Targeting Cancer- and Chemotherapy-Induced Anorexia and Cachexia using the GDF15/GFRAL Signalling System

A thesis submitted to the University of Manchester for the degree of Doctor of Philosophy in the Faculty of Biology, Medicine, and Health

2023

Rosemary HW Shoop

School of Medical Sciences

Contents

Word count: 51761

List of figures

List of tables

List of abbreviations

+ve   positive

-ve   negative

3V   3rd ventricle

4V   4th ventricle

AAV   Adeno-associated virus

ACS   Anorexia cachexia syndrome

AP   Area postrema

A/P   Anterior/posterior

ARC   Arcuate nucleus of the hypothalamus

BBB   Blood brain barrier

BMI   Body mass index

BNST   Bed nucleus of the stria terminalis

CA   Cyclophosphamide + adriamycin

cc   Central canal

CCK   Cholecystokinin

CeA   Central amygdala

ChR2	Channel rhodopsin-2
CGRP	Calcitonin gene related peptide
CINV	Chemotherapy induced nausea and vomiting
CIS	Cisplatin
clPBN	Central lateral PBN
CNO	Clozapine-N-oxide
COPD	Chronic obstructive pulmonary disorder
CPA	Conditioned place aversion
CRACM	Cre-assisted circuit mapping
Cre	Cre recombinase
CRH	Corticotropin releasing hormone
CTA	Conditioned taste aversion
D2R	Dopamine 2 receptor
DIO	Double inverted open reading frame
DMEM	Dulbeco's modified eagle medium
DMSO	Dimethyl sulphoxide
DMX	Motor nucleus of the vagus/10th cranial nerve

DREADD	Designer receptor exclusively activated by designer drug
D/V	Dorsal/ventral
DVC	Dorsal vagal complex
ELISA	Enzyme-linked immunosorbent assay
elPBN	External lateral parabrachial nucleus
eYFP	Endogenous yellow fluorescent protein
FBS	Foetal bovine serum
FG	Fluorogold (hydroxystilbamidine methanesulfonate)
GDF15	Growth differentiation factor 15
GEM	Gemcitabine
GFRAL	GDNF receptor alpha-like
GFRAL mAb	Monoclonal anti-GFRAL antibody
GIT	Gastrointestinal tract
GLP-1	Glucagon-like peptide-1
GLP-1R	Glucagon-like peptide-1 receptor
HG	Hyperemesis gravidarum
HPA	Hypothalamic-pituitary-adrenal

ic	Internal capsule
IHC	Immunohistochemistry
IL-1β	Interleukin-1 beta
IL-6	Interleukin-6
IL-8	Interleukin-8
IP	Intraperitoneal
ISH	In situ hybridisation
JIR	Jackson Immuno Research
KC	Keratinocyte chemoattractant
KO	Knock out
LLC	Lewis lung carcinoma
lPBN	Lateral parabrachial nucleus
LPS	Lipopolysaccharide
LV	Lateral ventricle
mAb	Monoclonal antibody
MC4R	Melanocortin 4 receptor
MCP-1	Monocyte chemoattractant protein-1

MCSF	Macrophage colony-stimulating factor
MIC-1	Macrophage inhibitory cytokine-1
M/L	Medial/lateral
mNTS	Medial portion of the nucleus of the solitary tract
NDS	Normal donkey serum
NSAID	Non-steroidal anti-inflammatory drug
NTS	Nucleus of the solitary tract
ovBNST	Oval nucleus of the bed nucleus of the stria terminalis
PB	Phosphate buffer
PBS	Phosphate buffered saline
PBT	Phosphate buffer with triton-X
PBN	Parabrachial nucleus
PDYN	Prodynorphin
PENK	Proenkephalin
PKCδ	Protein kinase C delta
Poly(I:C)	Polyinosinic:polycytidylic acid
POMC	Proopiomelanocortin

PPG	Pre-proglucagon
PrRP	Prolactin releasing peptide
PVH	Paraventricular nucleus of the hypothalamus
qPCR	Quantitative polymerase chain reaction
SC	Subcutaneous
scp	Superior cerebellar peduncle
SEM	Standard error of the mean
TAX	Paclitaxel (Taxol)
TGFβ	Transforming growth factor beta
TH	Tyrosine hydroxylase
TNFα	Tumour necrosis factor alpha
VEGF	vascular endothelial growth factor
VEH	Vehicle
VGLUT	Vesicular glutamate transporter
VTA	Ventral tegmental area
WT	Wild type

Abstract

Anorexia/cachexia syndrome (ACS) causes the mortality of 20-30% of cancer patients and worsens the prognosis of many more. The mechanisms underlying ACS are poorly understood and, therefore, there is currently no effective method to combat this condition. Growth differentiation factor 15 (GDF15) is a cytokine which is released in response to cell stress and damage, such as is caused by cancer and chemotherapy. The action of GDF15 on its cognate receptor, GDNF alpha-like receptor (GFRAL), has been linked to anorexia, cachexia and nausea. The GDF15/GFRAL signalling network may therefore be a good target for cancer- and chemotherapy-induced ACS.

In this thesis, I demonstrated that a low dose of exogenous GDF15 caused anorexia and aversion in healthy mice and pica behaviour in rats. Immunohistochemistry (IHC) showed that this low dose of GDF15 caused activation of neurons in the dorsal vagal complex (DVC), the lateral parabrachial nucleus, the central amygdala, the paraventricular nucleus of the hypothalamus, and the oval nucleus of the bed nucleus of the stria terminalis. These areas are known to be involved in signalling anorexia and weight loss. Retrograde tracing showed connections between activated neurons in these areas.

Furthermore, IHC illuminated different neuronal phenotypes activated by GDF15 in these areas, including neurons containing the neuropeptide, cholecystokinin (CCK), in the DVC. Signalling through this population and the consequent anorexia was prevented pharmacologically using a CCK receptor antagonist or by selectively ablating these CCK neurons genetically.

In future, it will be possible to directly manipulate GFRAL neurons using our bespoke *Gfral*-Cre mouse model, which I validated in my thesis. *Gfral*-Cre mice were crossed with a fluorescent reporter strain to show fidelity of Cre expression in GFRAL neurons. The mice were also crossed with a 1TB-hM3Dq^{mCherry} mouse, which caused the selective expression of a designer receptor, the activation of which caused anorexia and prevented gastric emptying.

GFRAL^{DVC} neurons were activated by GDF15, but not by other satiety or sickness signals. GFRAL neurons were, however, activated by chemotherapy treatments which caused anorexia, weight loss, and the increase of GDF15 in otherwise healthy mice. For these chemotherapy treatments, the prevention of GFRAL signalling by congenital knock out of the GFRAL receptor, or by treatment with a GFRAL-blocking antibody, reduced or reversed anorexia and weight loss.

Although three different murine cancer models were tested here, none showed a suitable ACS phenotype which would have allowed further study of the link between GDF15 and cancer ACS.

The effects of GDF15/GFRAL signalling during chemotherapy in this thesis, and reported during cancer in other literature, show the GDF15/GFRAL signalling network to be a promising target to combat ACS in cancer and chemotherapy.

Declaration

No portion of the work referred to in the thesis has been submitted in support of an application for another degree or qualification of this or any other university or other institute of learning.

Copyright statement

The author of this thesis (including any appendices and/or schedules to this thesis) owns certain copyright or related rights in it (the "Copyright") and they have given the University of Manchester certain rights to use such Copyright, including for administrative purposes.

Copies of this thesis, either in full or in extracts and whether in hard or electronic copy, may be made **only** in accordance with the Copyright, Designs and Patents Act 1988 (as amended) and regulations issued under it or, where appropriate, in accordance with licensing agreements which the University has from time to time. This page must form part of any such copies made.

The ownership of certain Copyright, patents, designs, trademarks and other intellectual property (the "Intellectual Property") and any reproductions of copyright works in the thesis, for example graphs and tables ("Reproductions"), which may be described in this thesis, may not be owned by the author and may be owned by third parties. Such Intellectual Property and Reproductions cannot and must not be made available for use without the prior written permission of the owner(s) of the relevant Intellectual Property and/or Reproductions.

Further information on the conditions under which disclosure, publication and commercialisation of this thesis, the Copyright and any Intellectual Property and/or Reproductions described in it may take place is available in the University IP Policy (see http://documents.manchester.ac.uk/DocuInfo.aspx?DocID=24420), in any

relevant Thesis restriction declarations deposited in the University Library, the

University Library's regulations (see

http://www.library.manchester.ac.uk/about/regulations/) and in the University's

policy on Presentation of Theses.

Acknowledgements

It is a time-honoured cliché to say that science does not happen without help, and this project was no exception, so I have a lot of people to thank for sharing with me their time, expertise, and resources.

Firstly, I'd like to thank Simon Luckman for hiring me as a technician in 2017, then almost immediately persuading me to do a PhD. This has been an amazing opportunity to do some truly inspiring science and I have met a lot of wonderful people working in his group. It has been a privilege and I could have worked on this project for the rest of my career.

Next, I would like to express my gratitude to the whole of the Luckman group, and later the D'Agostino group, a collection of lovely people and excellent scientists, who were kind enough to share their invaluable support and advice throughout. In particular, a massive thank you to Dr Amy Worth for her tireless efforts in training me in everything from *in vivo* and *ex vivo* techniques to teaching me skills necessary to be a functional lab member. Thank you for being an excellent mentor, and offering great advice on experimental design, writing, and where to get the best cake. Also, a massive thank you to Dr Nic Nunn, who volunteered to read drafts of my thesis and provided some cracking feedback, and to Jenna Hunter and Isabella Culotta who were both so generous with their time and skills, despite having their own hectic schedules.

Thanks also to Dr Claire Feetham and Valeria Collabolletta for stepping in during the final few months, running some rather complicated experiments, and getting the IHC for the *Gfral*-Cre::hM3Dq^{mCherry} sorted in time for me to add it into my thesis. I'm really excited that you're carrying on the GFRAL project and can't wait to see what you'll find out next.

Before this project, I had absolutely no experience in the field of cancer, so a big thank you to Dr Jamie Honeychurch for his help and knowledge with cancer experiments, advice on (chemo)therapeutics, and provision of cell lines used in

cancer studies. Thanks to Jamie also for his help with cell culture techniques and getting the ball rolling with our first cancer study.

A huge thank you also belongs to Dr Ray Wong for not only allowing me to use his cell culture facilities (and occasionally consumables), but for showing me how to use them and continuing advice and support on cell culture techniques and implantation methods. Massive thanks also go to Emily Rowling and Brian Telfer for sharing their wealth of knowledge on cancer models and then walking me through how to set them up and run studies with them. These lovely people did not need to offer me their time or help, but did anyway, and half of chapter 6 would be missing without their input.

On a more personal level, I'd like to thank my long-suffering family and friends for sticking with me and putting up with me and my bellyaching over the last 4-and-a-bit years. In particular, thank you to my lovely Jack for being a wonderful sounding board and for his continuing support through this whole process. Thank you to my wonderful sister and aunt, the Drs. Stevie Shoop-Worrall and Kate Weiner, for the open use of your living rooms for writing in, for the many many cups of tea, and for the reassurances that this was not a standard PhD experience. A massive thank you to my mum also, who picked up the phone on an almost daily basis to listen to a blow-by-blow account of this whole PhD process. Thank you all for bearing with me through this. All I can say is, it's finally over. Normal service can now be resumed.

And finally, having finished thanking all these wonderful people, I have a small request to make of the four horsemen of the modern apocalypse (Fire, Flood, Plague, and Brexit). Shall we not do that again? Please?

1 Introduction

1.1 Anorexia and cachexia

Anorexia (literally 'an' = without and 'orexis' = appetite) describes reduced food intake due to lack of appetite/motivation to eat. Anorexia can occur in healthy individuals when they are full or satiated, for example by the consumption of a significant volume of food to cause mechanical stretch of the stomach, or sufficient nutrients to trigger the release of satiating hormones. Anorexia also occurs during illness. This can be due to a range of reasons, including nausea, pain, aversion, or as an adaptive sickness response. Over time, anorexia can lead to weight loss. In some chronic diseases, for example cancer, this weight loss can include the loss of lean as well as fat mass. This more problematic form of weight loss is deemed cachexia.

Cachexia is known as a wasting disease, the etymology for which translates to 'bad condition'. Cachexia is characterised primarily by the loss of skeletal muscle, but also encompasses the loss of other muscle types and fat mass. Both anorexia and cachexia are associated with inflammation (Fearon *et al.*, 2011) and when seen together are referred to as anorexia cachexia syndrome (ACS). ACS is common in many chronic and inflammatory disease states, including, but not limited to, congestive heart failure, chronic kidney disease, rheumatoid arthritis, chronic obstructive pulmonary disorder (COPD), and cancer (Tisdale, 2004; Molfino, Laviano and Fanelli, 2010; Tazi and Errihani, 2010; von Haehling and Anker, 2010; Fearon *et al.*, 2011). Overall, approximately 30% of cancer patients are expected to experience cachexia, with that number rising to 90% for patients with liver cancer, lung cancer, or cancers affecting the gastrointestinal tract (GIT) (Anker *et al.*, 2019). ACS is predicted to be the cause of mortality for at least 20% of deaths amongst cancer patients (Argilés *et al.*, 2014).

Despite cachexia being so common amongst patients with cancer and having such detrimental effects, it has historically been difficult to diagnose due to there being no real definition of the condition. It was only in 2011 that a criteria for the definition of cancer cachexia was decided by an international consensus (Fearon *et al.*, 2011).

Cancer cachexia is now described as "a multifactorial syndrome characterised by an ongoing loss of skeletal muscle mass (with or without loss of fat mass) that cannot be fully reversed by conventional nutritional support" (Fearon *et al.*, 2011). Clinical criteria for the diagnosis of cachexia can be found in *Box 1*.

> **BOX 1:** *In cancer, these are the criteria for a diagnosis of cachexia, copied from Fearon et al. (2011):*
>
> *"• Weight loss >5% over past 6 months (in absence of simple starvation); or*
>
> *• BMI <20 and any degree of weight loss >2%; or*
>
> *• Appendicular skeletal muscle index consistent with sarcopenia (males <7·26 kg/m²; females <5·45 kg/m²)* and any degree of weight loss >2%†*
>
> **Defined reference values (sex-specific) and standardised body composition measurements are essential to undertake assessment of skeletal muscle depletion. Although there is a paucity of reference values related to cancer-specific outcomes (Prado et al., 2007; Prado, Birdsell and Baracos, 2009), a generally accepted rule is an absolute muscularity below the 5th percentile. This can be assessed as follows: mid upper-arm muscle area by anthropometry (men <32 cm², women <18 cm²); appendicular skeletal muscle index determined by dual energy x-ray absorptiometry (men <7·26 kg/m²; women <5·45 kg/m²); lumbar skeletal muscle index determined by CT imaging (men <55 cm²/m²; women <39 cm²/m²); whole body fat-free mass index without bone determined by bioelectrical impedance (men <14·6 kg/m²; women <11·4 kg/m²).*
>
> *†A direct measure of muscularity is recommended in the presence of fluid retention, a large tumour mass, or obesity (overweight)."*

The development of effective treatments for cachexia has been further impeded by poor understanding for the mechanisms by which it acts. Although there has been a large amount of research in the area, and many mechanisms have been suggested, there is still no evidence of what causes cachexia (Tazi and Errihani, 2010). The lack of understanding of the causes of cachexia have meant that it is extremely difficult to address.

As this classification suggests, whilst cachexia is frequently accompanied by anorexia, at least a portion of weight loss is independent of reduced food intake (Fearon *et al.*, 2011). Alterations in energy metabolism, nutrient utilisation, and the reduced ability to replace lost muscle mass in cachexia may be responsible for this weight loss (Argilés *et al.*, 2014; Lerner, Tao, *et al.*, 2016; Baracos *et al.*, 2018; Garcia-Jimenez

and Goding, 2019). Loss of muscle mass may be linked to increased inflammation as chronic inflammation leads to muscle breakdown (Narsale and Carson, 2014). In this case, inflammation causes loss of muscle mass both by increasing muscle degradation and decreasing synthesis of new muscle tissue (Narsale and Carson, 2014).

Many inflammatory cytokines and pathways have been implicated in ACS. Some of the cytokines most frequently found to increase during cachexia are interleukin-1β (IL-1β), interleukin-6 (IL-6) and tumour necrosis factor α (TNF-α) (Tijerina, 2004; Fearon, Glass and Guttridge, 2012; Onesti and Guttridge, 2014). Whilst these cytokines and others demonstrably contribute to anorexia and weight loss/cachexia, none have yet been found to be causative of this syndrome (Vaughan, Martin and Lewandowski, 2013). Monoclonal antibodies against some of these cytokines are currently used in the treatment of cancer (Korneev et al., 2017). However, as these cytokines are not the cause of ACS, prevention of their signalling is not sufficient to fully combat ACS (Fearon, Glass and Guttridge, 2012; Collin R. Elsea, Kneiss and Wood, 2015).

Whilst it affects many organs, cachexia has the greatest impact on adipose tissue and skeletal muscle (Weber, Arabaci and Kir, 2022). In addition to depletion of muscle mass and fat stores, cachexia literally causes wastage of energy as signals cause increased browning of white adipose tissue and thermogenesis (Weber et al., 2022) and a change from oxidative phosphorylation, to less efficient glycolysis in some affected cells (Molfino, Laviano and Fanelli, 2010; Donohoe, Ryan and Reynolds, 2011; Argilés et al., 2014), all of which increases energy expenditure.

At this time, ACS remains a very real problem faced by many patients with chronic diseases including cancer. Despite being the focus of a lot of research over many years, we are only now beginning to understand the causes and design treatments. Those listed above show promise, but as the causes of ACS during disease in general are so poorly understood, there is currently no effective strategy to combat it.

1.2   What causes weight loss in cancer?

Cancer is a disease which can affect any tissue of any person, regardless of gender, age, or ethnicity, and is predicted to affect between 1:2 and 1:3 people during their lifetimes (Ahmad *et al.*, 2015). Cancer is caused by mutations in cells, which allows them to grow and divide in an uncontrolled manner. In most tissues, uncontrolled division of mutated cells leads to the formation of solid masses, called tumours. ACS is extremely common amongst cancer patients, with approximately 50% of cancer patients expected to be affected (Argilés *et al.*, 2014), increasing to up to 90% of patients, depending on the type and stage of cancer (Ahmad *et al.*, 2015). Unfortunately, ACS during cancer can greatly increase risk of mortality (Siff *et al.*, 2021), with skeletal muscle atrophy being a predictive factor of survival (Daly *et al.*, 2018). During cancer, anorexia, weight loss, and cachexia can stem from several peripheral and central mechanisms.

On the most basic level, tumours can physically prevent the uptake of nutrients by forming in the GIT, or in key secretory organs such as the pancreas. During pancreatic cancer, tumours can interfere with insulin production and secretion, thereby interrupting normal glucose homeostasis (Ito, Igarashi and Jensen, 2012). On the other hand, tumour cells can release hormones which cause weight loss, e.g. tumours releasing gut hormones such as glucagon (Ito, Igarashi and Jensen, 2012), or waste products such as lactate which can lead to reduction of appetite (Baile *et al.*, 2017). Lactate released from tumour cells can circulate, crossing the blood-brain barrier (BBB), and then interact with glucose-sensing neurons and neurons involved in hunger and satiety signalling in the brainstem and hypothalamus (Baile *et al.*, 2017).

In addition, tumours are often accompanied by inflammation (Ezeoke and Morley, 2015). For example, pro-inflammatory cytokines, IL-1β, IL-6, and TNF-α are released by macrophages in the tumour microenvironment (Ramos *et al.*, 2004; Molfino *et al.*, 2010; Suzuki *et al.*, 2013; Lerner *et al.*, 2016). These factors induce anorexia by activating central anorectic signalling pathways via actions in the GIT and vagus, or directly in areas of the brain not protected by the BBB (Ezeoke and Morley, 2015). In the periphery, exposure to pro-inflammatory cytokines can cause alterations in the

tumour metabolism, which can lead to deficiency in minerals such as zinc (Siren and Siren, 2010; Hendifar *et al.*, 2019). Zinc is vital in a number of processes including nutrient absorption and sense of taste (Yagi *et al.*, 2013). It is very common for taste and smell perception to be altered during cancer, and this can be a strong factor influencing anorexia (Ezeoke and Morley, 2015).

Signalling by pro-inflammatory cytokines released by tumours and surrounding cells can also impact body composition by acting peripherally to induce proteolysis in muscle tissue (Yeh and Schuster, 1999; Fearon, Glass and Guttridge, 2012; Argilés *et al.*, 2014; Siff *et al.*, 2021). Whilst this mostly affects skeletal muscle, during more severe forms of cancer cachexia, this can include smooth and cardiac muscle, for example those muscles responsible for swallowing and breathing correctly (Rausch *et al.*, 2021; Malla *et al.*, 2022). This is one way in which cachexia can increase the risk of mortality. Inflammatory factors have also been shown to impact on lipogenesis, lipolysis, and thermogenesis (Arruda *et al.*, 2010; Siff *et al.*, 2021; Malla *et al.*, 2022; Weber, Arabaci and Kir, 2022), causing further depletion of energy stores.

Certain inflammatory cytokines such as TNF-α, IL-1, and IL-6 are known to decrease gastric motility, which can lead to severe feelings of nausea and emesis (Tijerina, 2004), as well as causing activation of areas of the brain which have direct influence on the degradation of peripheral energy stores. The hypothalamus is well documented to affect peripheral energy homeostasis via alterations in processes such as hepatic gluconeogenesis (Könner *et al.*, 2007) and modulation of energy expenditure (Arruda *et al.*, 2010). Hypothalamic signalling can affect muscle wasting directly by causing a switch between peripheral anabolism and catabolism. Ramos et al, (2004) show that hypothalamic signalling can directly cause peripheral muscle wasting. Though the main focus of research into the effects of central signalling on anorexia/cachexia has been on the hypothalamus, the hindbrain is now emerging as having an important role. The role of the dorsal vagal complex (DVC) in the hindbrain on food intake and energy homeostasis will be discussed more fully in section 1.6.

On a smaller scale, tumours often consist of fast-growing cells which are poorly supplied by vascular structures and, therefore, do not receive adequate nutrition or oxygen (Nagy *et al.*, 2009). For small groups of cells, nutrients and oxygen can be obtained via passive diffusion from the surrounding environment. During cancer, clusters of cells can form rapidly, growing large enough that cells towards the centre would require infrastructure, such as blood vessels to ensure a supply of oxygen and nutrients an adequate removal of waste products. However, often cells divide too rapidly for the necessary infrastructure, such as blood vessels, to form. Equally, when tumours do form vascular structures, they are often disorganised and inefficient (Nagy *et al.*, 2009). Without adequate vasculature, cells inside large tumours cannot access oxygen or nutrients, and waste products build up (Paredes, Williams and San Martin, 2021). For this reason, tumours can often feature stressed, starving cells and can have a large energetic demand.

This puts the body under stress to produce metabolic substrates as quickly as possible to meet the demand. During cancer ACS, the body increases the availability of metabolic substrates in three ways: promotion of lipolysis and tissue breakdown, inhibition of lipid storage enzymes, and a switch from full oxidative phosphorylation to glycolysis (Donohoe *et al.*, 2011; Weber *et al.*, 2022). Glycolysis is far less efficient than oxidative phosphorylation, so less ATP is produced per unit of substrate, exacerbating the problem of lack of energy (Molfino, Laviano and Fanelli, 2010; Argilés *et al.*, 2014; Paredes, Williams and San Martin, 2021).

Further to this, even under circumstances when glucose is available, cancer cells can be programmed to preferentially use amino and fatty acids as a metabolic substrate. For example, several studies have shown that cancer cells prefer to use the amino acids such as arginine, glutamine, and aspartate as respiratory metabolites (Argilés *et al.*, 2014; Lerner, Tao, *et al.*, 2016; Garcia-Jimenez and Goding, 2019). This preference further promotes muscle-wasting by encouraging the breakdown of muscle tissue to provide for amino acid demand (Argilés *et al.*, 2007; Lerner, Tao, *et al.*, 2016). Cachexia is therefore known as a 'wasting disease'; not just due to muscle wasting, but also due to wasting energy. Unfortunately, in addition to stress signalling

causing anorexia and cachexia, starvation and pseudo-starvation may also promote metastasis, making the disease worse (Garcia-Jimenez and Goding, 2019).

Despite signalling stress to promote neoangiogenesis (Chiavenna, Jaworski and Vendrell, 2017; Altorki *et al.*, 2019) and increase supply of metabolic substrates (Paredes, Williams and San Martin, 2021), it is still common for cancer cells to die from lack of nutrients, hypoxia, or simply being too mutated to survive (Brown and Wilson, 2004; Gatenby and Gillies, 2004). Under these circumstances, cell death occurs via necrosis, rather than apoptosis. When cells die in this disorganised manner, they release their contents, which can be toxic, which then comes into contact with surrounding cells, damaging those as well, causing dedifferentiation, inflammation, the release of more distress signals, and increasing waste build up in the tumour microenvironment (Gatenby and Gillies, 2004; Bredholt *et al.*, 2015). These waste products and the pro-inflammatory cytokines their release can trigger, are also able to pass through into circulation and reach receptors in the central nervous system, triggering negative responses, such as anorexia, nausea, and emesis (Ezeoke and Morley, 2015).

In summary, tumours initiate the breakdown of muscle and fat to supply their growing energy demands, and then release inflammatory cytokines and toxins into circulation. These signals can act peripherally to cause degradation of fat and muscle and act centrally to cause nausea, emesis, anorexia, and further depletion of peripheral energy stores. There have been many suggestions as to which signals cause ACS during cancer. Those commonly suggested are IL-1β, IL-6, and TNF-α. Whilst these cytokines certainly contribute to anorexia, weight loss, and muscle wastage, none have been found to be causative of cancer ACS. The lack of knowledge of the causes of ACS is one of the key reasons that there is currently no completely effective therapy.

1.3   What causes weight loss with cancer therapy?

During cancer, cytotoxic therapy can also be a cause of ACS. Current, non-surgical treatment strategies for cancers include any combination of chemotherapy,

radiotherapy, hormone therapy, and targeted therapies such as monoclonal antibodies and growth factor antagonists. Cytotoxic chemotherapy is one of the most commonly used strategies to combat cancer and there are many different types which act via different mechanisms to prevent cell division and bring about cancer destruction. Different classes of chemotherapy will be described in more detail in chapter 7. Common side effects of the majority of traditional chemotherapies include combinations of nausea, vomiting, stomach pain, anorexia, and weight loss (Joint Formulary Committee, 2022). For example, it is estimated that >90% of cancer patients receiving cisplatin, a commonly used chemotherapeutic, will experience nausea and vomiting (Rapoport, 2017).

Cancer therapies can destroy tumours by several mechanisms, for example, by preventing cell division by disrupting DNA, cytoskeletal structures, and enzymes involved in cellular maintenance and repair. Cancer therapies often target rapidly dividing cells. In adulthood, there are relatively few cell types which divide frequently. Those that do are often exposed to harsh environments in which they are subject to destruction by mechanical and chemical means (e.g., epithelial cells in the stomach are exposed to low pH stomach acid and abrasion by food). Therefore, whilst systemic therapies may be used to destroy rapidly dividing cancer cells, they may also be responsible for destroying these other, healthy cells.

As with spontaneous necrosis of cancer cells, cell death caused by cytotoxic therapies also causes an immune response and the release of a range of inflammatory cytokines which can lead to anorexia, cachexia, and visceral malaise. As discussed earlier, these cytokines and other factors released can act centrally and in the periphery and can lead to alterations in visceral hormone release, changes in taste perception, nausea, vomiting, and muscle and fat catabolism (Elsea *et al.*, 2015; Ezeoke and Morley, 2015).

In addition to the ways in which cancers cause anorexia and weight loss, chemotherapies can affect food intake and body composition/weight by destroying healthy cells in and around to GIT (Sonis, 2004; Wafai *et al.*, 2013). Non-specific, systemic chemotherapeutics have the greatest impact on rapidly dividing cells such

as the gut endothelium. Destruction of luminal epithelial cells limits surface area via which nutrients can be absorbed, further reducing the nutrients available to the body. Chemotherapies also damage and destroy the gut microbiota (Bajic *et al.*, 2018). The gut microbiota is plays an important role in maintaining the integrity of the intestinal lumen, and intestinal dysbiosis can therefore further compromise the intestinal endothelium, compounding the direct damage caused by chemotherapy (Bajic *et al.*, 2018).

Outside of the gut, it is common for chemotherapies to cause damage to peripheral enteric neurons, and this can contribute to disruption of vagal signalling, which in turn slows gastric emptying and leads to nausea and emesis (Wafai *et al.*, 2013; McQuade *et al.*, 2016). Additionally, damage to peripheral sensory neurons by chemotherapy can cause neuropathic pain (Park *et al.*, 2013; Bajic *et al.*, 2018). Together, interference with normal signalling of energy balance and pain caused by chemotherapy can lead to depression, anorexia, and cachexia (Ezeoke and Morley, 2015; Bajic *et al.*, 2018).

ACS has been found to decrease the efficacy of chemotherapies, the impact of which is worse prognosis (Bachmann *et al.*, 2008; Arthur *et al.*, 2016). For example, Daly *et al.* (2018) found that reduction in muscle mass was predictive of increased risk of mortality. Further to this, reduction in fat and muscle mass are associated with increased toxicity from chemotherapies (Dewys *et al.*, 1980; Donohoe, Ryan and Reynolds, 2011; Fearon, Arends and Baracos, 2013), meaning lower doses must be used, or that drug cannot be used at all (Donohoe, Ryan and Reynolds, 2011; Fearon, Arends and Baracos, 2013). There is also evidence that ACS/starvation situations place cancer cells into a 'dormant' state, in which they do not rapidly divide, thereby allowing them to avoid destruction and increasing chances of relapse (Prunier *et al.*, 2018; Garcia-Jimenez and Goding, 2019). In this way, chemotherapy treatment is a part of an unfortunate paradox, in which the therapy to treat the cancer causes cachexia, which in turn makes chemotherapy less effective.

Prophylactic antiemetic treatments given before chemotherapies have recently become more effective, reducing the incidence and severity of chemotherapy-

induced nausea and vomiting (Aapro, 2016). However, these side effects are still present for many drugs (Majem *et al.,* 2022). Nausea, emesis, anorexia, and the accompanying weight loss have been responsible for keeping many new and innovative cancer therapies off the market and are a common cause for patient non-compliance (Rapoport, 2017). In this "Catch-22" situation, patients receiving therapy which causes ACS show reduced response to treatment and, therefore, worsened prognosis (Bachmann *et al.*, 2008; Arthur *et al.*, 2016). Patients not receiving therapy may still experience ACS from the cancer itself, which will continue to delvelop due to lack of therapy.

It is important to note that whilst many chemotherapies and cancer therapies do cause nausea, emesis, anorexia, and weight loss, this is not the case for all chemotherapies (Joint Formulary Committee, 2022). As mentioned earlier, though many inflammatory signals are increased by chemotherapies which cause nausea, anorexia, and cachexia, and undoubtedly have a role in signalling these effects, none have been found to be causative of ACS. Investigation is needed to discover whether certain factor(s) are changed by chemotherapies which cause ACS, but not in those which do not. These factors could contribute to, or cause, ACS following chemotherapy treatment. This is something which will be explored further in chapters 7 and 8.

Recently, information regarding a cytokine which may be this signal has come to light. This cytokine, growth differentiation factor 15 (GDF15) is a main point of investigation in this thesis and will be discussed in more detail below.

1.4   Strategies to combat anorexia cachexia syndrome

The main challenges when treating ACS are to increase calorie intake and prevent loss of/maintain muscle mass. Current options to increase caloric intake are to encourage patients to consume a high-calorie diet and eat more of their favourite foods. This can be supported by treatment with appetite stimulants. Currently, available appetite stimulants include ghrelin-based treatments (Neary *et al.*, 2004; Tazi and Errihani, 2010; Mendes *et al.*, 2015; Duan, Gao and Zhu, 2021) or megestrol

acetate (megace). Cannabinoid receptor agonists are also being developed as appetite stimulants to treat patients with ACS (Tazi and Errihani, 2010; Ezeoke and Morley, 2015).

These appetite stimulants utilise endogenous signals which act on central feeding circuits to increase feelings of hunger and the drive to eat. Megace is a synthetic progesterone analogue which is additionally used to treat certain hormone-sensitive cancers (Yeh and Schuster, 2006). Megace can also combat cachexia to an extent via action on glucocorticoid receptors. This increases weight gain (Yeh and Schuster, 2006). However, megace-induced weight gain appears dependent on an increase in fat mass, without affecting lean mass. Whilst this is useful, this is not a therapy which is able to fully combat ACS. Appetite stimulants face further limitations when treating ACS as, although they can combat anorexia, cachexia cannot be fully reversed by increasing nutritional support (Fearon *et al.*, 2011).

Slightly more promising are analogues of the orexigenic hormone, ghrelin. Under healthy conditions, ghrelin is released in greatest quantity immediately prior to mealtimes. Not only does ghrelin act in the hypothalamus, DVC and on the vagus to stimulate hunger and promote increased energy intake (Pradhan, *et al*., 2013), ghrelin also decreases energy usage and promotes growth and expansion of energy stores. It does this by supressing thermogenesis (Lin *et al.*, 2011; Pradhan, Samson and Sun, 2013), promoting the release of growth hormone, which has anabolic properties (Kojima *et al.*, 1999; Sun *et al.*, 2004), and promoting adipogenesis and lipogenesis, whilst preventing proteolysis and protecting muscle cells from apoptosis (Mendes *et al.*, 2015).

The protective and proliferative actions of ghrelin on muscle occur during sarcopenia, another muscle-wasting condition (Porporato *et al.*, 2013; Wu *et al.*, 2020), and therefore may also occur during cachexia. This makes the ghrelin pathway a good target for both anorexia and weight loss/cachexia. However, caution must be applied to the use of ghrelin signalling pathways if treating cancer-induced ACS as there is evidence that increased ghrelin signalling can cause growth and proliferation of tumour cells (Majchrzak *et al.*, 2012; Lin and Hsiao, 2017). Ghrelin is also found at

high levels in certain metastatic tumours compared with non-metastatic tumours (Majchrzak *et al.*, 2012; Lin and Hsiao, 2017).

Treatment options which focus on combatting the cachexia component of ACS focus on preserving and increasing muscle mass. This can include encouraging the patient to participate in gentle exercise (Fearon, Arends and Baracos, 2013; Vaughan, Martin and Lewandowski, 2013; Crawford, 2019), treatment with non-steroidal anabolic hormone analogues (Coats *et al.*, 2011; Dobs *et al.*, 2013), and myostatin blockers (Busquets *et al.*, 2012; Duan, Gao and Zhu, 2021). There is some suggestion that, exercise can encourage maintenance of existing muscle mass, as well as promoting replacement of degraded muscle, and reduction of inflammation, which can minimise further muscle loss (Fearon, Arends and Baracos, 2013; Hardee, Counts and Carson, 2019; Hendifar *et al.*, 2019; Graham *et al.*, 2021; Siff *et al.*, 2021). Similarly, myostatin antagonists can help prevent further degradation of muscle, whilst androgen receptor modulators, such as enobosarm, can help to increase muscle mass during and after cancer therapy (Busquets *et al.*, 2012; Dobs *et al.*, 2013).

Despite appetite stimulants and attempts to build muscle mass, nutrition still may not be accessible to patients as cancers can cause changes in taste perception, making foods unbearable to consume, and certain changes made by cancers (e.g. blockage of GIT or zinc deficiency) may physically prevent nutrient absorption (Ezeoke and Morley, 2015). Though there is currently not a pharmacological method to combat changes in taste perception, many tumours can be removed surgically or shrunk/destroyed using other cancer therapy methods, thus removing physical barriers to nutrient absorption.

One of the most reliable methods of reversing cancer ACS available is to shrink or destroy the tumour (Weber, *et al.*, 2022). Unfortunately, this can be a complex process, with some tumours being inoperable and many cancer therapy options additionally contributing to ACS, nausea, and emesis. In particular, chemotherapy, radiation therapy, immune therapies, and opioid painkillers are known to cause nausea and emesis (Joint Formulary Committee, 2022). Reasons that cancer therapies induce nausea and emesis include reduced liver function, causing build-up

of waste products in circulation, reduced gastric emptying, and release of signals from the gut and other visceral organs, such as serotonin and substance P (Andrews and Horn, 2006; Lacy, Parkman and Camilleri, 2018). These then activate central nausea pathways, both directly through blood-borne signals and through signalling via the enteric nervous system and the vagus (Lacy, Parkman and Camilleri, 2018; Sanger and Andrews, 2018; Zhong *et al.*, 2021; Carson *et al.*, 2022). Depending on how therapies are causing nausea and emesis, different antiemetic drugs may be prescribed.

Though emesis is often accompanied by nausea, nausea and emesis work via similar, but separate pathways. Emetic pathways were discovered before nausea pathways, therefore historically, antiemetic drugs were effective against emesis, but not nausea (Andrews and Sanger, 2014; Sanger and Andrews, 2018). In more recent years, with increasing understanding of what causes nausea, more effective antiemetics have been developed which are better at combatting both nausea and emesis (Jones *et al.*, 2011; Lacy, Parkman and Camilleri, 2018).

It is now common for serotonin antagonists, neurokinin-1 inhibitors, antihistamines, and drugs which increase gastric motility to be prescribed alongside chemotherapies and radiotherapy which cause nausea and emesis (Joint Formulary Committee, 2016; Roila *et al.*, 2016). These help to prevent activation of peripheral and central nausea pathways by preventing signalling from the vagus as well as direct activation of neurons in the dorsal vagal complex (DVC), an area key in coordinating both satiety and sickness signalling and will be discussed more thoroughly below. These drugs are effective at increasing patient quality of life and nutrient uptake, but once again, are not fully effective at preventing ACS.

To understand how cancer and cancer therapies cause anorexia, cachexia, nausea, and emesis, it is necessary to briefly explore current understanding of appetite and body weight regulation.

1.5   Maintenance of body weight

Maintenance of energy balance is essential to remain healthy and functional. This is integrally linked with body composition and the maintenance of body weight, which represents our stores of the macronutrients that are needed to function.

Simply put, body weight is maintained as a balance between energy intake and expenditure. Energy intake occurs via feeding, and is spent in processes such as respiration, growth, and thermogenesis. If energy intake is greater than energy expenditure, then weight gain occurs, stores of glycogen and triglycerides increase, and growth of other tissues such as muscle is possible. The body can also compensate to a degree for an excess of energy intake by wasting energy through adaptive thermogenesis (Reddy *et al.*, 2014; Geary, 2020). If energy intake is less than expenditure, weight is lost, with energy stores being broken down to increase availability of metabolic substrates. Changes in body weight for healthy adults is generally accounted for by changes in fat mass (Heymsfield *et al.*, 2014; Geary, 2020).

To maintain energy balance and a healthy body, the brain and endocrine systems interact to control the availability of nutrients. As feeding is a behaviour, energy intake is under the control of central signalling networks. When the body is in caloric deficit or energy has been replenished, signals from the GIT and peripheral energy stores, such as adipose tissue and muscle, travel to the brain via either the peripheral nervous system or the endocrine system (Pradhan, Samson and Sun, 2013). The brain then coordinates responses to seek food, feed, or terminate feeding, depending on what is appropriate. This will be discussed in more detail below. Such signals regarding energy status can also act directly in the periphery to coordinate responses such as insulin release or to glucose storage (Baldini and Phelan, 2019). For example, the hormone ghrelin, released from the GIT, acts centrally to increase food intake, but also acts directly on adipose tissue to promote lipogenesis and adipocyte growth (Pradhan, Samson and Sun, 2013).

Body weight is also affected by central and peripheral signalling in times of stress and disease. During starvation, signals from the brain promote the breakdown of muscle

and fat stores to increase availability of metabolic substrates (Argilés *et al.*, 2007; Fearon, Arends and Baracos, 2013; Klaus, Igual Gil and Ost, 2021). Alternatively, when toxins are ingested, body weight can be affected by the actions of inflammatory cytokines directly on muscle and fat (Braun *et al.*, 2011; Glass and Olefsky, 2012; Liu *et al.*, 2022), and by central signalling pathways which cause anorexia, changes in thermogenesis and signal to peripheral energy stores to further cause proteolysis/lipolysis (Donohoe, Ryan and Reynolds, 2011; Duan, Gao and Zhu, 2021). Finally, emotional stress has the ability to alter feeding habits via signalling networks, including the hypothalamic-pituitary-adrenal (HPA) axis and central regions such as the bed nucleus of the stria terminalis (BNST) and the central amygdala (CeA) (Maniam and Morris, 2012; Di Bonaventura *et al.*, 2014; Sominsky and Spencer, 2014; Hardaway *et al.*, 2019). Activation of the HPA axis via stress and disease can further affect body weight by signalling to cause the breakdown of fat and muscle stores (Braun *et al.*, 2011; Peckett, Wright and Riddell, 2011). These central pathways are influenced by energy status, emotional status, sickness, and stress.

1.6 Anorectic pathways

Food intake is a key part of the maintenance of body weight. Most mammals eat in bouts, called meals. Under normal circumstances, meals are initiated by appetite, which describes the motivation to eat. Once enough is deemed to have been consumed, meals are terminated by satiation, a process by which the brain signals that enough volume and/or nutrients have been ingested. Satiety, a feeling of being replete, during which time there are enough nutrients to support normal functioning, growth and activity, then prevents further food seeking behaviour and ingestion until there is once again a caloric deficit (Greenway, 2015).

Feeding is a behaviour, and as such is controlled by central signalling pathways. Increases and decreases in feeding can lead to changes in body weight. These changes generally stem from changes in quantity of glycogen on a day-to-day basis (Wasserman, 2009; Duan, Gao and Zhu, 2021). In addition to feeding affecting body weight, activation of central signalling pathways can directly affect body weight by encouraging anabolism or catabolism of lipids, proteins and glycogen stores (Braun

et al., 2011; Mullur, Liu and Brent, 2014; Saito *et al.*, 2015). Generally, feeding and body weight are maintained as part of normal homeostasis, but changes can be made in response to sickness, stress, and reward stimuli.

Under homeostatic control, when there is a caloric deficit, we become hungry, seek food, and eat. Hunger is a negative emotional state (Betley *et al.*, 2015) and can be signalled by orexigenic hormones (Abizaid *et al.*, 2006; Chen *et al.*, 2009). Ingestion of food causes stretch in the GIT which is detected by mechanoreceptors. The intake of different nutrients is also detected in the GIT, causing the release of anorectic hormones (Konturek *et al.*, 2004). These signals can be received in the brainstem, specifically in the dorsal vagal complex (DVC), either via the vagus nerve as part of the enteric nervous system, or directly in the area postrema (AP) and the nucleus of the solitary tract (NTS) (Konturek *et al.*, 2004; Browning and Travagli, 2016).

The DVC is a term used to describe three regions in the brainstem: the AP, the NTS, and the motor nucleus of the vagus/10th cranial nerve (DMX) collectively. The AP is known as the chemoreceptive trigger zone in humans and has a major function in signalling emesis (Borison, 1974; MacDougall and Sharma, 2023). The structure is common to many species, including mice and rats (non-emetic species), and shrews, monkeys, and humans (emetic species). The AP is located next to the 4th ventricle (4V) and is a circumventricular area in the brain. This means that it is not protected by the BBB. This exposure allows neurons in the AP direct contact with factors circulating in the bloodstream. These signals include hormones, nutrients, and toxins. Whilst most renowned for signalling nausea and emesis, the AP also has a pivotal role in processing satiety cues (Grill and Hayes, 2012; Lutz, 2016).

The NTS is a much larger area than the AP, with the rostral and caudal regions performing different functions. The more rostral portions of the NTS mediate gustatory signalling, gastric motility, blood pressure and circulation around the gastrointestinal tract (GIT), and have a role in respiratory signalling (Browning and Travagli, 2016). The more caudal portion, like the AP, is involved in both nausea and satiety signalling (Browning and Travagli, 2016). In combination these areas affect nutrient uptake, firstly by influencing motivation to eat, then by controlling the rate

at which food travels through the GIT and the circulation of blood to transport the resulting substrates.

There are many separate populations of neurons in the AP and NTS which are responsible for the different functions which these areas perform. These neurons can be defined by their content of neuropeptides and neurotransmitters, their location within the DVC, and their projections to other parts of the brain. The different populations of neurons also respond to different stimuli. For example, some neurons are more responsive to toxic signals and others to nutritive cues (Heeley and Blouet, 2016; Roman, Derkach and Palmiter, 2016; Roman, Sloat and Palmiter, 2017; D'Agostino *et al.*, 2018).

There are some neurons in the DVC which respond preferentially to different elements of food, e.g. different chain lengths of lipid, different amino acids, or sugars (D'Agostino *et al.*, 2016; Heeley and Blouet, 2016). Even within populations of these neurons, it is possible to find different subsets which signal via different efferent pathways. For example, there is a population of neurons in the AP/NTS which contain the neurotransmitter cholecystokinin (CCK). Activation of these neurons causes a reduction in food intake (D'Agostino *et al.*, 2016). This is achieved by separate subsets of CCK neurons signalling to the hypothalamus, inducing anorexia, or to the PBN and CeA, a pathway involved in negative feelings of nausea and malaise (Roman *et al.*, 2017).

Typically, homeostatic control of food intake is described as a function of the hypothalamus. In this model, neurons containing agouti-related peptide (AgRP), neuropeptide Y (NPY) and GABA signal hunger and drive food seeking and ingestion, whilst inhibiting neighbouring anorectic neurons which contain pro-opiomelanocortin (POMC) (Cone *et al.*, 2001). AgRP/NPY neuronal activity is inhibited by circulating factors and hormones released in response to feeding. This then allows for activation of POMC neurons which signal anorexia and in turn inhibit AgRP/NPY neurons (Waterson and Horvath, 2015). These neurons are undoubtedly essential to feeding behaviour, as ablation of the ARC during adulthood leads to starvation and death in mice (Gropp *et al.*, 2005; Luquet *et al.*, 2005). However, feeding is essential

to continuing life, and therefore there is a lot of redundancy in networks controlling this behaviour. The role of the DVC in control of food intake in health and disease is now becoming more prominent in discussions around feeding. It is clear that the DVC has roles not just in 'general housekeeping' following feeding to coordinate efficient nutrient absorption, but also in signalling emotional responses and aversion or reward following feeding (Yagi *et al.*, 2013; Zhong *et al.*, 2021). This will ensure the right food substances are being sought.

For both input areas, neurons integrate feeding/hunger cues by projecting to other areas including the parabrachial nucleus (PBN) and hypothalamic nuclei, which then form networks by signalling to other regions such as the CeA or the BNST (Garfield *et al.*, 2015; Waterson and Horvath, 2015). In concert, these signalling networks coordinate the cessation of food seeking and consumption when energy balance has been restored, and project back down via the DVC to affect gastric motility, hormone release, and alterations in blood pressure necessary to utilise nutrients which have been consumed (Browning and Travagli, 2016).

On the other hand, feeding can be curtailed by negative stimuli which cause nausea, emesis, pain, or aversion. These stimuli seem to cause anorexia and weight loss using similar brain regions and signalling networks as those which cause satiety and satiation. The key difference is often the populations of neurons in those areas which are activated. A good example of this is the lateral PBN (lPBN), which is known to coordinate both satiating and aversive signals to terminate feeding, by integrating signals coming from the DVC and PVH and signalling to other regions such as the PVH, amygdala, or NTS (Alhadeff *et al.*, 2015; Garfield *et al.*, 2015; Campos *et al.*, 2016). Calcitonin gene related peptide (CGRP) neurons in the lPBN form a part of an aversive anorectic pathway. Satiating signals received in the lPBN are received by neurons separate from the neurons which contain CGRP (Garfield *et al.*, 2015). Similarly, whereas satiating signals are received in the DVC by neurons such as those expressing prolactin-releasing peptide (PrRP) (Lawrence, Ellacott and Luckman, 2002), it is common for sickness signals to activate neurons containing signalling peptides such as preproglucagon (PPG), serotonin, dopamine, and glutamate in the DVC (Roman,

Derkach and Palmiter, 2016; Alhadeff *et al.*, 2017; Leon *et al.*, 2021; Zhong *et al.*, 2021).

In addition to preventing food intake, emesis can contribute to anorexia during sickness and disease. Emesis, though often accompanied by nausea, is in fact a distinct process (Singh and Kuo, 2016). Emesis can be brought about in a number of ways, one of which is a response to toxins, such as ingested pathogens or drug therapies which damage the luminal cells in the GIT (Zhong *et al.*, 2021). In this case, it can be the vago-vagal reflex which causes emesis (Lacy, Parkman and Camilleri, 2018). Normally the vago-vagal reflex is activated by mechanical stretch in the GIT caused by the ingestion of food (Travagli and Anselmi, 2016). Signalling by sensory vagal afferents to the DVC and back via vagal motor efferents causes tonic inhibition of the muscles surrounding the stomach, allowing it to stretch and accommodate food (Travagli and Anselmi, 2016; Powley, 2021). In the presence of toxins and inflammatory cytokines, this reflex arc is interrupted, removing the tonic inhibition of muscles in the stomach wall and causing sudden contraction of the stomach, forcing the contents upward into the oesophagus for removal (Lacy, Parkman and Camilleri, 2018). Alternatively, toxins/inflammatory signals can act directly on the AP to activate both vagal efferents, and/or higher brain regions to cause emesis (Andrews and Horn, 2006; Browning and Travagli, 2016).

Alternatively, emesis can be linked to nausea. Nausea is caused by activation of neurons in the DVC, for example those containing cholecystokinin (CCK) or serotonin (Billig, Yates and Rinaman, 2001; Andrews and Horn, 2006; Ezeoke and Morley, 2015; Rapoport, 2017), which then signal to the PBN and CeA in a highly aversive pathway (Alhadeff *et al.*, 2015; Roman, Sloat and Palmiter, 2017; Palmiter, 2018) which, further to terminating food intake, causes learned aversion (Zhong *et al.*, 2021). In turn, the DVC may cause a decrease of gastric motility (Browning and Travagli, 2016), which further increases feelings of nausea, which may eventually lead to an emetic response processed with the involvement of higher brain regions (Zhong *et al.*, 2021). In all cases, afferent signalling causing emesis is integrated in the DVC and travels to the GIT via vagal efferents (Zhong *et al.*, 2021).

Central pathways which cause anorexia can further be involved in causing weight loss and changes in body composition during disease. For example, in addition to causing anorexia, the activation of certain hypothalamic neurons can increase thermogenesis and cause the catabolism of peripheral energy stores (Arruda *et al.*, 2010; Dodd *et al.*, 2014; Siff *et al.*, 2021) and can signal the breakdown of glycogen in visceral organs, muscle, and fat (Duan *et al.*, 2021). This can be in response to direct action of inflammatory signals in the hypothalamus, or as a result of signalling from areas like the DVC (Grill and Hayes, 2012; Siff *et al.*, 2021).

It is apparent that the DVC is an important integratory area, receiving both humoral and neuronal inputs to affect feeding behaviour and body composition. A major goal of this thesis is to explore the ways in which GDF15/GFRAL signalling causes anorexia and weight loss. GFRAL neurons, discussed in more detail below, are located in the DVC, and may use some of the above signalling pathways to cause anorexia and weight loss during cancer and chemotherapy.

1.7 GDF15

Growth differentiation factor 15 (GDF15) is a cytokine and a member of the TGFβ family. It was first described in the 1990s by the Breit group in Australia (Fairlie *et al.*, 1999) under the name of macrophage inhibitory cytokine 1 (MIC-1) and the Unsicker group in Germany (Strelau *et al.*, 2000) under the name of GDF15.

Under normal physiological circumstances in humans, GDF15 circulates at a low level of between 200-2150 pg/ml (Brown *et al.*, 2002; Tsai *et al.*, 2015; Welsh *et al.*, 2022). This figure increases with aging and pregnancy (Fujita *et al.*, 2016; Welsh *et al.*, 2022). This mostly originates from the liver, but can also be found at low levels in the heart, lungs, kidneys, testes, adipocytes, and epithelial cells (Fairlie *et al.*, 1999). GDF15 is often described as a pleiotropic hormone, due to its many roles in neural development, skin maintenance, influencing body composition, and disease development (Strelau *et al.*, 2000; Wang, Baek and Eling, 2013; Yang *et al.*, 2017; Tran *et al.*, 2018; Luan *et al.*, 2019).

GDF15 release is increased from cells which have been damaged or stressed, for example by radiation (Sándor *et al.*, 2015), hypoxia (Albertoni *et al.*, 2002; Hinoi *et al.*, 2012), mitochondrial stress (Kang *et al.*, 2021), amino acid deficiency/starvation (Patel *et al.*, 2019). These circumstances can come about during disease states such as rheumatoid arthritis (Brown *et al.*, 2007), obesity (Tsai *et al.*, 2015), congestive heart failure (Xu *et al.*, 2006; Kempf *et al.*, 2007; Wollert, Kempf and Wallentin, 2017), chronic kidney disease (Nair *et al.*, 2017), and cancer (Welsh *et al.*, 2003; Tsai *et al.*, 2018). During disease, the circulating concentration of GDF15 can increase by 10-100 times normal levels (Tsai *et al.*, 2012). In many cases, the circulating levels of GDF15 correlate with patient outcome, and so GDF15 is now beginning to be used as a prognostic biomarker for several diseases including cancer (Adela and Banerjee, 2015; Fujita *et al.*, 2016; Lerner, Gyuris, *et al.*, 2016; Wollert, Kempf and Wallentin, 2017; Cao *et al.*, 2021). Interestingly, drug therapies can also cause an increase in GDF15 (Altena *et al.*, 2015; Hsu *et al.*, 2017; Coll *et al.*, 2019).

The only non-pathophysiological situations when GDF15 is secreted in large amount is during pregnancy, when it is released by the placenta (Hromas *et al.*, 1997), and heavy exercise (Laurens *et al.*, 2020). The functional role of GDF15 during pregnancy at this time is unknown, though excessive secretion correlates with the presentation of morning sickness and *hyperemesis gravidarum* (Petry *et al.*, 2018; Fejzo *et al.*, 2019).

There is strong evidence that both cancer and cancer therapy can cause increases in GDF15. During cancer, GDF15 can be produced and released from the tumour and the tumour microenvironment (Bauskin *et al.*, 2005; Huh *et al.*, 2010; Bruzzese *et al.*, 2014). It is also possible that GDF15 is released from other affected tissues e.g., adipose and muscle, or tissues particularly affected by chemotherapy treatment. In fact, since the initiation of this research, evidence has emerged that *Gdf15* is increased in the liver during treatment with the chemotherapy, cisplatin (Patel *et al.*, 2019). Cancer therapies, by their nature, also cause cell damage and therefore the release of inflammatory signals (Elsea, Kneiss and Wood, 2015; Wong *et al.*, 2018; Loman *et al.*, 2019; Grant *et al.*, 2021). Several chemotherapy drugs, including

cisplatin and camptothecin have now been proven to cause increases in circulating GDF15 (Hsu *et al.*, 2017; Breen *et al.*, 2020; Worth *et al.*, 2020; Lu *et al.*, 2022).

Though GDF15 is present and increased during different disease states, it is not generally clear what role it plays during disease. In several cases, increased GDF15 can be a positive or a negative prognostic marker (Unsicker *et al.*, 2013, Emmerson, 2018). The best example of this is during cancer.

There have been many studies investigating the roles of GDF15 during cancer, but despite this, the actions of GDF15 during cancer are varied and sometimes opposing. In some cases, increased GDF15 can increase survival (Husaini *et al.*, 2015; Ratnam *et al.*, 2017; Lu *et al.*, 2018) and sensitise cancer cells to non-steroidal anti-inflammatory drugs (Baek *et al.*, 2000; Martinez *et al.*, 2006; Lincová *et al.*, 2009). However, GDF15 can also increase metastasis and invasion (Senapati *et al.*, 2010; Griner, *et al.*, 2013; Aw Yong *et al.*, 2014; Siddiqui *et al.*, 2022), increase neo-angiogenesis (Huh *et al.*, 2010; Song, *et al.*, 2012), and protect slower dividing cancer cells from chemotherapy drugs, promoting cancer relapse (Prunier *et al.*, 2018; Bellio *et al.*, 2022), with increased levels being associated with morbidity and mortality (Lerner *et al.*, 2015). Like other TGFβs, which can inhibit or stimulate the proliferation of cells (Prunier *et al.*, 2018), GDF15 increase has been linked to both inhibitory and proliferative effects on the growth of tumours (Emmerson *et al.*, 2018). The role that GDF15 plays in the growth and progression of tumours seems to depend on the type and stage of cancer, with positive effects being seen in less severe cancers.

Not in contention is the fact that increased GDF15 causes anorexia and weight loss. When GDF15 is increased in rodents, monkeys, or humans, whether by injection (Emmerson *et al.*, 2017; Hsu *et al.*, 2017; Yang *et al.*, 2017; Mullican *et al.*, 2017), genetic over expression (Macia *et al.*, 2012), or tumour expression (Johnen *et al.*, 2007; Chrysovergis *et al.*, 2014), food intake is decreased and consequently body weight is reduced.

A proportion of weight loss in response to GDF15 is due to reduced food intake (Johnen *et al.*, 2007; Emmerson *et al.*, 2017; Hsu *et al.*, 2017; Yang *et al.*, 2017; Mullican *et al.*, 2017; Xiong *et al.*, 2017; Luan *et al.*, 2019; Cimino *et al.*, 2021) as pair-

fed obese mice treated with GDF15 or vehicle lose comparable amounts of weight (Tsai *et al.*, 2016; Yang *et al.*, 2017; Mullican *et al.*, 2017). In mice which are not obese, GDF15 can impact body weight and composition by decreasing the rate of gastric emptying, (Xiong *et al.*, 2017), increasing lipolysis in white adipose tissue (Chung *et al.*, 2017; Laurens *et al.*, 2020; Suriben *et al.*, 2020), and causing the browning of white adipose, a key function in thermogenesis (Tsai *et al.*, 2018; Ost *et al.*, 2020), and reducing muscle mass (Johnen *et al.*, 2007; Breen *et al.*, 2020; Suriben *et al.*, 2020).

Though GDF15 causes decreases in brown adipose mass (Ost *et al.*, 2020; Suriben *et al.*, 2020), evidence that GDF15 alters energy expenditure is conflicting. Whilst some groups see an increase in energy expenditure/increased metabolic rate (Johnen *et al.*, 2007; Tsai *et al.*, 2013; Chrysovergis *et al.*, 2014; Lerner, Tao, *et al.*, 2016; Yang *et al.*, 2017; Tsai *et al.*, 2018; Tran *et al.*, 2018), others see no change (Macia *et al.*, 2012). Results seem to be dependent on whether the animal being treated with GDF15 is obese or not (Yang *et al.*, 2017; Tsai *et al.*, 2018). GDF15 may affect energy balance by increasing anxiety behaviours and altering locomotor activity (Low *et al.*, 2017).

Weight loss with GDF15 is accompanied by increased insulin sensitivity and improved glucose profile in diet induced obese mice (Yang *et al.*, 2017; Mullican *et al.*, 2017; Xiong *et al.*, 2017; Tran *et al.*, 2018). This may be due to effects of GDF15 on organs, such as the liver and pancreas, or is more likely explained by the loss of fat mass in obese rodents. As GDF15 release is not affected by time of day or mealtimes (Tsai *et al.*, 2015; Patel *et al.*, 2019), it is unlikely to be involved in the physiological control of energy balance on a day-to-day basis. However, GDF15 knock-out (KO) mice become obese to a greater extent than wild-type (WT) littermates (Mullican *et al.*, 2017), so GDF15 may act as a last line defence against obesity.

GDF15 also has less beneficial effects on control of energy balance. There is now evidence, from work in this thesis and by other groups, that GDF15 is aversive and causes anorexia by triggering nausea and emesis, and visceral malaise in rodents and lesser primates (Borner, Shaulson, *et al.*, 2020; Borner, Wald, *et al.*, 2020; Worth *et*

al., 2020; Sabatini *et al.*, 2021). This is supported by several human studies which find that severity of morning sickness and *hyperemesis gravidarum* are linked to levels of GDF15 during pregnancy (Fejzo *et al.*, 2018, 2019; Petry *et al.*, 2018), and the finding that GDF15 causes activation of aversive anorectic central signalling pathways (Hsu *et al.*, 2017; Worth *et al.*, 2020). Anorexia caused by this aversion and nausea leads not just to weight loss, but in mice with spontaneous or implanted tumours, excessive GDF15 can also lead to cachexia (Tsai *et al.*, 2012; Lerner *et al.*, 2016; Jones *et al.*, 2018; Suriben *et al.*, 2020; Albuquerque *et al.*, 2022). This may hold true for human patients as well as rodent models, as higher levels of GDF15 in cancer patients correlates with cachexia (Lerner *et al.*, 2015; Jones *et al.*, 2018; Ahmed *et al.*, 2021).

As GDF15 is increased by cancer and cancer therapy, and causes anorexia, weight loss, and cachexia in animal models, the GDF15 signalling pathway may be a good target to combat cancer and chemotherapy-induced ACS. To successfully manipulate GDF15 signalling, we must find out more about it.

1.8 GFRAL

Though GDF15 was discovered in 1999, it was more than 15 years before its cognate receptor was discovered. Johnen *et al*. (2007) initially proposed that hypothalamic TGFβ II receptors may play a role in signalling GDF15-induced anorexia and weight loss. However, it has since been shown that GDF15 does not act directly on these receptors. In 2017, four groups from different pharmaceutical companies published simultaneously in *Nature* and *Nature Medicine,* data showing that GDNF alpha-like receptor (GFRAL) is the cognate receptor for GDF15 (Emmerson *et al.*, 2017; Hsu *et al.*, 2017; Yang *et al.*, 2017; Mullican *et al.*, 2017).

GFRAL is a tyrosine kinase receptor and is a divergent member of the GDNF family of receptors. When activated, GFRAL dimerises with co-receptor RET and forms a receptor complex (Yang *et al.*, 2017; Mullican *et al.*, 2017). RET is necessary for GFRAL to function (Yang *et al.*, 2017; Mullican *et al.*, 2017). The four original papers each showed that GDF15 acts exclusively on the GFRAL receptor, and that GFRAL is likewise only activated by GDF15 (Emmerson *et al.*, 2017; Hsu *et al.*, 2017; Yang *et*

al., 2017; Mullican *et al.*, 2017). Although Xiong *et al.* (2017) found that an adapted, long-lasting form of GDF15 bound in the colon of healthy mice, these four groups each showed that GFRAL receptors are expressed exclusively in the brainstem. Despite its location in the brainstem, GFRAL neuronal activation is not reliant on vagal input (Borner *et al.*, 2017).

Since the discovery of GFRAL, there has been a great deal of interest in utilising the GDF15/GFRAL signalling network for therapeutic purposes, either to treat obesity and metabolic disease, or to combat anorexia and weight loss during disease. Several groups have now produced and successfully used antibodies against GDF15 or GFRAL to combat anorexia and weight loss during disease and therapy in murine models, including cancer (Joshi *et al.*, 2011; Wang *et al.*, 2014; Breen *et al.*, 2020; Ding *et al.*, 2020; Suriben *et al.*, 2020; Cimino *et al.*, 2021) and metformin therapy (Coll *et al.*, 2019).

To use the GDF15/GFRAL signalling system appropriately and effectively to combat cancer- and chemotherapy-induced anorexia and weight loss, more knowledge is required about GFRAL, its signalling network, and how GDF15/GFRAL signalling causes anorexia, weight loss, and cachexia. Thus far, only a small amount of research has been conducted to identify GFRAL neurons and their signalling pathways.

In 2017, Yang *et al.* showed that some GFRAL neurons express the catecholamine synthetic enzyme, tyrosine hydroxylase (TH), which was later confirmed by the Luckman group (Worth *et al.*, 2020), data for which is presented in chapter 4. GFRAL neurons have also been found to express the glucagon-like peptide 1 receptor (GLP-1R) (Frikke-Schmidt *et al.*, 2019) and neuropeptide FF (NPFF) (Zhang *et al.*, 2022). A population of TH^{DVC} neurons have a known role in control of energy balance as a part of a satiety signalling pathway (Dodd *et al.*, 2014). GFRAL neurons may therefore utilise satiety pathways to cause anorexia. $NPFF^{DVC}$ neurons seem to have a role in signalling glucose homeostasis, and may therefore be involved in the GDF15/GFRAL effect on glucose control (Zhang *et al.*, 2022).

In mice, GLP-1 is used centrally as a neuropeptide to signal anorexia via both reward/satiety pathways (Holt *et al.*, 2019; Brierley *et al.*, 2021) and aversive

pathways (Williams *et al.*, 2018; Holt *et al.*, 2019). Whilst GFRAL neurons activation is aversive (Borner, Shaulson, *et al.*, 2020; Borner, Wald, *et al.*, 2020; Worth *et al.*, 2020; Sabatini *et al.*, 2021), and there is precedent for aversive anorectic signalling to be a composite of aversive and rewarding signals (Roman, *et al.*, 2017), the anorectic actions of GLP-1 on GLP-1R neurons appears to be distinct from the actions of GDF15 on GFRAL neurons (Frikke-Schmidt *et al.*, 2019).

As fewer than half of GFRAL neurons express TH, and the actions of GDF15 are separate from GLP-1, there is still work needed to elucidate the identity of GFRAL^{DVC} neurons and find out which transmitters or peptides they might be using to induce anorexia and weight loss in response to activation by GDF15.

Likewise, only a little is known about the GFRAL signalling network outside of the DVC. Hsu *et al.* (2017) showed that GDF15 activates GFRAL^{DVC} neurons, neurons expressing CGRP in the PBN, and neurons in the CeA. Though they did not investigate the connections between these areas, GFRAL neurons could be utilising this aversive anorectic pathway as described by Carter *et al.* (2014), Cai *et al.* (2014), and Alhadeff *et al.* (2015).

The limited expression of GFRAL, its fidelity to GDF15, the anorectic/weight loss properties of GDF15/GFRAL signalling, and the increases of GDF15 in diseases including cancer and chemotherapy make the GDF15/GFRAL signalling system an interesting target to explore for treatment of cancer and chemotherapy ACS. Different central regions and pathways contribute to anorexia and weight loss in different ways. Finding out which pathways GFRAL neurons use to signal will aid the understanding of how GFRAL neuron signalling causes anorexia, weight loss, and cachexia. This may then provide options in the future to target specific parts of the signalling pathway to reduce anorexia, weight loss, and nausea/emesis during disease, without impacting on any beneficial effects GFRAL signalling may be having on tumour growth or survival. Therefore, GFRAL signalling networks will be explored in this thesis, as well as the viability of targeting this system to combat cancer and chemotherapy induced ACS.

1.9 Aims

The aims of my PhD relate to the six experimental chapters of my thesis, each of which will contain specific objectives (see Chapters 3-8). Thus, the aims of this thesis are as follows:

1. To understand the mechanism by which GDF15 interacts with the brain to reduce food intake (Chapter 3)
2. To describe the phenotype and function of GFRAL-expressing neurons (Chapter 4)
3. To discover central signalling pathways utilised by GFRAL neurons (Chapter 5)
4. To define GDF15 secretion in mouse models of cancer (Chapter 6)
5. To survey cancer treatments which cause the secretion of GDF15 (Chapter 7)
6. To prevent GFRAL signalling during chemotherapy (Chapter 8)

2 Methods

2.1 Reagents and antibodies

2.1.1 General

PB
0.1M phosphate buffer was produced by dissolving 6.24 g/l NaH2PO4.2H2O (Sigma Aldrich, UK) and 28.48 g/l Na2HPO4.2H2O (Sigma Aldrich, UK) in distilled water.

PBT
0.2% Triton X-100 (Sigma Aldrich, UK) in 0.1M PB.

PBS
Phosphate buffered saline (PBS) was made using PBS tablets (Sigma), according to the manufacturer's instructions.

2.1.2 Drugs and viruses

GDF15
Lyophilised recombinant human GDF15 (R&D Systems, Abingdon, UK. Cat#. 9279-GD-050) dissolved in 100 µl of 15 mM HCl. GDF15 solution was neutralised by adding 80 µl 7.5 mM NaOH. GDF15 was then diluted to the correct concentration using sterile saline. GDF15 was injected at 4 nmol/kg, in a volume of 4 ml/kg, subcutaneously unless stated otherwise.

Devazepide
Powdered devazepide (Tocris, Abingdon, UK) was reconstituted in pure DMSO, then diluted to a working concentration of 1 mg/4 ml in 40% DMSO using saline. Devazepide was administered IP at 1 mg/kg in a volume of 4 ml/kg. Control animals for the devazepide study were treated IP with 4 ml/kg saline containing 40% DMSO.

GFRAL mAb	GFRAL monoclonal antibody (Emmerson *et al.*, 2017) was reconstituted at 2.28 mg/ml in sterile PBS and was injected at 10 mg/kg intraperitoneally.
Fluorogold	Hydroxystilbamidine. 4% in sterile water (Invitrogen, Paisley, UK. H22845)
CNO	Clozapine-N-oxide (CNO) was reconstituted in sterile saline and injected IP at a volume of 4 ml/kg to give a dose of 3 mg/kg.

2.1.3 Genotyping

Lysis buffer	25 mM NaOH (Sigma Aldrich, UK) and 0.2 mM EDTA (Sigma Aldrich, UK) in DNAse/RNAse-free water (Life technologies Ltd, Paisley, UK)
Neutralising buffer	40 mM Tris HCl (Sigma Aldrich, UK) dissolved in DNAse/RNAse-free water
TAE	40mM Tris HCl (Sigma Aldrich, UK), 20mM acetic acid (Sigma Aldrich, UK) and 1mM EDTA (Sigma Aldrich, UK) in distilled water.

2.1.4 Histology

Heparinised saline	20 kU/l heparin (Sigma Aldrich, UK). 0.9% NaCl (w/v) in distilled water.
30% sucrose solution	Sucrose (Sigma Aldrich, UK) dissolved in 0.1M PB.
Cryoprotectant	30% each of ethylene glycol and glycerol in 0.05M PB.

Table 1. Antibodies for immunohistochemistry

Primary antibodies	Concentration	Company	Catalogue #
Rabbit anti-cFos polyclonal	1:1000	Abcam	ab190289
Rabbit anti-cFos polyclonal	1:1000	Santa Cruz	SC52
Goat anti-DsRed polyconal	1:500	Santa Cruz	33353
Mouse anti-PKCδ monoclonal	1:500	BD Biosciences	610398
Chicken anti-GFP polyclonal	1:2000	Abcam	ab13970
Sheep anti-GFRAL polyclonal	1:200	ThermoFisher Scientific	PA5-47769
Rabbit anti-TH polyclonal	1:2000	Abcam	ab112
Sheep anti-TH polyclonal	1:1000	Millipore	ab1542
Secondary antibodies	**Concentration**	**Company**	**Catalogue #**
Donkey anti-rabbit[biotin]	1:500	Jackson Immuno Research (JIR)	711-065-152
Donkey anti-mouseAlexa [594]	1:1000	JIR	715-585-150
Donkey anti-goatAlexa [594]	1:1000	JIR	705-585-147
Donkey anti-SheepAlexa [594]	1:1000	Molecular Probes	A11016
Donkey anti-chickenAlexa [488]	1:1000	JIR	703-545-155
Donkey anti-sheepAlexa [350]	1:1000	Molecular Probes	A21097
Streptavadin[594]	1:1000	JIR	016-580-084
Streptavadin[488]	1:1000	JIR	016-540-084

2.2 Animals

In vivo experiments described in this thesis were carried out at one of three locations: the University of Manchester (Manchester, UK), Alderley Park (Macclesfield, UK), and Eli Lily (Indianapolis, IN, USA). All experiments were carried out under the relevant ethical guidelines as laid out at each institution. UK experiments were carried out in accordance with Home Office regulations.

Non-transgenic "wild type" C57Bl/6 mice were obtained from Envigo (Huntingdon, UK) or Charles River (Manston, UK). All transgenic animals were bred in house on a C57Bl/6 background, with the exception of *Scl26a*-Cre mice, which were on a mixed C57BL/6;FVB/N;129S6 background.

Mice were kept on a 12 hr light/12 hr dark cycle (lights on 07:00-19:00 BST) in rooms maintained at a temperature of $21^{\circ}C$ ±2 and 40-60% humidity. Unless stated otherwise, mice were housed in groups of no more than 6 per cage, with *ad libitum* access to standard mouse chow (Special Diet Services, UK, or Envigo, UK) and water. Mice were not changed between diets whilst on study. In cases where mice were single housed for the purpose of a study, they were allowed a minimum of 1 week to acclimatise to new housing before any experimentation was carried out.

All mice were acclimatised to handling for at least 1 week prior to study. During this time, baseline food intake and body weight measurements were taken daily. All IP and SC injections were administered using 29G insulin syringes, which had the smallest possible gauge needle, to minimise pain from injection.

Table 2. Transgenic strains of mouse

Strain	Origin
Calca-Cre	Kindly gifted by Prof. Richard Palmiter (Carter *et al.*, 2013) PMID:24121436
Cck-Cre	Jackson Laboratories, stock#: 012706
Crh-Cre	Jackson Laboratories, stock#: 012704
Gcg-Cre	(Parker *et al.*, 2012) PMID:22638549
Gfral-Cre	Luckman group (unpublished)
Pdyn-Cre	Jackson Laboratories, stock#: 027958
Penk-Cre	Jackson Laboratories, stock#: 025112
Prlh-Cre	(Dodd *et al.*, 2014) PMID:25176149
Slc17a6-Cre	Jackson Laboratories, stock#: 016963
1TB-hM3Dq^{mCherry}	D'Agostino group (unpublished)
Ai32 (ChR2-eYFP)	Jackson Laboratories, stock#: 012569
Rosa26-loxSTOPlox-eYFP	Jackson Laboratories, stock#: 006148
GFRAL KO	Taconic, stock#: TF3754

2.2.1 Fluorescent reporter strains

Fluorescent reporter strains were generated by crossing 'Cre' lines with either a Rosa26-loxSTOPlox-eYFP mouse, which caused the expression of a yellow fluorescent marker in cell bodies, or an Ai32 mouse, which induced the expression of ChR2-eYFP on the membranes of neuronal cell bodies and their processes.

2.2.2 Genotyping

All heterozygous transgenic animals were genotyped to ensure expression of the correct genes. Ai32 (ChR2-eYFP), *Calca*-Cre, *Slc17a6*-Cre, and Rosa26-loxSTOPlox-eYFP animals were maintained as homozygous colonies. All homozygous breeders were checked for the correct genotype before being crossed. After this, any F1 offspring resulting from homozygous crosses were not genotyped for these traits.

To genotype heterozygous transgenic animals, ear punches were collected into Eppendorf tubes. 75 µl alkaline lysis buffer was added to each tube and samples were heated at 95 ^{O}C on a Grant QBD4 heating plate (Grant Instruments, Cambridge, UK) for 45 min. Samples were then removed from the heating plate, placed on ice, and an equal volume of acidic neutralising buffer was added. Samples were briefly vortexed to ensure tissue lysis and thorough mixing. 2.5 µl of each DNA sample was used per PCR reaction.

Genotyping PCR primers were obtained from Sigma (UK). PCR reactions were made using GoTaq Hot Start Polymerase Kit (Promega, Southampton, UK), according to the manufacturer's instructions and run on a PCR thermocycler. Specific primer sequences and thermal cycling protocols are stated below, in Table 3. All 'Cre' lines were genotyped using a generic 'Cre' protocol, except *Gcg*-Cre mice, which used an 'iCre' protocol.

Gel electrophoresis was used to separate DNA fragments in the PCR product. PCR product was run on a gel comprising of 1.5% agarose (Bioline, London, UK) and 0.005% SafeStain (Invitrogen, UK) in TAE solution. Gels were visualised on an Alpha Innotech Corporation open-source UV transilluminatior and imaged using a digital camera.

Table 3. Primer sequences used for genotyping of transgenic strains

PCR	PCR cycling protocol	Primer sequences
General 'Cre'	95 °C for 2 min, (95 °C for 30 s, 62 °C for 1 min, 72 °C for 1 min) x32 cycles, then 72 °C for 5 min, and hold at 4 °C indefinitely.	Cre target (F): GCC CTG GAA GGG ATT TTT GAA GCA Cre target (R): ATG GCT AAT CGC CAT CTT CCA GCA Cre control (F): GGT CAG CCT AAT TAG CTC TGT Cre control (R): GAT CTC CAG CTC CTC CTC TGT C
'1TB-hM3Dq'	94 °C for 30 s, (94 °C for 30 s, 56 °C for 30 s, 68 °C for 30 s) x35 cycles, then 68 °C for 5 min, and hold at 4 °C indefinitely.	1TB-lox-F2: CATCAAGCTGATCCGGAACCC 1TB-FRT-R1: GGGTACATCACGTGCTAGCTTT
'iCre'	95 °C for 2 min, (95 °C for 1 min, 57 °C for 1min, 72 °C for 1 min) x 35 cycles, then 72 °C for 5 min, and 4 °C indefinitely.	PPG Cre 002: GAC AGG CAG GCC TTC TCT GAA PPG Cre 003: CTT CTC CAC ACC AGC TGT GGA β catenin (Control F): AAG GTA GAG TGA TGA AAG TTG TT β catenin (Control R): CAC CAT GTC CTC TGT CTA TTC
'GFRAL KO'	95 °C for 15 min, (94 °C for 45 s, 60 °C for 1 min, 72 °C for 1 min) x35 cycles, then 72 °C for 5 min, and hold at 4 °C indefinitely.	GFRAL-15 (F): CAACAAATGAACACATATTGATTGAGTAGG GFRAL-16 (R): GTATGGATGACCTCCACTGTACAG NEO3B (Control R): GTGTGGCGGACCGCTATCAGGAC

2.3 Surgery

2.3.1 Preparation and recovery

Mice were anaesthetised by one of two methods. For all surgeries, barring those targeting the DVC, anaesthesia was induced using 3% isoflurane in oxygen. Once mice were anaesthetised, the fur was shaved, and skin swabbed with iodine at the incision site. The mouse was placed in a stereotaxic frame (Kopf Instruments, Tujunga, CA, USA). For surgeries using isoflurane, anaesthetic was decreased to 2-2.5% isoflurane in oxygen for maintenance during surgery.
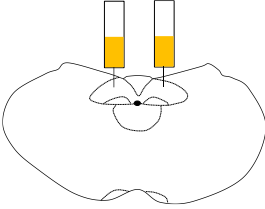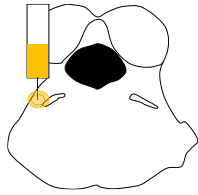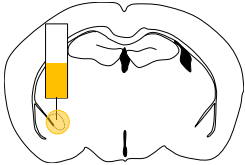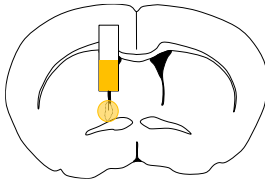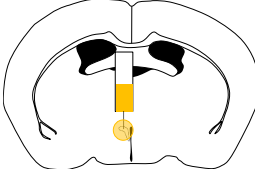
All animals were administered a SC injection of 1 ml of sterile saline and a SC injection of analgesic at the start of surgery. Analgesia consisted of 0.1 mg/kg buprenorphine. At the end of surgery, mice were placed in a warm cabinet maintained at 37 °C and returned to normal housing once they were fully mobile. All animals were allowed a minimum of 2 weeks recovery before participating in further studies. This also allowed time for expression of viral products.

2.3.2 Intracranial injections

Intracranial injections were targeted at specific brain regions, co-ordinates for which were estimated using a mouse stereotaxic brain atlas (Paxinos and Franklin, 2001). Co-ordinates can be found in Table 4, below. A small incision was made in the skin and small hole(s) were drilled above the area(s) of interest as estimated by distance from lambda using a Vernier scale. Viruses or tracers were injected into the brain using a glass pipette attached to a Drummond nanoinjector (Drummond Scientific Company, Broomall, PA, USA). An average of three injections were made at each injection site, 2 min apart, and moving dorsally by 0.1 mm between each injection. This was to reduce the chance of damaging brain tissue which can be caused by injecting higher volumes. This also reduced the amount the injected substance spread.

An additional modified surgical method was used to deliver viruses to the DVC (D'Agostino *et al.*, 2016, 2018). This is described in detail in chapter 4.

Table 4. Target regions for stereotaxic surgery

Region	Schematic	Co-ordinates
DVC (AP/NTS)		From Obex A/P: -0.2 mm M/L: 0 and ±0.2 mm D/V: -0.2 mm
lPBN		From Bregma A/P: -4.9 mm M/L: -1.4 mm D/V: -3.8 mm
CeA		From Bregma A/P: -1.4mm M/L: -2.7mm D/V: -5.1mm
ovBNST		From Bregma A/P: +0.3 mm M/L: -1.0 mm D/V: -4.5
PVH		From Bregma A/P: - 0.7 mm M/L: -0.3 mm D/V: -5.5 mm

2.4   Assignment of animals to studies

For all studies, animals were randomly assigned to groups using the Microsoft Excel (RAND) function. For studies investigating body weight and food intake, animals were pseudo-randomised to ensure similar average body weights and ratio of male:female within groups. This involved an initial sort of animals into groups using the (RAND) function, followed by manual adjustments.

Where possible, blinding was further ensured during analysis by not labelling each animal with group until it was necessary (for example during cell counts, see section 2.9.5).

2.5   Feeding experiments

Unless stated otherwise, mice were singly housed to permit measurement of individual food intake. If chow had been removed before the study, it was returned immediately after injection(s) were administered. Chow was weighed in the hopper, on digital scales (OHaus, Nänikon, Switzerland) accurate to 10 mg.

2.5.1 Night-time feeding

Mice were deprived of food for 2-3 hr before lights out. Experimental substances were administered within one hour before lights out. Food was weighed in the hopper before injection (0 hr), and then at 1 hr, 2 hr, 4 hr, and 24hr after injection(s).

2.5.2 Fasted re-feeding

Mice were deprived of food at lights out on the day before the study. The next morning (approx. 16 hr later), test substances were administered, and chow was immediately returned in a pre-weighed food hopper. The food hopper was weighed as described above at 1 hr, 2 hr, 4 hr, and 24 hr after experimental treatment.

2.5.3 Repeated dose of chemotherapy food intake measurements

These experiments were run over the space of a week for some chemotherapy treatments. On the morning of day 0, the first dose of chemotherapy drug was

administered IP. Food weight and body weight were measured at this time and then at the same time daily for the remainder of the study. Further doses of chemotherapy were administered at the time of food and body weight measures on days 3 and 5.

Mice were anaesthetised and culled via cardiac puncture on day 6, 24 hr after the final dose of chemotherapy. Food and body weight were measured immediately before cull.

2.6 Measuring body weight and composition

Mice were weighed using digital scales (OHaus), accurate to 10 mg. Body composition was measured by quantitative magnetic resonance using an EchoMRI-900 scanner (EchoMRI LLC, Houston, USA). The scanner was first calibrated using canola oil. Mice were then scanned with a gain of 3 and no water setting. Fat mass and lean mass were recorded in grams.

2.7 Blood collection and preservation of tissues

2.7.1 Blood sampling and plasma preparation

Heparinised tubes were prepared by coating clean Eppendorf tubes with pipetting 200KU/l heparin (Sigma Aldrich, cat. H5515), reconstituted in distilled water. Coated tubes were kept at 4°C until use.

Non-terminal bleeds were performed via tail tip puncture. Mice were placed in a hot box at 37°C for 5 min before blood samples were collected. Mice were then placed in a restraint tube and a sterile needle was used to puncture the tail tip. Gentle pressure was applied to the tail and blood was collected using a heparinised pipette tip to quickly transfer into a heparinised tube.

Terminal bleeds were performed under heavy isoflurane anaesthesia. Mice were anaesthetised with 3-4% isoflurane in oxygen at a rate of 1 l/s. Mice were either decapitated and trunk blood was collected, or cardiac puncture was performed.

All blood was collected into heparinised tubes, gently inverted several times to ensure thorough mixing of blood with heparin and placed on ice for a maximum of 2

hr. Blood was then centrifuged at 1000 XG for 20 min at 4°C and resulting plasma was stored at -80°C.

2.7.2 Preservation of tissue

Brains and lungs were dissected and post-fixed for 24 hr in 10% formalin (Merck, UK) at 4 °C. At this point, tissue was transferred into a 30% sucrose solution, and kept at 4 °C until equilibrated. Preserved tissue was rapidly frozen on dry ice and stored at -80 °C.

2.8 GDF15 ELISA

Initially, GDF15 in plasma was detected using a pre-assembled mouse/rat-specific GDF15 Quantikine enzyme-linked immunosorbent assay (ELISA) kit (R&D Systems, UK. Cat. MGD150) following manufacturer's instructions. GDF15 standards, samples or control samples were plated in duplicate and diluted 1:20 with assay diluent in each well. The plate was incubated at room temperature for 2 hr on an orbital plate shaker set at approximately 80 rpm, then thoroughly aspirated. Plates were washed four times with the wash buffer provided. Plates were aspirated and dried between each wash. Mouse/rat GDF15 conjugate was added to each well and the plate incubated for a further 2 hr at room temperature on the plate shaker. The plate was then washed four times with wash buffer as before, then incubated in substrate solution for 30 min at room temperature in the dark. Acidic stop solution was quickly added and the optical density of each well measured within 30 min of the addition of stop solution. Plates were read using a BioTek Synergy HT plate reader and BioTek Gen5 microplate reader and imager software at 450 nm with a correction at 630 nm.

To coat plates in house, later studies used an R&D Systems mouse/rat GDF15 DuoSet ELISA kit (cat. DY6385). GDF15 capture antibody was reconstituted at 800 ng/ml in PBS. Clean 96-well plates, provided in the relevant ancillary kit (R&D Systems, UK. Cat. DY008) were coated by adding 100 µl GDF15 capture antibody to each well and incubating overnight at room temperature. The GDF15 ELISA was then performed as described above.

The eight-point standard curve was established by reducing the data with a four-parameter logistic (4-PL) curve-fit using GraphPad Prism 8 software (GraphPad Prism, California, USA). This then allowed duplicate readings to be interpolated in the same programme. Averages of duplicate readings were used for statistical analysis.

2.9   Histology

2.9.1 Transcardial perfusion

Mice were heavily anaesthetised with 5% isoflurane in oxygen, until the pedal pinch withdrawal reflex was lost, and then transcardially perfused with heparinised saline then 10% formalin (Merck, London, UK) via a 23G needle clamped into the apex of the left ventricle of the heart. Following decapitation, the brain was removed and post-fixed overnight in 10 % formalin at 4 °C. Brains were then dehydrated in 30 % sucrose solution at 4 °C. Brains were rapidly frozen on dry ice and stored at -80 °C.

2.9.2 Sectioning tissue

Before sectioning, brains were blocked by making a coronal cut rostral to the cerebellum. Frozen, blocked, brains were fixed to the stage of a freezing sledge microtome (Bright 8000, Bright Instruments, Luton, UK) using distilled water. 30 μm sections were cut and placed in PB. For longer term storage, brains were transferred into cryoprotectant and stored at -20 °C. For caudal blocks, containing the DVC and PBN, sections were cut into 3 sets. For rostral blocks, containing PVH, CeA, and ovBNST, sections were cut into 4 sets.

2.9.3 Fluorescence immunohistochemistry

Sections were washed three times for 5 min in PBT, followed by blocking solution (5% normal donkey (NDS) serum in PBT) for 1 hr at room temperature, then incubated overnight with antibodies in 1% NDS in PB.

Sections were then washed three times for 5 min in PBT, then 2 hours with secondary antibodies diluted in 5% NDS in PBT. For experiments using biotinylated secondary antibodies, sections were washed three times in PB for 5 min then incubated for an hour in streptavidin conjugated to a fluorescent Alexafluor (see Table 1). Then, for all

protocols, sections were washed twice for 5 min in PB, three times for 5 min in distilled water, and mounted on non-adhesion slides in distilled water.

Slides were air-dried overnight and Prolong Gold anti-fade mountant (ThermoFisher, cat. P36930) was used to attach coverslips.

2.9.3.1   Validation of GFRAL primary antibody

As the GFRAL primary antibody (Thermofisher Scientific, cat. PA5-47769) was new to the group at the beginning of this project, validation was required. Initial experiments were performed with brain sections containing DVC which were exposed to only the primary GFRAL antibody, and sections without the DVC stained with both primary and secondary antibodies (data not shown). These experiments showed no fluorescence. Furthermore, sections of brain tissue containing DVC from *Gfral*^{-/-} mice was stained using the GFRAL antibody. In this tissue, there was also no evident fluorescent signal. An example of this tissue can be seen in section 8.4.1.2, Figure 8.2.

2.9.4 Microscopy

Fluorescently stained brain sections were visualised using a Zeiss snapshot Axiomanager.D2 upright microscope (Zeiss, Oberkochen, Germany) and images were captured using a Coolsnap HQ1 camera (Photometics, AZ) and Micromanager software v1.4.23 (https://imagej.net/Micro-Manager). A Texas Red Fs45 filter set was used to capture red Alexafluor[594] staining, a FITC Fs38 filter set was used to capture green Alexafluor[488] staining, and blue staining (fluorogold and Alexafluor[395]) was captured using a DAPI Fs49 filter set. Images were captured using a 5x or 10x objective lens.

2.9.5 Cell counts

Cell counts were performed using Fiji software (Schindelin *et al.*, 2012). DVC images were stitched together using the 'pairwise stitching' macro and a 'linear blending' method before cell counts were performed. Counts were performed using the 'cell

counter' macro. For counts on images which contained more than one colour channel, each channel was counted separately. For quantification of co-localisation of two or more channels, colour images were overlaid, and all markers were displayed to ensure fair counting.

Other brain areas (PBN, CeA, ovBNST, PVH), which were encompassed in a single image, were not stitched, but were processed and counted in the same way.

To ensure blinding of the user during cell counts, animals only labelled with their treatment groups during the in vivo portion of the study, and then again after cell counts had been completed.

2.10 Statistics

All raw data was entered manually into Microsoft Excel software. Basic calculations were performed in Excel (e.g., calculation of food intake, % body weight change, and average cell count/section). For all experiments, outliers were manually identified in Excel as $< \mu - 2$ standard deviations (SD) or $> \mu + 2SD$ and were excluded from the data set. Once data had been processed, it was analysed using GraphPad Prism software. Data was checked for normal distribution using a Shapiro-Wilk test and subsequent analyses were performed as described below:

For experiments which compared saline/vehicle vs. a single treatment group at a single time point (e.g., cell counts and certain ELISAs), data was analysed using an unpaired Student's t test or Mann-Whitney U test, as appropriate. For experiments which compared saline/vehicle vs. multiple treatment groups at a single time point (e.g., food intake over 24 hr following chemotherapy treatment in different genotypes of mice), data were analysed using a one-way ANOVA or non-parametric equivalent. This was then followed by a post hoc Sidak's multiple comparisons test.

Two-way ANOVA or non-parametric Kruskal-Wallis tests were performed to compare data collected across multiple time points, e.g. cumulative food intake and body weight change over the space of a week. This was followed by a post hoc Dunnett's or Sidak's multiple comparisons test.

Correlation analysis was performed to assess the connection between GDF15 concentration and food intake or body weight measurements. This was carried out using Pearson correlation analysis.

All data is plotted as mean, with error bars representing standard error of the mean (SEM). Significance is denoted on graphs as * $p < 0.05$, ** $p < 0.01$, *** $p < 0.001$.

3 The effects of exogenous GDF15

3.1 Introduction

GDF15 administration decreases food intake, causes weight loss, and improves insulin and glucose tolerance (Suriben *et al.*, 2020; Macia *et al.*, 2012; Emmerson *et al.*, 2017; Hsu *et al.*, 2017; Yang *et al.*, 2017; Mullican *et al.*, 2017; Tsai *et al.*, 2018; Day *et al.*, 2019; Worth *et al.*, 2020). Therefore, there is interest in GDF15 as a potential therapeutic target for obesity. However, GDF15 secretion is caused by cell stress and damage (Park *et al.*, 2012; Altena *et al.*, 2015; Patel *et al.*, 2019; Townsend *et al.*, 2021), which is present in such disease states as kidney disease, heart failure, arthritis and cancer (Bauskin *et al.*, 2010; Ho *et al.*, 2013; Unsicker *et al.*, 2013; Lerner *et al.*, 2015; Nair *et al.*, 2017; Johann *et al.*, 2021; Wang *et al.*, 2022), and not by meal times (Tsai *et al.*, 2015). This could indicate that GDF15 is not a regulator of normal energy balance.

In addition to weight loss and decreased food intake, GDF15 has been linked to nausea and emesis. This includes morning sickness, and its more severe form, *hyperemesis gravidarum* (Fejzo *et al.*, 2018; Petry *et al.*, 2018; Borner, Shaulson, *et al.*, 2020; Borner, Wald, *et al.*, 2020; Fejzo *et al.*, 2022). Increased GDF15 has also been linked to cachexia, a form of weight loss which can occur independently of food intake (Chrysovergis *et al.*, 2014; Suriben *et al.*, 2020) and encompasses loss of both fat and lean mass, in addition to inflammation (Fearon *et al.*, 2011). Understanding how GDF15 causes anorexia and weight loss is essential when deciding how and when to manipulate its actions in a therapeutic context. Thus far, there has been a lack of evidence of how GDF15 causes anorexia and weight loss.

Animals can decrease or stop feeding due to many reasons, including feeling full/satiated, pain, fear, nausea, or sickness (Aviello *et al.*, 2021; Cifuentes and Acosta, 2022). Valence is a term used in the field of psychology to describe the feeling a stimulus causes. Valence is positive if a feeling is good or pleasurable, such as satiety, or negative if the feeling is bad or unpleasant, for example, pain, sickness, or

nausea (Russell, 2003). Establishing the valency induced by GDF15 will be important if considering it as a therapeutic target. An early indicator that GDF15 might have negative valence came from Low et al. (2017), wherein GDF15 knock-out mice showed reduced anxiety behaviours compared with wild-type littermates (Low *et al.*, 2017). Following this study, further evidence, including work in this chapter, emerged that GDF15 signalling has a negative valence (Borner, Shaulson, *et al.*, 2020; Borner, Wald, *et al.*, 2020; Worth *et al.*, 2020). Though a signalling system may have negative valence, it is possible that it utilises additional pathways with varying effects (Roman *et al.*, 2017). It is, therefore, necessary to investigate the valence of GDF15 as well as its overall effects which may utilise different signalling pathways.

Feeding and feeding-related behaviours are controlled by a number of known central signalling pathways. Some of these are activated during the normal, physiological regulation of energy balance, some are specific to sickness and disease, and others may be activated by either. GDF15 may utilise one or several of these pathways to cause anorexia and weight loss.

Classically, the DVC and the hypothalamus, in particular the ARC and the PVH, have received the most attention when investigating the central control of feeding behaviour. These areas are not only involved in the maintenance of normal energy balance but are also involved in regulating feeding behaviour during sickness and disease (Cone *et al.*, 2001; Cimino *et al.*, 2021; Cifuentes and Acosta, 2022).

The DVC is comprised of three regions: the AP, NTS, and DMX. These areas respond locally to affect feeding behaviour and nutrient uptake as a part of circuits affecting gastric motility, emesis, gustation, and control of blood flow around the GIT (Browning and Travagli, 2016). The DVC also sends signals to, and receives descending signals from, higher cortical areas co-ordinating feelings of nausea, and satiety (Browning and Travagli, 2016). Therefore, this region is heavily involved in the control of food intake by co-ordinating both satiety and sickness.

Input to the DVC comes from the vagus relaying signals from the GIT, direct exposure of neurons to circulating factors via the AP, which is a circumventricular organ, and from other regions in the brain (Grill and Hayes, 2013; Sanger and Andrews, 2018).

In combination these areas affect nutrient uptake, firstly by influencing motivation to eat, then by controlling the rate at which food travels through the GIT and the circulation of blood around the GIT to transport the resulting substrates. In 2017, four groups published the finding that GDF15 acts exclusively on GFRAL receptors (Emmerson *et al.*, 2017; Hsu *et al.*, 2017; Yang *et al.*, 2017; Mullican *et al.*, 2017). These same groups found that GFRAL receptors are expressed exclusively in the DVC. This region is therefore the starting point in this chapter for investigations into how GDF15 causes anorexia and weight loss.

In the process of my investigations, in addition to the DVC and hypothalamus, other parts of the brain were found to be engaged by GDF15 signalling. These included the PBN, CeA, and ovBNST. The PBN and CeA are both known to play a critical roles in signalling pathways which affect satiety and sickness and therefore affect food intake (Carter *et al.*, 2013; Cai *et al.*, 2014; Alhadeff *et al.*, 2015; Zséli *et al.*, 2016; Chen *et al.*, 2018; Palmiter, 2018; Hardaway *et al.*, 2019). Though there has been less intensive investigation, the ovBNST has also been implicated in the control of feeding behaviour (Maracle *et al.*, 2019; Wang *et al.*, 2019).

Within these areas of the brain, specific populations of neurons are involved in the different aspects of feeding and energy balance. The DVC contains a highly heterogeneous population of neurons, many of which affect food intake via circuits which result in positive or negative valence (Browning and Travagli, 2016). Much is already known about neuronal types in the DVC which contribute to anorexia and weight loss. For example, a population of neurons in the NTS express prolactin-releasing peptide (PrRP). These neurons are activated by satiety-inducing signals such as feeding, ingestion of lipids, and systemic satiety hormones such as CCK (Dodd *et al.*, 2014). PrRP neurons in the DVC are a subpopulation of neurons which express TH (Dodd *et al.*, 2014), the rate limiting enzyme in the production of catecholamines. TH neurons are a part of several pathways affecting food intake and energy balance (Dodd *et al.*, 2014). On the other hand, another population of neurons in the caudal NTS express preproglucagon (PPG). These neurons are sensitive to stimuli which cause sickness and pain, such as LiCl and gastric stretch (Brierley *et al.*, 2021; Leon *et al.*, 2021).

A third population of neurons in the NTS and AP contain the neuropeptide, CCK. In addition to being a gut derived satiety hormone, CCK is produced and released by neurons in the DVC to decrease feeding via two separate pathways; one which aversion/negative valence (D'Agostino *et al.*, 2016; Roman *et al.*, 2017). Further examples of anorectic neuronal populations in the DVC are those containing pro-opiomelanocortin (POMC) (Fortin *et al.*, 2020), and those containing the vesicular glutamate transporter, VGLUT (Wu, Clark and Palmiter, 2012).

With the exception of the GFRAL[DVC] population (Yang *et al.*, 2017; Frikke-Schmidt *et al.*, 2019; Zhang *et al.*, 2021), little is known about the phenotype of neurons in the DVC which are activated by GDF15. It may be the case that GDF15 causes the activation of other, known, anorectic signalling networks. If this is the case, exploration of this knowledge could be informative of how GDF15 signalling influences feeding behaviour and may provide targets via which GDF15 signalling can be manipulated.

3.2   Aims and objectives

Hypothesis: GDF15 interacts with the brain, via known anorectic regions and cell populations, to induce anorexia and weight loss.

Aim: To understand the mechanism by which GDF15 interacts with the brain to reduce food intake.

1) What happens when circulating GDF15 is increased?
   - Establish a dose of GDF15 which causes anorexia in mice.
   - Discover the valency of exogenous GDF15 treatment by behavioural testing.
2) What central signalling pathways does exogenous GDF15 affect to cause anorexia?
   - Investigate whether GDF15 treatment activates neuronal types in the DVC which are known to affect food intake.
   - Explore which other areas of the brain are activated by an anorectic dose of GDF15.

3.3 Methods

3.3.1 Animals

Adult male C57BL6/J mice (Envigo, Hillcrest, UK) between the ages of 10 and 20 weeks were used for feeding studies and behavioural valence studies.

Male Sprague-Dawley rats (Envigo, Indianapolis, USA) at approximately 270 g at the start of the study were used in pica testing.

Pomc^{eGFP} mice were bred and housed by Dr Garron Dodd at the University Melbourne, Victoria, Australia. *Cck*-Cre, *Gcg*-Cre (Parker *et al.*, 2012), *Prlh*-Cre, or *Slc17a6*-Cre mouse lines were crossed with a Rosa26eYFP fluorescent reporter strain as described in 2.2.1 to generate fluorescent reporter lines. These animals were used in neuronal activation immunohistochemistry studies.

All animals were kept under standard conditions as described in General Methods 2.2 unless otherwise stated.

3.3.2 GDF15 treatment

GDF15 was administered SC to mice at 0 nmol/kg, 2nmol/kg, 4 nmol/kg, or 8 nmol/kg at a volume of 4 ml/kg. 0 mg/kg (VEH) groups were administered 4 ml/kg saline SC.

A night-time feeding study (2.4.1) and a fasted re-feeding study (2.4.2) were performed with these doses of GDF15 as described in General Methods.

3.3.3 Behavioural valence studies

3.3.3.1 Conditioned taste aversion

Male C57Bl6/J mice were given one week to acclimatise to single housing with two bottles containing water.

To condition mice, water was removed from cages overnight for 16 hr before SC injection VEH or 4 nmol/kg GDF15. Two bottles containing 30% sucrose in sterile water were returned to mice for 30 min immediately after injection. Bottles containing sucrose were weighed before and after the 30 min period. When bottles

containing sucrose solution were removed, mice were returned two bottles of water and allowed to recover for 24 hr.

After 24 hr, water was again removed overnight for 16 hr. On the next day, all mice were returned one bottle containing water and one containing 30% sucrose solution for 30 min. The side of the cage which the sucrose was placed was alternated within the group in order to avoid any placement bias. Sucrose and water bottles were weighed before and after the 30 min. % intake was measured for water and sucrose as the % of total weight of fluid consumed during the 30 min test period.

3.3.3.2   Conditioned place avoidance

To measure conditioned place avoidance, a two-chamber apparatus was used, in which a darker chamber, with rough black floor and black spotted walls, was connected to a lighter chamber, with smooth grey floor and grey striped walls, by a brightly lit corridor (Harvard Biosciences/Bio-chrom Ltd., Cambridge, UK). A digital camera was set above with a view of the whole apparatus and SMART software (Smart v3.0, Panlab, Harvard Biosciences/Biochrom Ltd.) was used to detect the mice and record time spent in each location.

A pre-test score was determined on day 1 by allowing mice free movement through both chambers and corridor for 30 min. Time spent in each area was recorded and the chamber in which mice spent most time was determined the preferred side. This was the darker side for all mice. On days 2 and 3, mice underwent training sessions in which they were injected SC with saline or 4 nmol/kg GDF15 in a volume of 4 ml/kg. Mice were given 10 min in their home cages after injection, before being placed for 30 min in the 'preferred' chamber, with the corridor removed. Day 4 was the test day. This followed the same protocol as day 1, the pre-test day, and mice were recorded for 30 min with freedom to move between both chambers but were not treated with any drugs.

A conditioned place avoidance (CPA) score was calculated for the pre-test and test days by subtracting the amount of time spent in the non-preferred side from the time spent in the preferred side during the 30 min of recordings.

Conditioned place avoidance testing was carried out by Dr Christopher Cook and Ms Katie Tye from the Luckman group at the University of Manchester.

3.3.3.3　　　Pica behaviour

Pica, the eating of non-nutritive substances, was measured in male Sprague-Dawley rats by collaborators at Eli Lily (Indianapolis, USA). In this study, rats were acclimatised to the presence of kaolin clay in their cages for 1 week prior to the study. Rats were then injected with vehicle (acetate buffer, pH 5.5, 1 ml/kg) SC, 0.2 mg/kg GDF15, reconstituted in acetate buffer, SC, 128 mg/kg LiCl, reconstituted at 0.3M in water, IP, daily for 3 days. Kaolin intake was measured daily during this time.

This pica behaviour study was carried out by Jesline Alexander-Chacko and colleagues at Lilly Research Laboratories, Eli Lilly & Company, Indianapolis, United States.

3.3.4 Neuronal activation

In all studies examining neurons activated by GDF15, mice were kept in their home room and cages. If they were moved to another room, they were placed there at least 3 hr before the start of the study and the room was kept quiet for the duration of the time that the mice were there. This allowed the mice to acclimatise to the new environment and gave time for any cFos generated by the stress of moving to subside before the start of the experiment.

Mice were injected SC with VEH or 4 nmol/kg GDF15 in a volume of 4 ml/kg and food was removed from mice at the time of injection to avoid the expression of cFos due to the consumption of food. For group-housed mice, food was removed at the time the first mouse in the cage was injected. 2 hr after injection, mice were transcardially perfused and brains dissected, fixed, and processed as described in General Methods 2.6.2 and 2.8.

3.3.5 Immunohistochemistry

A standard protocol, as described in General Methods (2.8.3) was used throughout this chapter.

3.3.6 Statistics and analysis

All raw data was entered into Microsoft Excel, where outliers, determined as being ±2 standard deviations from the mean, were removed. Data was then analysed using GraphPad Prism 7 or 8 software (GraphPad Software, San Diego, California, USA). All data were assessed for normal distribution using a Shapiro-Wilk test.

Food intake studies were analysed using a two-way ANOVA, followed by a *post hoc* Dunnett's multiple comparisons test. % fluid intake for conditioned taste avoidance test was analysed using a two-way ANOVA followed by *post hoc* Sidak's multiple comparisons test. Conditioned place avoidance was analysed using a paired t test and kaolin intake (pica behaviour) was compared using a mixed-effects two-way ANOVA analysis followed by *post hoc* Tukey's multiple comparisons test.

All data are presented as mean, with error bars representing SEM.

3.4 Results

3.4.1 Effect of exogenous GDF15 on food intake

To establish an anorectic dose of GDF15, the normal physiological drive for mice to eat was challenged by treating WT mice with 0 nmol/kg (vehicle), 2nmol/kg, 4nmol/kg, or 8nmol/kg GDF15 shortly before lights out. At 2 hr post-treatment, all doses of GDF15 caused anorexia in comparison with the 0 nmol/kg GDF15-treated group (Fig. 3.1A). The cumulative effect persisted for at least 24 hr after injection, with the greatest decrease being shown by the mice treated with the highest dose of 8 nmol/kg GDF15 ($p < 0.0001$ at 24 hr). The potency of the anorectic effect of GDF15 was tested with the stronger feeding stimulus of fast-refeeding. When mice were fasted for 16 hr overnight, the lowest dose of 2 nmol/kg GDF15 was no longer able to overcome the drive to feed by the morning (Fig. 3.1B). However, both higher doses of 4 nmol/kg and 8 nmol/kg were still able to overcome this stronger feeding stimulus and reduce food intake. As seen in the night-time feeding study, the anorectic effect of GDF15 lasted at least 24 hr. As 4 nmol/kg was the lowest dose consistently able to cause anorexia, this was the dose used moving forward.
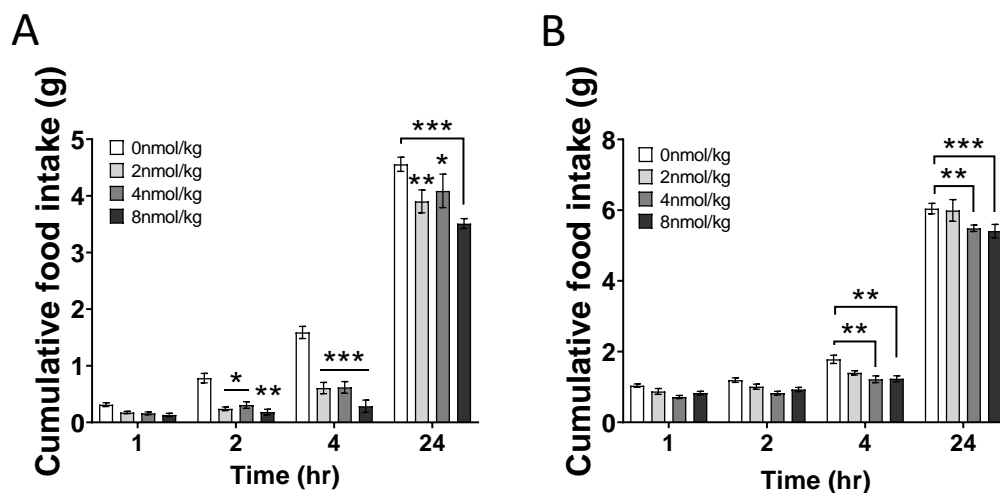
Figure 3.1. Effect of GDF15 treatment on food intake. Cumulative food intake of wild-type male mice treated with GDF15 A) just before lights out and B) during refeeding following a 16 hr fast. n=6/group. Data were analysed using two-way ANOVA with *post hoc* Dunnett's multiple comparisons test. Error bars represent SEM.* p <0.05, ** p <0.01, *** p <0.001.

3.4.2 Valency of GDF15

To begin investigating how GDF15 causes anorexia, conditioned taste aversion (CTA) and conditioned place avoidance (CPA) tests were performed. GDF15 induced aversion in both CTA (Fig. 3.2A) and CPA (Fig. 3.2C) tests.

In the CTA, mice were trained to associate a novel taste (sucrose) with an SC injection of saline vehicle (VEH) or GDF15. Mice treated with VEH showed a clear preference for sucrose after training, with 82 ±9% of their total fluid intake being sucrose during the test session. On the other hand, mice which associated sucrose with GDF15 strongly avoided it, with an average of 8% ±6 of their total fluid intake being sucrose.

In the CPA, mice were placed into a two-chamber apparatus, one side of which was 'light' and the other 'dark' (Fig. 3.2B). The preferred side was calculated as the chamber in which mice spent most time during the pre-test session. This was the 'dark' chamber for all mice. Association of the preferred chamber with GDF15 decreased the amount of time spent in the preferred chamber from an average of 534 s to 254 s (Fig. 3.2C).

Finally, GDF15 induced pica behaviour in rats (Fig. 3.2D). Pica, which was measured here by intake of kaolin clay, was greater in rats treated with GDF15 than those treated with LiCl by day 2 (2.98 g ±2.18 vs. 1.61 g ±2.29, respectively). This is an interesting result as LiCl is known to cause severe nausea and malaise in rodents (Andrews and Horn, 2006).
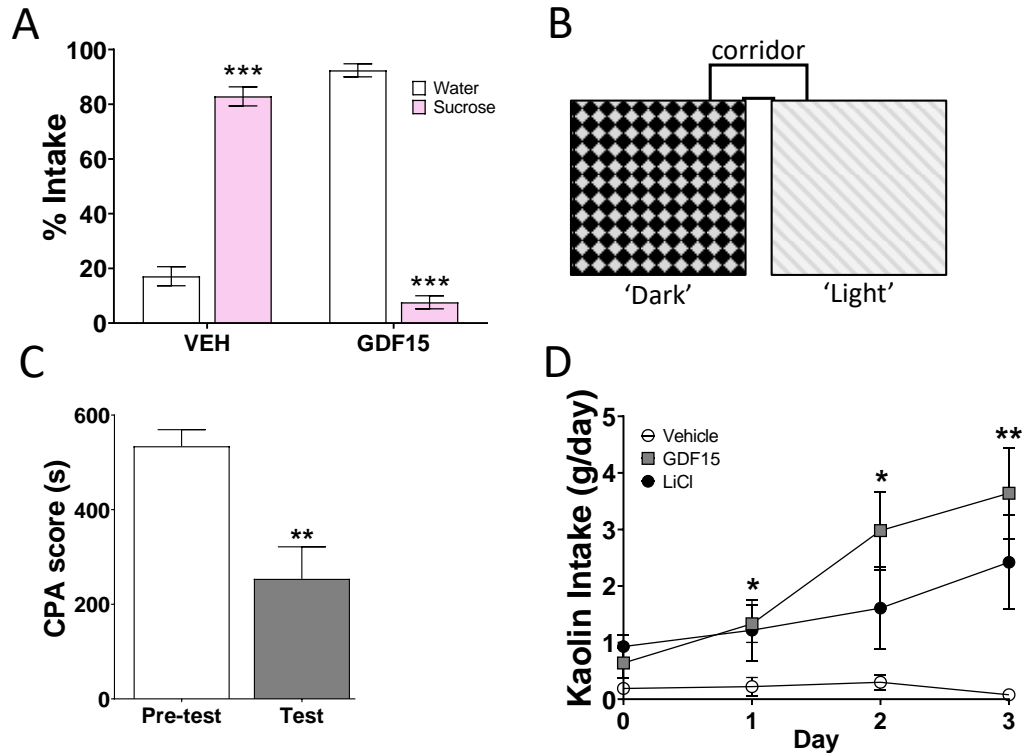
Figure 3.2. Valence of GDF15. Conditioned taste aversion was measured as A) % fluid intake of water or sucrose in wild-type mice, trained to associate sucrose solution with saline or 4 nmol/kg GDF15 administration. n = 6/group. Conditioned place aversion (CPA) was measured by placing wild-type male mice into a B) two-chamber apparatus which comprised of a dark, rough-floored chamber connected to a light, smooth-floored chamber by a brightly lit corridor. C) CPA score was compared before conditioning mice to associate the preferred chamber with saline (VEH) or 4 nmol/kg GDF15 treatment and after. n=6/group. % Fluid intake was analysed using a two-way ANOVA followed by post hoc Sidak's multiple comparisons test. CPA score was compared using a paired t test. D) Pica behaviour was measured in rats by measuring kaolin clay intake following daily injections of vehicle, 0.2 mg/kg GDF15 or 128 mg/kg LiCl. n = 9-10/group. Analysed using mixed-effects analysis followed by *post hoc* Tukey's multiple comparisons test. All error bars represent SEM. * $p < 0.05$, ** $p < 0.01$, *** $p < 0.001$ compared with VEH or pre-test scores. Contributions: B/C) CPA was performed by Dr Christopher Cook and Ms Katie Tye. D) Rat pica behaviour study was performed by Jesline Alexander-Chacko and colleagues at Eli Lilly, Indianapolis.

3.4.3 Activation of GFRAL^{DVC} neurons by GDF15

Fluorescence immunohistochemistry showed that within the DVC, GFRAL-immunoreactive neurons were found specifically in the AP and the dorsal region of the NTS at the level of the AP (Fig. 3.3A). The bulk of GFRAL neurons were found between Bregma −7.32 mm and −7.76 mm, with occasional GFRAL neurons seen slightly more rostrally or caudally in the NTS. On these occasions, there were between 1-3 GFRAL neurons present in the section. As these neurons were not consistently seen in these more rostral and caudal parts of the NTS, all cell counts involving GFRAL in the DVC were restricted to sections between Bregma −7.32 mm and −7.76 mm.

Whilst no GFRAL neurons in the DVC of mice treated with saline contained cFos, the lowest anorectic dose of 4 nmol/kg GDF15 caused activation of an average of 71% of GFRAL neurons the AP (p <0.0001) and 19% of GFRAL neurons in the NTS (p = 0.0012. Fig. 3.3B). In terms of numbers of cells, this represented an average of 15 out of 22 GFRAL^{+ve} neurons in the AP and 4 out of 18 GFRAL^{+ve} neurons in the NTS. There was another population of neurons in the medial NTS (mNTS) which were immunoreactive to cFos following GDF15 treatment which did not contain GFRAL.
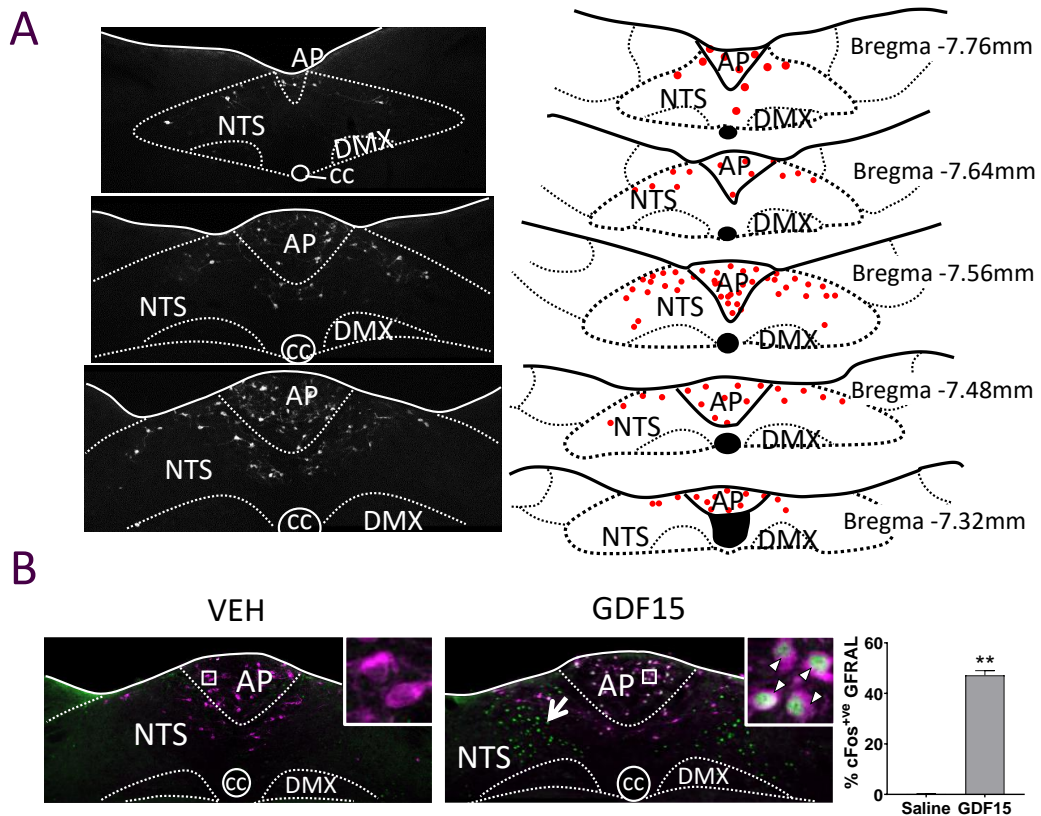
Figure 3.3. Location of GFRAL immunoreactive neurons in the dorsal vagal complex.
A) Fluorescence staining of native GFRAL receptor protein alongside a schematic of corresponding sections showing the location and density of expression GFRAL-immunoreactive neurons within the dorsal vagal complex (DVC). cFos, the transcription factor, was used as a proxy of neuronal activation. B) Dual fluorescence staining of GFRAL (magenta) with cFos (green) in the DVC of mice treated with vehicle (VEH) or GDF15 between Bregma −7.32 mm and −7.76 mm and quantification of the % of cFos^{+ve} GFRAL neurons in the DVC. Triangular pointers indicate GFRAL neurons expressing cFos following an exogenous dose of GDF15. Arrow indicates a population of neurons which do not express GFRAL which express cFos following an exogenous dose of GDF15 in the medial region of the nucleus of the solitary tract (NTS). AP = area postrema, cc = central canal, DMX = 10th cranial nerve/dorsal motor neuron of the vagus. % of cFos^{+ve} neurons was analysed using a Mann-Whitney U test. ** $p < 0.01$.

3.4.4 GDF15 activates anorectic neuronal populations in the DVC

To assess whether GDF15 utilises other known pathways to induce anorexia, other anorectic neuronal populations in the DVC were investigated using dual immunofluorescence. *Slc17a6* is the gene encoding the vesicular glutamate transporter, VGLUT2, *Prlh* is the gene encoding PrRP, and *Gcg* is the gene encoding PPG.

In addition to activating GFRAL-expressing neurons in the DVC, GDF15 treatment led to expression of cFos in 10% of approximately 170 neurons/section which expressed the neurotransmitter, CCK (Fig. 3.4A), 10% of approximately 90 neurons/section which expressed the catecholamine producing enzyme, TH (Fig. 3.4B), and 10% of approximately 330 neurons/section which expressed VGLUT2 (Fig. 3.4C). These neuronal types were activated in the AP and in the NTS. In all cases, a larger percentage of the neurons investigated were activated in the AP than in the NTS.

By contrast, GDF15 activated only one or two neurons containing PrRP per animal (Fig. 3.4D). This was not a significant increase from the number of neurons activated in saline-treated animals (p = 0.0631). GDF15 did not activate any neurons containing PPG (Fig. 3.4E), or POMC (Fig. 3.4F).

In the DVC, there were two distinct groups of neurons activated: one in the AP and dorsal NTS, and another in the medial NTS. In the AP, approximately 58% of neurons contained CCK, 24% contained TH, and 54% contained VGLUT. In terms of the number of cells, this represented approximately 10 ±2 neurons/section expressing CCK-Cre::eYFP, 4 ±1 neurons/section containing TH, and 10 ±1 neurons/section expressing VGLUT2-Cre::eYFP. No GFRAL[AP] neurons contained POMC and there were no PrRP or PPG neurons in the AP. In the NTS there was an average of approximately 80 neurons immunoreactive to cFos. Of these, approximately 11% per section contained CCK, 6% per section contained TH, and 26% per section contained VGLUT. No neurons activated in the mNTS contained PPG or POMC.
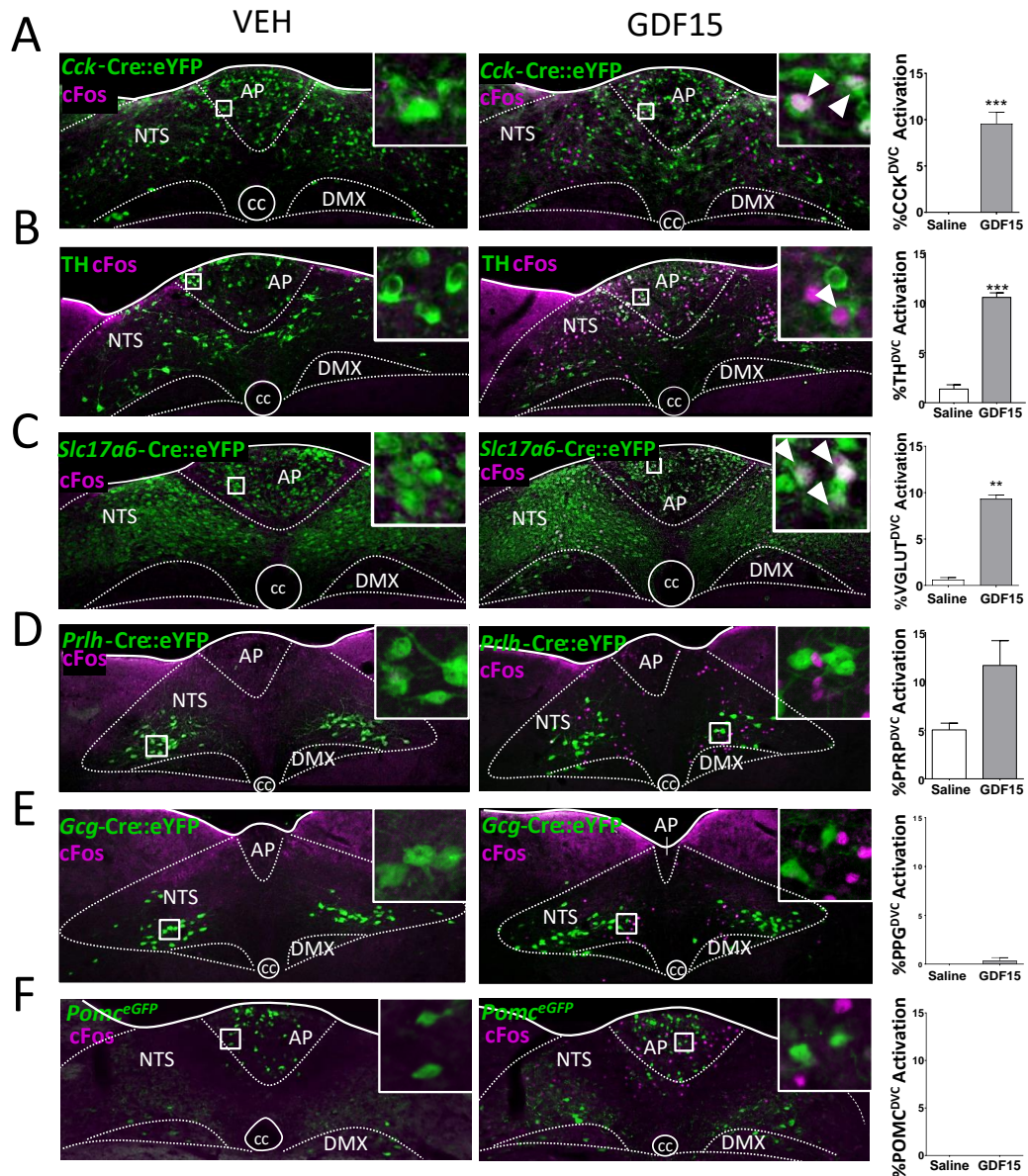
Figure 3.4. GDF15 activates neurons in the DVC. Different neuronal populations in the dorsal vagal complex (DVC) containing A) cholecystokinin (*Cck*)-Cre::eYFP, B) tyrosine hydroxylase (TH), C) vesicular glutamate transporter 2 (VGLUT2. *Slc17a6*)-Cre::eYFP, D) preproglucagon (PPG. *Gcg*)-Cre::eYFP, E) prolactin-releasing peptide (PrRP. *Prlh*)-Cre::eYFP, or F) pro-opiomelanocortin (*Pomc*)[eGFP] were stained using fluorescence immunohistochemistry (green) in mice which had been treated with saline or GDF15. The number of DVC neurons activated in the dorsal vagal complex by GDF15 was determined by presence of cFos (magenta) in those neurons. Co-localisation with cFos was quantified and analysed using an unpaired t-test or Mann-Whitney U-test as appropriate. Error bars represent SEM. n= 2-7/group. ** $p < 0.01$, *** $p < 0.001$. AP = area postrema, cc= central canal, DMX = 10th cranial nerve/dorsal motor neuron of the vagus, NTS = nucleus of the solitary tract. Contributions: F) experiment performed by Dr Garron Dodd, who kindly provided the images.

3.4.5 Activation of other brain regions by GDF15

Activation of other brain regions associated with regulating food intake was investigated following GDF15 treatment. In the PBN, exogenous GDF15 administration cause the expression of cFos specifically in a small, distinct population in the external lateral region (elPBN. Fig. 3.5A). GDF15 treatment also led to cFos expression in neurons in the CeA (Fig. 3.5B), the ovBNST (Fig. 3.5C), and the PVH (Fig. 3.5D). The identity of the neurons activated in these areas will be explored in Chapter 5.
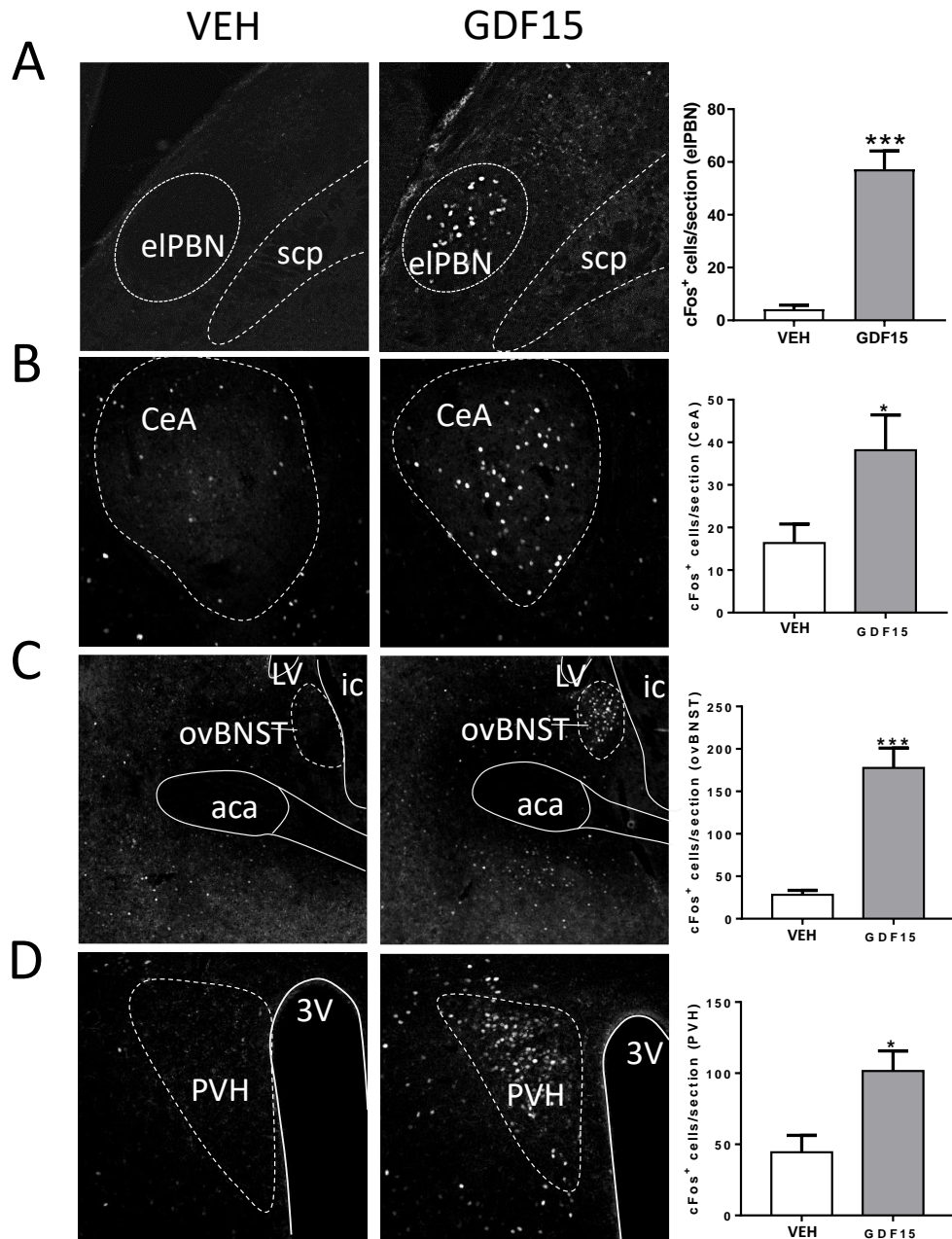
Figure 3.5. Brain regions activated by exogenous GDF15. cFos expression in neurons in A) the external lateral parabrachial nucleus (elPBN) between Bregma -5.02mm and −5.20 mm, B) the central amygdala (CeA) between Bregma −0.82mm and −0.94 mm, C) the oval nucleus of the bed nucleus of the stria terminalis (ovBNST) between Bregma +0.14 mm and +0.38 mm, and D) the paraventricular nucleus of the hypothalamus (PVH) between Bregma −0.70 mm and −1.06 mm in mice treated subcutaneously with saline vehicle or 4 nmol/kg GDF15. Neuronal activation was estimated by the presence of cFos (white). aca = anterior commissure, ic = internal capsule, LV = lateral ventricle, scp = superior cerabellar peduncle, 3V = 3rd ventricle. n= 4/group PBN, n=6-7/group CeA, ovBNST, and PVH. Cell counts were analysed via unpaired t test or Mann-Whitney U-test as appropriate. All error bars represent SEM. * p<0.05, *** p <0.001. Contributions: B)-D) IHC, imaging, and counts performed by Dr Amy Worth.

3.5   Discussion

3.5.1 Dose of GDF15

Tsai et al. (2018) stated in their review that GDF15 circulates at a concentration of 20–1200 pg/ml in normal physiological conditions in humans. In a more recent study, Welsh *et al.* (2022) found this figure to be higher, but both found that this quantity can greatly increase during aging and disease (Tsai *et al.*, 2018; Welsh *et al.*, 2022). However, there is no recommendation in literature of the concentration at which GDF15 circulates in mice during normal, healthy conditions. There is also variation in doses of exogenous GDF15 with which mice are reported to have been treated to cause anorexia and weight loss (Emmerson *et al.*, 2017; Hsu *et al.*, 2017; Miyake *et al.*, 2021). It was, therefore, necessary to establish an anorectic dose of GDF15 in mice. The lowest anorectic dose was used in order to engage the minimal effective neuronal circuitry and so obtain the clearest idea of what the actions of GDF15 are. In this chapter, a dose of 4 nmol/kg GDF15 was chosen as a model of GDF15-induced anorexia as this was the lowest dose to consistently induce anorexia (Fig. 3.1).

Though this is a much lower dose than is used in most of the literature, this dose of 4 nmol/kg may still equate to a large amount of GDF15 in circulation. In 2019, Patel *et al*. published a study in which mice were injected with varying doses of GDF15, which was subsequently measured in the plasma of those mice for 24 hr after. According to their study, an exogenous dose of 4 nmol/kg GDF15 administered subcutaneously results in roughly 4000-5000 pg/ml GDF15 in circulation 2 hr after injection, the time point at which blood and brain tissue were collected in these studies. In the rest of this thesis, the 'low' dose of 4 nmol/kg GDF15 therefore produces a far greater quantity of circulating GDF15 than endogenous GDF15 released in response to various stimuli examined in this thesis (which increases to an average of approximately 500 - 1800 pg/ml, depending on the chemotherapy applied. See Chapter 7).

Furthermore, there is very little evidence in literature regarding concentrations of endogenous GDF15 during disease in mice. The only evidence thus far comes from Breen *et al.* (2020), who found endogenous levels of GDF15 in the plasma of anorectic/cachectic tumour-bearing mice was significantly less than 1 ng/ml. This, therefore, leaves an important gap in knowledge. In future, endogenous GDF15 levels should be measured in mouse disease models to gain a better understanding of what quantities of GDF15 are relevant to the symptoms of diseases such as cancer.

3.5.2 GDF15 is an aversive stimulus

To understand how GDF15 causes anorexia and weight loss, its valency was investigated. Initial indicators that GDF15 might have a negative valency came from Low *et al.*, who found that GDF15 KO mice showed reduced anxious behaviours which are associated with stimuli which cause a negative valency (Low *et al.*, 2017). In this chapter, this is confirmed as when paired with a positive stimulus (sucrose or 'dark' in the CTA or CPA studies, respectively), GDF15 caused avoidance, indicating that its effects are unpleasant (Fig. 3.2A&C). In addition, GDF15 caused increased pica behaviour in rats, even in comparison with LiCl, a potent nauseating stimulus (Fig. 3.2D). These findings are also consistent with those of Borner *et al.*, who published twice in 2020 showing that GDF15 causes anorexia and aversion by inducing nausea, emesis, and visceral malaise in rodent models (Borner, Shaulson, *et al.*, 2020; Borner, Wald, *et al.*, 2020). The studies by Borner *et al.* were published the same year as the findings in Figure 3.2, and together, these data contribute to the current understanding of how GDF15 causes anorexia and weight loss in rodents.

The effects of GDF15 on inducing nausea and emesis seem to be consistent across species, including primates (Breen *et al.*, 2020) and potentially humans. Circulating GDF15 levels have previously been linked to morning sickness and its more severe form, *hyperemesis gravidarum* in pregnant women (Petry *et al.*, 2018; Fejzo *et al.*, 2019). Although pregnancy is a physiological state, it does cause significant stress to the body. Throughout literature, circulating GDF15 is associated disease states and in response to cell stress and damage (Park *et al.*, 2012; Altena *et al.*, 2015; Fujita *et al.*, 2016; Patel *et al.*, 2019), which can also be associated with nausea and emesis.

3.5.3 Central activation of neurons following GDF15 administration

In this chapter, I confirmed that GFRAL is expressed in a very limited area in the AP and the dorsal region of the NTS at the level of the AP. Administration of GDF15 caused cFos expression of an average of 47% of these GFRAL neurons in the DVC, with a much higher proportion of neurons activated being in the AP than the NTS (Fig. 3.3B). This could be because, unlike the NTS, the AP is a circumventricular area. As GDF15 acts directly on GFRAL receptors, it likely has easier access to GFRAL receptors in the AP than the NTS.

When considering GFRAL as a therapeutic target, it is worth noting that the location of GFRAL noted here and elsewhere in literature has only ever been assessed in healthy individuals. It is possible that in disease states, GFRAL could be expressed elsewhere, e.g., on tumours, thereby allowing GDF15 to act on other parts of the body, and potentially have effects other than anorexia and weight loss.

Literature shows that GDF15 acts exclusively through GFRAL receptors (Emmerson *et al.*, 2017; Hsu *et al.*, 2017; Yang *et al.*, 2017; Mullican *et al.*, 2017). However, there were many non-GFRAL neurons activated in the DVC following GDF15 injection (Fig. 3.3B). Most notably, there is a group of neurons in the mNTS whose phenotype is still unknown. These activated neurons are located in an area in which known populations of anorectic neurons, which respond to both satiety and sickness signals, reside. Information about the identity of these non-GFRAL neurons which are activated by GDF15 would aid a better understanding of which signalling pathway(s) are activated by GDF15. This would not only allow an assessment the mechanism(s) by which GDF15 causes anorexia but could also allow the manipulation of GDF15 signalling using established drugs and techniques.

Studies in this chapter revealed that some GDF15-activated mNTS neurons contained CCK, TH, and VGLUT (Fig. 3.4). However, no more than a quarter of this population contained any of these markers. Therefore, the identity of this population remains relatively unknown. It is possible that this group of neurons activated by GDF15 is heterogeneous, and therefore expression of GFRAL is the unifying phenotype for these neurons. Whilst I have employed a direct technique, investigating whether

neurons expressing GFRAL also express known anorectic markers, in 2021, Zhang *et al.* successfully applied a more general technique, RNASeq, to discover the different phenotypes of AP neurons mediating nausea behaviour. In their publication, Zhang *et al.* (2021) found that a group of glutamatergic neurons in the AP could be distinguished by the fact they also contained *Gfral*. This technique could also be employed to further explore the phenotype of GFRAL[NTS] neurons in the future.

Outside of the DVC, exogenous GDF15 caused cFos expression in a small area of the PBN, here described as the elPBN. This is a similar area in which Carter *et al.* (2013) and others describe a population of anorectic neurons containing the gene *Calca*, which encodes calcitonin gene-related peptide (CGRP). These neurons are part of a well-established aversive signalling network which includes the CeA, also activated by GDF15 administration. Therefore, *Calca*[elPBN] neurons will be investigated in future chapters. The ovBNST and the PVH were also activated by GDF15. All these areas are capable of reducing feeding behaviour when activated and represent parts of the circuitry which cause anorexia by responding to both aversive and satiating signals.

At this point, GDF15 has been shown to cause anorexia and have a negative valence. Judging by the phenotype of neurons activated in the DVC and the central regions activated by GDF15, it is still possible that GDF15 causes anorexia and weight loss via more than one pathway, much like CCK[DVC] neurons (Roman *et al.* 2017). As GDF15 acts exclusively on GFRAL receptors, the next chapter seeks to expand knowledge about GFRAL[DVC] neurons and how they signal in the hope of further understanding how activation of GFRAL neurons causes anorexia and finding ways in which to manipulate the GDF15/GFRAL signalling network.

3.6 Conclusions

- Low doses of GDF15 cause anorexia
- Increased GDF15 has a negative valence
- GDF15 activates GFRAL neurons in the AP and NTS, plus another population of non-GFRAL-expressing neurons in the mNTS
- GDF15 causes expression of cFos in areas in the mid- and forebrain which have known roles in the regulation of food intake and body weight

4 The phenotype and function of GFRAL-expressing neurons

4.1 Introduction

Due to the ability of the GDF15/GFRAL signalling system to induce anorexia and weight loss, there is currently interest in this system both as a target to reduce obesity and to prevent weight loss in disease states (Wischhusen *et al*., 2020; Fung *et al.*, 2021; Lu *et al.*, 2022; Wen *et al.*, 2022). In the previous chapter, I showed that increased GDF15 causes anorexia and aversion and this has been corroborated by other published works (Borner, Shaulson, *et al.*, 2020; Borner, Wald, *et al.*, 2020). However, at this point, relatively little is known about the phenotype of the GFRAL[DVC] neurons which GDF15 acts on. This information is essential to provide a greater understanding of how the GDF15/GFRAL signalling system causes anorexia and may provide avenues via which the system may be manipulated therapeutically.

In recent years, GDF15 has been shown to be increased by noxious stimuli, such as certain drug therapies (Altena *et al.*, 2015; Hsu *et al.*, 2017; Coll *et al.*, 2019; Breen *et al.*, 2020; Worth *et al.*, 2020), exogenous toxins (Luan *et al.*, 2019) and various disease states, including cancer (Breit *et al.*, 2011; Chung *et al.*, 2017; Luan *et al.*, 2019; Patel *et al.*, 2019; Breen *et al.*, 2020). These stimuli can cause an inflammatory response, mitochondrial stress, and/or cellular damage and are often accompanied by anorexia, nausea, and weight loss, including cachexia. GDF15 can also be increased by chronic high fat feeding and exercise (Kleinert *et al.*, 2018; Patel *et al.*, 2019; Zhang *et al.*, 2019; Laurens *et al.*, 2020), which are not generally associated with nausea or aversion. As GDF15 acts exclusively on GFRAL receptors (Emmerson *et al.*, 2017; Hsu *et al.*, 2017; Yang *et al.*, 2017; Mullican *et al.*, 2017), GFRAL[DVC] neurons may be sensitive to different kinds of anorectic stimuli, such as those which are involved in signalling satiety and reward, or those involved in signalling nausea and aversion.

In this chapter, the response of GFRAL neurons to a range of anorectic stimuli will be tested. Satiety-associated stimuli investigated will be an IP dose of the intestinal

satiety hormone, CCK, and an oral dose of lipid. The potent nausea-inducing stimulus, LiCl, will also be tested. Although GDF15 levels are not affected by acute food intake (Tsai *et al.*, 2015; Patel *et al.*, 2019), it is possible that GFRAL neurons are responsive to more than one type of signal and may use multiple signalling pathways to cause anorexia.

To date, there has been relatively little work investigating the phenotype of GFRAL neurons. What is known is that some GFRAL neurons express TH (Yang *et al.*, 2017), and in mice and humans, GFRAL is a sub-population of DVC neurons which express the GLP-1 receptor (Frikke-Schmidt *et al.*, 2019; Zhang *et al.*, 2021). There are several neuronal populations in the DVC, in the location where GFRAL neurons are found, which are known to be involved in signalling anorexia and weight loss. Examples of these include neurons expressing CCK, PPG, and PrRP, (Dodd *et al.*, 2014; D'Agostino *et al.*, 2016; Holt *et al.*, 2019; Brierley *et al.*, 2021). As GDF15 activates neurons which express CCK, TH and VGLUT (Fig. 3.2), it is possible that neurons which express GFRAL may also express one or more of these neuropeptides. This will be investigated using fluorescence IHC and *in situ* hybridisation.

A more direct way of investigating the phenotype and function of GFRAL neurons and the GFRAL neuronal signalling network would be by targeting or manipulating GFRAL neurons directly using a transgenic *Gfral*-Cre mouse model. During the course of these studies, one such model was created by the Luckman group. The presence of Cre recombinase exclusively in neurons expressing GFRAL allows for both the cell bodies and the processes of Cre-expressing neurons to be fluorescently marked, showing more about the location and projections of GFRAL neurons. The Cre also enables the manipulation of GFRAL neurons specifically by causing the expression of actuating channels or receptors (e.g., channel rhodopsin for optogenetic experiments, or designer receptors exclusively activated by a designer drug (DREADDs) for chemogenetic manipulation).

4.2   Aims and objectives

Hypothesis: GFRAL^{DVC} neurons are activated following application of anorectic stimuli, and contain other known anorectic markers.

Aim: To describe the phenotype and function of GFRAL-expressing neurons

1) Increase understanding of how GFRAL^{DVC} neurons induce anorexia and weight loss

- Establish what types of stimuli activate GFRAL neurons
- Investigate the phenotype of GFRAL^{DVC} neurons using IHC
- Investigate what neuropeptides GFRAL neurons release to induce anorexia

2) Validate the new *Gfral*-Cre mouse model

- Establish the location of Cre expression
- Compare the effects of activating GFRAL neurons using GDF15 (native GFRAL) vs. artificially activating GFRAL neurons in the *Gfral*-Cre model

4.3 Methods

4.3.1 Animals

Cck-Cre, *Gcg*-Cre, *Prlh*-Cre and *Slc17a6*-Cre mice were crossed with the Rosa26eYFP fluorescent reporter strain as described in General Methods 2.2.1 to generate fluorescent reporter strains for IHC experiments.

Gfral-Cre mice were newly generated by the Luckman group over the course of this project. *Gfral*-Cre mice were crossed with Ai32 (ChR2-eYFP) mice to generate *Gfral*-Cre::ChR2-eYFP mice which express a fluorescently marked channel rhodopsin on the cell bodies and processes of *Gfral*-Cre neurons. *Gfral*-Cre mice were also crossed with 1TB-hM3Dq^{mCherry} mice (D'Agostino, unpublished) to generate *Gfral*-Cre::hM3dq^{mChery} mice, which express the stimulatory DREADD in neurons expressing *Gfral*-Cre.

4.3.2 Drugs and viruses

GDF15 – administered subcutaneously as described in General Methods (2.1.2), with the exception of the CCK neuronal knock-down study (4.3.4.1). In this study, mice were administered 8 nmol/kg GDF15, rather than the usual 4 nmol/kg.

AAV8-hSyn-DIO-mCherry (Addgene, cat. 50459-AAV8)

AAV5-flex-taCasp3-TEVp: (Addgene. PMID:23663785)

CCK - administered IP at a concentration of 6 µg/kg at a volume of 4 ml/kg.

Oral lipid – 0.3ml 20% intralipid emulsion (Sigma Aldrich, cat. I141) was via oral gavage.

LiCl - 128 mg/kg LiCl was administered IP at a volume of 10 ml/kg.

Devazepide – administered IP at a concentration of 1 mg/kg and a volume of 4 ml/kg

CNO – 3 mg/kg CNO administered via intraperitoneal route as described in General Mehtods (2.1.2).

4.3.3 Stereotaxic surgery

AAV-mCherry (n = 7) or AAV-caspase (n = 7) were injected bilaterally into the NTS of 9-11 week old male *Cck*-Cre mice (D'Agostino *et al.*, 2016, 2018). Mice were anaesthetised with an IP injection of ketamine and xylazine (80 mg/kg and 10 mg/kg, respectively, administered at a volume of 10 ml/kg). Following confirmation of anaesthesia by toe-pinch, the mouse was placed in a stereotaxic frame with its nose tilted downwards at roughly a 45° angle. An incision was made at the level of the cisterna magna, and neck muscles were carefully retracted. Following dura incision, the obex served as reference point for injections with a glass micropipette. AP/NTS coordinates were approximatively -0.2 mm A/P, 0 and ±0.2 mm M/L, -0.2 mm D/V from the obex. A schematic of these injections can be found in Table 4. 150 nl of virus was delivered during each of the three microinjections. Animals were administered analgesia (5 mg/kg Carprofen, SC) for 2 days post-operatively and given a minimum of 14 days recovery before experiments. Surgeries in this chapter were performed by Dr Giuseppe D'Agostino.

4.3.4 Feeding studies

4.3.4.1 Viral knock down of CCK neurons

Cck-Cre mice which had been injected into the DVC with AAV-mCherry or AAV-Caspase were acclimatised to new home cages in a Sable Promethion Core feeding system (Sable Systems International, Berlin, Germany) for at least one week prior to the feeding study. Mice underwent a night-time feeding study as described in General Methods (2.4.1) in a cross-over format. In this study, half of mice injected with AAV-mCherry and half of the mice injected with AAV-caspase were treated SC with saline (VEH), whilst the other half were treated with 8 nmol/kg GDF15 in a volume of 4 ml/kg. The Sable system recorded food weight every 3 s for the next 24 hr. Mice were given one week to recover before the experiment was repeated, with mice previously treated with VEH being treated with GDF15, and vice versa. This experiment was carried out by Dr Amy Worth.

4.3.4.2 Pharmacological antagonism of CCK signalling

This feeding study was carried out using 12-week-old male C57BL6/J mice (Envigo) as described in General Methods (2.4.1). Devazepide was administered 50 min before injection of GDF15.

4.3.4.3 Chemogenetic activation of GFRAL neurons

This study was carried out using 10-16 week old, male and female *Gfral*–Cre::hM3Dq^{mCherry} mice, as described in 2.4.1 General Methods.

Mice were treated IP with either saline (n = 6) or 3 mg/kg CNO (n = 6) at a volume of 10 ml/kg.

In this study, the effects of CNO were more severe than when treating wild-type animals with GDF15. Unlike SC GDF15, animals treated with CNO showed obvious physical signs of sickness including squinting, hunching, and decreased mobility, resulting in the euthanasia of one mouse on humane grounds before the final time point.

4.3.5 Gastric emptying

Rate of gastric emptying was measured in the same *Gfral*-Cre::hM3Dq^{mCherry} animals described in 4.3.4, using a Cambridge Life Sciences Paracetamol assay kit (cat. K8002).

Food was removed from animals overnight before the study. Mice were weighed and injected IP with either saline control (n = 5) or 3 mg/kg CNO (n = 6) at a volume of 4 ml/kg. 30min later, mice were gavaged with 10 µl/kg paracetamol. Blood was collected by tail tip puncture using heparinised pipette tips immediately before paracetamol gavage (0 min), and 15 min, 30 min and 60 min after paracetamol gavage. Blood was immediately placed into heparinised Eppendorf tubes and placed on ice for a maximum of 2 hr. Blood was centrifuged for 20 min at 4 °C at 13,000 XG and resulting plasma was aliquoted and stored at -80°C until assayed.

The assay was run using the 'reduced-volume assay' protocol according to manufacturer's instructions. Absorbance was read on a BioTek Synergy HT plate reader using BioTek Gen5 microplate reader and imager software at 620/690 nm.

4.3.6 Neuronal activation studies

Activation of GFRAL neurons is explored in this chapter in sections 4.4.1, 4.4.3, and 4.4.5.2. In each of these studies, mice were briefly fasted from the time of treatment, barring mice which were orally gavaged with intralipid ('oral gavage'. Fig.4.1D). These mice were instead fasted for overnight before treatment. All mice underwent transcardial perfusion, as described in General Methods 2.8.1, 90 min following treatment, with the exception of those treated SC with GDF15, which were perfused 2 hr following treatment. Mice were treated as follows:

4.3.6.1 GDF15

12-week-old male C57BL6/J (Envigo) mice were injected SC with saline (VEH. n = 6) or 2 nmol/kg GDF15 (n =6) at a volume of 4 ml/kg.

12-week-old male *Cck*-Cre::eYFP mice were injected SC with saline (VEH. n = 6) or 4 nmol/kg GDF15 (n = 7) at a volume of 4 ml/kg.

4.3.6.2 Satiety and sickness signals

10-12-week-old male *Cck*-Cre::eYFP mice were injected IP with saline vehicle (VEH. n = 5) or 6 μg/kg CCK (n = 6) at a volume of 4 ml/kg.

10-12-week-old male *Cck*-Cre::eYFP mice were administered 0.3 ml saline (VEH) or 0.3 ml of 20% intralipid emulsion (oral lipid. Sigma Aldrich, cat. I141) via oral gavage.

10-12-week-old male *Cck*-Cre::eYFP mice were injected IP with saline (VEH. n = 6) or 128 mg/kg LiCl (n = 6) at a volume of 10 ml/kg, giving a final dose of 0.15 M LiCl.

The tissue for LiCl, IP CCK, and oral lipid treated mice was kindly supplied by Dr Amy Worth.

4.3.6.3 Chemogenetic activation of *Gfral*-Cre neurons

14-21 week old male and female *Gfral*-Cre::hM3Dq[mCherry] mice were injected IP with saline (n = 5) or 3 mg/kg CNO (n = 6) at a volume of 4 ml/kg.

4.3.7 Histology

IHC was carried out as described in General Methods 2.8.3. Images were collected using the standard protocol described in 2.8.4, barring images captured for Fig. 4.4. Images for this study were acquired using a Panoramic-250 microscope slide scanner (3D-Histech, Budapest, Hungary) using a *40x/0.95 Plan Apochromat* objective (Zeiss) and the *TRITC and FITC* filter sets. Snapshots of the slide scans were taken using Case Viewer software (3D-Histech) and any further processing required was carried out using Fiji software (Schindelin *et al.*, 2012). Red channels were pseudo-coloured magenta for the purposes of presentation only. IHC in Fig. 4.4 was carried out by Ms Sangavy Loganathan. IHC and imaging in Fig. 4.5 was carried out by Ms Valeria Collabolletta, both under under Rosemary Shoop's instruction.

4.3.8 RNAscope *in situ* hybridisation

Four or five 10 μm-thick tissue sections at the level of the AP were collected from 8-week-old C57BL/6J mice (n = 3). *Cck* (cat# 402271-C1) and *Gfral* (cat#417021-C3) mRNA was detected using RNAscope Multiplex Fluorescent Assay reagent kits (Advanced Cell Diagnostics, Inc, Newark, CA), according to the manufacturer's instructions, at Gubra (Hørsholm, Denmark). Slides were counter stained with DAPI to identify cellular nuclei. Slides were scanned under a 20X objective in an Olympus VS120 Fluorescent scanner.

4.4 Results

4.4.1 GFRAL-expressing neurons are activated by GDF15, but not by other satiety or sickness signals

To better understand how GFRAL^{DVC} neurons induce anorexia, mice were treated with a range of stimuli known to cause anorexia via different mechanisms. GDF15 activated GFRAL-expressing neurons in a dose dependent manner, with VEH activating an average of 0% GFRAL neurons, 2 nmol/kg GDF15 activating an average of 24% GFRAL neurons (Fig. 4.1A) and 4nmol/kg activating an average of 47% GFRAL neurons (Fig. 4.1B).

GFRAL neurons were not activated by a satiety-inducing dose of CCK (p > 0.9999, Fig. 4.1C), or an oral infusion of lipids (p > 0.9999, Fig. 4.1D), both of which generally caused high levels of neuronal activation in the DVC.

Very few GFRAL-expressing neurons were activated when mice were treated with the nausea-inducing drug LiCl (Fig. 4.1E). Though the difference in activation between saline- and LiCl-treated mice was statistically significant (p = 0.0304), the average number of GFRAL neurons activated by LiCl was between 1 and 2 per section.
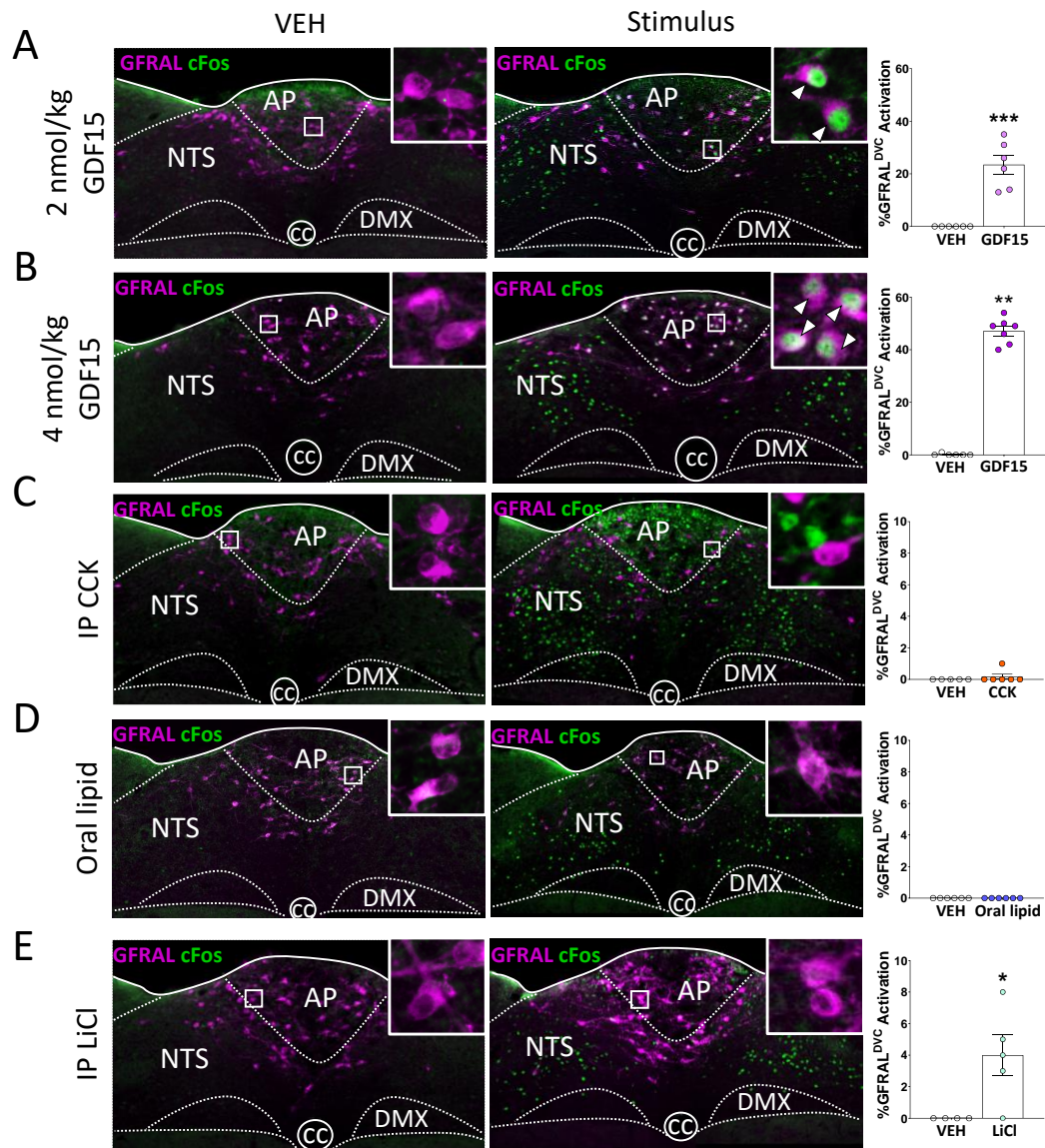
Figure 4.1. GFRAL-expressing neurons are activated by GDF15, but not by other satiety or sickness signals. Activation of GFRAL-expressing neurons (magenta) in the dorsal vagal complex (DVC) as measured by co-localisation with the transcription factor, cFos (green), following treatment with vehicle (VEH) or A) SC 2 nmol/kg GDF15, B) SC 4 nmol/kg GDF15, c) IP 6 µg/kg CCK, D) oral gavage of lipid (20% intralipid emulsion), or E) IP 128 mg/kg LiCl. n= 6/group. Data analysed using an unpaired t test or Mann-Whitney U test as appropriate. * $p < 0.05$, ** $p < 0.01$, *** $p < 0.001$. Contributions: C)-E) Sectioned tissue kindly provided by Dr Amy Worth.

4.4.2 Phenotype of GFRAL neurons

To further understand how GFRAL^{DVC} neurons affect anorexia, co-localisation of GFRAL receptors with other neuronal markers associated with anorexia was investigated. A series of Cre-expressing mice were crossed with the Rosa26EYFP reporter strain. Fluorescence immunohistochemistry revealed that an average of 58% of GFRAL^{AP} and 33% of GFRAL^{NTS} neurons (visualised by immunohistochemistry for the native receptor protein) co-localised in *Cck*-Cre::eYFP neurons. (Fig. 4.2A).

24% of GFRAL^{AP} neurons and 31% of GFRAL^{NTS} neurons contained the catecholamine marker, TH (Fig. 4.2B), and 54% of GFRAL^{AP} and 21% of GFRAL^{NTS} neurons contained the vesicular glutamate transporter, VGLUT2 (Fig. 4.2C). There was no co-localisation of GFRAL in *Prlh*-Cre::eYFP- or *Gcg*-Cre::eYFP-expressing neurons (Fig. 4.2D and E, respectively). PrRP was expressed in neurons in a more ventral portion of the NTS than GFRAL, and the bulk of neurons expressing PPG in the DVC are expressed more caudally than GFRAL neurons. There were very few sections available which contained both PPG and GFRAL neurons.

As there were concerns that the *Cck*-Cre::eYFP model may have some developmental expression of eYFP, RNAscope analysis also was carried out. 69% of *Gfral*^{AP} neurons and 35% *Gfral*^{NTS} mRNA-containing neurons also contained *Cck* mRNA, a higher percentage than was estimated by immunohistochemistry in the reporter mouse (Fig. 4.2F).
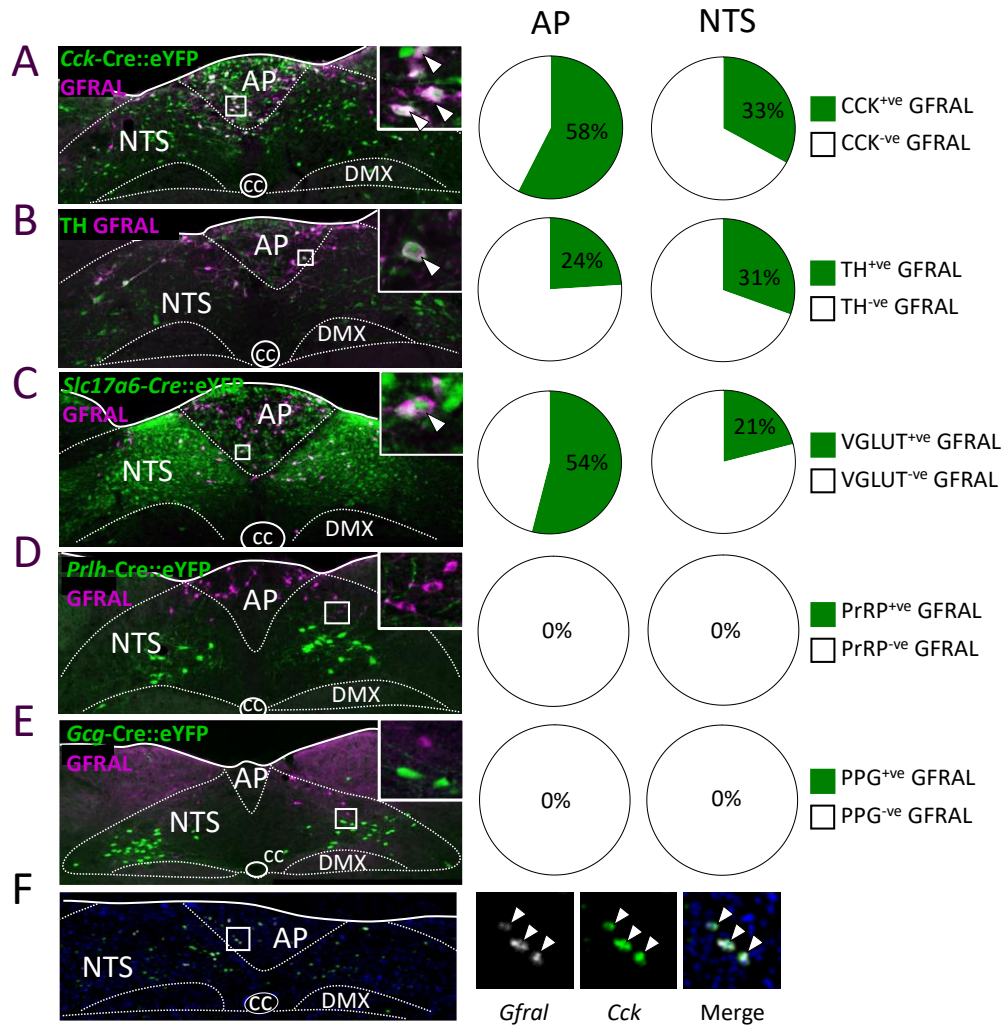
Figure 4.2. Phenotype of GFRAL neurons in the dorsal vagal complex. A series of Cre-expressing mice were crossed with a fluorescent reporter strain. Dual fluorescence staining of GFRAL (magenta) with A) *Cck*-Cre::eYFP, B) TH, C) VGLUT (*Slc17a6*)-Cre::eYFP, D) PrRP (*Prlh*)-Cre::eYFP, and E) PPG (*Gcg*)-Cre::eYFP (green) in the DVC between Bregma -7.32 mm and -7.76 mm. Pie charts represent the % GFRAL neurons in the area postrema (AP) and nucleus of the solitary tract (NTS) which co-localise with neuronal markers. F) In situ hybridisation histology of *Gfral* and (white) and *Cck* (green) with DAPI (blue) staining in the DVC. n=3-4 mice for each study. cc= central canal, DMX =motor nucleus of the vagus/10th cranial nerve. Contributions: F) experiment commissioned to Gubra, who provided raw images. Resulting counts performed in collaboration with Dr Amy Worth.

4.4.3 CCK[+ve] GFRAL[DVC] neurons use CCK as a neurotransmitter to signal and cause anorexia

Dual-label fluorescence immunohistochemistry and *in situ* hybridisation studies revealed that the majority of GFRAL neurons contain CCK (Fig. 4.2A and F) and that GDF15 caused activation of both GFRAL[+ve] and CCK[+ve] neurons in the DVC (Fig. 4.1A and B and Fig. 3.4A respectively). In order to confirm that neurons which co-express GFRAL and CCK in the DVC are activated by GDF15, triple-label fluorescence staining was carried out in *Cck*-Cre::eYFP mice which had been treated with saline or GDF15. A mean of 59% of activated GFRAL[DVC] neurons also contained CCK in animals treated with GDF15, compared with 0% in animals treated with saline control (p <0.0001. Fig. 4.3A).

To investigate whether CCK[DVC] neurons and CCK neurotransmitter mediate GDF15-induced anorexia, a two-fold approach was taken. Firstly, CCK neurons were ablated in the DVC by injecting a Cre-inducible caspase virus (AAV5-flex-taCasp3-TEVp) into the DVC of male *Cck*-Cre::eYFP. The caspase virus caused a significant reduction in the number of CCK[+ve] neurons (p = 0.0004, Fig. 4.3B). During a night-time feeding study, caspase-treated mice were protected from the anorectic effects of GDF15 compared with mice which had received a control AAV-mCherry injection into the DVC (Fig. 4.3C).

Secondly, CCK signalling was prevented by pharmacological antagonism. 12-week-old, male C57 mice were injected IP with devazepide, a selective CCK_1 receptor antagonist, before being treated with GDF15 in a night-time feeding study (Fig. 4.3D). Signalling from CCK_1 receptors is anorectic (Konturek *et al.*, 2004), therefore preventing their signalling could have caused an increase in food intake. However, preventing CCK signalling with devazepide alone did not significantly affect food intake at any time point (vehicle-saline vs. devazepide-saline). GDF15 caused a decrease in food intake by 4 hr (p <0.0001, vehicle-saline vs vehicle-GDF15). Animals pre-treated with devazepide were completely protected from this GDF15-induced anorexia (Fig. 4.3D).
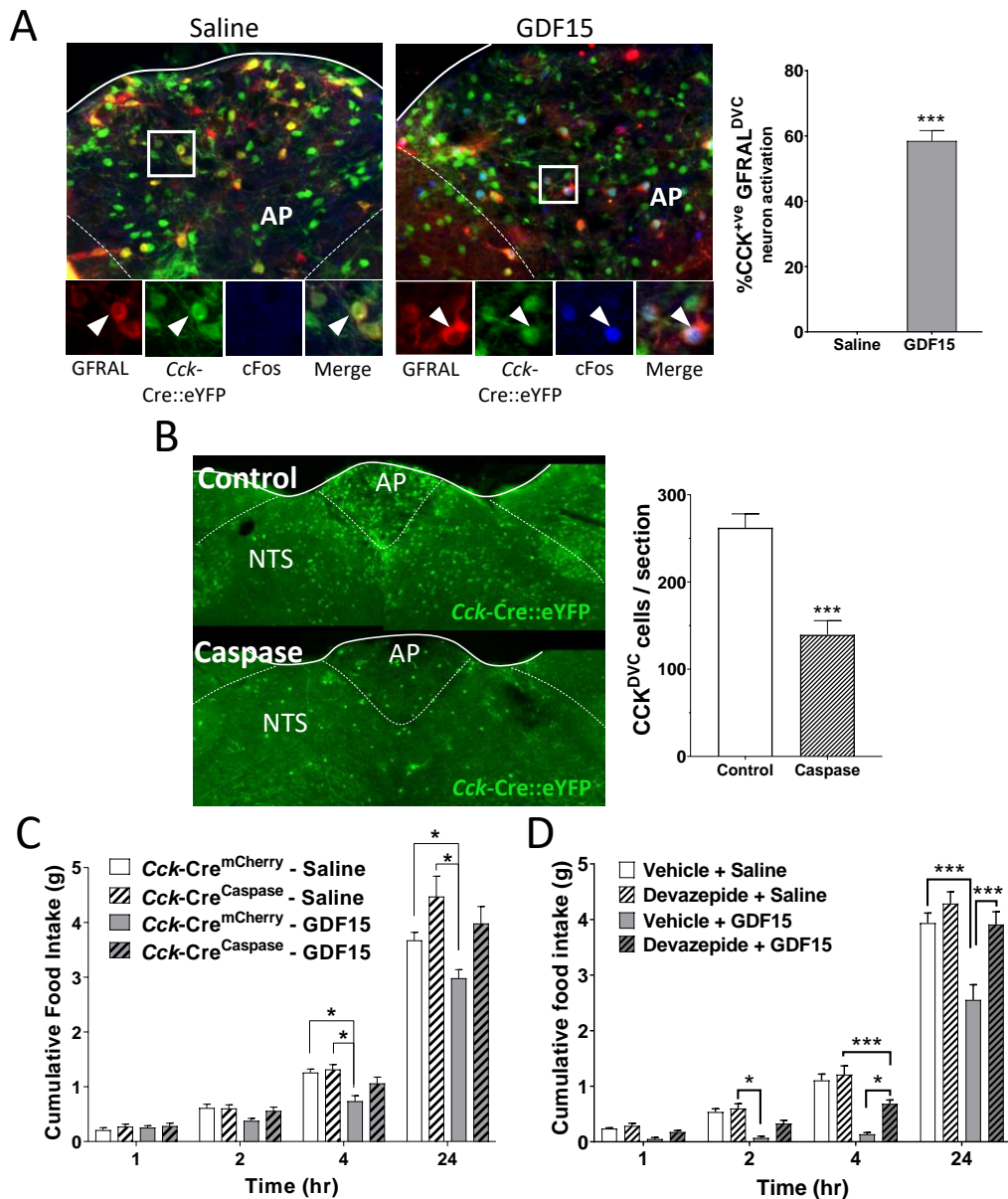
Figure 4.3. GFRAL neurons use CCK to send anorectic signals. *Cck*-Cre::eYFP mice were treated with 4 nmol/kg GDF15. A) Triple-label fluorescence staining was used to show co-localisation between GFRAL (red), *Cck*-Cre::eYFP (green), and cFos (blue). Percentage of cFos-immunoreactive GFRAL neurons which also contain CCK was quantified. AP= area postrema, cc= central canal, DMX = motor nucleus of the vagus/10th cranial nerve, NTS = nucleus of the solitary tract. *Cck*-Cre::eYFP mice were injected into the dorsal vagal complex with a control virus or a virus inducing the expression of caspase. B) The number of CCK[+ve] neurons was quantified following injection of virus. C) Food intake was measured in control- or caspase-treated mice following an injection of 8 nmol/kg GDF15. In another experiment, wild-type mice were treated with CCK-receptor antagonist, devazepide (1 mg/kg), followed by 4 nmol/kg GDF15. D) Food intake was measured for 24 hr afterwards. n = 5-6/group. Quantification of neuronal expression analysed using a Student's t-test or Mann-Whitney U-test as appropriate. Food intake data were analysed using two-way ANOVA followed by *post hoc* Tukey's multiple comparisons test. * p <0.05, ** p <0.01, *** p <0.001. Contributions: Surgery for B) and C) performed by Dr Guiseppe D'Agostino. B) IHC and cell counts performed by Dr Amy Worth. C) Data collection and analysis performed by Dr Amy Worth

4.4.4 Validation of a *Gfral*-Cre mouse model

4.4.4.1   Colocalisation of native GFRAL with *Gfral*-Cre

To validate the newly generated *Gfral*-Cre mouse, the fidelity of Cre expression with native GFRAL protein needed to be proven. *Gfral*-Cre mice were crossed with a reporter strain, causing the expression of ChR2-eYFP on the cell bodies and processes of neurons expressing Cre. Immunohistochemical analysis of the brains from the resulting offspring showed high levels of co-localisation between native GFRAL protein and *Gfral*-Cre::ChR2-eYFP (Fig. 4.4A), with a mean of 85% of *Gfral*-Cre cells marked with ChR2-eYFP co-localising with native GFRAL staining, and 71% of neurons stained for native GFRAL co-localising with *Gfral*-Cre::ChR2-eYFP in the DVC (Fig. 4.4B). Occasional ChR2-eYFP-marked cells (<3 per section) were seen in isolation in the cortex, the medial lemniscus or the nucleus of the trapezoid body (Fig. 4.4C). These cells did not have the same morphology as GFRAL neurons seen in the DVC and are likely ectopic expression of ChR2-eYFP in glial cells. These occasional cells did not express native GFRAL protein and were not activated by GDF15.
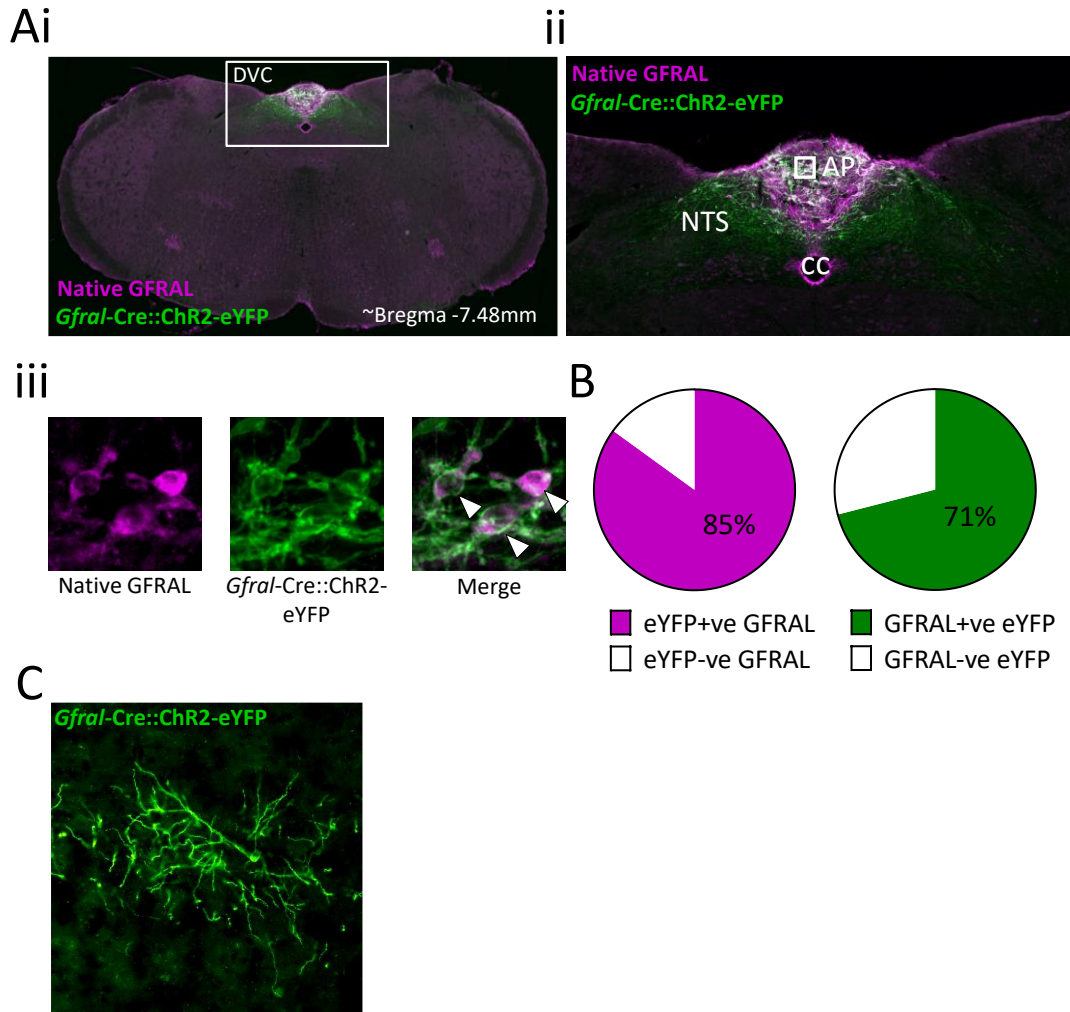
Figure 4.4. Fidelity of *Gfral*-Cre to neurons expressing native GFRAL in the *Gfral*-Cre mouse model. *Gfral*-Cre mice were crossed with a DIO-ChR2-eYFP strain to validate expression of Cre in neurons expressing native GFRAL. A) i) A representative section of hindbrain stained for native GFRAL (magenta) and ChR2-eYFP (green), ii) the dorsal vagal complex (DVC) and iii) a zoomed section of the DVC split into the separate colour channels showing co-localisation between native GFRAL and the eYFP reporter. B) Pie charts quantifying the percentage of neurons expressing native GFRAL which contain ChR2-eYFP (magenta), and the percentage of neurons containing ChR2-eYFP which express native GFRAL (green). C) An example of ectopic Cre-induced ChR2-eYFP expression in the cortex. Percentages calculated as an average of counts from 6 animals. Contributions: IHC performed by Ms Sangavy Loganathan.

4.4.4.2   The effects of activating of *Gfral*-Cre neurons

Having established that the Cre is expressed in GFRAL neurons, it was necessary to establish whether activation of *Gfral*-Cre neurons caused similar effects to activation of GFRAL neurons. *Gfral*-Cre mice were crossed with a 1TB-hM3Dq^{mCherry} line, which allows the expression of a stimulatory DREADD, marked with a fluorescent mCherry reporter, exclusively in *Gfral*-Cre neurons.

During a night-time feeding study, activation of *Gfral*-Cre neurons using the stimulatory DREADD prevented feeding for at least 4 hr following injection of CNO (Fig. 4.5A). By 24 hr after injection, there was no longer a significant difference between food intake for saline- vs. CNO-treated groups. Injection of CNO activated an average of 63% of *Gfral*-Cre neurons in the DVC vs. 2% neurons in animals treated with saline vehicle (Fig. 4.5B).

Furthermore, activation of *Gfral*-Cre neurons by the stimulatory DREADD almost entirely prevented gastric emptying as measured using a paracetamol assay (Fig. 4.5C). During the 60 min following oral gavage of paracetamol, the concentration of paracetamol in the plasma of mice treated with saline increased and peaked at 0.32 mmol/l at 15 min. The plasma concentration of paracetamol for CNO-treated mice peaked at 0.04 mmol/l at 15 min. Area under the curve analysis shows that there was a significant difference in the quantity of paracetamol in the plasma of saline vs. CNO-treated mice during the experiment ($p = 0.0408$, Fig. 4.5D).
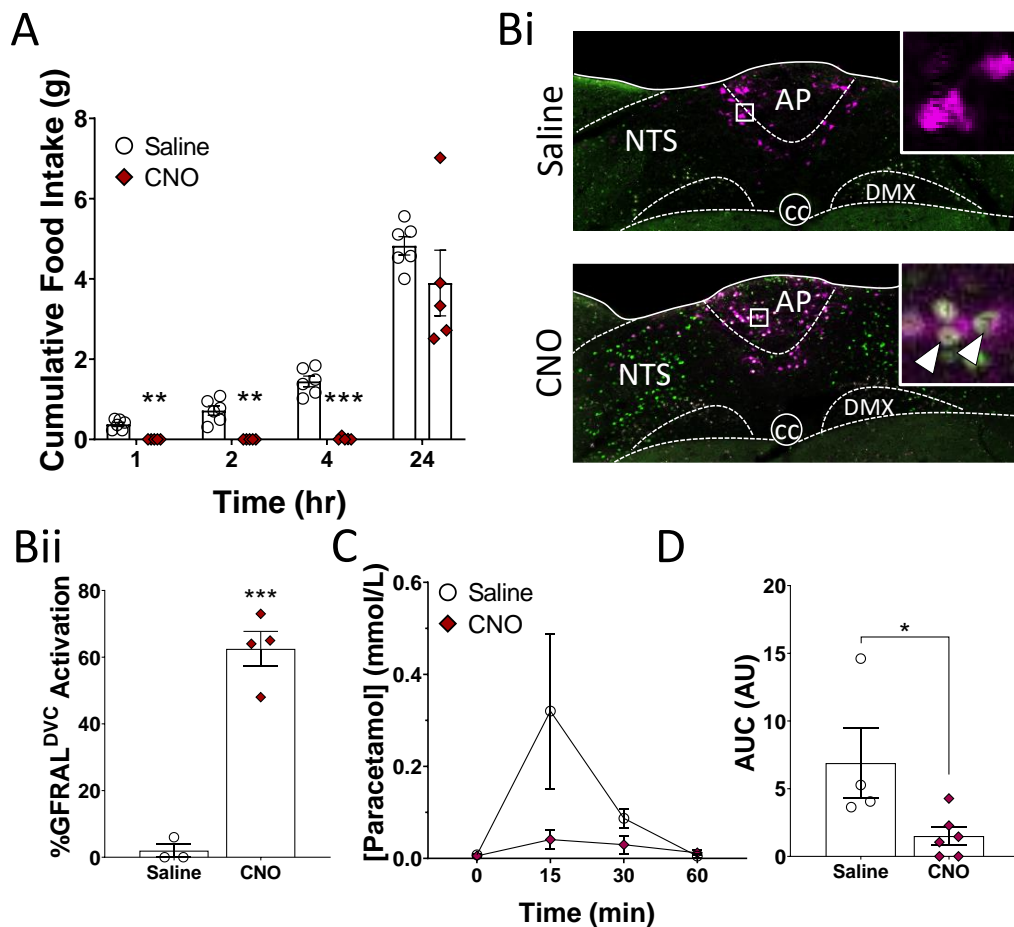
Figure 4.5. Actions of *Gfral*-Cre neuronal activation. *Gfral*-cre mice were crossed with a 1TB-hM3Dq^{mCherry} strain, which caused the expression of a stimulatory DREADD in neurons expressing Cre. A) Cumulative food intake after *Gfral*–Cre::hM3Dq^{mCherry} mice were injected with saline or 3 mg/kg CNO and Bi-ii) activation of *Gfral*-Cre neurons 2 hr after treatment with CNO. *Gfral*-Cre::hM3Dq^{mCherry} mice were treated with saline or 3 mg/kg CNO, then given an oral gavage of 10 μl/kg paracetamol. C) Concentration of paracetamol was measured in plasma for 60 min after. D) Area under the curve (AUC) analysis of quantity of paracetamol in plasma of *Gfral*–Cre::hM3Dq^{mCherry} mice for 60 min following oral gavage of paracetamol. n=5–6/group for cumulative food intake and paracetamol assay. n= 3-4/group activation of *Gfral*-Cre neurons by CNO. Cumulative food intake and paracetamol concentration were analysed using two-way ANOVA followed by post hoc Sidak's multiple comparison test. Activation of *Gfral*-Cre neurons was analysed using an unpaired t test. * $p < 0.05$, ** $p < 0.01$, *** $p < 0.001$. Contributions: *In vivo* studies run with the help of Dr Claire Feetham and Dr Nicolas Nunn. IHC and imaging for Bi performed by Ms Valeria Collabolletta.

4.5 Discussion

4.5.1 Activation of GFRAL^{DVC} neurons

At the beginning of this project, literature had shown that GDF15 acts through GFRAL, and that GFRAL is expressed exclusively in the brainstem (Emmerson *et al.*, 2017; Hsu *et al.*, 2017; Yang *et al.*, 2017; Mullican *et al.*, 2017). However, it was not known if GDF15/GFRAL-induced anorexia plays a role in normal physiological control of energy balance, was a part of a sickness response, or both. Therefore, this chapter explored whether GFRAL neurons were responsive to known sickness and satiety signals.

In this chapter, neurons expressing GFRAL were activated by GDF15 in a dose-dependent manner but were not activated by satiety signals such as oral infusion of lipids or an IP dose of CCK (Fig. 4.1). This is perhaps not surprising as we had found that GDF15 causes a negative valence and work by other groups has shown that GDF15 is released in response to cellular damage or stress (Park *et al.*, 2012; Fujita *et al.*, 2016; Chung *et al.*, 2017; Patel *et al.*, 2019; Townsend *et al.*, 2021) – neither of which are associated with satiety. Additionally, though the level of circulating GDF15 may be linked to body mass index in humans, it is not affected by meal times (Tsai *et al.*, 2015). Therefore, satiety signals released in response to physiological feeding are unlikely to utilise the GDF15/GFRAL signalling network to cause anorexia.

More surprisingly, GFRAL neurons were not particularly activated by the sickness mimetic, LiCl (Fig.4.1E). This contrasts with the findings of Sabatini *et al.* (2020), who found that LiCl did activate *Gfral*-Cre neurons in their *Gfral*^{eGFP} model. However, their model showed a large amount of ectopic expression in non-GFRAL^{DVC} neurons. Though there was a slight increase in %GFRAL neuron activation caused by LiCl in my study, this amounted to an average of one neuron per section activated in the LiCl group. This is unlikely to be enough to cause the anorexia phenotype. It may be that LiCl, whilst acting on neurons in the DVC to cause nausea, does not cause cell damage or stress sufficient to induce the release of GDF15, and therefore causes nausea and anorexia via a different pathway. In support of this idea, LiCl causes the activation of populations of neurons in the DVC which do not co-localise with GFRAL-expressing

neurons, such as PPG neurons (Luckman, unpublished). This evidence does not disprove the idea that GFRAL neurons are activated in response any signals which induce aversive anorexia and nausea, particularly as there is evidence LPS and Poly(I:C), bacterial and viral toxins respectively, do cause the release of GDF15 and subsequently, the activation of GFRAL neurons (Luan *et al.*, 2019; Cimino *et al.*, 2021). Rather, it is more likely that GFRAL neurons are activated indirectly by noxious stimuli, which cause the release of GDF15.

In this chapter, GFRAL receptors were found in the same neuronal populations which were activated by GDF15 in the Fig. 3.4. These were neurons expressing CCK, TH, and VGLUT, but not PPG or PrRP (Fig. 4.2). Since the beginning of this work, two groups have also shown that GFRAL^{DVC} neurons express GLP-1Rs (Frikke-Schmidt *et al.*, 2019; Zhang *et al.*, 2021).

When considering manipulating the activation of GFRAL neurons, TH and VGLUT are not appropriate targets via which to manipulate GFRAL signalling, as both are widely expressed throughout the brain and are used in multiple different signalling pathways. Targeting either of these populations would therefore cause multiple confounding side-effects alongside any alterations in feeding behaviour and body weight caused by GDF15/GFRAL signalling.

Additionally, although GFRAL neurons do express GLP-1Rs, Frikke-Schmidt *et al*. (2019) show that very few neurons in the AP which express both GFRAL and GLP-1R are responsive to GDF15. As Frikke-Schmidt *et al.* (2019) do not quantify the percentage of GFRAL neurons express GLP-1R or vice versa, it is possible that GLP-1R is expressed on a sub-population of GFRAL^{DVC} neurons which are not responsive to GDF15. This would make sense as no matter the dose of GDF15, only around 70% of GFRAL^{AP} neurons are activated (discussed in later chapters). As these GLP-1R-expressing GFRAL neurons are unresponsive to GDF15, manipulation of GLP-1Rs would also provide an accurate model to study GDF15/GFRAL signalling.

However, although CCK is expressed widely in the brain, CCK neurons outside the blood-brain barrier (i.e., in the AP) might be open to systemic manipulation. Provided

that GFRAL neurons use CCK to signal, CCK could be a possible target to affect GFRAL signalling.

4.5.2 GFRAL neurons use CCK as a neurotransmitter to induce anorexia

This chapter provided evidence that GFRAL neurons use CCK to signal and that GDF15-induced anorexia can be decreased or prevented by preventing CCK signalling (Fig. 4.3). Up to this point, I have shown that GDF15 activates CCK^{DVC} neurons (Fig. 3.4A) and GFRAL neurons contain CCK (Fig. 4.2A). However, this does not prove that GFRAL neurons use CCK to induce anorexia. With GFRAL being a subpopulation of CCK^{DVC}, it was possible that GDF15 activated DVC neurons and CCK+ve GFRAL neurons were separate from each other.

To begin investigating whether GFRAL neurons might use CCK to induce anorexia, *Cck*-Cre::eYFP animals were treated with GDF15 and activation of GFRAL neurons which contained CCK was sought using triple-label fluorescence IHC. As CCK+ve GFRAL neurons evidently were activated by GDF15 (Fig. 4.3A), it is possible that GFRAL neurons, utilising CCK as the transmitter, mediate the anorectic effects of GDF15. To explore this possibility, CCK signalling in the DVC was prevented in two different ways – by specifically destroying CCK neurons in the DVC and by pharmacological antagonism of CCK signalling.

When CCK signalling from the DVC was prevented, both by destroying the neurons using the caspase virus (Fig. 4.3B) and pharmacological block using devazepide (Fig. 4.3D), the anorectic response to GDF15 administration was prevented. Unlike pharmacological block of CCK signalling, in which food intake trended towards an increase following devazepide treatment (Fig. 4.3D), there was no difference in food intake between the control-saline and caspase-saline groups (Fig. 4.3C). This may be because CCK signalling was only prevented in the DVC in the caspase-treated mice, whereas it was prevented everywhere in devazepide-treated mice, both for central and gut derived CCK signalling.

Interestingly, *Cck*-Cre mice treated with mCherry/caspase virus were unresponsive to the dose 4 nmol/kg GDF15 which is used elsewhere throughout this thesis. The

addition of the Cre to CCK neurons should not have a phenotypic effect on mice, however *Cck*-Cre mice do become obese when they age. Due to the time taken for mice to undergo surgery and recovery, mice in this study had already somewhat aged and become overweight by the time the night-time feeding study was performed. There is now evidence that GFRAL becomes unresponsive to GDF15 during obesity (Chow *et al.*, 2022). In this study, it is possible that, due to being overweight, these mice were less able to respond to GDF15, and therefore a higher dose was needed to overcome this. This does not make results from this experiment invalid, as they still describe the effects of reducing or preventing CCK signalling on food intake during GDF15 treatment. Furthermore, 8 nmol/kg GDF15 which was used in this experiment is still a lower dose of GDF15 than is used in most published literature, with which results in this thesis are compared.

An IP dose of devazepide, a selective antagonist for the CCK_1 receptor, is likewise a valid model to demonstrate the role of central CCK signalling during GDF15 treatment. Activation of central CCK_1 receptors causes the reduction of food intake and satiety (Konturek *et al.*, 2004). Contrary to original belief, CCK_1 receptors are found centrally in several areas of the brain (May *et al.*, 2016; Zeng *et al.*, 2020), including the elPBN (Worth *et al.*, 2020), an area activated by GDF15 (Fig. 3.5A). Devazepide is also able to cross the BBB to act on central CCK_1 receptors (Woltman *et al.*, 1999).

Though CCK signalling also occurs outside of the brain, predominantly through CCK_1 receptors on vagal afferents (Konturek *et al.*, 2004), the effects of GDF15 are not dependent on signalling from the gut via the vagus (Borner *et al.*, 2017). The systemic effects of devazepide are therefore unlikely to impact on the effects of GDF15. This was proven to be the case when comparing the vehicle/saline and vehicle/devazepide groups, which did not show any difference in food intake, except at the 24 hr time point, when devazepide-treated mice had a trend towards increased food intake (p = 0.2338. Fig 4.3D).

Taken together, it is evident that devazepide can affect central CCK signalling, with its systemic effects being irrelevant to the effects of GD15 on feeding behaviour and

is therefore a good model to assess whether GFRAL neurons use CCK to induce anorexia. Indeed, if the actions of devazepide by itself increase feeding, this is not a negative effect if the proposition is to treat unwanted anorexia and weight loss.

As CCK receptors are frequently expressed on cancer cells and CCK signalling has been shown to have proliferative effects (Zeng *et al.*, 2020), CCK antagonists may be attractive for the treatment of cancer on two fronts – for the prevention of ACS, and the prevention of tumour growth. However, though CCK antagonists are currently used clinically and devazepide itself is used in human trials (Berna *et al.*, 2007), devazepide has a half-life of around 4 hr (Reidelberger *et al.*, 2003). If treating during chronic conditions such as cancer or chemotherapy-induced anorexia/weight loss, devazepide would need to be administered several times per day for weeks or months until the disease had been effectively treated/cured. A better option may then be to target the GFRAL receptor with a longer-lasting therapy. Fortunately, such therapies have already begun to be developed, and one such antibody treatment will be further explored in Chapter 8.

In summary, GFRAL neurons in the DVC are activated by GDF15, but not other satiety and sickness signals, and use CCK to induce anorexia. It is therefore likely that GFRAL neurons play a role in signalling anorexia and weight loss during situations which cause the increase of GDF15, and not during normal energy homeostasis. Whilst it is possible to manipulate the GDF15/GFRAL signalling pathway via CCK, the half-life of CCK receptor antagonists may be short enough to limit their usefulness in treating chronic anorexia and weight loss as would be seen in many disease states, so it would still be useful to find a longer acting drug or target the GFRAL receptors themselves.

4.5.3 Evaluation of the *Gfral*-Cre model

The *Gfral*-Cre mouse represents an excellent opportunity to investigate the GDF15/GFRAL signalling system in detail. As this was a newly generated mouse line, it required validation to ensure that it would be suitable for future use. To confirm this, I investigated whether the Cre was expressed only on neurons expressing native GFRAL protein and whether activation of *Gfral*-Cre neurons had similar effects to treating with GDF15.

IHC in the *Gfral*-Cre::ChR2-eYFP mice showed a high percentage of co-localisation between Cre-expressing neurons and native GFRAL staining and very little ectopic expression throughout the brain (Fig. 4.4A and B). The few cells which did express ChR2-eYFP outside of the DVC were not activated following administration of GDF15 and appeared either alone or in clusters of fewer than three cells. Furthermore, these ectopic cells had significantly different morphology to GFRAL[DVC] neurons, bearing most resemblance to glial cells, and did not express native GFRAL protein. Therefore, these ectopic cells are unlikely to have significant measurable effects when attempting to manipulate GFRAL signalling via *Gfral*-Cre neurons. Although Cre is not expressed in 100% of neurons which have positive staining for native GFRAL, when comparing the number of *Gfral*-Cre-expressing neurons in the DVC from both *Gfral*-Cre::ChR2-eYFP and *Gfral*-Cre::hM3dq[mCherry] mice to the number of native GFRAL neurons detected with IHC, there was no significant difference. It is therefore likely that the majority of GFRAL neurons express Cre in the *Gfral*-Cre model, and that this is sufficient to represent the activity of the population of GFRAL[DVC] neurons.

That a sufficiently high number of GFRAL neurons contain Cre to represent the population seems likely as activating *Gfral*-Cre neurons using chemogenetics produced similar results as when treating with GDF15 (Fig. 4.5). Administration of CNO to *Gfral*-Cre::hM3Dq[mCherry] mice caused anorexia (Fig. 4.5A). The severity of the anorexia in the *Gfral*-Cre::hM3Dq[mCherry] animals compared with wild-types treated with GDF15 (Fig. 3.1) may be due to increased numbers of GFRAL neurons being activated by the DREADD (Fig. 4.5Bi) than by 4 nmol/kg GDF15 (Fig. 3.3B), which was judged to be a low anorectic dose. In terms of number of neurons activated, CNO activated 50% more GFRAL neurons compared with GDF15 (mean 30 ±6 neurons/section CNO vs 19 ±2 neurons/section GDF15).

In addition to the activation of *Gfral*-Cre neurons by chemogenetic stimulation, there was also increased cFos expression in neurons which did not express *Gfral*-Cre the mNTS of *Gfral*-Cre::hM3Dq[mCherry] mice (Fig. 4.5Bi). Surprisingly, there was no difference in cFos expression or % GFRAL (/*Gfral*-Cre) activation in the AP in mice treated with GDF15 vs CNO, meaning that the difference was generated in the NTS.

The lack of difference in activation of GFRAL[AP] neurons may be because 60-70% represents maximal activation of the population in this area.

The increased activation of GFRAL[NTS] neurons may be due to a matter of access. The AP is a circumventricular area and is therefore exposed to circulating factors including cytokines like GDF15. The NTS however, is at least partially protected by the BBB. CNO may be more effective at crossing the BBB than GDF15, and therefore would have had direct access to neurons in the NTS. Though it bears further investigation, as GDF15 and chemogenetic activation of *Gfral*-Cre neurons cause similar effects despite differences in the number of NTS neurons activated, it is likely that GFRAL neurons in the AP and NTS act as one continuous population to cause anorexia.

Research by other groups shows that treatment with GDF15 delays gastric emptying (Xiong *et al.*, 2017; Hinke *et al.*, 2018; Borner, Wald, *et al.*, 2020). The chemogenetic activation of *Gfral*-Cre neurons by CNO in our model almost prevented gastric emptying (Fig. 4.5C&D). Again, a more severe phenotype was seen than when treating with GDF15, as before this was likely due to increased numbers of GFRAL-expressing neurons activated by the DREADD than by GDF15.

The reduction in gastric emptying in *Gfral*-Cre::hM3Dq[mCherry] mice following CNO treatment may be as severe as to be classified as gastroparesis. Gastroparesis can be a reason for anorexia itself (Webb and Fogel, 1995). Dramatic reduction or cessation of gastric motility prevents gastric emptying, therefore maintaining gastric stretch following feeding. This not only maintains satiety signals to prevent further feeding but can also be very uncomfortable or even painful. Indeed, following injection of CNO during the night-time feeding study, one mouse showed signs of pain and lack of mobility severe enough that it was destroyed on humane grounds. It is certainly true that delayed gastric emptying can contribute to feelings of nausea (Lacy, Parkman and Camilleri, 2018; Carson *et al.*, 2022). Delayed gastric emptying may therefore be one of the mechanisms via which GDF15 and activation of GFRAL neurons leads to nausea and emesis.

Whilst assessing the effect of *Gfral*-Cre neuron activation by DREADD receptors, it is worth bearing in mind that whilst DREADDS are useful, they can present a less subtle method of testing the behavioural output following stimulation of a neuronal population. This may be another reason why the effect of CNO on Gfral-Cre neurons is greater than the effect of GDF15 on native GFRAL receptors.

Generally, when receptors are activated, they trigger a specific intracellular signalling cascade within the cell. Activation of different receptor types can trigger different intracellular signalling cascades. In neurons, this can cause the release of signalling molecules which affect other cells. In this way, a neuron expressing multiple receptors can have different responses when different receptors are activated.

When using DREADDs, all intracellular signalling cascades are activated. Therefore, activation of DREADDs in a neuronal population which expresses several different receptors may give a composite effect. For example, GFRAL neurons also express GLP-1Rs. The phenotypic effects of GFRAL activation are reported to be similar, but separate, from GLP-1R activation (Frikke-Schmidt *et al.*, 2019). Therefore, activation of neurons expressing GFRAL using DREADDs is likely to show similar downstream effects as stimulating both of these receptors, which will be very difficult to separate.

Furthermore, in Fig. 4.5, there was no negative control group of CNO-treated hM3Dq-negative animals. Whilst the effects of CNO on negative controls are now well known, in this instance, the absence of a negative control may have posed an issue. Some commercially available CNO has been known to be contaminated with small amounts of clozapine (Mahler and Aston-Jones, 2018), which does have an impact on food intake and gastric emptying (Joint Formulary Committee, 2023). Mice which were positive for *Gfral*-Cre, but negative for 1TB-hM3Dq[mCherry], could have been treated with CNO as a negative control when investigating the effects of DREADDs on food intake and gastric emptying in the *Gfral*-Cre model. Fortunately, effects of DREADD activation on food intake and gastric emptying in this chapter were far more drastic than would be seen with contaminated CNO. Therefore, these results should not be discounted as the effect of low-level clozapine contamination.

Taken together, the high percentage of Cre expression in GFRAL neurons with low expression in other cells and the similarity in effect of treating with exogenous GDF15 and activation of the *Gfral*-Cre neurons shows that the *Gfral*-Cre mouse is a good model to investigate the GDF15/GFRAL signalling network. This now opens up many opportunities to dissect the function of the different parts of the GFRAL signalling pathway which is being carried forward by the Luckman lab.

For example, the *Gfral*-Cre mouse will allow deeper exploration of neurons and areas directly activated by GFRAL neurons. For example, the model could be used to confirm that GFRAL neurons directly activate neurons in the PBN and NTS using Cre-assisted circuit mapping (CRACM). There has also been suggestion that activation of the PBN is anorectic but does not cause aversion (Sabatini *et al.*, 2020). With the *Gfral*-Cre mouse, it will be possible to examine role of neurons these PBN neurons using optogenetic stimulation.

The expression of Cre will also allow the selective knock-down of GFRAL neurons in the DVC using a virus such as the AAV-caspase used in Fig. 4.3. A model like this would be useful to explore the effects of preventing GFRAL signalling in different diseases and therapies including cancer and chemotherapy. This could in some ways be preferable to using a congenital knock out model, because GFRAL KO mice are known to become obese as they age. As circulating GDF15 is increased by obesity (Tsai *et al.*, 2015), this could affect feeding and body weight results in a way which a knock-down model would not. This would also be preferable to using a proxy, such as the *Cck*-Cre animals used in Fig. 4.3B&C, as the virus would target GFRAL neurons only, to give more specific results.

This *Gfral*-Cre model therefore represents an exciting opportunity to help uncover information about the GFRAL signalling network and continue investigations into the role of GDF15/GFRAL signalling, not just in the context of cancer and chemotherapy, but other diseases.

4.6 Conclusions

- GFRAL neurons are activated by GDF15, but not satiety signals

- GFRAL-expressing neurons also contain CCK, TH, and VGLUT

- GFRAL neurons use CCK as a neurotransmitter to cause anorexia

- GDF15/GFRAL signalling can be manipulated by targeting CCK signalling

- The *Gfral*-Cre mouse faithfully recapitulates the GFRAL expression pattern

- Selective activation of GFRAL neurons causes anorexia and slows gastric emptying

5 The GFRAL signalling network

5.1 Introduction

To date, relatively little research has been published about the central GDF15/GFRAL neuronal signalling network. To understand how GDF15 signals to cause anorexia and weight loss and gain further understanding of how this system might be manipulated in a therapeutic context, further information about where GFRAL neurons project and the identity of GDF15-activated neurons should be sought.

Data from Chapter 3 and published literature show that GFRAL receptors are only expressed in the brain, in the AP and the dorsal region of the NTS at the level of the AP (Emmerson *et al.*, 2017; Hsu *et al.*, 2017; Yang *et al.*, 2017; Mullican *et al.*, 2017). GDF15 causes a GFRAL-dependent anorexia, aversion and weight loss (Emmerson *et al.*, 2017; Hsu *et al.*, 2017; Yang *et al.*, 2017; Mullican *et al.*, 2017; Worth *et al.*, 2020). Though GDF15 administration produces negative valency, there are a number of potential pathways which can affect anorexia and weight loss and which, individually, can have either positive or negative valency.

In Chapter 4, I demonstrated that GFRAL neurons in the DVC contain and use CCK to signal. Roman *et al*. (2017) showed that activation of CCK neurons in the DVC which project to either the PBN or to the PVH cause anorexia. Though the net valency of CCK^{DVC} signalling is negative, Roman *et al*. showed that CCK^{DVC}→PVH signalling has positive valency, whilst CCK^{DVC}→ PBN has negative valency. As such, CCK^{DVC} signalling can potentially induce anorexia via two separate pathways. As GFRAL neurons are a sub-population of CCK^{DVC} neurons and GDF15 causes activation of both the PBN and PVH, it is possible that GFRAL neurons cause anorexia in the same way as CCK^{DVC} neurons.

There are several known central signalling pathways which cause anorexia and weight loss via different mechanisms. Areas known to be involved in regulating food intake and body weight outside of the DVC include the PBN, the CeA, the ovBNST,

and the hypothalamus, in particular the ARC and the PVH. Though GDF15 does not affect activation of neurons in the ARC (Johnen *et al.*, 2007; Hsu *et al.*, 2017), all of these other areas are activated when GDF15 is increased. In addition, published data describes some of the neuronal populations within these areas which affect feeding behaviour. These populations contain phenotypic markers, such as calcitonin gene-related peptide (CGRP), proenkephalin (PENK), prodynorphin (PDYN), protein kinase Cδ (PKCδ), and corticotropin releasing hormone (CRH). This chapter will therefore explore different neuronal types and pathways which cause anorexia, associated with either positive or negative valency.

5.1.1 Areas of the brain activated by exogenous GDF15

5.1.1.1 Parabrachial nucleus

The PBN is a heterogeneous structure which can be divided anatomically into several different regions involved with different functions, such as water and salt balance, pain, visceral malaise, taste, and blood CO_2 levels. PBN neurons are also a part of circuits influencing glucose homeostasis, body temperature, breathing, cardiac function and importantly in the context of these studies, feeding (Palmiter, 2018). Exogenous GDF15 causes the activation of unidentified neurons in the lPBN. There are a number of different candidate neuronal types in the lPBN potentially associated with the control of feeding behaviour, which will be investigated in this chapter; those containing CGRP*,* PENK, or PDYN.

A subset of glutamatergic neurons in the elPBN express the *Calca* gene, which encodes the protein, CGRP (Carter *et al*., 2014). Over the last 10 years, work by the Palmiter group has shown these *Calca*[elPBN] neurons are activated by 'illness mimetics,' such as lipopolysaccharide (LPS) and LiCl (Carter *et al.*, 2013); anorectic signals, including CCK and leptin (Campos *et al.*, 2016); affect meal size and duration (Carter *et al.*, 2013); cause conditioned taste aversion (Carter *et al.*, 2015; Chen *et al.*, 2018). *Calca*[elPBN] neurons form part of a well-studied and highly aversive anorectic signalling pathway from CCK[DVC] → *Calca*[elPBN]→PKCδ[CeA] (Carter *et al.*, 2013; Cai *et al.*, 2014; Alhadeff *et al.*, 2015; Roman, *et al.*, 2017). As exogenous GDF15 causes activation in the DVC, elPBN, and CeA and GFRAL[DVC] neurons contain and use CCK to induce

anorexia, it is likely that GDF15/GFRAL signalling causes anorexia and weight loss via this signalling pathway.

There are two more populations of neurons in the lPBN which may cause anorexia. These populations contain the opioid peptides, PENK and PDYN (Khachaturian *et al.*, 1983; Kim *et* al., 2020; Norris *et al.*, 2021). Evidence for the actions of PENK neurons in the PBN is scarce, however, in the forebrain (specifically the PVH and the CeA), PENK neurons form a part of a reward signalling pathway (Le Merrer *et al.*, 2009) and the pathway which signals binge eating in rodents in response to stress (Welch *et al.*, 1996; Blasio *et al.*, 2014). To induce binge eating, the cleavage products of PENK, met-enkephalin and leu-enkephalin, act on central opioid receptors (Blasio *et al.*, 2014). Peripherally there is also a high level of innervation of the gut from PENK and PDYN neurons in response to the consumption of palatable diet (Clement-Jones and Rees, 1982). PENK signalling therefore clearly plays a role in the central control of feeding, using similar brain nuclei as GDF15/GFRAL signalling.

Although the current knowledge about PENK signalling indicates a role in increasing food intake in response to physical/emotional stress (such as foot shock and restraint stress) (Martin-Garcia *et al.*, 2011; Blasio *et al.*, 2014), rather than decreasing food intake in response to stress at a cellular level such as would cause the increase of GDF15, there is no information about the role of PENK^{elPBN} neurons, which may affect feeding differently. Alternatively, if all PENK neurons signal to increase food intake, GFRAL neuron activation may reduce PENK signalling to induce anorexia. As PENK neurons are located in the lPBN and may have a role in the control of food intake, it is worth investigating whether these neurons are being utilised by the GDF15/GFRAL signalling network to induce anorexia and weight loss.

The effect of PDYN^{lPBN} neurons on food intake has been more thoroughly explored. In their publication in 2020, Kim *et al.* described an aversive anorectic circuit from gut$\rightarrow$ vagus $\rightarrow$ NTS $\rightarrow$ PDYN^{lPBN} $\rightarrow$PVH. This pathway was activated by the mechanoreception of both solids and fluids and shares characteristics of GDF15/GFRAL signalling in that it is part of an aversive signalling pathway, involving activation of similar brain regions. Furthermore, chemogenetic activation of GFRAL

neurons (see Chapter 4) caused severe delay of gastric emptying. Such a delay in gastric emptying may cause the activation of stretch receptors in the gut. Therefore, it is possible that GDF15/GFRAL signalling has some effect by acting on mechanoreceptors and may utilise PDYN[IPBN] signalling to cause aversion and anorexia.

5.1.1.2   Central amygdala

The CeA is a large, complex region in the forebrain which forms a part of several signalling pathways with various purposes. The functions of these include those regulating fear (Haubensak *et al.*, 2010), anxiety (Pérez De La Mora *et al.*, 2007), pain (Okere *et al.*, 2000), addiction (Pursey *et al.*, 2019), learning (Ma *et al.*, 2011), reward (Douglass *et al.*, 2017; Hardaway *et al.*, 2019), salt intake (Andrade-Franzé *et al.*, 2015; Guan *et al.*, 2018), food motivation (Douglass *et al.*, 2017; Anesten *et al.*, 2019), sickness and aversion (Ma *et al.*, 2011; Carter *et al.*, 2013; Alhadeff *et al.*, 2015), and anorexia (Kovács *et al.*, 2012; Park-York *et al.*, 2013; Cai *et al.*, 2014). The CeA therefore affects food intake via several different mechanisms. The CeA is both responsive to normal physiological feeding signals, such as systemic or centrally released neuropeptide, GLP-1 (Parker *et al.*, 2013; Anderberg *et al.*, 2014; Anesten *et al.*, 2019), and systemically released gut hormone, CCK (Billig *et al.*, 2001; Haubensak *et al.*, 2010), and also stress and sickness/malaise stimuli (Elmquist *et al.*, 1996; Alhadeff *et al.*, 2015). Different populations of neurons within the CeA coordinate anorexia in response to these different signals.

In the same way that the CeA forms a part of a diverse range of signalling pathways, the CeA is also comprised of multiple different neuronal phenotypes. Those which are known to induce anorexia include a population of neurons containing the enzyme, protein kinase C delta (PKCδ). This population seems to be a part of networks inducing anorexia in response to both satiety and sickness stimuli. For example, a satiety-inducing dose of systemic CCK has been shown to cause anorexia via activation of a pathway involving the DVC, ventral tegmental area, and CeA[PKCδ] neurons (Cai *et al.*, 2014; Sanchez *et al.*, 2022). On the other hand, these same neurons are also responsive to aversive sickness stimuli such as LiCl and the

chemotherapy drug, cisplatin, again resulting in anorexia (Cai *et al.*, 2014; Alhadeff *et al.*, 2015). In addition to PKCδ, the CeA also contains a separate population of neurons which contain corticotropin releasing hormone (CRH). This population in the CeA modulates feeding behaviour in response to physical/emotional stress (Haubensak *et al.*, 2010) and may also form a part of the physiological control of feeding.

It is possible that the GFRAL signalling network is utilising one, or both, of these neuronal populations to induce anorexia. As shown in Figure 4.3, GFRAL neurons utilise CCK to induce anorexia. Central release of CCK from the DVC has been shown to activate the lPBN as part of an aversive signalling pathway (Roman, Sloat and Palmiter, 2017), and there is an established aversive signalling pathway from DVC→lPBN→CeA (Alhadeff *et al.*, 2015), which causes similar nausea/emesis effects as the central release of CCK and increased GDF15. Likewise, GDF15 has been shown to affect CRH signalling pathways in other parts of the brain in response to injection of LPS or infection with *Escherichia* coli (Cimino *et al.*, 2021). As the CeA also utilises CRH neurons as a part of a stress signalling pathway, it is possible these neurons also form a part of the GDF15/GFRAL signalling network.

Finally, the CeA is known to have anorectic projections to other areas of the brain which are activated by GDF15, such as the PBN, BNST, and NTS (Zséli *et al.*, 2018). In this chapter, retrograde tracing will be utilised to establish where the CeA lies in the GDF15/GFRAL signalling network to induce anorexia, and therefore understand which anorectic pathways GDF15 might be activating.

5.1.1.3   Oval nucleus of the bed nucleus of the stria terminalis

Whilst signalling from the ovBNST can certainly impact feeding behaviour (Hao *et al.*, 2019; Wang *et al.*, 2019), its role is less well characterised than other brain regions which are activated by GDF15. In the ovBNST, two populations of neurons have been identified which affect feeding behaviour. One is a GABAergic population which signals to the lateral periaqueductal grey matter, increasing feeding (Hao *et al.*, 2019). Another is a population containing PKCδ. The latter receive input from the

PBN and coordinate anorexia during inflammation (Wang *et al.*, 2019). It is possible that this second population may be a part of the GDF15/GFRAL signalling network.

Other regions of the BNST have better established roles in feeding behaviour. Several studies connect the BNST with binge-eating behaviours in response to stress. One such study shows that stress-induced anorexia is caused by signalling of BNST neurons expressing CRH receptors (Ciccocioppo *et al.*, 2004). This anorexia is counteracted via dopaminergic and opioid signalling which cause binge-eating behaviour (Di Bonaventura *et al.*, 2014).

Only one study links the ovBNST to dopamine signalling and binge-eating (Maracle *et al.*, 2019). As these studies of stress/binge-eating behaviour implicate the lateral BNST, and the stress described is physical/emotional (foot shock and restraint stress), rather than cellular stress which would cause the release of GDF15, this circuit is likely to lie outside of the ovBNST and be separate from the anorexia induced by GDF15.

5.1.1.4 Paraventricular nucleus of the hypothalamus

The hypothalamus rightfully receives a lot of attention in experiments concerning the neuronal control of food intake. Two of the best characterised areas within the hypothalamus which affect feeding behaviour are the ARC and the PVH. There is conflicting evidence in the literature about whether GDF15 increases activation of neurons in the ARC, with some studies showing activation and others not (Johnen *et al.*, 2007; Hsu *et al.*, 2017). Scanning through images taken for this thesis, it appears that ARC neurons are not activated by GDF15. However, there is unanimous agreement here, in Fig. 3.5D, and in literature that the PVH is activated by GDF15 (Johnen *et al.*, 2007; Worth *et al.*, 2020; Cimino *et al.*, 2021).

The PVH is a key area in regulating the body's stress response via the hypothalamic-pituitary-adrenal (HPA) axis and it does this using neurons containing CRH. CRH[PVH] neurons are responsive to such stressors as bacterial infection, endoplasmic reticulum stress, and genotoxins (Cimino *et al.*, 2021). As GDF15 is increased by cellular stress, many or all of these stimuli also increase the release of GDF15 (Park *et al.*, 2012; Altena *et al.*, 2015; Hsu *et al.*, 2017; Luan *et al.*, 2019; Scheffer *et al.*,

2020; Cimino *et al.*, 2021). Activation of the PVH by GDF15 and the emerging relationship between GDF15 and glucocorticoid release (Melvin *et al.*, 2020; Cimino *et al.*, 2021) implicate CRH[PVH] neurons in the GFRAL signalling network.

Discovering the pathways via which GFRAL signals will allow us to find out more about how GDF15 causes anorexia and weight loss and could provide targets by which to manipulate the signalling system. We can explore how these areas connect to each other by using techniques such as retrograde tracing and fluorescence immunohistochemistry. A fluorescent tracer, such as fluorogold (FG), can be injected into an area of interest, where it will be taken up by terminals and transported back to cell bodies, thus enabling the discovery of direct connections between activated neurons in areas of interest.

With the availability of the *Gfral*-Cre mouse, it is also possible to fluorescently label Cre-expressing GFRAL neurons by crossing the *Gfral*-Cre mouse with a channelrhodopsin-eYFP (ChR2-eYFP) line. This will cause the expression of ChR2-eYFP in the cell bodies and neuronal processes of Cre-expressing GFRAL neurons and enable the visualisation of GFRAL projections to other parts of the brain. These projections may also be in close apposition to neuronal populations of interest, and so will direct future studies of the functional connections of GFRAL neurons.

There are several known anorectic connections between areas shown to be affected by GDF15 (Chapter 3). These connections are summarised in Fig. 5.1 and will be investigated as a part of this chapter.
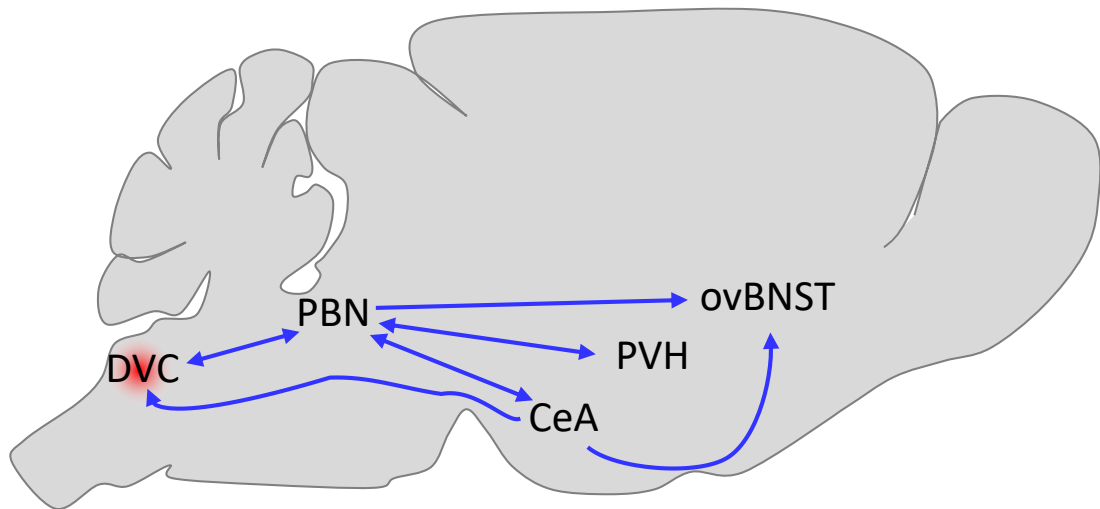
Figure 5.1 Known central anorectic connections. Schematic of a mouse brain showing known anorectic connections between different regions. Each of the areas shown is affected by exogenous GDF15, therefore these connections may form part of the GDF15/GFRAL central signalling network.

5.2 Aims and objectives

Hypothesis: GDF15 causes activation of GFRAL neurons, which then induce anorexia using known anorectic signalling pathways.

Aim: To discover central signalling pathways utilised by GFRAL neurons

1) Investigate the phenotype of neurons activated by GDF15 outside of the DVC
    - Use fluorescence IHC to investigate the activation of different neuronal populations in the lPBN, CeA, PVH, and ovBNST
2) Find connections between different brain regions activated by GDF15 to discover whether known anorectic pathways might be used by GDF15/GFRAL to reduce food intake
    - Investigate connections between brain regions activated by GDF15 using the retrograde tracer, FG
    - Investigate projections of GFRAL^{DVC} neurons using the *Gfral*-Cre mouse model

5.3 Methods

5.3.1 Animals

11-12-week-old male and female *Calca*-Cre^GFP, 14-week-old male and female *Penk*-Cre::eYFP, 12-24-week-old male and female *Pdyn*-Cre::eYFP, 14-week-old male and female *Crh*-Cre::eYFP, and 14-21-week-old make and female *Gfral*-Cre::ChR2-eYFP mice were used for neuronal activation studies.

11-12-week-old male and female *Calca*-Cre^GFP and 14-week-old male C57BL/6J (Charles River, UK) mice were used for retrograde tracing FG studies.

Details of these lines can be found in Table 1.2. All mice were kept under standard conditions as described in General Methods (section 2.2)

5.3.2 Drugs and tracers

4 nmol/kg GDF15 was administered subcutaneously to mice 2 hr before transcardial perfusion as described in General Methods section 2.1.2 and 2.8.1 respectively.

Hydroxystilbamidine methanesulfonate (FG; Life Technologies ltd. Cat. H22845) was reconstituted at 4% in sterile water and 12-18 nl was injected unilaterally into the PBN, CeA, PVH, or BNST (for coordinates, see Table 4).

AAV8-hSyn-DIO-mCherry (Addgene, cat. 50459-AAV8) was reconstituted in sterile saline to a titre of 2.2×10^{13} gc/ml and was injected bilaterally into the lPBN a volume of 150 nl/side.

5.3.3 Stereotaxic surgery

Surgeries were performed using the standard protocol as described in 2.3.2. mCherry was injected bilaterally into the lPBN of *Calca*-Cre^GFP mice. FG was injected unilaterally for all targets into C57BL6/J mice, co-ordinates for which can be found in Table 1.4. Injections of FG into the CeA were performed by Dr Nicolas Nunn. Injections of FG into the PBN, PVH, and ovBNST were performed by Dr Amy Worth.

After surgery, mice were given at least 2 weeks before transcardial perfusion. This allowed the mice time to recover and gave time for axonal transport of FG or expression of mCherry.

5.3.4 Immunohistochemistry

All IHC was carried out using the standard protocol described in 2.8.3 and imaged using a fluorescent microscope (2.8.4), barring sections stained for PKCδ, which required an antigen retrieval step. The antigen retrieval step was carried out immediately before the normal IHC protocol and was as follows:

Sections were washed three times for 5 min in neutral 0.1M phosphate buffer (PB; pH 7.4; prepared in-house by dissolving 14.24g/l $Na_2HPO_4 \cdot 2H_2O$ (Sigma-Aldrich, cat. 71645) and 3.12g/l $NaH_2PO_4 \cdot 2H_2O$ (Sigma-Aldrich, cat. 71500) in water). Sections were then transferred into 10-50 mM sodium citrate solution at a pH of 8.5-9.0 and heated at 80°C for 30 min. Sections were removed from the heat and allowed to cool to room temperature in sodium citrate solution. Finally, sections were washed three times for 5 min in 0.1M PB. Normal IHC protocol was then followed from this point.

FG was not counter-stained as its own fluorescence was enough to be detected using the DAPI filter (350 nm) of a Zeiss Snapshot microscope.

Images for PKCδ staining in Figure 5.2 and *Gfral*-Cre::ChR2-eYFP sections in Figure 5.3 were acquired using a Panoramic-250 microscope slide scanner (3D-Histech, Budapest, Hungary) using a *40x/0.95 Plan Apochromat* objective (Zeiss) and the *TRITC and FITC* filter sets. Snapshots of the slide scans were taken using Case Viewer software (3D-Histech) and any further processing required was carried out using Fiji software (Schindelin *et al.*, 2012). All cell counts were carried out using Fiji software (Schindelin *et al.*, 2012) as described in General Methods.

Dr Amy Worth carried out IHC and subsequent image processing and analysis for PKCδ and *Crh*-Cre::eYFP forebrain studies in Figure 5.2. Ms Sangavy Loganathan carried out IHC and imaging on *Gfral*-Cre::ChR2-eYFP sections in Figure 5.3 and PBN sections from *Calca*-Cre[GFP] animals which had been injected into the CeA with FG in Figure 5.4F under Rosemary Shoop's instruction.

5.4 Results

5.4.1 Neuronal types activated following exogenous GDF15 treatment

5.4.1.1 PBN

In *Calca*-Cre mice which had been injected bilaterally into the elPBN with AAV8-hSyn-DIO-mCherry, GDF15 treatment caused cFos immunoreactivity in an average of 46% of *Calca*–Cre neurons whereas just 1.8% of *Calca*-Cre neurons contained cFos in the elPBN of saline-treated mice (p <0.0001. Fig. 5.2A).

In contrast, GDF15 treatment did not cause cFos expression in *Penk*-Cre-expressing neurons in the elPBN (Fig. 5.2B). Nor did GDF15 treatment cause cFos expression in *Pdyn*-Cre-expressing neurons in the elPBN (Fig. 5.1C). The bulk of *Pdyn*-Cre::eYFP neurons were located in a more dorsal region of the lateral PBN than those neurons affected by GDF15 treatment. Of the few *Pdyn*-Cre::eYFP found in the elPBN, none were affected by exogenous GDF15.
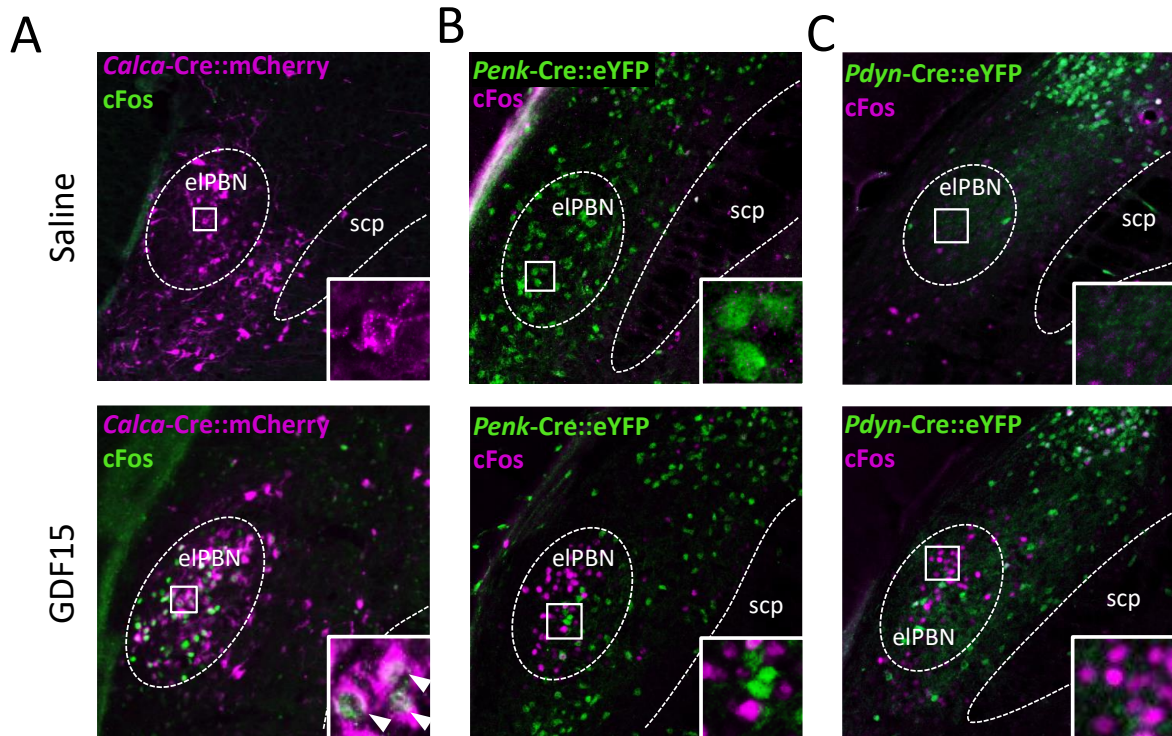
Figure 5.2. Phenotype of neurons activated by GDF15 in the PBN. *Calca*-Cre mice were injected into the external lateral portion of the parabrachial nucleus (elPBN) with AAV8-hSyn-DIO-mCherry and were treated with saline or GDF15. A) Activation of *Calca*–Cre::mCherry neurons (magenta) was determined by co-localisation with the neuronal activation marker, cFos (green). Proenkephalin (*Penk*)–Cre and prodynorphin (*Pdyn*)–Cre mice were crossed with the Rosa26eYFP fluorescent reporter strain and activation of B) *Penk*–Cre::eYFP neurons (green) and C) *Pdyn*–Cre::eYFP neurons (green) in the elPBN following GDF15 injection was investigated, again via co-localisation with cFos (magenta). Contributions: Surgery in panel A performed by Dr Amy Worth.

5.4.1.2   Forebrain

Activation of PKCδ neurons in the CeA, ovBNST, PVH following GDF15 treatment was investigated. In saline-treated animals, approximately 1% of PKCδ neurons contained cFos in the CeA. This increased to an average of 14% for GDF15-treated animals (p = 0.0012. Fig. 5.23i). In the ovBNST, an average of 35% of PKCδ neurons were activated by GDF15 compared with 2% in saline-treated mice (p = 0.0012. Fig. 5.3Aii). PKCδ was not expressed in neurons in the PVH (Fig. 5.3Aiii).

Activation of neurons expressing *Crh*-Cre::eYFP was also investigated. GDF15 did not significantly increase the activation of neurons containing *Crh*-Cre::eYFP in the CeA (Fig. 5.3Bi). There were very few *Crh*-Cre::eYFP neurons in the ovBNST, with an average of 6 neurons per side for each section. Many more *Crh*-Cre::eYFP neurons were observed in the dorsal and ventral regions of the BNST, with an average of 27 and 36 neurons per section per side, respectively. For the neurons which did appear in the ovBNST, an average of 7% of *Crh*-Cre::eYFP neurons were activated, which was equivalent to approximately one neuron activated per section (Fig. 5.3Bii). GDF15 treatment did not cause a statistically significant activation of *Crh*-Cre::eYFP neurons here or in the rest of the BNST.

GDF15 treatment caused an increase in cFos immunoreactivity in *Crh*-Cre::eYFP neurons in the PVH, with saline treated controls having an average of 6% of Crh-Cre::eYFP neurons colocalising with cFos, vs. an average of 26% in GDF15-treated animals (p = 0.0291. Fig. 5.3Biii). Unlike other populations we have examined, there was a large amount variation in the level of activation of *Crh*–Cre::eYFP neurons in the PVH, with a range of 5-50% of *Crh*-Cre::eYFP neurons containing cFos after GDF15 treatment. Activation in saline-treated control was much more consistently between 5-10% of the population.
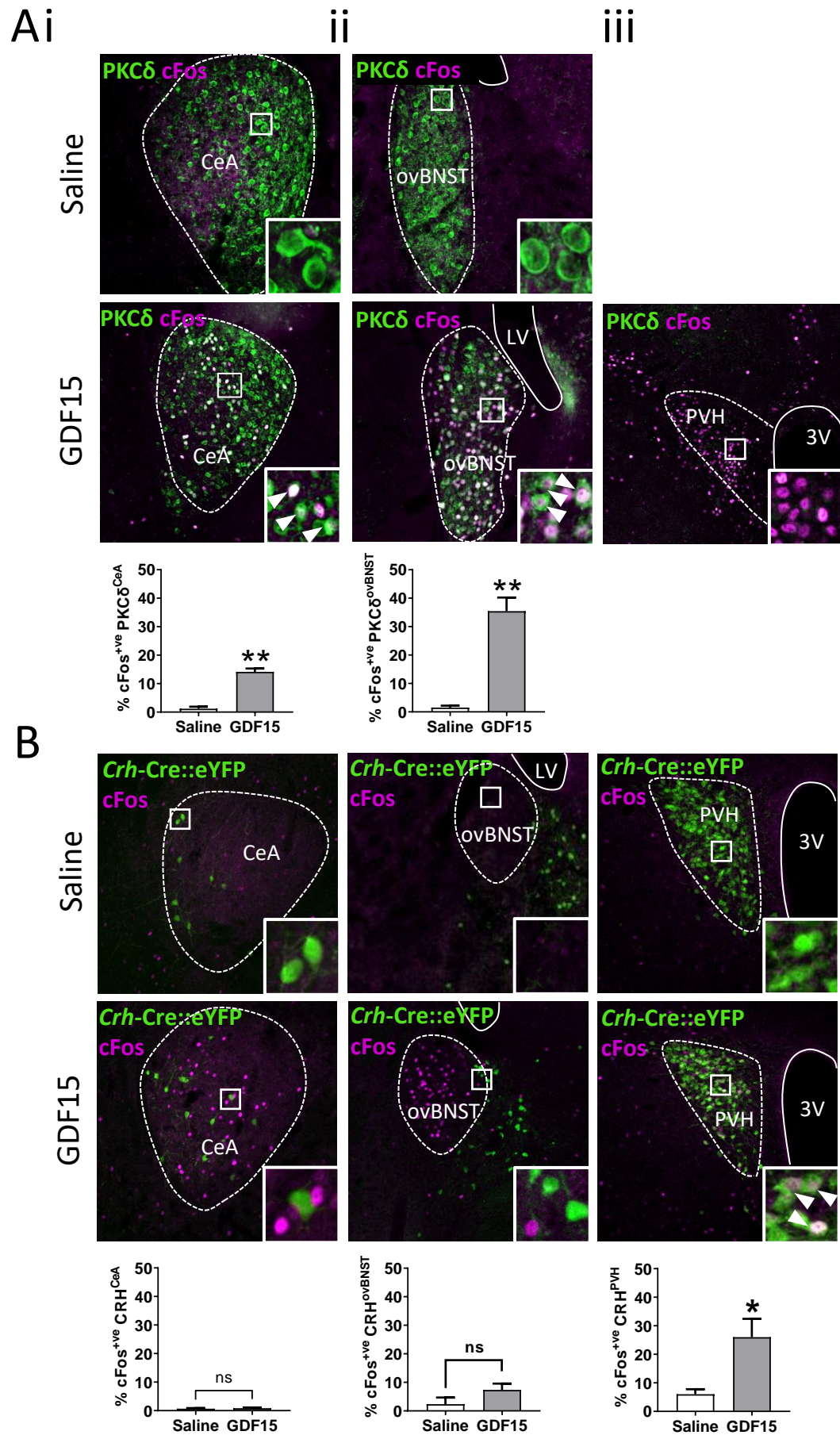
Figure 5.3. Phenotype of neurons activated by exogenous GDF15 in the forebrain. Quantification of the percentage activation of neurons containing A) PKCδ or B) *Crh-*Cre::eYFP (green) in the central amygdala (CeA), the oval nucleus of the bed nucleus of the stria terminalis (ovBNST), and the paraventricular nucleus of the hypothalamus (PVH) in mice treated with saline or 4 nmol/kg GDF15. Activation of neurons was determined by the co-localisation with the neuronal activation marker, cFos (magenta). n=6-7/group. LV = lateral ventricle, 3V = 3rd ventricle. Data analysed using t-test or Mann-Whitney U−test as appropriate. * $p < 0.05$, *** $p < 0.001$. Contributions: IHC, imaging and cell counts performed by Dr Amy Worth.

5.4.2 Direct projections of GFRAL neurons

Two techniques were utilised to discover the direct projection sites of GFRAL^{DVC} neurons. Firstly, the fluorescent retrograde tracer, FG, was injected unilaterally into areas shown to be activated by GDF15 (the lPBN, CeA, ovBNST, and PVH – Fig 3.5). Correct targeting of FG was confirmed at the site of injection (Fig. 5.4Ai-iv). GFRAL neurons which were activated by GDF15 administration in the AP and the NTS co-localised with FG which had been injected into the PBN (Fig. 5.4B). FG from the CeA did not co-localise with activated GFRAL^{DVC} neurons (Fig. 5.4C), nor did FG from the ovBNST (Fig. 5.4D) or the PVH (Fig. 5.4E). This suggests that GFRAL neurons which are activated by GDF15 have direct projections to the PBN, but not to the CeA, ovBNST, or PVH.

From these studies, it is also possible to determine connections between areas activated by GDF15 and non-GFRAL^{DVC} neurons which are activated by GDF15. Non-GFRAL neurons in the mNTS do not project to the PBN as they do not co-localise with FG from this area (Fig. 5.4B). One to two non-GFRAL^{mNTS} neurons per section co-localised with FG from the CeA (Fig. 5.4C). Several non-GFRAL^{mNTS} neurons co-localised with FG from the ovBNST (Fig. 5.4D), and a substantial number co-localised with FG from the PVH (Fig. 5.4E). Quantification of the amount of co-localisation with FG was not performed as the targeting and uptake of FG will differ between animals, making absolute comparisons invalid.

Secondly, *Gfral*-Cre::ChR2-eYFP mice were generated. The advantage of the ChR2-eYFP fluorescent marker over the eYFP used in other strains was that it marks neuronal processes as well as cell bodies. Projections from *Gfral*-Cre neurons were present in high density close to the population of mNTS neurons which were activated by GDF15 (Fig. 5.4F). There was also a high density of projections around neurons activated by GDF15 in the elPBN (Fig. 5.4G). In accordance with FG results, there were no projections present in the CeA (Fig. 5.4H), the ovBNST (Fig. 5.4I) or the PVH (Fig. 5.4J).
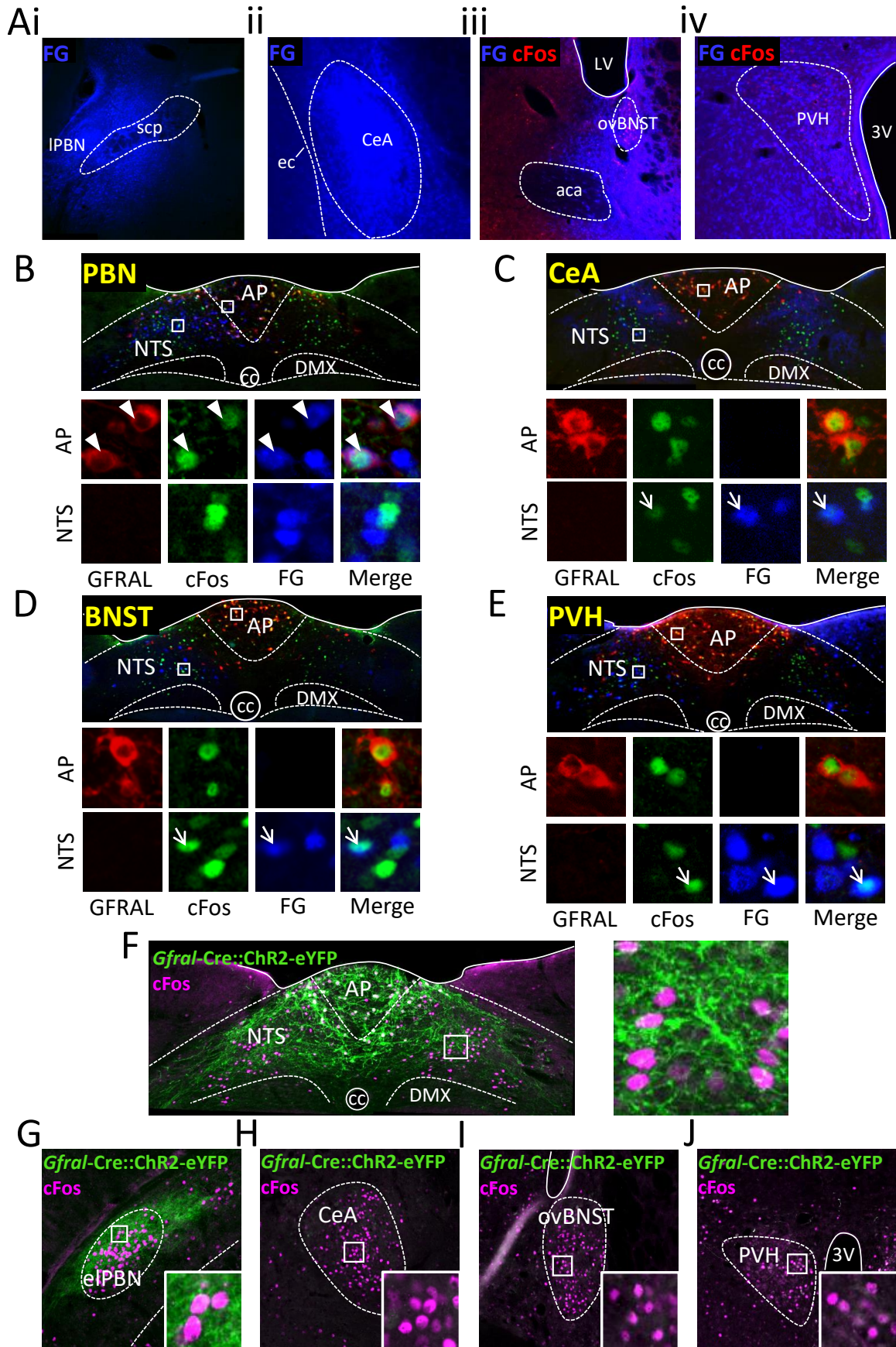
Figure 5.4. Direct projection sites of GFRAL^DVC neurons. Targeting of unilateral injections of the retrograde tracer, fluorogold (FG, blue) into wild-type mice was confirmed in Ai) the parabrachial nucleus (PBN), ii) the central amygdala (CeA), iii) the bed nucleus of the stria terminalis (BNST), and iv) the paraventricular nucleus of the hypothalamus (PVH). Co-localisation of FG with activated GFRAL neurons (red, native GFRAL + green, cFos) in the dorsal vagal complex (DVC) following GDF15 treatment in mice injected into B) the lateral portion of the PBN (lPBN), C) the CeA, D) the BNST, or E) the PVH with FG. *Gfral*-Cre::ChR2-eYFP mice were treated with 4 nmol/kg GDF15. Projections form *Gfral*-Cre::ChR2-eYFP neurons in F) the DVC, G) the external lateral portion of the PBN (elPBN), H) the CeA, I) the oval nucleus of the BNST (ovBNST), and J) the PVH, areas which are activated following GDF15 treatment (cFos, magenta). aca = anterior commissure, AP = area postrema, cc = central canal, DMX = motor nucleus of the vagus, ec = external capsule, NTS = nucleus of the solitary tract, 3V = 3rd ventricle. Contributions: Images for Aii-iv collected by Dr Amy Worth. Tissue processing, IHC, and imaging for F-J performed by Ms Sangavy Loganathan.

5.4.3 The GFRAL signalling network

FG was also utilised to investigate connections between brain regions activated by GDF15. In the same animals as described previously, the majority of neurons activated in the elPBN projected to the CeA (Fig. 5.5A). In these mice, there was also a more dorsal portion of the elPBN which contained FG, but not cFos.

FG injected into the PBN co-localised with neurons in the CeA and the PVH containing GDF15-induced cFos. Though there was FG present in the ovBNST, it did not correspond with neurons activated by GDF15 (Fig. 5.5B). This suggests that some GDF15-activated neurons in both the CeA and PVH, but not in the ovBNST, project to the PBN.

A substantial number of GDF15-activated neurons in the elPBN co-localised with FG from the ovBNST, demonstrating that they project directly to that nucleus. There were also many non-GDF15 activated neurons in the elPBN which contained FG from the ovBNST. In addition, a small number of GDF15-activated neurons in the medial portion of the CeA projected to the ovBNST. There was a small amount of FG from the ovBNST in the PVH, but this did not co-localise with GDF15-induced cFos (Fig. 5.5C).

Finally, there was no co-localisation of FG injected into the PVH with GDF15-activated neurons in the elPBN, CeA, or ovBNST (Fig. 5.5D). In fact, FG from the PVH did not appear in any of these areas at all. The appearance of FG in the elPBN from terminals in the CeA and ovBNST showed that there are populations of elPBN neurons which both are and are not activated by GDF15 project to the CeA and ovBNST.

Having confirmed that GDF15 activates *Calca*-Cre neurons in the PBN (Fig. 5.1A) and that neurons in the PBN project to the CeA (Fig. 5.5A), FG was injected into the CeA of *Calca*-Cre[GFP] mice to investigate whether *Calca*-Cre neurons, activated by GDF15, project to the CeA. An approximate count revealed that 20-30% of *Calca*-Cre[GFP] neurons co-localised with FG. The majority of these *Calca*-Cre neurons, which projected to the CeA, contained cFos. Further investigation showed that additional *Calca*-Cre[GFP] neurons were present more rostrally and more ventrally than the

neurons which were activated by GDF15. Thus, GDF15 did not activate the majority of the population of *Calca*-Cre neurons but did activate a substantial number of them which project to the CeA (Fig. 5.5E).
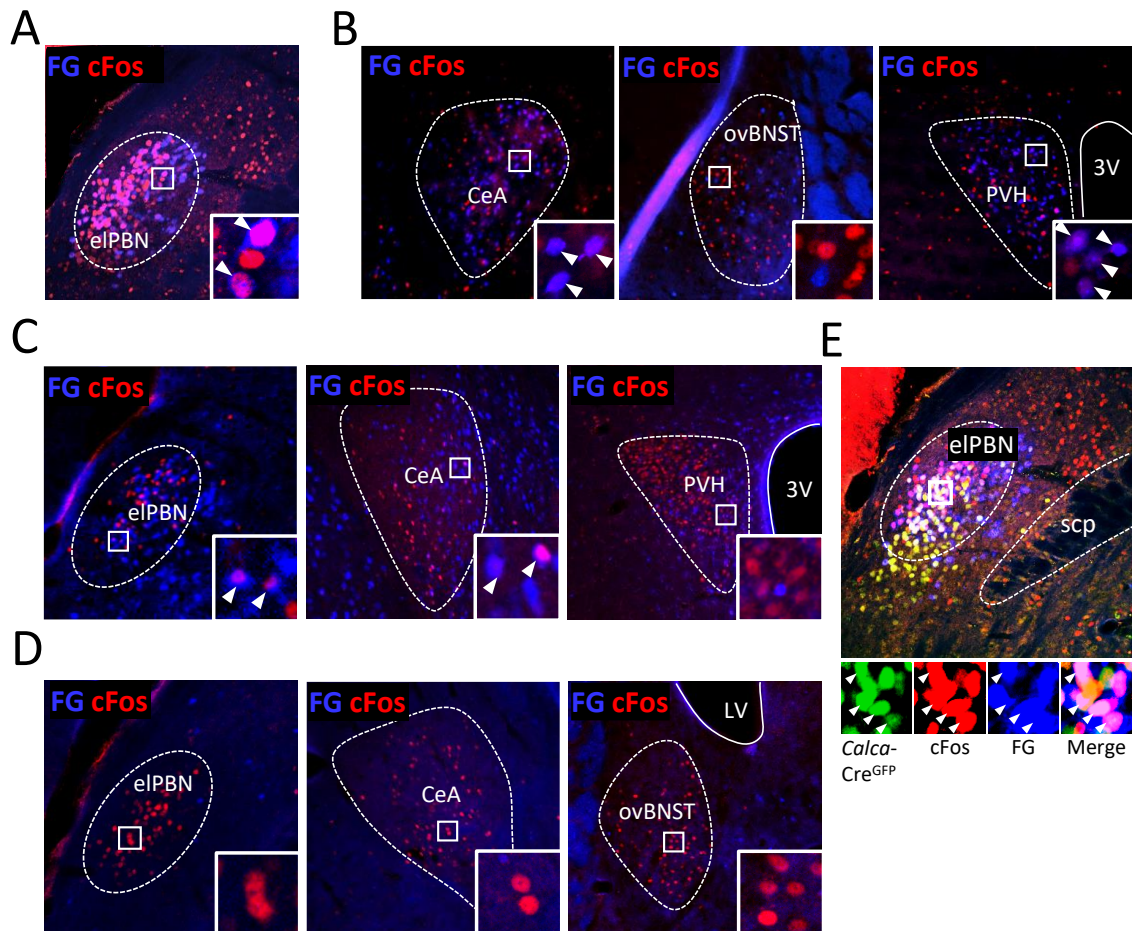
Figure 5.5. Tracing connections between mid- and forebrain areas activated by GDF15 treatment. Co-localisation of neurons activated by GDF15 (cFos, red) with the retrograde tracer, fluorogold (FG, blue) which had been injected into A) the central amygdala (CeA), B) the lateral portion of the parabrachial nucleus (lPBN), C) the bed nucleus of the stria terminalis (BNST), and D) the paraventricular nucleus of the hypothalamus (PVH), in areas which are activated by GDF15. *Calca*-Cre[GFP] mice were injected into the CeA with FG and treated with GDF15. E) Co-localisation between *Calca*-Cre[GFP] (green), cFos (red) and FG (blue) was sought in the PBN. ec = external capsule, elPBN = external lateral PBN, LV = lateral ventricle, scp = superior cerebellar peduncle, 3V = 3rd ventricle. Image from panel E collected by Ms Sangavy Loganathan.

5.5 Discussion

5.5.1 Phenotype of neurons activated by GDF15

To date, little work has been conducted to uncover the phenotype of neurons activated by GDF15 administration outside of the DVC. This information could give better clues as to how GDF15/GFRAL signalling causes anorexia and weight loss as the signalling system could be using known pathways. It could also provide further targets via which the GDF15/GFRAL signalling system could be manipulated for study and in therapy. Therefore, one of the aims of this chapter was to further the knowledge of the identity of neurons activated outside of the DVC by GDF15. Previous chapters have shown that GDF15 is anorectic and causes conditioned taste aversion. In this chapter, neuronal types which cause these effects in areas activated by GDF15 were investigated using immunohistochemistry and neuronal activation studies.

5.5.1.1 PBN

The PBN is an area involved in a diverse range of activities and contains several different neuronal types. Within the PBN, there are neurons expressing specific neuropeptide markers which are known to be involved in, or have been linked with, signalling anorexia and food reward. The role of three of these neuronal types in GDF15/GFRAL signalling was investigated.

The first population of these neurons investigated were those expressing CGRP. There are many similarities between the actions of GDF15 and effects caused by the activation of CGRP neurons in the elPBN, such as anorexia and conditioned taste aversion (Carter *et al.*, 2015; Palmiter, 2018). Chapter 4 provided evidence that GFRAL neurons in the DVC co-localise with those expressing CCK (Fig. 4.2A). CCK^{NTS} neurons have been shown to signal to the elPBN, causing anorexia (Roman, Sloat and Palmiter, 2017). In addition, data in Chapter 3 showed GDF15 treatment caused the activation of neurons in the elPBN and CeA (Fig. 3.5). As CGRP neurons are found in the elPBN, express CCK receptors (Worth *et al.*, 2020), and project to the CeA, causing anorexia and aversion, it was probable that GDF15 signals anorexia and aversion via

these neurons. GDF15 did indeed cause the activation of approximately 45% of *Calca*–Cre[mCherry] neurons in the elPBN (Fig. 5.2A). The majority of *Calca*-Cre[elPBN] neurons activated by GDF15 projected to the CeA (Fig. 5.5A). This gives compelling evidence that the GFRAL signalling system utilises the known aversive DVC → PBN →CeA pathway described by Alhadeff *et al.* (2015) and the Palmiter group (Roman *et al.* 2016; Palmiter, 2018).

However, not all *Calca*[elPBN] neurons were activated by GDF15, and not all neurons activated by GDF15 in the elPBN expressed *Calca*-Cre. The fact that GDF15 did not activate the entire population of *Calca*-Cre[elPBN] neurons is understandable as CGRP neurons in the elPBN carry out multiple functions. Neurons in the lPBN have been shown to be activated by sickness signals, such as LiCl, LPS and GDF15, as well as forming part of a satiety circuits via signalling from AgRP neurons in the ARC (Garfield *et al.*, 2015; Campos *et al.*, 2016). Judging by the neuronal subtypes and connections shown to be involved in the GFRAL signalling network, and as it is debatable whether GDF15 causes activation of the ARC, it seems likely that the role of CGRP[elPBN] neurons in GDF15/GFRAL signalling is aversive, rather than satiating.

GDF15 did not activate the whole population of CGRP[elPBN] neurons (Fig. 5.2A). As CGRP[elPBN] neurons are involved in signalling anorexia by different pathways, it may be the case that there are different subsets of CGRP[elPBN] neurons which cause anorexia via different mechanisms. Future investigations could be performed to discover whether this is the case, and it may be that aversive anorectic CGRP signalling in the lPBN is generated by neurons which express CCK receptors and/or are activated by GDF15.

As GDF15 also cause the activation of non-*Calca* neurons in the elPBN, other neuronal types in this area were also investigated. PENK and PDYN are opioid peptides which are known to be affected by the ingestion of food and are involved in the regulation of feeding behaviour during stress in forebrain regions (Clement-Jones and Rees, 1982; Christiansen *et al.*, 2011). These peptides are both expressed in the lPBN.

Though GDF15 did not activate PENK neurons in the PBN, due to the uncertainty of the nature of PENK signalling in the PBN, this does not provide evidence that GDF15

might be causing anorexia via more than just aversive pathways. Further research on the action of PENK[PBN] neurons would be needed to confirm this. The involvement of PENK[PBN] neurons in control of food intake could be assessed by preventing signalling of these neurons with a caspase virus during a feeding study. Alternatively, PENK[PBN] neurons could be induced to express a stimulatory DREADD or channel rhodopsin, and this population could be stimulated, and food intake measured. The valency of these neurons could then be measured using CTA or CPA coupled with the chemogenic or optogenetic activation of this neuronal population to assess whether food intake is affected due to satiety or aversion.

Although PENK neurons clearly affect food intake and are located in a similar region of the PBN that is activated by GDF15, it is unlikely that GDF15/GFRAL signalling would utilise PENK neuronal signalling to cause anorexia. As mentioned earlier, PENK neurons elsewhere in the brain are involved in signalling to increase food intake in response to types of stress which do not cause the release of GDF15 (Patel *et al.*, 2019; Lockhart, Saudek and O'Rahilly, 2020). Like GDF15/GFRAL signalling, PENK signalling does not seem to be a part of normal homeostatic control of feeding and rather than reducing feeding by inducing satiety through reward pathways, it increases feeding in response to stressors. The result of this is a dampening of stress pathways which GDF15/GFRAL signalling activates (Blasio *et al.*, 2014; Di Bonaventura *et al.*, 2014; Cimino *et al.*, 2021). Although enkephalins act on opioid receptors and there is an abundant expression of mu opioid receptors in the lPBN (Huang *et al.*, 2021), enkephalins preferentially act on delta opioid receptors (Le Merrer *et al.*, 2009). Furthermore, evidence thus far indicates that GFRAL neurons are excitatory, containing both glutamate (Fig. 4.2C) and catecholamines (Fig. 4.2B). It is therefore unlikely that GFRAL neurons inhibit PENK neurons in the lPBN to prevent their effect of increasing food intake.

Though activation of PDYN[lPBN] neurons has a similar effect to increasing GDF15 (Kim *et al.*, 2020), PDYN neurons were not activated by GDF15. This is to be expected when considering the following: 1) though PDYN neurons receive input from neurons in the NTS, the projecting neurons are located more medial in the NTS than where GFRAL neurons are located. Also, PDYN neurons appear not to receive input from the AP. 2)

PDYN neurons are activated by different stimuli than GFRAL neurons. Whilst PDYN neurons are activated by mechanoreception in the digestive tract, the release of GDF15, and therefore activation of the GFRAL signalling network, is unaffected by meal times and food consumption (Tsai *et al.*, 2015). Finally, 3) though PDYN neurons are expressed in the lateral portion of the PBN, much like neurons activated by GDF15, the bulk of PDYN neurons were seen in a more dorsal portion of the PBN. This dorsal region of the PBN in which PDYN neurons were found also did not co-localise with the area in which *Gfral*-Cre neurons were seen to project.

5.5.1.2   Forebrain

Moving outside of the PBN, the activation by GDF15 of neurons expressing PKCδ and CRH in the CeA, ovBNST, and PVH were explored. PKCδ neurons in the CeA are part of an anorectic pathway and are activated by both satiety and sickness signals (Cai *et al.*, 2014). Cai *et al.* (2014) showed that PKCδ neurons are activated by LPS. LPS causes the release of GDF15 (Luan *et al.*, 2019), which also causes the activation of PKCδ^{CeA} neurons (Fig. 5.3Ai). It is, therefore, possible that on exposure to sickness signals like LPS, PKCδ^{CeA} neurons are activated by the subsequent release of GDF15 as a part of the GFRAL signalling network.

Cai *et al.* (2014) also showed that *Calca* neurons in the lPBN signal directly to PKCδ in the CeA. The circuit from CGRP^{lPBN} to neurons in the CeA has been shown to be highly aversive in several publications and can be activated by stimuli which cause sickness and nausea such as LPS, LiCl, and the chemotherapy drug, cisplatin (Cai *et al.*, 2014; Alhadeff *et al.*, 2017). In this chapter, GDF15 caused the activation of *Calca*-Cre^{elPBN} neurons (Fig. 5.2A) and PKCδ^{CeA} neurons (Fig. 5.3Ai). FG studies also showed that *Calca*-Cre neurons activated by GDF15 in the elPBN signal to the CeA (Fig. 5.5E). Therefore, it is likely that GDF15 is activating the circuit described by Cai *et al.* (2014).

In the CeA and ovBNST, CRH neuron signalling is involved in binge eating (Iemolo *et al.*, 2013; Di Bonaventura *et al.*, 2014). In the PVH, CRH neurons are involved in signalling stress as a part of the HPA axis, which is necessary to coordinate the body's response to stress, including infection and disease (Turnbull and Rivier, 1999). The

activation of the HPA axis has well documented effects on food intake and body weight (Sominsky and Spencer, 2014).

There is emerging evidence that GDF15 plays a role in activating the HPA axis during infection and disease (Melvin *et al.*, 2020; Cimino *et al.*, 2021). As shown in this chapter, GDF15 caused the activation of CRH neurons in the PVH (Fig. 5.3B). We published this finding (Worth et al., 2020) and this was reaffirmed a year later in a publication by another group (Cimino *et al.*, 2021). Activation of CRH[PVH] neurons by GDF15 supports the theory that GDF15 is increased as a part of a stress response and that GDF15/GFRAL signalling is not part of the normal physiological control of food intake.

Interestingly, only an average of 31% of neurons activated by GDF15 in the PVH contained CRH (Fig. 5.3B). Therefore, whilst bearing in mind the fluorescent reporter may not have been present in every CRH[PVH] neuron, it is likely that GDF15 activated more than one neuronal type in this area. There are several different cell types in the PVH which affect food intake, including those which express MC4Rs, PENK and PDYN. It is unlikely that GDF15-activated PVH neurons contain any of these markers. PENK and PDYN positive PVH neurons are involved in signalling reward during binge eating (Christiansen, *et al.*, 2011; Martín-García *et al.*, 2011) and Hsu *et al.* (2017) showed that *Mc4r* KO in rats did not impact the effects of GDF15 on food intake or body weight. However, as a minority of neurons activated by GDF15 in the have been identified, it would still be worth further investigation to phenotype the rest of these neurons and gain a more complete picture of the role of the PVH in the GFRAL signalling network.

Overall, data in this chapter further supports results in Chapter 3 which indicate that GDF15 has negative valency and triggers anorexia and weight loss via aversive central signalling pathways. Immunohistochemistry performed to investigate neuronal activation by GDF15 revealed that GDF15 activated several neuronal types known to be a part of aversive pathways, such as neurons which contain *Calca*, in the PBN, neurons which contain PKCδ in the CeA and ovBNST, and neurons which contain CRH in the PVH. Though CCK[NTS] neurons which signal to the PVH have been shown to have

positive valence (Roman, Sloat and Palmiter, 2017), the majority of data here highlight anorectic signalling pathways which cause nausea, malaise, and aversion. Therefore, the GDF15/GFRAL signalling network may cause anorexia using pathways with both positive and negative valence, with the overall effect being aversive. The aversive nature of GDF15 should perhaps not be surprising, as it is released in circumstances of disease and cellular stress.

5.5.2 GFRAL signalling network

The second objective of this chapter was to establish connections between the different regions of the brain involved in GDF15 signalling. This again was to further understand how GDF15/GFRAL signal to cause anorexia and weight loss. In this chapter, two methods were used to address this goal.

Firstly, the retrograde tracer, FG, was injected into regions which had been shown to be activated by GDF15 in Chapter 3. FG is taken up in the synapses of neurons at the injection site and carried back to the cell bodies. Co-localisation between FG and neurons activated by GDF15 in other regions suggests which areas project to neurons at the FG injection site. In this chapter, FG was successfully utilised to show connections from the following types of neurons which are activated by GDF15:

- GFRAL[DVC] neurons to the PBN
- From mNTS neurons which are responsive to GDF15 to the PVH
- From *Calca*-Cre[elPBN] neurons to the CeA and back from the CeA to both *Calca*–Cre and non-*Calca*-Cre neurons in the elPBN
- From The elPBN to the BNST
- From the PVH to the PBN
- From the CeA to the BNST

This effectively links all areas activated by GDF15 to each other and implicates several known anorectic signalling pathways which GDF15/GFRAL could be using to reduce food intake and body weight. These connections are summarised in Figure 5.6.

Whilst FG is a useful tool and has provided plenty of information here, it does have some drawbacks. Namely, that FG spreads at the site where it is injected. Therefore,

if the area targeted is very small, FG is likely to reach other areas around the target, potentially confusing the results. This is especially pertinent when interpreting results for FG injections targeted at the ovBNST. In this experiment, though coordinates were refined, and the smallest possible volume of FG was injected, there was still spread to the rest of the BNST. As there are known connections between the NTS and other areas of the BNST (Berthoud *et al.*, 1990; Williams *et al.*, 2018), it is impossible to be certain which part of the BNST the small number of GFRAL-negative, GDF15-activated neurons in the mNTS (Fig. 5.4D) project to.

For the same reason, FG would not have been suitable to investigate the potential connection between GFRAL[DVC] neurons and non-GFRAL neurons in the mNTS which are activated by GDF15. Therefore, another technique had to be employed to discover whether GFRAL neurons in the DVC connect with non-GFRAL neurons in the mNTS. To investigate this connection, the *Gfral*-Cre mouse was crossed with the ChR2-eYFP line, which caused the expression of eYFP in the cell bodies and the neuronal processes of *Gfral*-Cre neurons. This allowed visualisation of projections from GFRAL neurons to their target sites, including the mNTS. This model also supported FG data, showing that GFRAL neurons project directly to the elPBN, but not to other forebrain structures.

Though these studies show connections between different areas of the brain, they do not prove functional connection. The final step in investigating the connections between regions in the GFRAL signalling network would therefore be to use a technique such as channel rhodopsin-assisted circuit mapping, to prove functional connections between GFRAL and other neuronal types in the GDF15/GFRAL signalling network. This is now possible due to the development of our *Gfral*-Cre mouse line, and the availability of other mouse lines such as the *Calca*-Cre, *Crh*-Cre, and PKCδ–Cre. Before, a proxy for these populations would have been required, such as using a *Cck*-Cre mouse to investigate connections of GFRAL neurons or *Slc17a6*-Cre mouse to investigate the connections of CGRP neurons. This would have given less accurate results as GFRAL and CGRP neurons are subpopulation of CCK neurons in the DVC and glutamatergic neurones in the PBN, respectively.

5.5.3 Summary
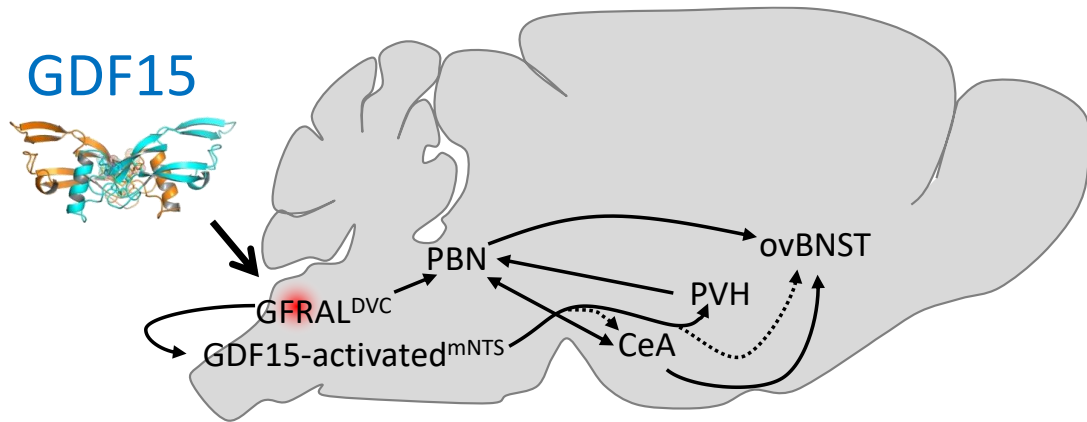
Figure 5.6. Summary of GDF15/GFRAL signalling network. Connections between GFRAL neurons activated by GDF15 in the DVC (GFRAL^{DVC}) and neurons activated by GDF15 in the medial portion of the nucleus of the solitary tract (mNTS), the parabrachial nucleus (PBN), the central amygdala (CeA), the oval nucleus of the bed nucleus of the stria terminalis (ovBNST) and the paraventricular nucleus of the hypothalamus (PVH). Solid arrows denote connections between areas. Dotted arrows denote weak connections with very few neurons involved.

5.6   Conclusions

- The phenotypes of many neurons activated by GDF15 outside of the DVC have now been established, with GDF15 causing the activation of neuronal types in the PBN, CeA, ovBNST, and PVH which are known to be connected to signalling stress and aversion

- Connections between areas activated by GDF15 have successfully been explored using retrograde tracing studies and fluorescent marking of *Gfral*–Cre neurons

- GDF15 activates known pathways which cause anorexia via aversion

- GFRAL neurons project directly to the mNTS and elPBN, but indirectly to other areas which are activated as a result of the administration of exogenous GDF15

6 GDF15 secretion in mouse models of cancer

6.1 Introduction

Anorexia and weight loss, in particular cachexia, pose a significant threat to cancer patients. Between 40% and 80% of cancer patients are expected to experience anorexia and weight loss, depending on the type and stage of cancer (Argilés *et al.*, 2014). Furthermore, ACS increases patient mortality and was responsible for up to 20% of cancer deaths in 2014 (Argilés *et al.*, 2014). Sometimes, weight loss and anorexia during cancer is caused by physical blockage of the GIT or the tumour impacting the ability to absorb nutrients in another way (e.g. neuroendocrine pancreatic tumours altering the release of hormones such as gastrin, somatostatin, or glucagon) (Hendifar *et al.*, 2019). However, there are many other cancer types which also feature anorexia and weight loss. As of yet, the cause in these cases is not certain and there is no effective treatment for anorexia and weight loss during cancer.

There is evidence across different types of cancers, from preclinical rodent models and humans, that cancer can cause an increase in circulating GDF15 (Altena *et al.*, 2015; Lerner *et al.*, 2015; Suriben *et al.*, 2020). Elevated GDF15 causes anorexia, weight loss and nausea. Evidence for additional roles in cancer is conflicting. Like other members of the TGFβ family, GDF15 can either be a positive or a negative prognostic marker during cancer.

Historically, synthetically derived GDF15 has been shown to be contaminated with very small quantities of other TGFβs (Olsen *et al.*, 2017). Unfortunately, even in such small quantities, TGFβs can affect tumour growth and development. Therefore, results of studies investigating the effects of GDF15 on cancers in *vitro* should be interpreted with care. However, there is also substantial data from humans, rats, and mouse models showing a range of effects of GDF15 on cancer in *vivo*, though results are often conflicting.

In some scenarios, the presence or increase of GDF15 is a positive prognostic marker, with GDF15 promoting apoptosis by sensitising cancer cells to non-steroidal anti-inflammatory drugs (NSAIDs) (Baek *et al.*, 2000; Martinez *et al.*, 2006; Lincová *et al.*, 2009) and allowing the anti-proliferative effects of other cancer therapy drugs (Zimmers *et al.*, 2010). GDF15 can slow tumour growth, repress tumour cell proliferation, promote infiltration of macrophages into the tumour, and increase rates of survival (Husaini *et al.*, 2015; Ratnam *et al.*, 2017; Lu *et al.*, 2018).

On the other hand, an increase in GDF15 during cancer is frequently detrimental to a good prognosis. GDF15 can promote cancer cell invasion and metastasis (Senapati *et al.*, 2010; Griner, *et al.*, 2013; Aw Yong *et al.*, 2014; Siddiqui *et al.*, 2022), promote neoangiogenesis alongside vascular endothelial growth factors (VEGF) (Huh *et al.*, 2010; Song, *et al.*, 2012), increase tumour growth and proliferation (Brown *et al.*, 2003; Chen *et al.*, 2007; Griner *et al.*, 2013), promote drug tolerance of cancer cells (Bellio *et al.*, 2022), and decrease immune response by suppressing macrophage activity (Ratnam *et al.*, 2017). These effects may occur as GDF15 suppresses the release of TNFα, IL-1, IL-6, and macrophage colony-stimulating factor (MCSF) (Bootcov *et al.*, 1997). In general, increased circulating GDF15 can lead to decreased survival rate/increased risk of mortality (Lerner *et al.*, 2015). The determining factor for GDF15 to be a positive or a negative marker seems to depend on both the type and severity of the cancer.

Alongside these effects, GDF15 has been linked with cancer-induced anorexia and weight loss (Johnen *et al.*, 2007). In particular, increased GDF15 has been linked to cancer cachexia (Lerner, Tao, *et al.*, 2016; Suriben *et al.*, 2020). Since cachexia is known to greatly impact risk of mortality for cancer patients, there is a clear need to study anorexia and weight loss in cancer and GDF15 provides an interesting target to focus on.

Many cancer studies investigating GDF15 have used patient-derived xenograft models, which have been screened for cells known to release GDF15, or otherwise have used cells specifically engineered to over produce GDF15. I aimed to use a syngeneic tumour model, one where the tumour cells originate in the same strain of

mouse, in order that we did not need to use immunocompromised mice and, therefore, have a more relevant response to the presence of a tumour. Likewise, engineered cells were not used in the hope that different types of tumours could be tested to see if there is a relationship between different types of cancer and GDF15 secretion.

Subcutaneous Lewis lung carcinoma (LLC) and CT26 colon carcinoma cells are two of the best established mouse cachexia models and are commonly used in cancer anorexia and weight loss/cachexia studies (Ballarò *et al.*, 2016). LLC cells originate in C57Bl6/J mice, however, CT26 cells were originally derived from Balb/c mice. Therefore, LLC cells were favoured for the following studies. MC38 colon carcinoma cells, originating in C57Bl6/J mice, have also been shown to cause weight loss (Bae *et al.*, 2019). The approach in this chapter was designed to explore the relationship between cancer anorexia and weight loss and the secretion of GDF15 in different mouse models, in the hope of ascertaining whether the GDF15/GFRAL signalling network might be a good target to combat cancer anorexia and weight loss.

6.2   Aims and objectives

Hypothesis: Cancer anorexia and weight loss is associated with the expression of circulating GDF15.

Aim: To define GDF15 secretion in mouse models of cancer and establish whether there is a link between GDF15 secretion and anorexia and weight loss in murine cancer models.

1) Establish murine cancer models which do, and do not, display anorexia and weight loss
   - Run a pilot study to measure food intake, body weight, and body composition in known cancer cachexia mouse models
2) Explore effects of cancer on the GDF15/GFRAL signalling network
   - Measure GDF15 in plasma and activation of GFRAL neurons in murine cancer models

3) Perform correlation analysis to establish whether there is a correlation between cancer-induced anorexia and weight loss and GDF15.

6.3 Methods

6.3.1 Animals

12-week old male C57BL6/J mice (Charles River, UK) were used in the subcutaneous tumour study using either LLC or MC38 colon carcinoma cells. 6-week old female C57BL6/J mice (Charles River, UK) were used for the orthotopic LLC study. All mice were kept under standard conditions as described in General Methods 2.2.

6.3.2 Cells and cell culture

All cells were kindly gifted by Dr Jamie Honeychurch and his colleagues in the Tim Illidge group at Cancer Research UK, Manchester Institute. LLC cells and MC38 colon carcinoma cells were grown *in vitro* in complete media, which was composed of high glucose Dulbecco's Modified Eagle's Medium (DMEM. Sigma Aldrich, UK) containing 10% FBS (Thermofisher, UK). Cells were split when they had reached 80-90% confluency, as assessed by observing the cells under a light microscope. Cells were passaged no more than three times before inoculation into mice.

To prepare cells for injection, cells were washed in sterile PB (Sigma Aldrich, UK), then detached from the flask by incubating in trypsin-EDTA (Sigma Aldrich, UK) for 3 min at 37°C. Detachment was assessed by visual inspection at 10x magnification on a light microscope. If cells were still adhered, then the flask was incubated for a further 2 min and the process repeated until cells were no longer adhered (incubation in trypsin did not exceed a maximum of 15 min). When cells were free-floating, complete media was added to neutralise the trypsin and then the cell solution was centrifuged at 500 XG for 5 min. Supernatant was removed and cells re-suspended in 1 ml serum-free media.

Concentration of cells was estimated by counting the number of cells in 10 μl free-floating cells solution within the grid of a haemocytometer. Free-floating cells were then diluted with serum-free media to produce 2×10^7 cells/ml.

All manipulations of cells were performed using aseptic technique in a laminar flow hood.

6.3.3 Subcutaneous tumour study

This study was carried out at the University of Manchester under Prof. Simon Luckman's project licence.

The day before the start of the study, mice were scanned in an EchoMRI 9000 scanner as described in General Methods (2.5). On day 0, mice were anaesthetised using 3% isoflurane in oxygen, which was decreased to 2% for maintenance. Fur over the flank was shaved and skin was swabbed with iodine. Mice were then inoculated with 100 µl serum-free media (n=4, Sigma Aldrich, UK), 100 µl serum-free media containing $2x10^6$ LLC cells at P10 (n=4), or 100 µl high glucose DMEM (serum-free media) containing $2x10^6$ MC38 cells at P7 (n=4) subcutaneously into the flank. From this point food intake, body weight and tumour volume were measured daily until mice reached a humane end point. Humane end points were defined as loss of 20% of initial body weight or when the tumour had reached a volume of 1500 mm^3. On the final day of the study, mice were scanned in the EchoMRI immediately before decapitation under deep isoflurane anaesthesia.

Blood and brains were collected and processed as described in General Methods (2.6.1 and 2.6.2 respectively). Tumours were also dissected, formalin-fixed overnight, and paraffin-embedded.

6.3.4 Orthotopic lung cancer study

This study was carried out at Alderley Park, under Dr Jamie Honeychurch's project licence. This licence did not permit the single housing of mice, therefore, female C57 mice were housed in groups of five. Ten mice (2x cages) were inoculated with $1x10^5$ LLC cells in 50 µl PB orthotopically into the left lung, using the finest gauge needle possible, under isoflurane anaesthesia. These mice formed the LLC group. Control mice were not injected into the lung. From this point, food intake for the cage and individual body weight were measured three times per week. As mice were group-housed, cumulative food intake for this study was calculated and presented per cage.

Body weight calculations remained as per animal. This study was designed to end when mice had either lost up to 15% of original body weight or started to show signs of respiratory distress.

At time of cull, mice were anaesthetised using isoflurane in 3% oxygen and cardiac puncture was performed. Blood, brains, and lungs were dissected and processed as described in General Methods (2.6).

Formalin-fixed lungs were placed into 70% ethanol for four days before images were taken.

6.3.5 Immunohistochemistry

As mice in these studies were culled via cardiac puncture, it was not possible to perform a transcardial perfusion. Instead, brain tissue was dissected, post-fixed in 4% paraformaldehyde overnight at 4 °C and then placed in 30% sucrose until it sank. All IHC was carried out using the standard protocol described in 2.8.3 and imaged using a fluorescent microscope (2.8.4). Antibodies used for fluorescence IHC can be found in General Methods (2.4.1. Table 1)

6.4   Results

6.4.1 Subcutaneous LLC and MC38 tumours

A small pilot study was performed to find potential models of cancer-induced anorexia and weight loss. Food intake, body weight, GDF15 concentration in plasma, and fat/lean mass were measured in mice bearing subcutaneous LLC or MC38 tumours.

In this study, neither subcutaneous LLC nor subcutaneous MC38 tumours affected food intake (Fig. 6.1A) or body weight (Fig. 6.1B) compared with control animals. When the weight of the tumour was removed from total body weight, mean body weight of control animals increased from 26.75 ±0.71 g to 27.98 ±0.61 g over the 15 days of the study ($p = 0.0028$). However, mean body weight for the LLC and MC38 groups did not increase ($F_{(9, 135)} = 10.30$, $p = 0.1659$ and $p = 0.1047$, respectively. Fig. 6.1C).

Similarly, there was no statistically significant difference between days 0 and 15 for fat or lean mass in any group (Fig. 6.1 D&E respectively. $F_{(9, 9)} = 2.043$, $p = 1510$ and $F_{(9, 9)} = 8.515$, $p = 0.0019$ respectively). In the control group, there was a trend towards an increase in fat mass, with fat increasing from a mean of 2.04 ±0.35 g to 2.89 ±0.21 g ($p = 0.0725$). This trend was not present in either cancer group. Neither tumour type caused an increase in GDF15 release (Fig. 6.1F).

This study was terminated after 15 days as tumours were reaching maximum allowable volume, and several had begun to ulcerate. As these models did not display anorexia, significant changes in body weight, or changes in circulating GDF15, further investigation into central activation of the GFRAL signalling network was not performed.
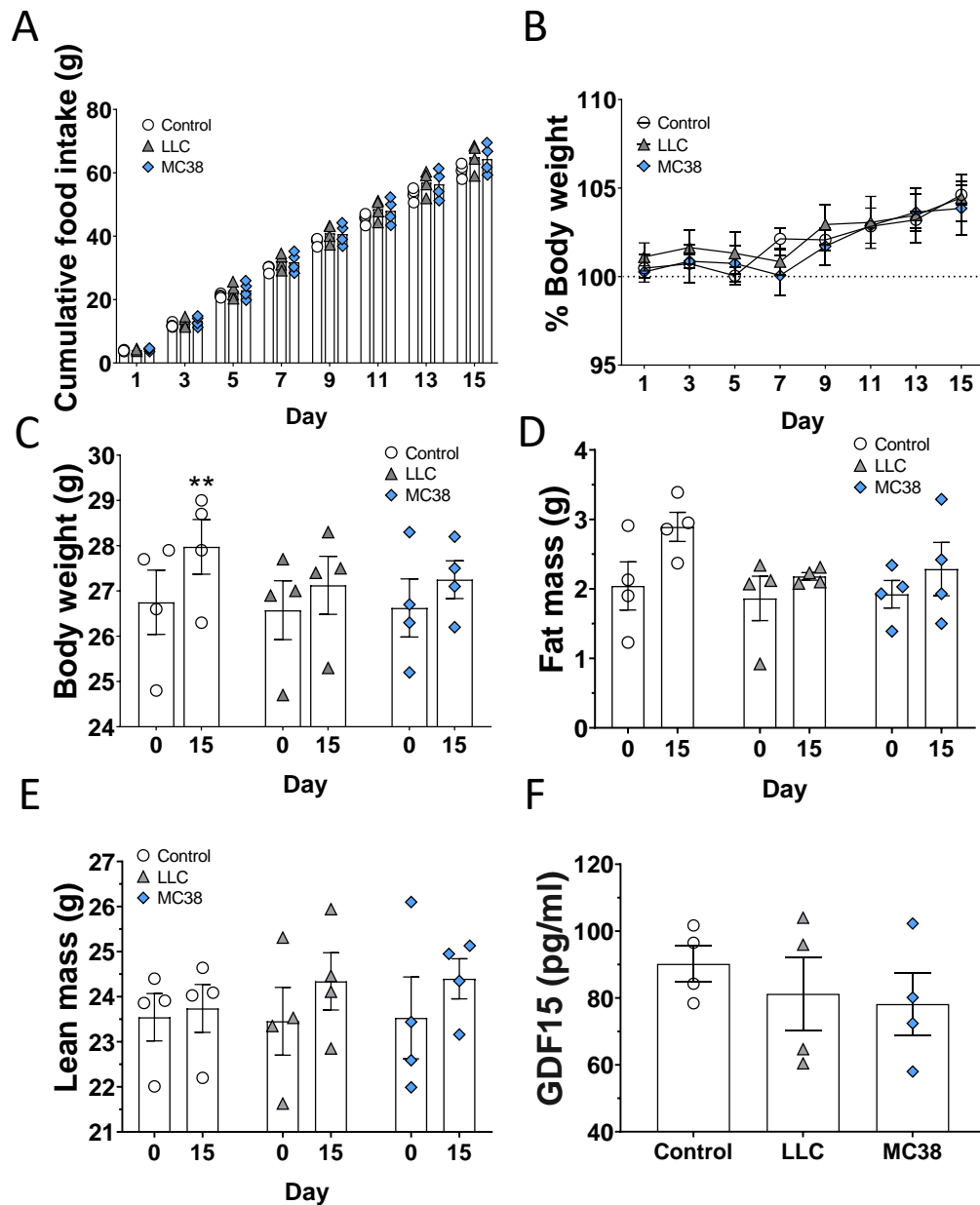
Figure 6.1. The effect of subcutaneous tumours on food intake, body weight and plasma GDF15. Male C57 mice were implanted subcutaneously with serum-free media (control) Lewis lung carcinoma (LLC) cells or murine carcinoma 38 (MC38) colon carcinoma cells into the flank. A) Food intake and B) % body weight change were measured over the next 15 days. Weight of the tumour was subtracted from the total body weight on day 15, and C) Tumour-free body weight, D) fat mass, and E) lean mass at day 0 and 15. F) Plasma GDF15 concentration on day 15. n = 4/group. Food intake and % body weight were analysed using a two-way ANOVA with a post hoc Tukey's multiple comparisons test. Body weight compared within groups over the course of the study, fat mass, and lean mass were analysed using a two-way ANOVA with a post hoc Sidak's multiple comparisons test. GDF15 concentration was compared using a one-way ANOVA with a post hoc Dunnett's multiple comparisons test. ** p < 0.01.

6.4.2 Orthotopic lung carcinoma

Another LLC cancer model was also investigated. In this model, LLC cells were injected orthotopically into one lung. Orthotopic LLC tumours caused a trend towards decreased food intake from approximately day 6 after inoculation with LLC cells, which became more pronounced as time passed (Fig. 6.2A). As mice were group housed, there were only two data points recorded for each group at each time point. Therefore, the food intake measurements were not significantly different at any time point in this study.

Over the course of the 15-day study, the control group gained significantly more body weight than the LLC group, the difference becoming apparent by day 13 ($p < 0.0463$. Fig. 6.2B). Within the LLC group, there was substantial variability in body weight change, with body weight change being between -15% and +6%. For some mice in the LLC group, body weight had begun to decrease as early as day 3. In this study, time did have a statistically significant effect on body weight ($F_{(18, 108)} = 24.30$, $p < 0.0001$)

By day 15, mice were showing signs of respiratory distress caused by tumour growth in their lungs (Fig. 6.2C). Therefore, on humane grounds, mice were culled, and blood was taken. GDF15 concentration in plasma collected on day 15, immediately before cull, was increased in the LLC group compared with the control group ($p = 0.0399$. Fig. 6.2D). The concentration of GDF15 in the plasma of these mice did not correlate with body weight loss (Fig. 6.2E).

Though there was an increase in activation in the DVC caused by the LLC tumours as measured by the presence of cFos (Fig. 6.2F&G), there was no activation of GFRAL neurons (Fig. 6.2G) in either group.
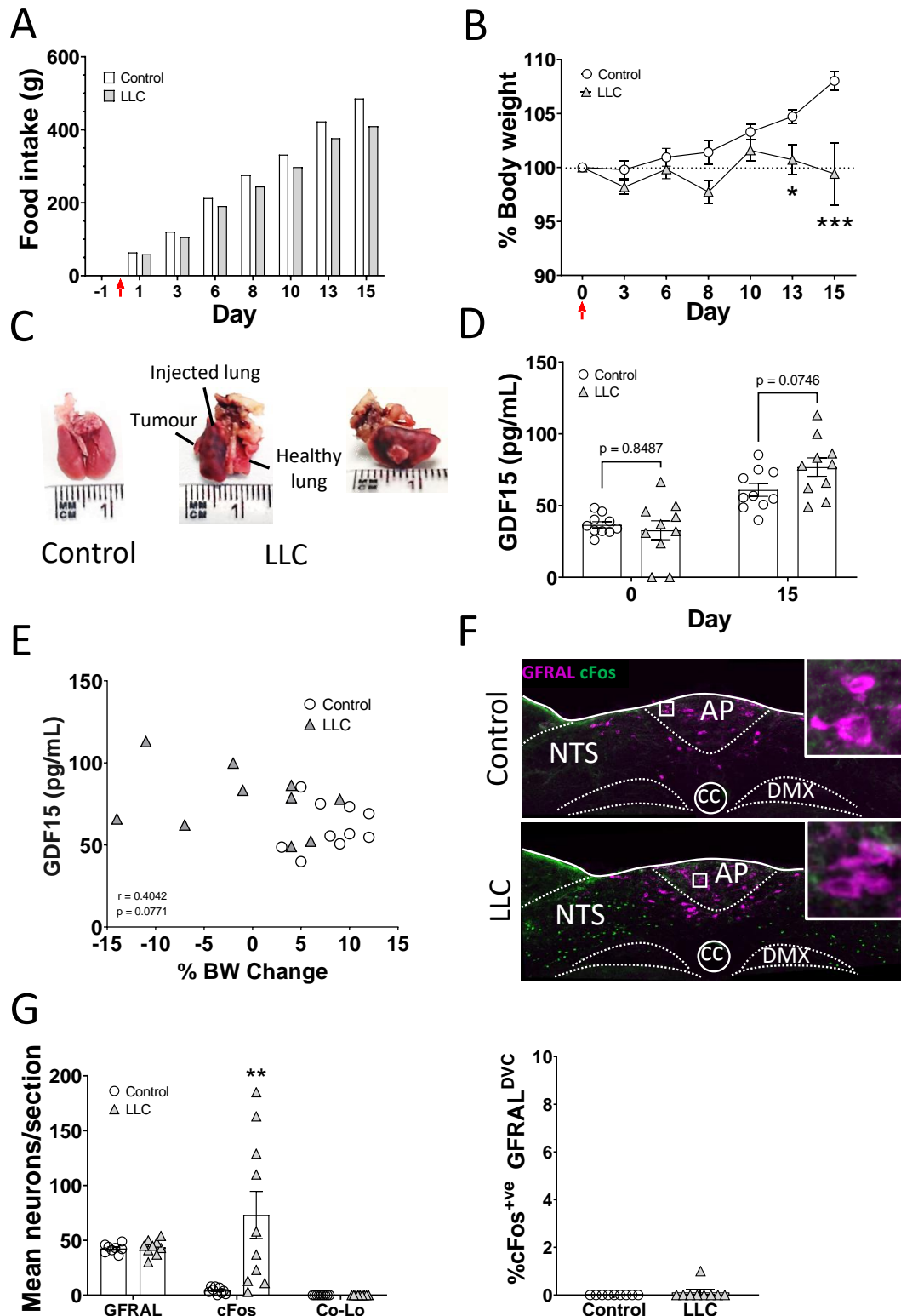
Figure 6.2. Effect of orthotopic lung carcinoma on feeding, body weight, and GDF15/GFRAL signalling. A) Food intake per cage (n = 5 mice/cage. n = 2 cages/group) and B) individual body weight of wild-type mice for 15 days following no intervention (control) or inoculation with Lewis lung carcinoma (LLC) cells into the left lung. Red arrow indicates day of inoculation with LLC cells. C) Examples of healthy control lungs vs. lungs of a mouse which had been inoculated with LLC cells. Lungs taken on day 15 after inoculation. D) GDF15 concentration in plasma taken from mice

on day 0, the day of inoculation, and day 15, at time of cull. E) The correlation between GDF15 concentration and % body weight change for mice in control and orthotopic LLC groups. F) the effect of orthotopic LLC burden on GFRAL^{DVC} activation after 15 days; GFRAL-expressing neurons (magenta) and cFos (green). G) Quantification of the mean number of neurons/section which express GFRAL, cFos, and both GFRAL and cFos (co-lo) and the percentage of GFRAL^{DVC} neurons activated. AP = area postrema, cc = central canal, DMX = motor nucleus of the vagus/10th cranial nerve, DVC = dorsal vagal complex, NTS = nucleus of the solitary tract. n = 10/group. Data checked for normal distribution using a Shapiro-Wilk test and analysed using two-way ANOVA followed by post hoc Sidak's multiple comparisons test. Mean neurons/section analysed using multiple t tests. * $p < 0.05$, ** $p < 0.01$, *** $p<0.001$.

6.5 Discussion

The studies in this chapter sought to establish different murine cancer models which show anorexia and weight loss caused by signalling from either the tumour or its extracellular matrix, in order to investigate whether cancer anorexia and weight loss might be linked to the secretion of GDF15. Models which show anorexia and weight loss due to other known reasons, such as physical blockage of the GIT or interference with food digestion and absorption (i.e., gut, colon, or pancreatic tumours, where the mechanism of weight loss is due to the inability of the animal to absorb nutrients) were avoided to establish whether GDF15 might be a contributing or causative factor of cancer anorexia and weight loss. The ideal model would also have been syngeneic in C57Bl/6 mice, for this reason, LLC and MC38 cell lines were used to generate tumours.

The subcutaneous LLC model was chosen as it is one of the two most common models used to study cancer cachexia (Ballarò, et *al.*, 2016) and originates from C57Bl/6 mice. Beyond this, there are many murine cancer models, with cells originating in C57Bl/6 mice, which can cause weight loss or cachexia. Amongst these is the MC38 colon carcinoma cell line, which were available in, and kindly donated by, Dr Jamie Honeychurch's group. Subcutaneous models were preferred over orthotopic cancers as tumours growing subcutaneously do not interfere with the normal functioning of vital organs, and therefore allow the effects of the tumour alone to be studied.

In 2017, Campos *et al*. published a set of experiments in which LLC cells were implanted subcutaneously into the left flank of *Calca*-Cre mice, very similar to the subcutaneous LLC model described and used in Fig. 6.1. In their publication, Campos *et al*. showed that subcutaneous LLC tumours caused anorexia, weight loss, and activation of *Calca*-Cre (CGRP) neurons in the elPBN, activation of the ovBNST and CeA. They also caused a decrease in fat mass, and increases in sickness behaviour (Campos *et al.*, 2017). These findings were confirmed by Bae *et al*. (2019). In their publication, subcutaneous LLC tumours also caused weight loss, and in addition, muscle weakness, muscle wasting, fatigue, and an increase in inflammatory cytokines

in circulation (Bae *et al.*, 2019). Bae *et al*. (2019) also measured these parameters in mice with subcutaneous MC38 tumours, finding similar results.

In this chapter, subcutaneous LLC and MC38 models did not increase in body weight/fat mass during the study in the way which non-tumour bearing controls did, which suggests that the cancers were having an effect (Fig. 6.1C). However, the mice could not be maintained to assess whether they would have deteriorated over a longer time period as tumour size and condition for both models meant that the outlined humane endpoints had been reached by day 15. In contrast to effects of these tumours reported in literature, these LLC and MC38 tumours did not cause body weight loss, anorexia, or change lean or fat mass (Fig. 6.1A-E). These models therefore did not behave in the way expected by examining the literature and so were not viable models of cancer anorexia/cachexia for use in my studies.

The difference between the LLC and MC38 models used in the current study and the subcutaneous LLC and MC38 models used by Campos *et al*. (2017) and Bae *et al*. (2019) may be due to divergence in the cell lines used by each group. For researchers studying the mechanics of tumour growth and metastasis, or for those whose research is concerned with treating tumours, body weight is used as a measure of wellbeing for mouse models and humane end points are often based on body weight loss. In these scenarios, having a cancer model which causes weight loss would be detrimental to the research. It therefore follows that most models used by cancer-research groups have been selected as they do not affect food intake or body weight.

As the LLC and MC38 cells in the current model were kindly donated by a group which investigates the treatment of tumours, it is possible that divergence has occurred in this line over time, with mutations in the cell lines which cause a greater or lesser impact on food intake and body weight being selected for dependent on what research was being performed. CT26 cells were also available from this group, but as this cell line is derived from Balb/c mice and has been extensively studied by the group and never found to cause weight loss, it was decided not to investigate this cell line.

Seemingly, cancer weight loss studies are mostly performed by groups in the USA and Japan, so finding a cancer model with anorexia and weight loss, not caused by physical abnormalities in the GI tract or digestive system and available in the UK, proved challenging.

As the two subcutaneous tumour models did not provide significant anorexia, weight loss, or GDF15 secretion, it was decided that a different form of LLC should be investigated. An orthotopic MC38 was not explored as MC38 cells originate from the colon, and disruption of the gastrointestinal tract would have introduced confounding causes of anorexia and weight loss. In the orthotopic LLC study (Fig. 6.2), LLC cells were injected directly into one lung of the mice, causing disruption to the function of a vital organ. This was unlike the SC tumours, which simply grew under the skin.

Orthotopic LLC tumours and, seemingly, time, caused a small, but statistically significant, increase in circulating GDF15 between and within groups of mice (Fig. 6.2D). As GDF15 is released in response to hypoxia (Hinoi *et al.*, 2012) and is increased by aging (Liu *et al.*, 2021; Welsh *et al.*, 2022), the presence of tumours in the lungs could explain the increase between groups. However, at 14 weeks (the age of mice at the termination of the study), mice might not be particularly considered 'aged'. As circulating GDF15 was increased in both groups, it is unlikely that this increase in GDF15 was due to any pathology. For both groups of mice, the increase in GDF15 was not sufficient to cause the activation of GFRAL neurons in the DVC (Fig. 6.2F).

Orthotopic LLC tumours also caused a variable change in body weight and possibly anorexia. In this study, some mice in the LLC group lost weight, others followed the same trajectory as the control group, and gained weight (Fig. 6.2B). Due to licencing restrictions, it was necessary to group house the animals in this experiment and consequently, there were only two values for food intake recorded at each time point. This effectively decreased the n number for food intake measurements. Although there was no significant difference in food intake between groups during this study (Fig. 6.2A), it is probable some LLC tumour-bearing mice were also anorectic. This variability could have been due to the cancer being more developed

in some mice than others, and therefore causing some mice to become unwell and not others in the cancer group. Indeed, there were near significant differences in absolute GDF15 levels (p = 0.0746) and the correlation of GDF15 and weight loss (p = 0.0771). This suggests that significance may have been reached with larger group size.

On the other hand, two animals in the orthotopic LLC group had to be culled on day 14, one day before the other mice. For these mice, one had lost weight over the course of the study, whilst the other had gained and was still showing increased body weight vs. the start of the study on the day of cull. This may indicate that the size/impact of lung tumours was not strongly linked to the cause of weight loss in these mice.

The orthotopic lung cancer model caused significant morbidity in comparison with the subcutaneous model, with the animals reaching the humane endpoint of respiratory distress. However, evidence in this study would indicate that effects on food intake and body weight were not due to GDF15/GFRAL signalling. in this orthotopic model, the humane endpoint reached was laboured breathing due to the size of tumours present in the lungs. Though mice could have been hypoxic at this point, GDF15 in the LLC group was only slightly increased compared with the control group (Fig. 6.2D) and GFRAL neurons were not activated (Fig. 6.2F&G).

In the orthotopic LLC model, some mice started showing weight loss as early as day 3 after inoculation and though there was no activation of GFRAL neurons, there was increased cFos in the DVC of tumour-bearing mice (Fig.6.2F&G). Perhaps then in this model, lung tumours caused weight loss and activation of the DVC via another signal such as IL-6 or TNF-α, both of which are known to be increased by subcutaneous LLC tumours (Ballarò, et *al.*, 2016) and have been linked with weight loss during cancer (Fearon *et al.*, 2012; Narsale and Carson, 2014; Onesti and Guttridge, 2014).

Unfortunately, due to Covid and difficulties in arranging experiments between collaborating labs working under different Home Office licences, it was difficult for me to progress this part of my project. If I had, the orthotopic lung cancer model

could have been altered by initially injecting a smaller number of cells to achieve slower tumour growth. This would then allow us to assess whether GDF15 would increase if given more time. However, as the weight-loss effects were so dramatic in some mice in this cohort, and in the absence of GFRAL activation, it is unlikely that weight loss in these mice is being caused by GDF15/GFRAL signalling. This would indicate that the use of these LLC cells is not a good model to investigate whether GDF15/GFRAL signalling causes cancer anorexia and weight loss.

As neither the subcutaneous or orthotopic tumours here caused the expected anorectic and weight loss/cachexia effects described in literature, these are not suitable models of ACS and should not be used to assess whether GDF15 has a role in causing anorexia/weight loss. However, this should not stop further investigation into the usefulness of preventing GDF15/GFRAL signalling during cancer in future. Despite these initial results, there is ample evidence that GDF15 is linked to cancers, both in human patients and rodent models. Several groups have shown that there is a link between GDF15 and cancer anorexia and cachexia (Johnen *et al.*, 2007; Tsai *et al.*, 2016; Borner *et al.*, 2017; Suriben *et al.*, 2020; Ahmed *et al.*, 2021). Indeed, Suriben et al. (2020) show that cachexia can be caused by cancers in rodent models, and that this can be combatted by blocking GFRAL signalling.

6.6 Conclusions

- Subcutaneous LLC and MC38 tumours did not cause anorexia, weight loss or affect GDF15

- Orthotopic LLC tumours caused rapid weight loss in some mice and may have caused anorexia, without significantly affecting the concentration of circulating GDF15 or causing activation of GFRAL^{DVC} neurons

- GDF15 in cancer anorexia and weight loss/cachexia is still a valid avenue of investigation, but appropriate models still need to be found

7 GDF15 secretion in mouse models of chemotherapy

7.1 Introduction

As previously outlined, many cancers cause anorexia and weight loss/cachexia, with detrimental effects to the patient in terms of both quality of life and prognosis. In addition to cancer, chemotherapy treatment can also cause ACS. In the British National Formulary, a significant number of cancer therapeutic agents will show side effects, including 'nausea', 'sickness', 'vomiting', 'lack of appetite', 'stomach pain', and several other effects that will reduce food intake and lead to weight loss (Joint Formulary Committee, 2022). Whilst anorexia is a major factor leading to weight loss, many chemotherapy drugs are also associated with cachexia. This is particularly pertinent as cachexia can decrease the efficacy of chemotherapy treatment. This occurs by increasing the toxicity of many drug therapies, making lower doses less tolerable (Dewys et al., 1980; Molfino et al., 2010). There is also evidence that starvation caused by cachexia induces cancer cells to enter a dormant state, helping them to avoid being destroyed by chemotherapy (Prunier et al., 2018).

Cachexia is a condition which often features inflammation (Fearon *et al.*, 2011) and many pro-inflammatory markers have been shown to increase in preclinical models of chemotherapy-induced ACS and in human patients (Argilés *et al.*, 2014; Ezeoke and Morley, 2015; Ünal *et al.*, 2015; Lerner *et al.*, 2016; Cao *et al.*, 2021). Previously, studies investigating the causes of chemotherapy ACS have implicated the peripheral and central actions of pro-inflammatory markers. The markers most commonly found to be increased during cancer and following chemotherapy include, but are not limited to, IL-1β, IL-6, IL-8, TNF-α, and macrophage chemoattractant protein-1 (MCP-1) (Elsea *et al.*, 2015; Ezeoke and Morley, 2015; Ünal *et al.*, 2015; Lerner *et al.*, 2016; Wong *et al.*, 2018; Cao *et al.*, 2021).

Release of IL-1β, IL-6, the murine IL-8 homologue, keratinocyte-derived chemokine (KC), TNF-α, and MCP-1 are commonly affected by inflammatory disease and during

cachexia and chemotherapy treatment. In particular, IL-6 is associated with anorexia and cachexia (Yeh and Schuster, 1999; Ando *et al.*, 2014; Narsale and Carson, 2014; Elsea *et al.*, 2015). Intracerebroventricular (ICV) administration of IL-1β into the third ventricle (3V) causes muscle wasting (Braun *et al.*, 2011) and ICV TNF-α into 3V causes anorexia, weight loss, and increased oxygen consumption in rats (Arruda *et al.*, 2010). Interestingly, IP administration of IL-1β does not cause changes in muscle mass (Braun *et al.*, 2011), indicating that cachectic effects are directly from central signalling.

Up to this point, research investigating inflammatory markers and cachexia in mice have used gene knock out models or monoclonal antibodies to prevent the functioning of these markers. These have shown an effect on food intake and body weight but have not yet proven that any of these signals are the main cause of anorexia and weight loss (Cao *et al.*, 2021). Therefore, chemotherapy-induced ACS remains as challenging to treat as cancer-induced ACS. As GDF15 is increased by some drug therapies which cause anorexia and weight loss/cachexia (Hsu *et al.*, 2017; Coll *et al.*, 2019; Breen *et al.*, 2020), it is possible that GDF15 is increased by many different chemotherapy drugs and signals to cause ACS.

To begin to assess whether this is the case, chemotherapy models first had to be established. Though GDF15 is released in response to cell damage and stress (Chung *et al.*, 2017; Patel *et al.*, 2019) and chemotherapies are designed to cause cell damage/death, not all chemotherapies cause anorexia and weight loss. It was therefore essential to establish chemotherapy models which did and did not show these effects. This would allow us to elucidate whether GDF15 is responsible for the anorexia and weight loss. Therefore, chemotherapy drugs from different classes, with different mechanisms of action, were investigated. In this chapter, the four different chemotherapy treatments were selected based on literature search. As relatively few chemotherapy studies are designed to investigate anorexia and weight loss, some drug regimens were selected as they commonly appeared in studies aimed to treat tumours in mice.

The involvement of GDF15/GFRAL signalling in chemotherapy ACS has been most thoroughly investigated with regards to cisplatin (CIS) and other platinum-based therapies. It is thought that the main mechanism via which CIS, and other platinum-based drugs, cause cell death is by causing cross-links between strands of DNA, preventing their separation, and making transcription of new strands of DNA impossible (Riddell and Lippard, 2018; Ghosh, 2019). This prevents replication of DNA, leading the cells to apoptosis. CIS has previously been shown to cause anorexia and weight loss in mice (Hsu *et al.*, 2017; Borner, Shaulson, *et al.*, 2020; Breen *et al.*, 2020; Worth *et al.*, 2020), rats (Alhadeff *et al.*, 2015), and up to 90% of human patients (Altena *et al.*, 2015; Rapoport, 2017). CIS is known to induce the release of GDF15 and activate regions of the GFRAL signalling network, in rats and mice (Alhadeff *et al.*, 2015; Hsu *et al.*, 2017; Worth *et al.*, 2020).

The taxane drug, paclitaxel (TAX), and the nucleoside drug, gemcitabine (GEM), are also cytotoxic chemotherapeutics. TAX and GEM bring about cell death via different mechanisms. TAX causes the stabilisation of microtubules in cells, preventing mitosis and thereby inducing apoptosis (Matson and Stukenberg, 2011). As a nucleoside, GEM is an analogue for normal nucleotides. When GEM is incorporated into DNA during replication, it causes destabilisation or early termination of the strand, leading to apoptosis (Plunkett *et al.*, 1995). Common side-effects of both TAX and GEM treatment in humans include nausea, vomiting, and loss of appetite. TAX also frequently causes anorexia (Joint Formulary Committee, 2022). In addition to their use in human therapy, TAX and GEM are both frequently used to investigate the effects of chemotherapies in preclinical cancer models (Vassileva *et al.*, 2008; Zhang *et al*., 2014; Loman *et al.*, 2019; Ryu *et al*., 2019; Breen *et al.,* 2020; Sullivan *et al.,* 2021). In preclinical studies, TAX and GEM have been administered at a range of doses, and either as a single dose or as part of a chronic dosing regimen, depending on what is being investigated. Chemotherapy models in this chapter aim to reflect these different dosing regimens.

During cancer, it is common for patients to be treated with a combination of chemotherapy drugs. This allows each individual chemotherapeutic to be dosed at a lower level, reducing its side-effects, and the chance of cancer cells developing drug

resistance. Therefore, the final chemotherapy model selected used a combination of the immunosuppressant, cyclophosphamide, and the anthracycline, adriamycin (also known as doxorubicin). There are several proposed mechanisms of action for anthracyclines. The most accepted is that they can bring about cell death by intercalating in DNA and inhibiting the action of topoisomerases, thereby preventing DNA replication (Venkatesh and Kasi, 2022). These drugs are often dosed together as a treatment for breast cancer in human patients and has been shown to cause ACS in healthy C57Bl/6j mice (Wong *et al.*, 2018).

In this chapter, food intake, body weight and plasma GDF15 concentration are investigated in each of these chemotherapy models to find out whether GDF15 is a common factor in those drugs which do decrease food intake and body weight. Though other proinflammatory markers may not be causative of ACS, they may contribute to this phenotype. Therefore, the effect of chemotherapy treatment on a selection of proinflammatory signals will also be investigated in addition to activation of the central GFRAL signalling network.

7.2   Aims and objectives

Hypothesis: anorexia and weight loss during chemotherapy correlates with circulating GDF15 and activation of brain regions affected by GDF15.

Aim: To survey different types of chemotherapy treatment to establish whether different types of chemotherapy drug which cause anorexia and weight loss also affect GDF15/GFRAL signalling.

1) Develop murine chemotherapy models which do and do not cause anorexia and weight loss.

   - Establish which of these models affect GDF15 release.

   - Investigate whether other proinflammatory signals are affected by chemotherapy treatments which cause anorexia and weight loss.

2) Establish whether the GFRAL signalling network is exclusively activated in those models which display anorexia and weight loss.

7.3 Methods

7.3.1 Animals

Male C57BL6/J mice (Charles River, UK) between the ages of 10 and 15 weeks were under standard conditions as described in 2.2. All mice had *ad libitum* access to SDS standard mouse chow, except those in the CA study, which were kept on Envigo (UK) standard mouse chow. All mice were single housed for the purpose of chemotherapy studies.

7.3.2 Chemotherapy models

Chemotherapy drugs were selected based on published literature which either showed these treatments to cause anorexia and weight loss in mice, or showed treatments used to treat tumours in murine cancer models. Doses for all treatments, bar CA, were established following preliminary feeding dose response studies. Doses of cyclophosphamide and adriamycin used had previously been shown to cause anorexia and cachexia in C57Bl/6j mice (Wong *et al.*, 2018).

Paclitaxel (TAX. ApeXBio, Houston, USA, cat. A4393-APE) was reconstituted in 20% dimethyl sulfoxide (DMSO) in 0.9% sterile saline (Kent scientific, UK) and was dosed IP at a concentration of 20 mg/kg at a volume of 4ml/kg. Vehicle-treated (VEH) animals received an IP injection of 20% DMSO in sterile saline at a volume of 4 ml/kg. TAX was dosed either once in 24 hr or three times over the space of one week.

Gemcitabine (GEM. Merck, UK. cat. G6423) was reconstituted in 0.9% sterile saline and dosed IP at a concentration of 120 mg/kg at a volume of 4 ml/kg. Vehicle-treated (VEH) animals received an IP injection of sterile saline at a volume of 4 ml/kg. GEM was dosed either once in 24 hr or three times over the space of one week.

Cisplatin (CIS. Merck, UK. cat. PHR1624) was reconstituted in 0.9% sterile saline, warmed to 60°C, and kept warm until the time of injection. CIS was dosed IP at a concentration of 4 mg/kg at a volume of 4 ml/kg. Vehicle-treated (VEH) animals received an IP injection of sterile saline at a volume of 4 ml/kg.

Cyclophosphamide (Merck, cat. C0768) was combined with adriamycin (Merck, cat. D1515) to form the treatment 'CA'. Both drugs were reconstituted in 0.9% sterile saline, thoroughly vortexed, and cyclophosphamide was gently heated to encourage dissolving. Cyclophosphamide and adriamycin were each injected IP at 4 ml/kg, the final concentration of cyclophosphamide being 167 mg/kg, and adriamycin being 4 mg/kg and the final volume being 8 ml/kg (4 ml/kg + 4 ml/kg). Vehicle-treated (VEH) animals therefore received an IP injection of sterile saline at a volume of 8 ml/kg.

7.3.3 Feeding and body weight studies

For all chemotherapy models, chow and mice were weighed and body composition was measured using an EchoMRI scanner as described in 2.4 and 2.5, approximately 5 hr following lights on. Mice were then immediately dosed IP with chemotherapy. Mice were not fasted before chemotherapy treatment.

For single dose models (CIS, CA, 1x TAX, 1x GEM), chow, body weight and body composition were measured again 24 hr later. Repeated dose models (3x TAX and 3x GEM) were run over the space of a week. Following the initial dose of chemotherapy on day 0, food intake and body weight were measured every 24 hr. Further doses of chemotherapy were administered at the time of food and body weight measures on days 3 and 5 (Fig 7.1).

All mice were culled 24 hr following (final) injection of chemotherapy under isoflurane anaesthesia in 3% oxygen via cardiac puncture. Cardiac puncture was performed within 15 min of EchoMRI scan to prevent further expression of cFos due to stress.

Blood and brain tissue were collected and processed as described in 2.6. Liver, heart, gut, white adipose tissue, interscapular brown adipose tissue, gastrocnemius muscle, and tibialis anterior muscle were also collected, weighed, and rapidly frozen on dry ice for future biomarker analysis.

Day: 0   3   5   6
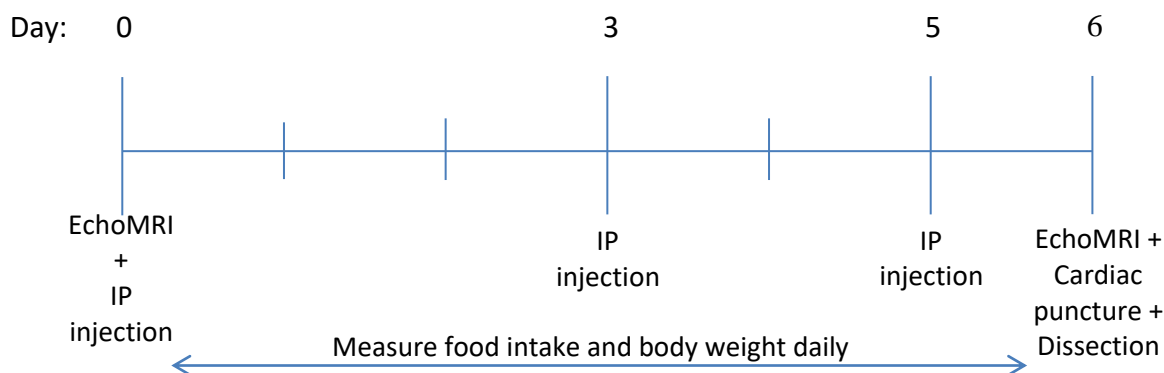
Figure 7.1. Timeline for repeated dose of chemotherapy models

7.3.4 Quantification of cytokines/chemokines

GDF15 was measured in heparinised plasma by ELISA. Two different R&D Systems mouse GDF15 ELISA kits were used. These kits were identical, except that one was pre-assembled. GDF15 plasma concentration was measured using the self-assemble R&D Systems DY6385 and DY008 kits for all experiments, barring the 1x TAX study, for which the pre-assembled R&D Systems MGD-150 mouse GDF15 kit was used. All plasma GDF15 was measured as according to manufacturer's instructions, details of which are provided in 2.7.

IL-1β, IL-6, KC, TNFα, and MCP-1 were quantified using a bespoke multiplex ELISA kit (MesoScale Diagnostics, U-PLEX cat. K15069L-1), according to manufacturer's instructions. In short, antibodies for mouse IL-1β, IL-6, KC, TNF-α, and MCP-1 were mixed with linkers, which were then applied to the plate and incubated overnight at 4 °C to allow conjugated linkers to coat specific spots in the well.

An eight-point standard curve was created by performing a 1:4 serial dilution and was plated in duplicate. Samples were also plated in duplicate and were diluted 1:2 with assay buffer. Standards and samples were incubated on a rotating plate shaker at room temperature for 1 hr at a brisk rotation speed.

Plates were washed three times using 0.05% Tween-20 (Sigma Aldrich, cat. P1379) in phosphate buffered saline (PBS. Sigma Aldrich). Detection antibody was then added, and plates were incubated for an hour on a rotating plate shaker at room temperature. Plates were again washed three times in 0.05% Tween-20 in PBS.

Read buffer was added immediately before reading on a MesoScale Diagnostics MESO QuickPlex SQ 120 reader using Methodical Mind software. Standard curves were calibrated

using a 4PL curve fit of log(concentration) with $1/y^2$ weighting. Absorbance readings were then interpolated using these curves to obtain quantities of cytokine/chemokine in pg/ml.

Data was checked for normal distribution using a Shapiro-Wilk test and analysed using unpaired Student's t test or Mann-Whitney U test as appropriate.

7.3.5 Immunohistochemistry

Fluorescence immunohistochemistry was performed on brain sections containing DVC, as described in 2.8.3. Antibodies used in this chapter can be found in General Methods.

7.4 Results

7.4.1 Chemotherapies which do and do not cause anorexia and weight loss

A single dose of CIS reduced food intake by around 45% compared with VEH control animals, ($p < 0.0001$. Fig. 7.2A) and a single dose of CA reduced feeding by approximately 35% ($p = 0.0005$. Fig. 7.2B). However, neither a single dose of TAX nor a single dose of GEM caused anorexia ($p = 0.4674$ and $p = 0.4530$ respectively. Fig. 7.2C & D respectively). Likewise, CIS caused an average of 5% body weight loss ($p = 0.0003$. Fig. 7.2E) and CA 7% loss ($p < 0.0001$. Fig. 7.2F), whilst TAX and GEM did not affect body weight (Fig. 7.2G & H).

In preclinical cancer studies, it is relatively uncommon for single doses of chemotherapy to be used. Therefore, repeated doses of TAX and GEM were also trialled to ensure an additive effect was not being missed by the single dose. Three repeat doses of TAX did not affect food intake ($p = 0.4995$. Fig. 7.2I) and although body weight was decreased in comparison with the VEH group on days 3 and 4, this represented a prevention of weight gain, rather than weight loss (Fig. 7.2J).

For animals treated with repeated doses of GEM, food intake was decreased after the second dose (Fig. 7.2K). However, there was no difference in body weight between VEH and GEM groups at any time point (Fig. 7.2L).
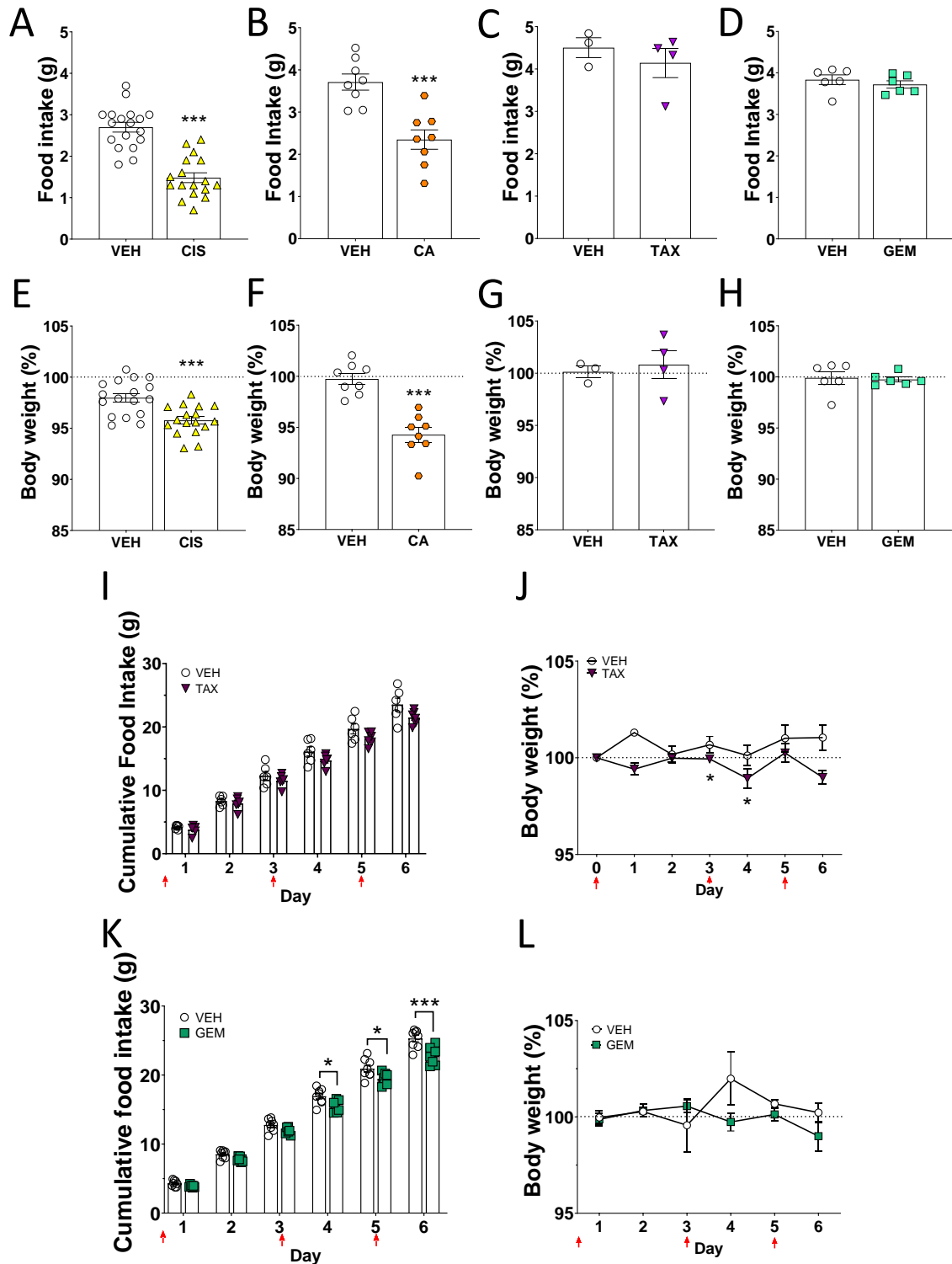
Figure 7.2. Effect of different chemotherapies on feeding and body weight. Food intake of wild-type mice 24 hr after a single dose of A) cisplatin (CIS), B) cyclophosphamide + adriamycin (CA), C) paclitaxel (TAX), or D) gemcitabine (GEM) and body weight change for the same drugs at 24 hr (E-H). Data were checked for normal distribution using a Shapiro-Wilk test and analysed using unpaired t tests. I) Cumulative food intake and J) % body weight change in wild-type mice treated with three doses of TAX over the space of week and K) cumulative food intake and L) % body weight change of wild-type mice treated with three doses of GEM in the same

time frame. Red arrows indicate days on which mice were dosed. Data analysed using a two-way ANOVA followed by post hoc Sidak's multiple comparisons test.n=6/group except in CIS study, where n=18/group and single dose TAX, where n = 3-4/group. All graphs show mean ±SEM * $p<0.05$, *** $p<0.001$.

7.4.2 Effect of chemotherapy treatment on GDF15

At 24 hr after treatment, plasma GDF15 concentration was approximately 8-fold higher in CIS-treated animals vs. VEH (Fig. 7.3A) and approximately 14-fold higher in CA-treated animals vs. VEH (Fig. 7.3B). Single doses of TAX or GEM did not cause an increase in plasma GDF15 concentration (Fig. 7.3C & D respectively).

For repeated dose models, three doses of TAX caused a slight increase in GDF15 (p = 0.0033), with a mean of 66 ±7 pg/ml VEH and 135 ±17 pg/ml 3x TAX (Fig. 7.3E). Three doses of GEM, which caused mild anorexia, also increased GDF15 (p = 0.0021) with a mean of 53 ±6 pg/ml GDF15 and 162 ±30 pg/ml in in VEH- and GEM-treated animals, respectively GEM (Fig. 7.3F). Although these differences are statistically significant, the increase of GDF15 caused by 3x TAX and 3x GEM was far less than that caused by CIS or CA treatment.

The concentration of circulating GDF15 in all mice treated with chemotherapeutics correlates with food intake, with r=-0.7331 and p < 0.0001 (Fig. 7.3G) and amount of weight loss, with r=-0.7767 and p < 0.0001 (Fig. 7.3H).
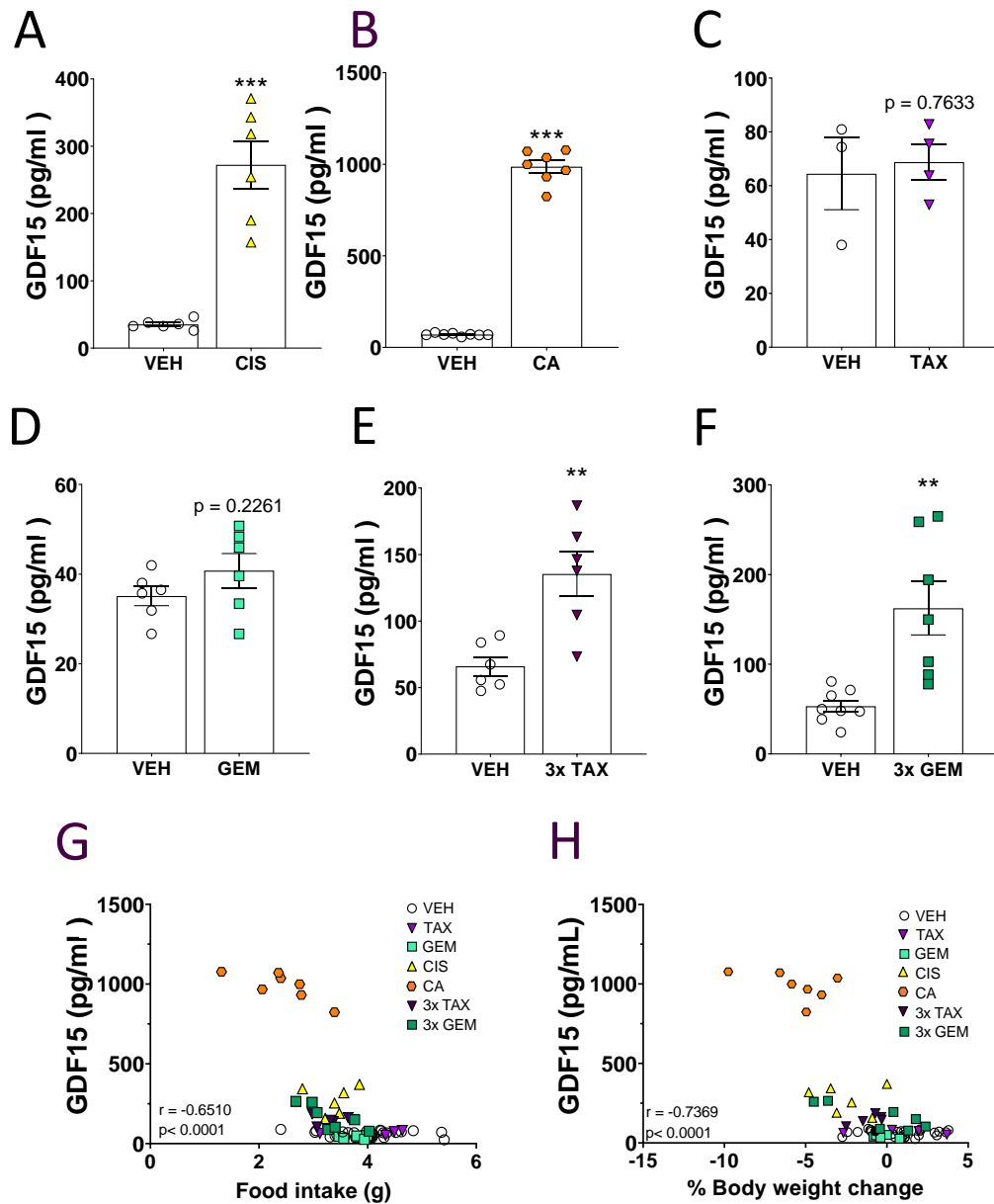
Figure 7.3. The effect of chemotherapy treatments on circulating GDF15. GDF15 concentration in plasma of mice 24 hr after being treated with vehicle (VEH) or a single dose of A) cisplatin (CIS), B) a combination of cyclophosphamide and adriamycin (CA), C) a single dose of paclitaxel (TAX), or D) a single dose of gemcitabine (GEM), and plasma GDF15 concentration 24 hr after the final of three doses of VEH or E) TAX (3x TAX) or F) GEM (3x GEM). Correlation analysis of G) food intake vs quantity of GDF15 and H) % body weight change vs quantity of GDF15. Differences in circulating GDF15 analysed using unpaired t tests. All graphs show mean+/- SEM. ** $p<0.01$ *** $p<0.001$.

7.4.3 Effect of chemotherapy treatment on other circulating factors

To investigate whether other circulating factors might be contributing to chemotherapy anorexia and weight loss, IL-1β, IL-6, KC, TNF-α, and MCP-1 were measured using a multiplex ELISA for each chemotherapy model.

IL-1β was increased by CA treatment ($p = 0.0011$) and three doses of TAX or GEM ($p = 0.0020$ and $p = 0.0436$ respectively. Fig. 7.4A). IL-6 was increased by CA and three doses of GEM ($p < 0.0001$ and $p = 0.0098$ respectively. Fig. 7.4B). KC, an IL-8 homologue, was increased by CIS ($p = 0.0491$), CA ($p = 0.0076$), and 3x GEM treatment ($p = 0.0025$. Fig. 7.4C). TNF-α was increased only in mice which had been treated with three doses of TAX ($p = 0.0297$. Fig. 7.4D). And finally, MCP-1 was increased by CA and three doses of GEM ($p = 0.0003$ and $p = 0.0007$ respectively. Fig. 7.4E). None of these cytokines/chemokines were increased in all chemotherapy treatment models which caused anorexia and weight loss, and some were increased by chemotherapies which do not cause anorexia and weight loss.
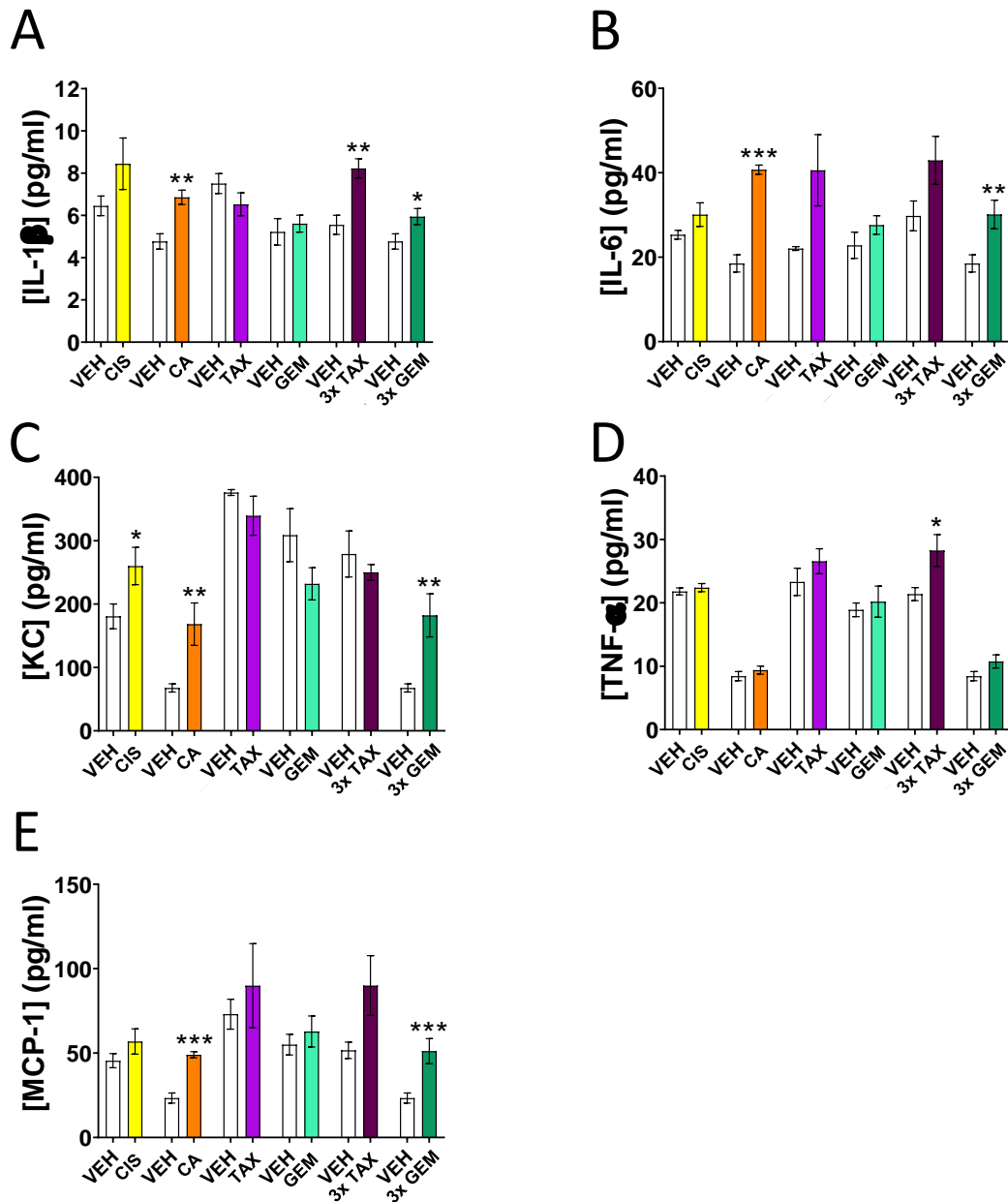
Figure 7.4. The effect of chemotherapy treatments on circulating inflammatory factors. Multiplex ELISA showing concentration of A) IL-1β, B) IL-6, C) KC, D) TNF-α, and E) MCP-1 in plasma of mice treated with vehicle (VEH) or chemotherapy. Chemotherapies tested were cisplatin (CIS), a combination of cyclophosphamide + adriamycin (CA), paclitaxel (TAX), and gemcitabine (GEM). All plasma measured was collected 24hr after treatment. In the case of the '3x' studies, three doses of chemotherapy were administered over the space of a week and plasma measured was taken 24hr after last dose. n=6/group for GEM, CIS, and 3x TAX studies. n=7-8/group for CA and 3x GEM studies. n=2-3/group for TAX study. All data were checked for normal distribution using a Shapiro-Wilk test and analysed using an unpaired t-test or Mann-Whitney U test as appropriate. * p<0.05, ** p<0.01, *** p<0.001.

7.4.4 Effect of chemotherapy on the central GFRAL signalling network

7.4.4.1 GFRAL^{DVC} neurons

Current evidence suggests that GFRAL is activated exclusively by GDF15 (Emmerson *et al.*, 2017; Hsu *et al.*, 2017; Yang *et al.*, 2017; Mullican *et al.*, 2017). Dual immunostaining of the DVC of chemotherapy-treated mice supports this evidence.

CIS induced cFos expression in approximately 19% of GFRAL^{DVC} neurons where 0% of GFRAL^{DVC} neurons were activated by vehicle treatment, $p < 0.0001$ (Fig. 7.5A). The majority of CIS activated GFRAL neurons were in the AP, rather than the NTS. CA activated an average of 20% of GFRAL^{DVC} neurons ($p<0.0001$), again, with the majority of those being found in the AP (Fig. 7.5B). Both CIS and CA caused activation of a group of non-GFRAL neurons in the mNTS in addition to GFRAL neurons. Single doses of TAX or GEM, which did not increase GDF15, did not activate GFRAL neurons nor any other neurons in the DVC (Fig. 7.5C &D, respectively).

In the case of repeated dose models, 3x TAX activated very few GFRAL^{DVC} neurons, the average being less than 5% of GFRAL^{DVC} neurons, which amounted to approximately one neuron per section (Fig. 7.5E). As there was no activation of GFRAL neurons in VEH-treated animals, this difference was statistically significant ($p = 0.0193$). Three doses of GEM activated approximately 12% GFRAL^{DVC} neurons, $p = 0.0079$ (Fig. 7.5F). There was a variable amount of activation in the DVC of mice treated with 3x GEM, with some having an average of 9 GFRAL neurons/section containing cFos, and others having none. More noticeable was the difference in overall amount of cFos expression in the GEM-treated animals, which varied between an average of 5 neurons/section and 216 neurons/section.

Overall, there was a strong correlation between the % of GFRAL neurons activated in the DVC and the level of GDF15 achieved following the different chemotherapy treatments (Fig. 7.5G).

Figure 7.5. The effect of chemotherapy treatment on activation of GFRAL^{DVC} neurons. GFRAL activation as measured by co-localisation of GFRAL (magenta) with the neuronal activation marker, cFos (green), in the DVC of mice 24 hr after treatment with A) cisplatin (CIS), B) cyclophosphamide + adriamycin (CA), C) paclitaxel (TAX), and D) gemcitabine (GEM). GFRAL activation 24hr after 3rd treatment with E) paclitaxel (x3 TAX) and F) gemcitabine (3x GEM) over a one-week period. G) Correlation between GDF15 concentration in plasma and %GFRAL activation in the dorsal vagal complex (DVC). n = 6 animals/group except TAX (3-4

animals/group) and 3x GEM (7-8 animals/group). AP = area postrema, cc = central canal, DMX = motor nucleus of the vagus/10thcranial nerve, NTS = nucleus of the solitary tract, Data were checked for normal distribution using Shapiro-Wilk normality test, then analysed by unpaired t test or Mann-Whitney U test as appropriate. * p<0.05, ** P<0.01, *** p<0.001.

7.4.4.2 Parabrachial nucleus

Looking outside of the DVC and GFRAL neurons, chemotherapy treatments which caused activation of GFRAL^{DVC} neurons also caused the activation of the elPBN. CIS (Fig. 7.6A) and CA (Fig. 7.6B) also caused activation of a second area in the lPBN, which here is defined as the central lateral PBN (clPBN). Though 3x TAX (Fig. 7.6C) and 3x GEM (Fig. 7.6D) did cause activation of elPBN, they did not cause the activation of this second area in the PBN.
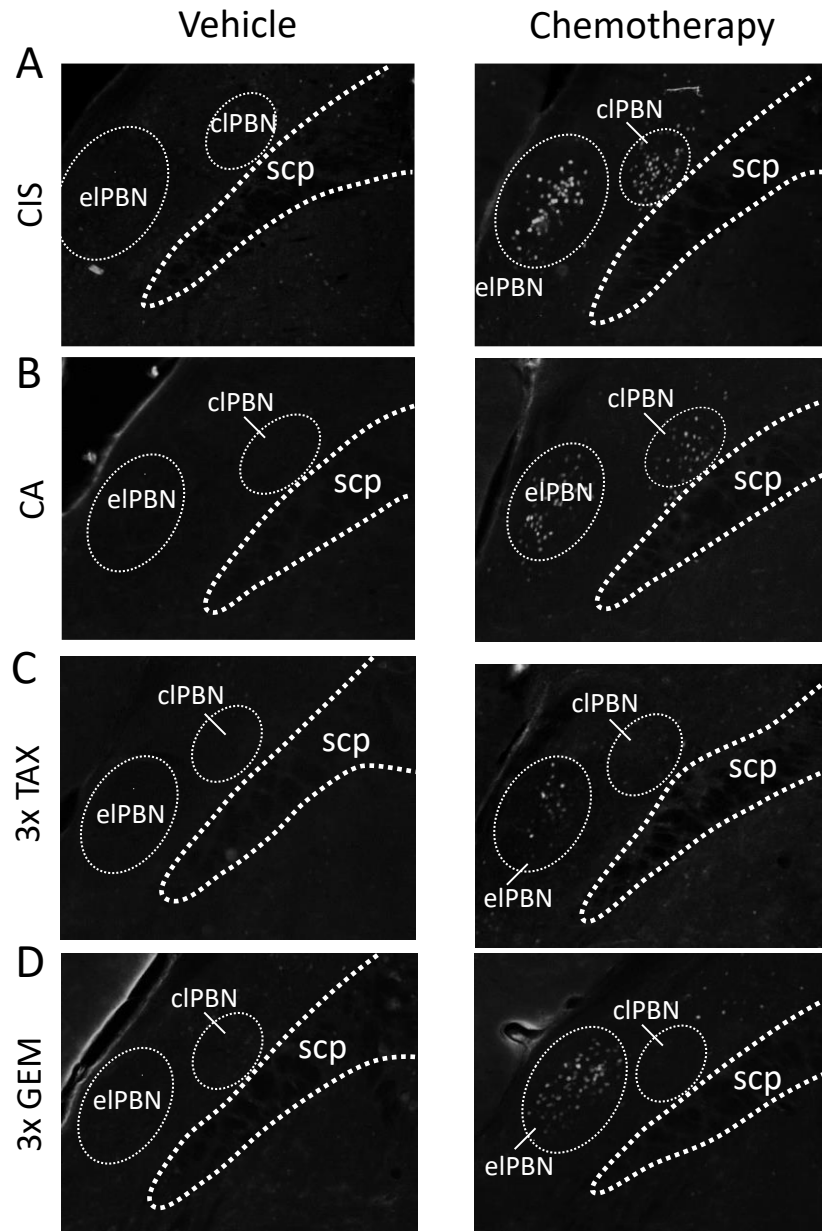
Figure 7.6. The effect of chemotherapy treatment on activation of neurons in the PBN. Activation as measured presence of the neuronal activation marker, cFos (white) in the parabrachial nucleus (PBN) of mice 24 hr after treatment with A) cisplatin (CIS), B) cyclophosphamide + adriamycin (CA), and 24 hr after the final dose of C) three repeat doses of paclitaxel (3x TAX), and D) three repeat doses of gemcitabine (3x GEM). elPBN = external lateral parabrachial nucleus, clPBN = central lateral PBN, scp = superior cerebellar peduncle.

7.5 Discussion

7.5.1 Chemotherapy treatments which caused anorexia and weight loss also increased GDF15

Of the different chemotherapy regimens tested, some had a much clearer effect on food intake and body weight than others. Single doses of CIS or CA strongly reduced feeding and body weight. These two therapies also caused a significant increase in circulating GDF15 which translated to a consequent activation of GFRAL neurons in the DVC and activation of the elPBN, in a similar pattern to SC injection of GDF15 (Fig.3.3B). On the other hand, a single dose of TAX or GEM had no effect on any parameter measured, from behaviour to circulating signalling factors or activation of the brain.

Repeated doses of TAX or GEM produced slightly less clear results. Three doses of TAX produced a small increase in circulating GDF15 (Fig. 7.3E), which in turn caused the activation of approximately one GFRAL^{DVC} neuron/section counted (Fig. 7.5E). There were also a several neurons activated in the elPBN for these animals (Fig. 7.6C). Although food intake was not significantly affected over the week of treatment, by day 4 of the study, there was beginning to be a trend towards a decrease in food intake (Fig. 7.2I).

Similarly, three doses of TAX did produce a difference in body weight compared with VEH-treated controls (Fig. 7.2J). However, on examination of the data, TAX prevented the small increase in body weight that is expected for VEH-treated animals, rather than causing a decrease in body weight. In context, the mean body weight change for mice treated with three doses of TAX was -1.02% over the week. During baseline measurements for these studies, before the mice had been treated with VEH or chemotherapy, it was normal for mice to gain or lose 1-2% body weight over a 24-hr period.

Although GDF15 was slightly increased for animals treated with 3x TAX (Fig. 7.3E), it seems unlikely that GDF15/GFRAL signalling was the reason for changes in feeding and body weight. As this level of GDF15 was associated with only one activated

GFRAL[DVC] neuron/section it is more likely that elPBN activation was caused by another signal induced by 3x TAX treatment. It is possible that if the study had run for longer, there could have been more pronounced effects on GDF15, food intake and body weight, bringing at least food intake and body weight results more in line with what is reported elsewhere in literature (Loman *et al.*, 2019; Grant *et al.*, 2021; Sullivan *et al.*, 2021).

Repeated doses of GEM produced variable results. In some animals, circulating GDF15 was increased, which correlated with both the activation of GFRAL[DVC] neurons (Fig. 7.5F) and a decrease in food intake after the second injection (Fig. 7.2K). This, however, did not correlate with a reduction in body weight (Fig. 7.2J). As would be expected, in mice with GFRAL[DVC] activation, there was corresponding activation of the elPBN (Fig. 7.6D). As with repeated doses of TAX, it is possible that a longer treatment regimen of GEM could have caused more pronounced effects on food intake and body weight, particularly as body weight could have been trending towards a decrease by day 6 for GEM (Fig. 7.2J). However, different to repeated doses of TAX, it seems that the feeding and body weight effects of repeated GEM were reliant on GDF15/GFRAL signalling. This can be seen as individual mice showing increased GDF15 also showed activation of GFRAL[DVC] neurons, activation of the elPBN, and anorexia, whereas the mice which did not have increased GDF15 showed none of these effects.

Throughout this thesis, VEH-treated control animals have consistently had plasma [GDF15] at or below 100 pg/ml (Fig. 6.1F, 6.2D, 7.3A-F, and 8.1C). In these animals there was no activation of GFRAL[DVC] neurons. For drug-treated groups, activation of GFRAL[DVC] neurons was seen when [GDF15] reached approximately 150 pg/ml. As GFRAL[DVC] activation correlated with plasma [GDF15], it would be interesting to see if the same holds true for the PBN and other areas of the GFRAL signalling network. This could easily be accomplished by performing a cell count of activated neurons in these areas.

7.5.2 Activation of the GFRAL signalling network by chemotherapies

Unexpectedly, both CIS and CA treatment also caused the activation of a second area of the PBN, the clPBN. There are several possibilities which could explain the activation of this second area. The first possibility was that this area requires higher levels of GDF15 to be activated. This could explain why the elPBN is activated by CIS, CA, and 3x GEM, but the clPBN is not activated by 3x GEM, which caused a smaller increase in GDF15. However, the clPBN was not activated by a dose of exogenous GDF15 (Fig. 3.5A). In light of the data in Patel *et al*. (2019), this explanation can be debunked as, according to their results, at 2 hr post-dosing plasma [GDF15] would have been approximately 4-5 ng/ml, far higher than the amount of GDF15 induced by CIS or CA treatment.

A second possibility is that chemotherapy treatment induced the release of other signals and that the clPBN was activated by one of these. In this chapter, five such signals were investigated (Fig. 7.4). Although no other signal was found to be increased only in those groups which had clPBN activation, the signals measured are by no means the only ones increased by chemotherapy or associated with anorexia and/or cachexia. There may be others which were not investigated here that causes the effect.

Finally, clPBN activation could have been related to the time after GDF15 increase that brains were collected. For mice treated with a dose of exogenous GDF15, brains were collected 2 hr post-dosing. For mice treated with chemotherapy drugs, brains were collected 24 hr following final dose. It is possible that this second area is being activated at a later in time point after GDF15 increase.

To investigate whether the clPBN is activated as a consequence of GDF15 or another signal, other pro-inflammatory/anorectic/pro-cachectic signals could be investigated, as they have above, using an ELISA. However, it would be simpler to block GDF15/GFRAL signalling using either a knockout model or a monoclonal antibody. This would establish the role of GDF15/GFRAL signalling in the activation of the clPBN, and this is what has been done in chapter 8. Next, brains could be collected 24 hr following treatment with GDF15. For this though, it is worth bearing

in mind that the half-life of GDF15 is significantly less than 24 hr (Xiong *et al.*, 2017). If the clPBN is activated as a delayed response to GDF15 increase, then it may be activated after 24 hr. However, if the clPBN is activated because of a prolonged increase of GDF15, it might be better to explore clPBN activation in the brains of animals which have been dosed with GDF15 multiple times over the space of a week.

The function of clPBN signalling and the phenotype of neurons activated in this region are still unknown. As the clPBN and elPBN are in such close proximity, exploring this prospect will only be possible if a distinct phenotype of clPBN neurons can be discovered. If this can be achieved, then this population of neurons can be selectively targeted, for example using optogenetic or chemogenetic technology.

As the clPBN is an area activated 24 hr-post chemotherapy treatment, but not 2 hr-post GDF15-treatment, cFos-immunoreactivity in the rest of the brains of CIS- and CA-treated animals should be investigated. If the clPBN is indeed activated as a part of the GDF15/GFRAL signalling network, there may be other areas which are involved at a later time point also. This would mean that the current understanding of the GFRAL signalling network, summarised in Fig. 5.5, is incomplete. Alternatively, this summary may be accurate for GDF15 actions acutely, but not chronically, as may be relevant during diseases and therapies such as cancer and chemotherapy.

When considering all chemotherapy treatments together, the concentration of circulating GDF15 correlated with the level of weight loss and severity of the anorexia (Fig. 7.3 G&H respectively). These data suggest that GDF15 was the causative factor for anorexia and weight loss following chemotherapy treatment, though this requires further evidence. Similarly, GFRAL[DVC] neuron activation also correlated with amount of GDF15 in circulation (Fig. 7.5G). The idea that GDF15 is causative of chemotherapy anorexia and weight loss is supported by the fact that no other signal associated with anorexia and weight loss measured was found to be affected universally by chemotherapies which cause a decrease in food intake and body weight. Based on these results, the GDF15/GFRAL signalling network seems to be a good target to combat chemotherapy-induced anorexia and weight loss.

7.6 Conclusions

- Chemotherapy treatments which increase [GDF15] above a threshold cause anorexia and weight loss, whereas chemotherapy treatments which do not increase [GDF15] above a threshold also do not induce anorexia or weight loss.

- A plasma [GDF15] of approximately 150 pg/ml is required to cause activation of GFRAL^{DVC} neurons in wild-type mice.

- The concentration of circulating GDF15 correlates with the severity of anorexia and weight loss.

- Chemotherapy treatments which increase GDF15 cause activation of GFRAL^{DVC} neurons and neurons in the elPBN.

- Some chemotherapy treatments which increase GDF15 also cause the activation of the clPBN.

8 Preventing GFRAL signalling during chemotherapy

8.1 Introduction

In this final results chapter, the role of GFRAL signalling in chemotherapy-induced anorexia and weight loss will be investigated with the aim of establishing whether the GDF15/GFRAL signalling network may be a good target to treat anorexia and weight loss in patients undergoing chemotherapy. In order to do this, GFRAL signalling will be blocked in murine chemotherapy models which cause anorexia and weight loss. The tools available to us in the lab include congenitally knocking out the GFRAL receptors using a GFRAL KO mouse, and pharmacological antagonism using the monoclonal antibody against the GDF15 receptor (GFRAL mAb), developed by Emmerson *et al*. (2017). Should prevention of GFRAL signalling remedy anorexia and weight loss in mice, GFRAL may prove a useful target to alleviate these symptoms in humans undergoing chemotherapy treatment.

Whilst it is not feasible to genetically knock out receptors in humans, there is precedent for the use of monoclonal antibodies to treat cancer. Many are already in use in a variety of forms. In cancer treatments, there are different forms of antibody treatment which act in different ways to bring about destruction of cancer cells. Some mAbs prevent cancerous cells from dividing, for example by antagonising growth factor receptors. Others are conjugated to cytotoxic/radioactive molecules to cancer cells, and so deliver doses of therapy directly to the cancerous tissue. This allows higher doses of drug to be used as there will less impact on surrounding tissues. Some mAbs are antiangiogenic, meaning that new blood vessels will not be created to supply a tumour, starving it of oxygen and nutrients. Yet other mAbs are able to manipulate immune responses to target cancerous cells e.g. by blocking T-cell checkpoint inhibitors or attracting immune cells to the cancer (Chiavenna, Jaworski and Vendrell, 2017; Liu Yang *et al.*, 2017; Seebacher *et al.*, 2019).

Monoclonal antibodies against GDF15 and GFRAL have also been developed and tested in preclinical cancer models. Several groups have shown ways in which neutralising GDF15 with an antibody therapy may be useful in treating cancer. In two separate studies, a GDF15 antibody improved the destruction of tumours by chemotherapy agents (Yu *et al.*, 2020; Wang *et al.*, 2021), with another publication showing decreased tumour growth following GDF15 antibody treatment due to decreased neovascularisation (Wang *et al.*, 2014). In line with this, an anti-GDF15 antibody was shown to prevent invasive and metastatic behaviours of colon cells *in vitro* (Ding *et al.*, 2020). Away from the treatment of tumours, Laurens *et al*. (2020) found that GDF15 was released by muscle cells which had undergone contraction similar to that induced by moderate to severe exercise, and which was predicted to cause cell stress. In this publication, the GDF15 neutralisation prevented lipolysis in adipose tissues – a quality which may be useful in the treatment of weight loss/cachexia.

To date, three groups have published research using mAbs against GFRAL. Instead of destroying neurons which express GFRAL, these antibodies block GFRAL receptors. Initially, GFRAL mAbs were used to investigate the effects of GFRAL signalling on energy balance, including feeding and body weight, in healthy rodents. Emmerson *et al*. (2017) published that a GFRAL mAb greatly reduces GDF15 binding to GFRAL receptors in rats. This had the effect of preventing anorexia and body weight loss induced by daily dosing of GDF15.

Coll *et al.* (2019) showed that an antibody against GFRAL could recover body weight and decrease energy expenditure in mice treated with metformin on a high fat diet. Later work from the same group in Cambridge focused more on disease models. Using the same antibody as before, Cimino *et al*. (2021) uncovered a role of GDF15/GFRAL signalling in activating the HPA axis in response to infection-related stimuli and toxins. In particular, intact GDF15/GFRAL signalling was required to activate the HPA axis in response to challenges which did not cause an increase in circulating cytokines.

In 2020, the Allan group showed that their GFRAL mAb, called 3P10, was also capable of preventing GDF15 binding to GFRAL, and activation of GFRAL neurons, in mice (Suriben *et al.,* 2020). In their publication, mice were protected from anorexia and weight loss induced by both treatment with GDF15 and from GDF15-releasing tumour xenografts. Furthermore, in a murine patient-derived xenograft model which did not show anorexia but did show pronounced cachexia, their 3P10 antibody recovered loss of white and brown fat mass, loss of skeletal muscle mass loss and skeletal muscle function, and decreased lipid metabolism, whilst increasing glucose metabolism, more in line with healthy, non-tumour bearing mice. In short, the 3P10 GFRAL mAb can combat cancer cachexia independently of the impact of food intake. Importantly, this antibody has been tested in both syngeneic and patient derived xenograft models. This group has shown that preventing GFRAL signalling did not impact on tumour growth.

Up to now, the role of GDF15/GFRAL signalling during drug-induced anorexia has been most thoroughly investigated during CIS therapy. Hsu *et al.* (2017) and Breen *et al.* (2020) show that blocking GDF15/GFRAL signalling using GDF15 or GFRAL KO models can prevent anorexia and weight loss in mice. In addition, Breen *et al.* (2020) go on to show that GDF15 KO mice are also protected from anorexia and weight loss during treatment with other platinum-based therapeutics. However, there is nothing in the literature to show that blocking GDF15/GFRAL signalling is effective at preventing anorexia and weight loss during other types of chemotherapy. This is something that this chapter aims to address.

Knowing that GFRAL mAbs can prevent anorexia and weight loss in animals with increased GDF15 and cancer, we aim to discover whether a GFRAL mAb will have similar beneficial effects during chemotherapy treatment. This will be done by testing treatment regimens which cause anorexia and weight loss (here, CIS and CA) using both the Taconic GFRAL KO mouse and the Emmerson group's GFRAL mAb. After this, further tests will be needed to prove that blocking GFRAL signalling does not have a negative impact on outcome in cancer models (e.g., promoting tumour growth or metastasis, or impacting the effects of cytotoxic therapy). However, providing that a GFRAL mAb can reduce or prevent the chemotherapy's effect on food intake/body

weight, there could be a future for a GFRAL mAb to be used to treat chemotherapy-induced anorexia and weight loss.

8.2 Aims and objectives

Hypothesis: The interaction of GDF15 with GFRAL is necessary for anorexia and weight loss following chemotherapy treatment in mouse models.

Aim: Prevent GFRAL signalling during chemotherapy to establish whether GFRAL signalling is responsible for anorexia and weight loss during chemotherapy treatments which cause an increase in GDF15.

1) Measure the effect of preventing GFRAL signalling on feeding and body weight in mice treated with chemotherapy.
    - Congenital knock out of GFRAL receptors – measure food intake and body weight in GFRAL KO mice treated with CA.
    - Pharmacological antagonism of GFRAL receptors – measure food intake and body weight following CIS or CA-treatment in wild-type mice which have been pre-treated with an anti-GFRAL monoclonal antibody (GFRAL mAb).
2) Measure GDF15 in the plasma of GFRAL KO mice and wild-type mice which have been treated with GFRAL mAb following CIS and CA treatment.
3) Explore what effect GFRAL mAb has on activation of the GFRAL signalling network during chemotherapy

8.3 Methods

8.3.1 Animals

14–16-week-old male and female GFRAL wild-type and null mice ($Gfral^{+/+}$ and $Gfral^{-/-}$), 18–25-week-old male and female *Calca*-Cre mice, and 14-week-old male C57Bl6/J mice (Charles River, UK) were kept under standard conditions as stated in General Methods (2.2), with *ad libitum* access to food and water at all times.

All mice were singly housed, for the purpose of food intake measurements, for at least 1 week prior to study.

8.3.2 Drug treatments

CA (167 mg/kg cyclophosphamide + 4 mg/kg adriamycin) was administered IP to male and female GFRAL KO or male C57Bl6/J mice, as described in 2.1.2. Vehicle-treated control animals were treated with an equivalent volume of saline IP (VEH).

4 mg/kg CIS was administered IP to male and female *Calca*-Cre mice as described in 2.1.2. Vehicle-treated control animals were treated with an equivalent volume of saline IP (VEH).

A monoclonal mouse anti-GFRAL antibody (mAb) was administered IP to male and female *Calca*-Cre mice or male C57Bl6/J mice as described in 2.1.2. Vehicle-treated control animals were treated with an equivalent volume of PB IP.

8.3.3 Feeding studies

8.3.3.1   Congenital knock out of GFRAL receptors

Single-housed male and female GFRAL KO mice ($Gfral^{+/+}$ and $Gfral^{-/-}$) were randomised into groups using the Microsoft Excel (RAND) function, then pseudo-randomised based on body weight and sex to ensure similar mean body weight and ratio of male:female animals in each group. Mice were administered saline (VEH) or CA IP during the morning of day 0. Food and body weight were weighed at this time.

24 hr later, food intake and body weight were measured again, and mice were culled via cardiac puncture under isoflurane anaesthesia at a rate of 3% in oxygen. Blood

and brains were processed and stored as described in General Methods (2.6) for later assays.

8.3.3.2 Pharmacological block of GFRAL receptors

Calca-Cre mice were treated IP with PB or mAb during the morning on day 0. 24 hr later, mice were injected IP with VEH or CIS. On day 2 (48 hr after injection of PB/mAb), mice were culled by cardiac puncture under isoflurane anaesthesia at a rate of 3% in oxygen. Blood and brains were processed and stored as described in General Methods (2.6) for later assays.

To investigate the effects of pharmacological block of GFRAL during CA treatment, this experiment was run a second time using male C57Bl6/J mice and CA instead of CIS.

8.3.4 Immunohistochemistry

Immunohistochemistry was carried out following standard protocols described in General Methods (2.8.3-5). Antibodies used can be also be found in General Methods.

Cell counts for the GFRAL mAb + CIS experiment (Co-localisation of GFRAL with cFos in the DVC and quantification of cFos in the PBN) were performed as described in General Methods (2.8.5) by Ms Amelia Catton under the guidance of Rosemary Shoop.

8.4 Results

8.4.1 Effect of congenital knock-out of GFRAL receptors during CA treatment

This experiment aimed to discover the anorectic/weight loss effects of chemotherapy in the complete absence of GFRAL signalling. As a similar experiment with GFRAL KO mice treated with CIS has already been published by Hsu et al. (2017), these studies with GFRAL KO animals focus on CA treatment.

8.4.1.1 Feeding and body weight

Each group of mice began the experiment at an average of 27.0 - 27.6 g. Injection with the chemotherapy combination CA caused a decrease in food intake and body weight in adult mice with intact GFRAL receptors ($Gfral^{+/+}$; Fig 8.1A and B respectively). However, there was no change in food intake or body weight after CA injection in littermates lacking GFRAL receptor ($Gfral^{-/-}$; Fig 8.1A and B respectively). CA caused an increase in circulating GDF15 in both $Gfral^{+/+}$ and $Gfral^{-/-}$ mice (Fig 8.1C). This fits the hypothesis that CA is causing an increase in circulating GDF15, which then acts via the GFRAL receptor to reduce food intake. To confirm this is the case, we investigated the action of CA on neuronal signalling in GFRAL neurons.
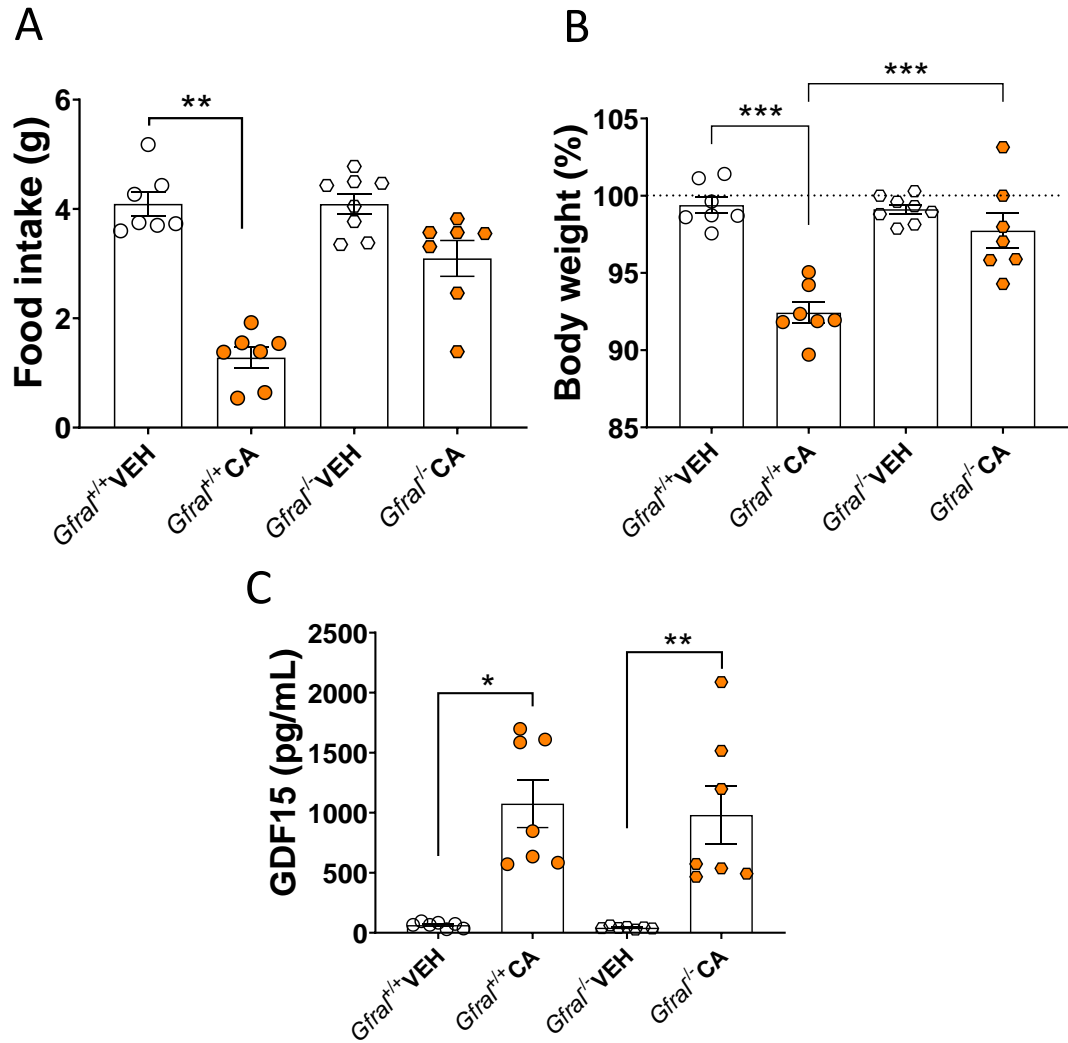
Figure 8.1. Effect of congenital GFRAL KO on feeding and body weight during chemotherapy. A) Food intake and B) body weight change of male and female GFRAL KO (*Gfral*^{-/-}) mice and wild-type litter mates (*Gfral*^{+/+}), 24 hr after treatment with the chemotherapy CA (cyclophosphamide + adriamycin). C) GDF15 concentration in plasma of *Gfral*^{+/+} and *Gfral*^{-/-} mice 24 hr after treatment with CA. n=7-8/group. Results were analysed using one-way ANOVA or Kruskall-Wallis test, followed by a post hoc Tukey's or Dunn's multiple comparisons test as appropriate.

8.4.1.2 Activation of DVC and PBN

No GFRAL immunoreactivity was detected in *Gfral^-/-* mice. Injection of CA in *Gfral^+/+* mice caused activation of GFRAL neurons (as indicated by the induction of cFos expression 24 hr after treatment) in *Gfral^+/+* mice, but not in *Gfral^-/-* mice (Fig. 8.2A and B). There was increased cFos expression in the mNTS of both *Gfral^+/+* and *Gfral^-/-* mice which were treated with CA in comparison with mice treated with VEH (Fig.8.2C). However, there were far fewer cFos^{+ve} neurons in the mNTS *of Gfral^-/-* mice treated with CA than were seen in the mNTS of *Gfral^+/+* mice (Fig. 8.2C).

There was also activation of neurons in the elPBN and clPBN of *Gfral^+/+* mice, but no activation in these areas for *Gfral^-/-* mice. Sections containing PBN from VEH- and CA-treated *Gfral^-/-* were indistinguishable (Fig. 8.2D).
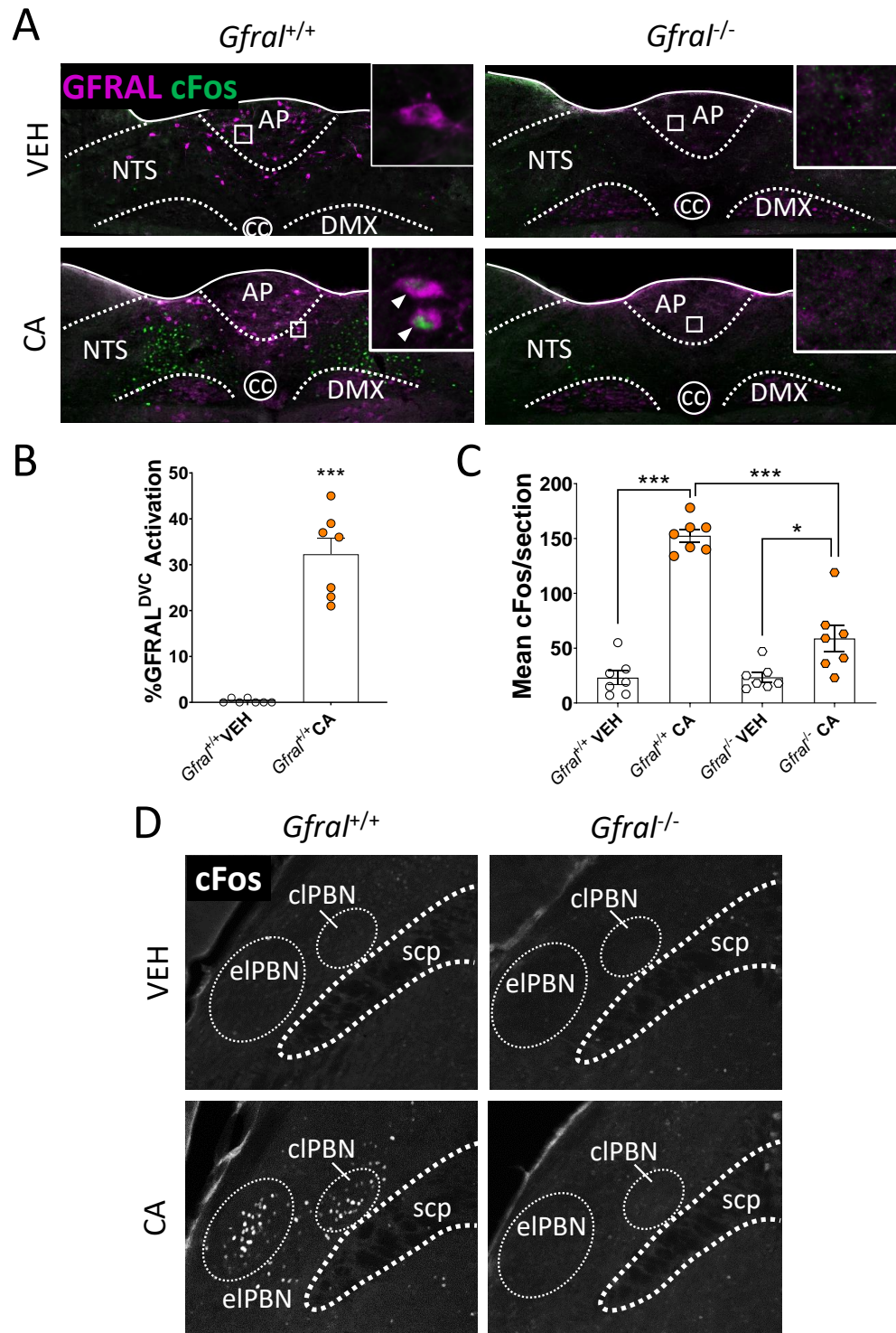
Figure 8.2. The effect of GFRAL KO on DVC and PBN activation following CA treatment. A) Immunohistochemistry showing activation of GFRAL neurons (magenta) in the dorsal vagal complex (DVC) as determined by co-localisation with cFos (green) in GFRAL wild-type mice (*Gfral*$^{+/+}$) or homozygous GFRAL null mice (*Gfral*$^{-/-}$), treated with vehicle (VEH) or cyclophosphamide and adriamycin (CA). B) Quantification of the percentage of GFRAL neurons activated in the DVC and C) of the mean number of cFos-expressing neurons in the DVC of *Gfral*$^{+/+}$ and *Gfral*$^{-/-}$ mice. D) Activation of the parabrachial nucleus (PBN) of *Gfral*$^{+/+}$ and *Gfral*$^{-/-}$ mice 24 hr after treatment with VEH or CA. n=7-8/group. AP = area postrema, cc = central canal,

DMX = motor nucleus of the vagus/10th cranial nerve, NTS = nucleus of the solitary tract, elPBN = external lateral PBN, clPBN = central lateral PBN, scp = superior cerebellar peduncle. Results were checked for normal distribution using a Shapiro-Wilk test, and analysed using one-way ANOVA, followed by a post hoc Tukey's multiple comparisons test. * $p < 0.05$, ** $p < 0.01$, *** $p < 0.001$

8.4.2 Pharmacological block of GFRAL receptors during CIS and CA treatment

8.4.2.1 Feeding and weight loss

An GFRAL mAb was used to pharmacologically block the GDF15/GFRAL signalling network during chemotherapy treatment. CIS caused a decrease in food intake in *Calca*-Cre mice (Fig 8.3A), with mean of 4.4 ±0.2 g for the PB-VEH treated group and 3.3 ±0.2 g for PB-CIS (p = 0.0243). By itself, the GFRAL mAb did not affect food intake (Fig. 8.3A).

In line with the decrease in food intake, CIS caused a significant decrease in body weight in WT mice (Fig. 8.3B). For animals pre-treated with the mAb, CIS did not cause significant difference in weight loss (Fig. 8.3B). The average body weight of groups of mice at the beginning of the study was between 29.30 g and 31.97 g.

In a similar experiment, wild-type C57 mice were treated with CA instead of CIS. Mice began this study at an average of 27.14 g – 29.14 g. In this study, CA caused a decrease in food intake in mice pre-treated with PB (Fig. 8.3C). The decrease in food intake was lost after mAb pre-treatment (Fig. 8.3C). However, block may not have been complete as the effects on body weight were almost equivalent between groups (p = 0.0538 mAb-VEH vs. mAb-CA. Fig. 8.3D). There was also no difference in body weight change between PB-CA and mAb-CA groups (Fig. 8.3D).
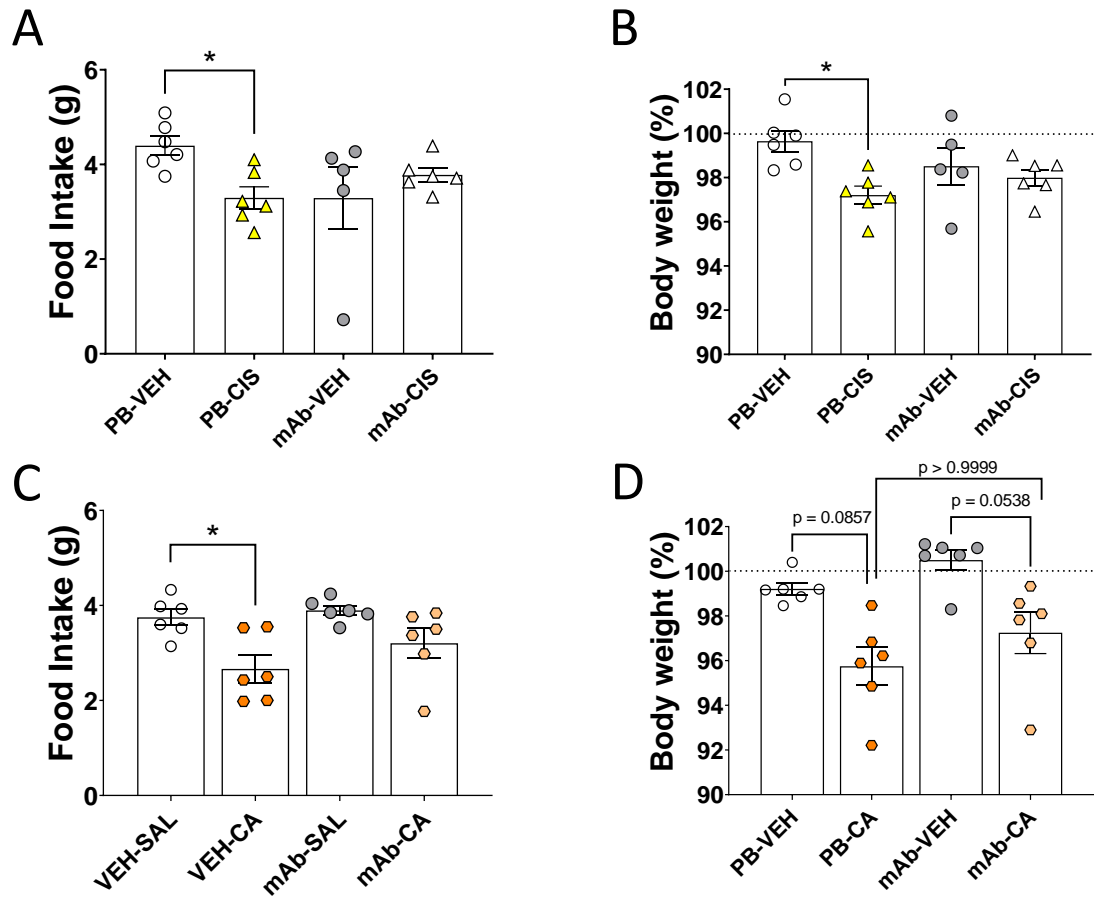
Figure 8.3. Effect of pharmacological block of GFRAL receptors on feeding and body weight and plasma GDF15 during chemotherapy. A) Food intake and B) body weight change 24 hr after treatment with vehicle (VEH) or cisplatin (CIS) in mice pre-treated with a sterile phosphate buffer control (PB) or a monoclonal antibody against the GFRAL receptor (mAb). C) Food intake and B) body weight change 24 hr after treatment with VEH or a combination of cyclophosphamide and adriamycin (CA) in mice pre-treated with PB or mAb. All data checked for normal distribution using a Shapiro-Wilk test, then analysed by 2-way ANOVA or Kruskal-Wallis test as appropriate, followed by a post hoc Tukey's or Dunn's multiple comparison test. * $p < 0.05$, ** $p < 0.01$.

Chapter 8: Preventing GFRAL signalling during chemotherapy

8.4.2.2   Activation of the DVC

CIS activated fewer GFRAL^{DVC} neurons in *Calca*-Cre mice when they had been pre-treated with GFRAL mAb vs. those which had not (Fig. 8.4A). GFRAL mAb also decreased GFRAL^{DVC} activation in WT mice treated with CA from an average of 38% (PB-CA) to an average of 17% GFRAL^{DVC} activation (mAb-CA. Fig. 8.4B).

As with food intake and body weight, the effect of CA on GFRAL^{DVC} activation was not completely blocked, however there was significantly reduced activation of GFRAL-expressing neurons in the presence of the mAb than without ($p = 0.0278$, PB-CA vs mAb-CA. Fig. 8.4B).

Likewise, mAb treatment prevented the increase in cFos in the mNTS following CIS treatment (mAb-VEH vs. mAb-CIS. Fig. 8.4A), and reduced, but did not prevent the increase in cFos^{mNTS} during CA treatment (mAb-VEH vs. mAb-CA. Fig. 8.4B).
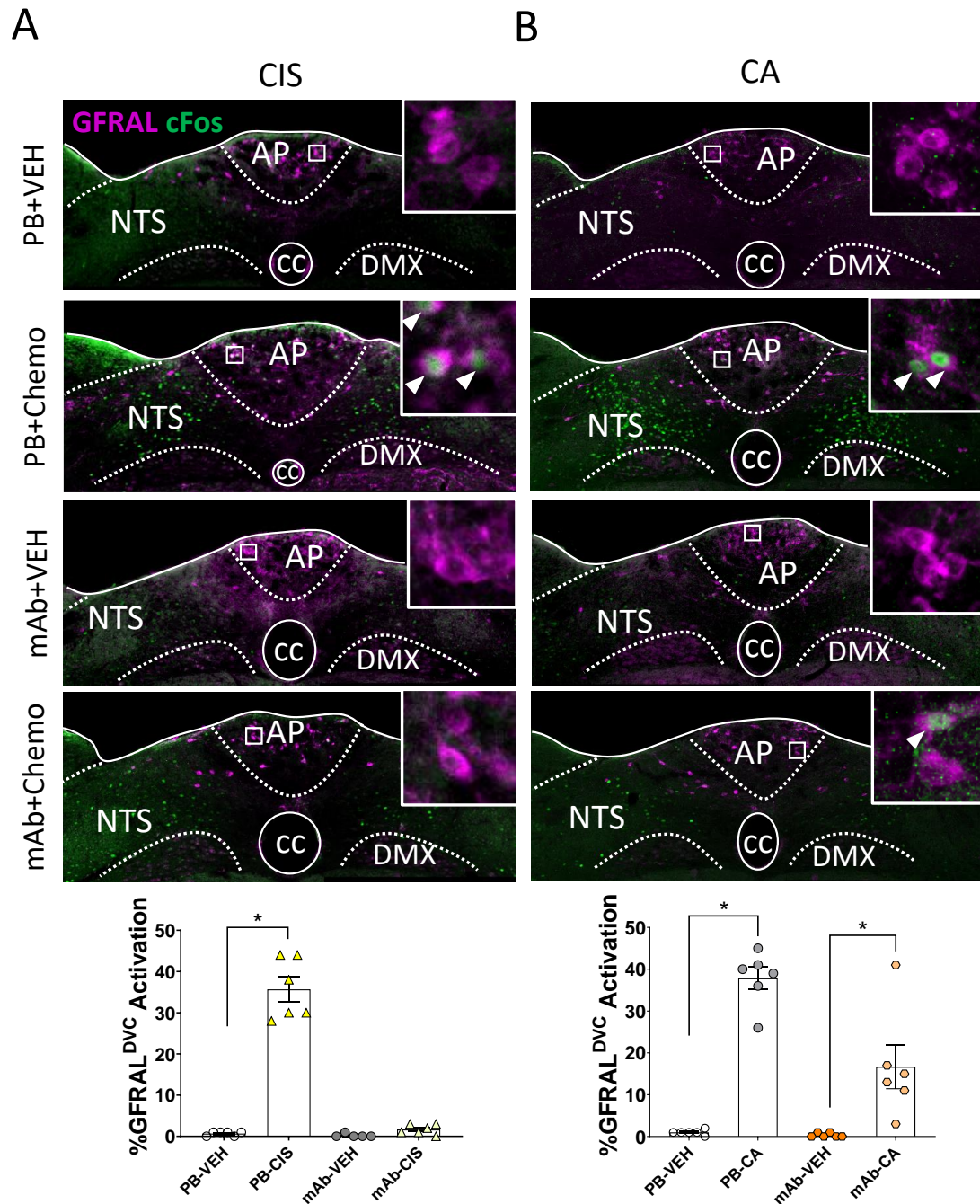
Figure 8.4. Effect of GFRAL mAb on activation of GFRAL^{DVC} neurons following chemotherapy. Activation of GFRAL-expressing neurons (magenta) in the dorsal vagal complex (DVC) as measured by co-localisation with cFos (green) in animals treated with control (PB) or a monoclonal antibody raised against the GFRAL receptor (mAb) and then vehicle (VEH), A) cisplatin (CIS) or B) cyclophosphamide + adriamycin (CA) 24 hr later. Images of sections from brains collected 24 hr after treatment with VEH or chemotherapy. n=6/group. AP = area postrema, cc = central canal, DMX = motor nucleus of the vagus/10th cranial nerve, NTS = nucleus of the solitary tract, Quantification of % GFRAL activation was analysed using a Kruskal-Wallis test, followed by a post hoc Dunn's multiple comparisons test. * p < 0.05. Cell counts for pannel A performed by Ms Amelia Catton.

8.4.2.3   Activation of the PBN

CIS or CA activated neurons in the elPBN and clPBN (Fig. 8.5A&D respectively). The GFRAL mAb completely prevented CIS-induced activation of the elPBN and clPBN (Fig. 8.5B&C respectively), and reduced CA-induced activation of the elPBN (Fig. 8.5E). GFRAL mAb did not significantly decrease activation of the clPBN in mice treated with CA (Fig. 8.5F).

Figure 8.5. GFRAL mAb effect on PBN activation following chemotherapy. A) Sections containing the parabrachial nucleus (PBN) of mice treated with phosphate buffer control (PB) or monoclonal antibody against GFRAL (mAb) followed by cisplatin (CIS) and the quantification of cFos expressing neurons in B) the external lateral PBN (elPBN) and C) the central lateral PBN (clPBN). D) PBN sections from mice treated with PB or mAb followed by VEH or a combination of cyclophosphamide + adriamycin (CA) and the quantification of cFos in E) the elPBN and F) clPBN. Images of PBN sections are approximately Bregma -5.02mm to -5.20mm. All data were checked for normal distribution using a Shapiro-Wilk test, then analysed using a one-way ANOVA or Kruskall-Wallis test, followed by post hoc Tukey's or Dunn's multiple comparison test as appropriate. n= 5-6 animals/group for mAb + CIS experiment and n=6 animals/group for mAb + CA experiment. scp = superior cerebellar peduncle.

8.5 Discussion

This chapter aimed to investigate whether GDF15/GFRAL signalling was responsible for anorexia and weight loss during chemotherapy. To achieve this, GFRAL signalling was prevented during chemotherapy treatment, either by congenital KO of GFRAL receptors in GFRAL KO mice, or pharmacological block of GFRAL receptors using an anti-GFRAL mAb. Chemotherapy treatments chosen were CIS and CA, as they have now been shown to cause anorexia and weight loss by myself (Fig. 7.2A, B, E, and F) and others (Alhadeff *et al.*, 2017; Hsu *et al.*, 2017; Wong *et al.*, 2018; Breen *et al.*, 2020).

8.5.1 Preventing GFRAL activation is effective at preventing chemotherapy-induced anorexia and weight loss

First and most promisingly, both congenital KO and pharmacological block of GFRAL receptors were able to reduce or prevent anorexia and body weight loss following chemotherapy treatment (Fig. 8.1A&B and 8.3A-D). Here, I show that blocking GFRAL receptors with a mAb inhibits the anorexia and weight-reducing effects of two chemotherapies. Some of my findings were published (Worth *et al.*, 2020) and confirmed by Breen *et al.* (2020). Here, I also have shown that, like with CIS treatment (Hsu *et al.*, 2017), the anorexia and weight-reducing effects of a different class of chemotherapy, CA treatment, are also blocked in *Gfral*$^{-/-}$ mice (Fig. 8.1A&B).

For CIS therapy, GDF15/GFRAL signalling seemed to be a causative factor affecting food intake and body weight loss. The GFRAL mAb was not only able to prevent anorexia and weight loss in *Calca*-Cre mice treated with CIS (Fig. 8.1A&B), but also prevented activation of GFRAL^{DVC} neurons, the group of neurons in the NTS, and both the elPBN and clPBN (Fig. 8.4A and Fig. 8.5A-C). These results confirm what had previously been shown by Hsu *et al.* (2017) using their GFRAL KO model and Breen *et al.* (2020), who prevented GDF15 signalling using both a GDF15 mAb and GDF15 KO mice.

Arguably, GFRAL signalling was also causative of CA-induced anorexia and weight loss. Although the GFRAL mAb was not able to prevent weight loss in WT mice treated with CA (Fig. 8.3D), congenital KO of GFRAL receptors was (Fig. 8.1A&B). The difference between these two models was likely that whilst there were no GFRAL receptors in $Gfral^{-/-}$ mice (Fig. 8.2A) and no consequent activation of the PBN (8.2D), the GFRAL mAb was not completely able to prevent activation of GFRAL^{DVC} neurons, with 17% of GFRAL^{DVC} neurons still being activated in mAb-CA treated mice (approximately 42 neurons. Fig. 8.4B), and therefore was not able to prevent activation of other areas of the GFRAL signalling network following CA treatment (Fig. 8.5D). This would mean that CA was still able to induce anorectic signals via the GFRAL signalling network in mice treated with mAb and would explain the incomplete protection from anorexia and weigh loss in this experiment.

Further support for the idea that GFRAL signalling is responsible for CA-induced anorexia and weight loss comes from the fact that CA treatment caused the increase of other anorectic, pro-cachectic signals such as IL-1β, IL-6, KC, and MCP-1 in WT mice (Fig. 7.4A-C &E) and following CA treatment in $Gfral^{-/-}$ mice, there was still increased activation of neurons in the NTS in comparison with VEH-treated littermates (Fig. 8.2C). It is possible that one or more of these other signals caused the activation of the NTS, without affecting food intake (Fig. 8.1A) or body weight (Fig. 8.1B) or causing activation of other parts of the GFRAL signalling network (Fig. 8.2D). Whilst GDF15 is increased by CA in $Gfral^{-/-}$ mice (Fig. 8.1C) in a similar way as it is in WT mice (Fig. 7.3B), it would be worth checking if these other signals are also increased in CA-treated $Gfral^{-/-}$ animals before drawing this conclusion about the lack of effect of these signals on food intake and body weight during CA-treatment.

If it is true that GFRAL signalling is responsible for CA-induced anorexia and weight loss, there is no clear reason why the GFRAL mAb should not have been as effective against CA as it was against CIS. Emmerson *et al.* (2017) successfully prevented anorexia and weight loss in mice treated with 0.1 mg/kg GDF15 using the same GFRAL mAb as described in this chapter. Although CA induced a larger increase in GDF15 than CIS (Fig. 7.3B and A respectively), the quantity of GDF15 in circulation following either of these treatments is still likely to be far less than the amount than

would be induced the dose used by Emmerson *et al.* (Emmerson *et al.*, 2017; Patel *et al.*, 2019). It therefore would also not follow that the quantity of GDF15 in circulation following CA treatment was able to overcome the block of GFRAL receptors by the mAb.

As GDF15 was only measured at 24 hr following treatment with CA for this study, it may be the case that CA caused a much larger increase in GDF15 at an earlier time point. If this is the case, perhaps the GFRAL mAb was not sufficient to block GFRAL signalling with this kind of challenge. Although this option seems unlikely as mice did not show sickness behaviours which would be associated with very high levels of GDF15, which are known to cause nausea, pica, and vomiting, depending on species (Borner, Wald, *et al.*, 2020; Breen *et al.*, 2020; Worth *et al.*, 2020), this could be confirmed by measuring GDF15 at earlier time points following CA treatment.

Alternatively, GDF15 is known to have a short half-life of 3 hr (Xiong *et al.*, 2017). GDF15 would therefore have been increased for only a few hours at a time in the Emmerson *et al.* (2017), as opposed to potentially being maintained at a higher level for 24 hr as a consequence of CA treatment. The increased time of exposure of the mouse to GDF15 may have been able to overcome the antagonism of the mAb if this is the case. Again, this seems unlikely as the GFRAL mAb was able to prevent activation of the GFRAL signalling network (Fig. 8.4A), anorexia (Fig. 8.3A) and weight loss (Fig. 8.3B) following CIS treatment.

Perhaps the best explanation then, is that this experiment was somewhat underpowered. In the study in which mice were treated with GFRAL mAb and CA (Fig. 8.3C&D), differences between different groups were very close to being significant which brings into question the accuracy of the outcome. This being the case, a power analysis should be carried out and the experiment repeated with more mice.

However, it is worth noting that the CA treatment did not behave as expected in this study. For other studies in which mice were treated with CA, average food intake over a 24-hr period was less, between to 1.3-2.3g (Fig. 7.2B and Fig. 8.1A). Additionally, in this chapter CA did not significantly decrease the body weight of mice pre-treated with PB in comparison with PB-VEH treated mice (Fig. 8.3D). Again, in

previous studies using this treatment, CA caused an average of 7% body weight loss in 24 hr, whereas in this chapter, PB-CA treated mice lost an average of 4% body weight (Fig. 8.3D). The reduced potency of CA treatment on food intake and body weigh in this chapter may have been related to a building fire shortly before this study was carried out, which may have affected the temperature at which the cyclophosphamide and adriamycin were stored. If the efficacy of the drugs was compromised by this, then this study should be repeated to ensure accurate results.

Likewise, there was an unexpected amount of variability for in the food intake and body weight of mice in the GFRAL mAb+CIS study (Fig. 8.3A&B). In particular, in the mAb-VEH group, one mouse had exceptionally low food intake of less than 1g in 24 hr, which was around 2.5g less than any other mouse in the entire cohort (Fig. 8.3A). In this study, a different mouse in the mAb-VEH group lost around 5% of body weight over the 24-hr period, when the rest of the group did not vary by more than 2%. These unusual results may have been due to the animals being stressed at some point during the study and again, greater n numbers or repetition of the study may be necessary to clarify the effect of the GFRAL mAb on feeding and body weight.

From these data, however, it is clear that GFRAL signalling is responsible for feeding and body weight effects during at least two different types of chemotherapy treatment. Moving forward, further classes of chemotherapies could be used to investigate whether this holds true across all classes of chemotherapies which cause anorexia and weight loss. This work has been begun by Breen *et al*. (2020), who investigated weight loss and nausea caused by different types of chemotherapy and cancer in relation to GDF15/GFRAL signalling. The investigation of cancer therapeutics could also be expanded to include other types of cancer therapy, such as radiotherapy. Radiotherapy is also known to cause anorexia (Zhang *et al.*, 2014), weight loss (Lau and Iyengar, 2017), and increase GDF15 (Sándor *et al.*, 2015; Park *et al.*, 2022).

8.5.2 Reducing/preventing GFRAL activation reduces or prevents activation of the GFRAL signalling network

8.5.2.1 mNTS

In this chapter, activation of other, non-GFRAL, neurons in the mNTS and the PBN was investigated. Both of these areas are activated following GDF15 administration (Fig.3.3B and 3.5A) and are activated by other aversive anorectic stimuli including CIS (Carter *et al.*, 2013; Alhadeff *et al.*, 2015).

Activation of the mNTS seemed to be affected by GFRAL signalling but was not entirely reliant on its presence. In *Calca*-Cre mice treated with GFRAL mAb-CIS, there was no GFRAL activation and decreased activation of the NTS compared with PB-CIS treated littermates (Fig. 8.4A). As there was no difference in the amount of cFos in the NTS of mAb-CIS vs mAb-VEH or PB-VEH groups (Fig. 8.4A), this would indicate that central activation of anorectic feeding pathways following CIS-treatment hinges on the activation of GFRAL^{DVC} neurons and activation of the GFRAL signalling network.

However, whilst both congenital KO of GFRAL and the GFRAL mAb were effective at reducing cFos in the DVC, neither condition was able to prevent cFos increase in the DVC in response to CA treatment (Fig. 8.2A and 8.4B). As there was increased cFos in the NTS of *Gfral*$^{-/-}$ mice treated with CA compared to those treated with VEH, there must have been another signal activating these neurons. It is possible that this may have been another pro-inflammatory signal such as IL-1β or IL-6 which were increased by CA treatment (Fig. 7.4 A&B) and which affect neuronal activation in the NTS (Turnbull and Rivier, 1999).

8.5.2.2 PBN

In contrast to the mNTS, the activation of the lPBN does appear to be dependent on intact GFRAL signalling. In animals treated with GFRAL mAb-CIS, which had no GFRAL^{DVC} activation, there was no activation of either lPBN region (Fig.8.5A-C). Likewise, in CA-treated *Gfral*$^{-/-}$ animals, there was no activation of the elPBN or clPBN (Fig. 8.2D), despite there being an increase of cFos in the NTS (Fig. 8.2C). This

indicates that chemotherapy-induced PBN activation occurs as a consequence of GFRAL signalling, and is not influenced by any other signals which are being released.

As activation of the clPBN, a region which was not activated by treatment with exogenous GDF15 in chapter 3 (Fig. 3.5A), was apparently not caused by another signalling molecule, I hypothesised that the additional activation of the clPBN following chemotherapy treatment could be due to a differing quantity of GDF15 in circulation following GDF15 injection vs. chemotherapy treatment or due to time of cull.

On closer inspection, activation of the clPBN is not likely to be due to a dose effect, despite 4 nmol/kg being a low anorectic dose and a lower dose than is used in most published literature. As discussed previously, Patel *et al*. (2019) investigated the concentration of GDF15 in plasma at various time points after injection of exogenous GDF15. Using their data, 2 hr after injection of 4 nmol/kg GDF15, GDF15 concentration in plasma should be between 4000-5000 pg/ml. This is significantly more than is found in the plasma of mice treated with CIS or CA at the time of cull in these studies, which was roughly between 180-1800 pg/ml. If this is accurate, there additional activation of the clPBN would not have been caused by a greater quantity of GDF15 in circulation. It is therefore more probable that the clPBN is activated as a delayed response to GDF15 increase.

In this thesis, mice treated with exogenous GDF15 were culled and brains collected at 2 hr after injection, whereas brains of mice treated with chemotherapies were collected 24 hr after final treatment with chemotherapy. The fact that the elPBN is activated and the clPBN is not following 3x TAX or 3x GEM treatments in the previous chapter can be interpreted to support the idea that the clPBN is activated as a result of a delayed response to increased GDF15. In these two treatment regimens, after three repeated doses, there was a decrease in feeding or body weight, which could indicate that the anorectic/weight loss effects were beginning to be expressed at the time of cull. If this was the case, then the brains of these animals would have been taken at a similar point in the GDF15/GFRAL signalling response as seen in brains of mice treated with exogenous GDF15, i.e., after the elPBN had been activated, but

before the clPBN activation had occurred. This theory could be explored in future by treating mice with GDF15 and collecting brains 24 hr after injection, rather than 2 hr, then examining the neuronal activation pattern in the PBN. In addition, the TAX and/or GEM treatment regimens could be extended to include another dose of TAX/GEM and food intake/body weight could be compared with PBN activation.

At this point, it is uncertain what the identity or the function of the clPBN neurons which are activated in consequence of increased GDF15 is. Future investigation of the phenotype of these neurons could provide information about an additional pathway being activated by GDF15, or another effect it may have over the longer term. These neurons could be involved in causing anorexia, weight loss, and even cachexia.

8.5.3 Efficacy of reducing/preventing GFRAL signalling at reversing chemotherapy anorexia and weight loss

In this chapter, prevention, or reduction of GFRAL signalling during chemotherapy prevented or reduced the anorectic and weight loss effects of chemotherapy treatment. Though treatment with a GFRAL mAb here was not totally effective, results do show that chemotherapy-induced anorexia and weight loss can be affected by targeting the GDF15/GFRAL signalling network. This is encouraging for several reasons, including that, as of yet, there is no effective treatment for any form of anorexia and weight loss/cachexia.

In addition to their effects on feeding and body weight during disease and therapy, GFRAL receptors provide an attractive therapeutic target due to their limited expression in the DVC and their being solely activated by GDF15. Unlike many neurotransmitters, such as CCK, glutamate, or catecholamines, GDF15 only acts on one receptor and seemingly only in disease situations. This would mean that other signalling pathways would not be altered, minimising unwanted side-effects. Furthermore, whilst it is not possible to prevent GFRAL receptor expression in human patients, mAb treatment is a viable option as a therapy. It may be possible to increase the efficacy of the GFRAL mAb against anorexia/weight loss by altering the dose or

the structure of the antibody could be altered to combat increases in GDF15 more effectively.

Taken together, data in this chapter shows that for chemotherapy treatments which increase GDF15, the GFRAL signalling network is activated and the cause of anorexia and weight loss. Though there are many more chemotherapy treatments and other cancer therapies which cause anorexia and weight loss, the prevention of anorexia and weight loss caused by different therapies with different mechanisms of action here would indicate that prevention of GFRAL signalling could be a useful co-treatment for cancer patients undergoing chemotherapy.

8.6 Conclusions

- Preventing GFRAL signalling reduces the effect of chemotherapy treatments on food intake and weight loss
- Preventing GFRAL signalling in the DVC prevents activation of other areas of the GFRAL signalling network
  - o Activation of both the elPBN and the clPBN are a result of GFRAL signalling during chemotherapy treatment.
- GFRAL mAb reduces GFRAL signalling without affecting GDF15 release.
- Though other signals during chemotherapy are still relevant to feeding behaviour and weight loss, prevention of GFRAL signalling could be a viable treatment to combat chemotherapy anorexia and weight loss.

9 General discussion

In this thesis, I aimed to discover how the GDF15/GFRAL signalling network causes anorexia and weight loss; whether that was related to ACS during cancer and chemotherapy; and, whether GDF15/GFRAL could be a target to combat cancer and chemotherapy ACS. The work presented in this thesis began in 2018, one year after the initial publications identifying GFRAL as the cognate receptor for GDF15 were released. Since this point in time, there has been a lot of interest in the GDF15/GFRAL signalling system from within both the academic and commercial communities as a target for both obesity and ACS. This has meant that the field has moved rapidly over the last few years.

The competitiveness of the GDF15/GFRAL field meant that the first three experimental chapters describe work which I performed as part of a group, but I have stated clearly my role in each experiment. Due to this teamwork, we were the first to publish a comprehensive description of the phenotype and connections of GFRAL neurons in a paper on which I was second author (Worth *et al.*, 2020). Our paper also contained data regarding the negative valence of the GDF15 signal, though other groups also published their own data on this specific aspect of GDF15's biology at around the same time (Borner, Shaulson, *et al.*, 2020; Borner, Wald, *et al.*, 2020; Sabatini *et al.*, 2020).

The remaining chapters of this thesis explore the possible translation of our knowledge to the fields of cancer and chemotherapy. Although an appropriate model of murine ACS was not available, data from Chapters 7 and 8 explore novel aspects of the relationship between GDF15 and different chemotherapy treatments which we hope to publish soon.

Finally, this thesis contains validation of our own bespoke *Gfral*-Cre mouse model. The late availability of this mouse due to the coronavirus pandemic meant that it could unfortunately not be utilised in experiments for my thesis. However, validation results which were obtained and presented in Chapters 4 and 5 show the high quality of this model, which will be of enormous value to the lab in their research to better

understand the GDF15/GFRAL signalling system moving forwards. Our lab's first paper using this model, on which I am a co-author, will hopefully be published in 2023. Although another group has published work using their own *Gfral*-Cre model (Sabatini *et al.*, 2021), their work mostly only confirms what we had published in our own original paper (Worth *et al.*, 2020).

9.1 GDF15/GFRAL signalling

When beginning this research, it was not clear whether GDF15/GFRAL signalling forms a part of normal physiological control of food intake and body weight, affects feeding and body weight as a part of a stress signalling pathway in response to damage or disease, or both. With the evidence now available, it seems clear that the main role of GDF15/GFRAL signalling is a response to cell damage and stress. This conclusion can be drawn based on the types of stimuli which cause the release of GDF15, the central signalling network activated in response to GFRAL neuron activity, the overall effect of aversion caused by the activation of the GFRAL signalling network, and the fact that preventing GFRAL signalling using an anti-GFRAL mAb or congenital KO did not affect food intake or body weight (Fig. 8.1A/B and 8.3).

Prior to the publication of our data in Worth *et al*. (2020), there was relatively little evidence showing the phenotype of GFRAL^{DVC} neurons. Results from Chapter 4 (published in Worth *et al*. (2020)), and other literature, show that neurons in the DVC which express GFRAL also express CCK (Fig.4.2A), TH (Fig.4.2B) (Yang *et al.*, 2017), VGLUT (Fig.4.2C), and GLP-1Rs (Frikke-Schmidt *et al.*, 2019; Zhang *et al.*, 2021). Although GLP-1 signalling is likely to be separate from the effects of GDF15, each of these neuronal markers which co-localise with GFRAL have an involvement in anorectic signalling as part of satiety-inducing and/or aversive signalling pathways (Rinaman, 1999; Seeley *et al.*, 2000; Wu, Clark and Palmiter, 2012; Dodd *et al.*, 2014; Roman, Sloat and Palmiter, 2017).

One way to establish whether GFRAL signalling is relevant to satiety-induced anorexia, aversive anorexia, or both, was to investigate the types of anorectic stimuli which activate GFRAL neurons. In Fig. 4.1, GFRAL neurons were not activated by

satiety signals such as an oral dose of lipids or an IP dose of CCK. This would imply indirectly that these satiety signals do not cause the release of GDF15. This could easily be confirmed by taking blood following administration of these stimuli to be analysed using a GDF15 ELISA.

In contrast, GDF15 is increased during disease, particularly that which leads to inflammation and cellular damage (Welsh *et al.*, 2003; Xu *et al.*, 2006; Brown *et al.*, 2007; Ho *et al.*, 2013), and by aversive and cytotoxic stimuli (Fig.7.2) (Hsu *et al.*, 2017; Breen *et al.*, 2020; Lu *et al.*, 2022). In Chapter 7, the cytotoxic chemotherapy treatments, CIS and CA caused the release of GDF15 and activation of GFRAL neurons (Fig. 7.3A/B and Fig. 7.5A/B respectively). Other groups have also shown that other inflammatory stimuli or drug therapies, such as LPS, Poly(I:C), metformin, and camptothecin cause an increase in GDF15 and activation of GFRAL neurons (Coll *et al.*, 2019; Luan *et al.*, 2019; Lu *et al.*, 2022).

Results from Chapters 3 and 4 show that GDF15 causes the activation of neurons in the DVC, elPBN, CeA, PVH, and ovBNST, which form components of know aversive signalling pathways. My tracing studies in Chapter 5 confirmed GDF15 activates the previously described aversive pathway between DVC$\rightarrow$CGRP^{elPBN}$\rightarrow$PKCδ^{CeA} pathway (Cai *et al.*, 2014; Alhadeff *et al.*, 2015) and the PBN$\rightarrow$ PKCδ^{ovBNST} connection which is also activated by inflammation (Wang *et al.*, 2019). The possible involvement of the lPBN, CeA, and PVH in GDF15 signalling had been inferred before my work commenced (Johnen *et al.*, 2007; Hsu *et al.*, 2017) We were, however, the first group to provide direct evidence that GDF15 activated GFRAL/CCK neurons which project to the PBN, and to describe the involvement of the ovBNST in this signalling network. Each of these regions of the brain can affect anorexia and weight loss either through signalling satiety and/or aversion.

Through work presented in this thesis, and subsequent work published by other groups, it is clear that GDF15/GFRAL signalling is highly aversive in rodents (Fig. 3.2) (Borner, Shaulson, *et al.*, 2020; Borner, Wald, *et al.*, 2020; Breen *et al.*, 2020; Sabatini *et al.*, 2021), primates (Breen *et al.*, 2020), and potentially humans (Petry *et al.*, 2018; Fejzo *et al.*, 2019), causing avoidance behaviour, nausea, and emesis. With this

information, we have concluded that GDF15/GFRAL signalling is not used under normal physiological circumstances to maintain energy balance, but is instead a response to stress.

9.2   A potential role of GDF15 in disease

Results presented here and in other published work show that increases in GDF15 lead to the activation of GFRAL neurons, which in turn induce sickness behaviours: nausea, aversion, anorexia (and subsequent weight loss). Although the malaise caused by GDF15 is frequently reported to have detrimental effects during disease and therapy, the release of GDF15 during disease states and cell stress is likely to have an adaptive advantage. Several theories propose benefits of anorexia and malaise during inflammatory diseases, and GDF15 seems to promote adaptive responses which may lead to increased chances of survival.

Firstly, anorexia and nausea may be adaptive as they prevent (further) ingestion of noxious substances, thereby preventing a greater pathogen or toxin load. GDF15 is aversive, causing anorexia and reduces or prevents the ingestion of otherwise palatable substances. This theory could be stretched further when taking into account evidence connecting GDF15 to nausea and vomiting during pregnancy (Fejzo *et al.*, 2018, 2019; Petry *et al.*, 2018). In this case, GDF15 release from the placenta might prevent ingestion of potentially teratogenic substances which may harm a vulnerable, developing foetus (O'Rahilly, 2017).

Secondly, there is evidence that anorexia is adaptive during some cases of inflammation. As reported in a series of studies dating back to the 1970s, negative energy balance in rodents infected with *Listeria monocytogenes* increases survival and rates of positive outcomes, where force-feeding, or even fed-state, leads to greater rates of mortality and worse outcomes (Aviello *et al.*, 2021). GDF15 release during disease and therapy may therefore be a response aimed to induce adaptive anorexia. Indeed, Luan *et al.* (2019) found that GDF15 KO mice had reduced survival in comparison with WT littermates when challenged acutely with an anorectic dose of LPS (Luan *et al.*, 2019).

In addition, both Luan *et al.* (2019) and Suriben *et al.* (2020) found that GDF15 causes changes in metabolism towards fats rather than carbohydrates. Although Luan *et al.* (2019) show that GDF15 causes a decrease in hepatic triglyceride production, they also found evidence that GFRAL signalling might affect hepatic triglyceride release via a sympathetic pathway. Suriben *et* al. (2020) found that GDF15 induces lipid mobilisation and oxidation, and that prevention of GFRAL signalling is protective of body weight, likely via the preservation of muscle. Like Luan *et al.* (2019), Suriben *et al*. (2020) show that GDF15-induced weight changes are dependent on peripheral adrenergic signalling. This swap from carbohydrate to fatty acid metabolism may be important for the protection of vital organs, such as the heart, during times of disease.

Finally, there is suggestion that nausea and malaise during disease may increase survival by promoting an animal to remain in the nest. This would lead to reduced energy expenditure which would otherwise be used to keep warm, move around, and forage. In the nest, animals also have reduced chances of predation whilst being in a weakened state due to illness (Aviello *et al.*, 2021). This could also be an adaptive role for GDF15, as GDF15 KO mice show increased locomotion and reduced anxiety behaviours (Low *et al.*, 2017).

In all of these cases, short term anorexia and malaise over the space of a few hours or days may be useful and promote the survival of the animal (or offspring, in the case of pregnancy). In the longer term, GDF15 causing anorexia, reduced gastric emptying, nausea, weight loss, chronic activation of the HPA axis, and general malaise is likely to become maladaptive, as energy stores become depleted and vital organs begin to be affected. These are symptoms which are commonly seen during cancer in both pre-clinical models and patients. At this point, prolonged anorexia and catabolism of fat and muscle leads to cachexia.

As previously discussed, during cancer and chemotherapy, ACS will further worsen the disease state by promoting survival of cancer cells and causing resistance or increased sensitivity to cancer therapies (Dewys *et al.*, 1980; Molfino, Laviano and Fanelli, 2010; Prunier *et al.*, 2018). In this way, GDF15 release may have evolved as

an adaptive response to disease and can be a positive or a negative prognostic biomarker, depending on the type and stage of disease.

9.3   Limitations of methods

Throughout this thesis, several methods, such as the quantification of cFos as a marker of neuronal activation, have been relied upon. These are valid and commonly used methods, however, it should be noted, as with all techniques, particularly when using proxies, that there are some drawbacks.

9.3.1   The use of cFos as a marker of neuronal activation

cFos is a transcription factor which is upregulated in many neuronal types in response to neuronal activation (action potential). Whilst the quantification of cFos using IHC is a common method to measure the response of neurons to various stimuli, it should be noted that not all neurons produce cFos in response to activation.

Also, each image depicting cFos expression should be regarded as a 'snapshot' in time. Images of brains were taken 90 min to 24 hr following administration of the stimulus of interest, whilst cFos remains detectable for several hours after neuronal activity. Immunoreactivity to cFos is therefore representative of a time range following a stimulus.

This is particularly relevant when looking at cFos immunoreactivity of GFRAL-expressing neurons and other populations of neuron in the DVC. Following administration of GDF15, GFRAL neurons express cFos, as well as another population in the mNTS. From the 'snapshot' image that we get from IHC, it could be possible that either both populations are directly responsive to GDF15, or that the mNTS population express cFos as a downstream response to GDF15 administration/increase.

In the case of the mNTS population, it is more likely that the latter is true as there has been research showing that GDF15 exclusively binds to GFRAL receptors (Emmerson *et al.,* 2017; Hsu *et al.,* 2017; Mullican et al., 2017; Yang *et al.,* 2017).

However, the use of cFos IHC alone does not prove this following GDF15 administration. Therefore, other techniques, such as prevention of GFRAL receptor activation, were employed. In this case, it was possible to see that mNTS cFos expression following GDF15 administration was dependent on GFRAL signalling being intact (Worth *et al.*, 2020; Emmerson *et al.*, 2017).

Therefore, quantification of cFos and investigation of co-localisation of cFos expression in specific neuronal populations is a useful tool to establish a response of neuronal populations to various stimuli. However, the above limitations should be kept in mind when interpreting results.

9.3.2 Ratio of male and female mice used across experiments

Throughout this thesis, predominantly male mice have been used for in vivo investigation, in particular, when investigating the effects of various stimuli in WT mice.

In this thesis, male mice were used when studies required only WT mice, and a mixture of male and female mice were used for studies using transgenics. In the case of transgenics, this decision was made so as to ensure adequate numbers of animals on study, and so as not to waste animals with the correct genotype.

Whilst male mice can sometimes cope better with single-housing conditions required to accurately measure food intake than female mice (for example, they can be less likely to become stressed and lose weight), this is an acknowledged issue with a lot of scientific research produced historically and currently, as male and female animals can respond differently to drug treatments.

Throughout this thesis, where both male and female mice were used in the same experiment, both sexes had similar responses to chemotherapies and other stimuli which caused activation of GFRAL neurons. In addition, work published by other groups shows that male and female mice have similar responses to the application of exogenous GDF15 (Mullican *et al.*, 2017).

Having said this, different sexes of mice may present different phenotypes during disease or other drug therapies. Therefore, both sexes of mice should be used equally in experiments for further investigation of the role of GDF15 and GFRAL neurons on anorexia and weight loss during disease.

9.3.3 The use of rodents to model nausea and emesis

Nausea and emesis are amongst the negative side-effects for many chemotherapy treatments (Joint Formulary Committee, 2023) and are a major cause of non-compliance/reason to discontinue therapy (Rapoport, 2017). It would therefore be very useful to understand the causes of chemotherapy-induced nausea and vomiting (CINV), in order to tackle the issue and treat patients more effectively.

It is very standard to use rodent models in preclinical trials of drugs; in particular, mice and rats. However, measuring nausea and emesis in mice and rats can be difficult.

When assessing nausea in rodent models, it is common to measure a proxy, such as pica behaviour in rat. In general, it is easier to assess general malaise in mice and rats, by recording the presence of 'illness behaviours', such as reduced locomotion, piloerection, squinting, and hunching.

Unfortunately, these are quite general responses and could also signify other issues such as pain or anxiety.

Emesis is even more difficult to assess as most rodents are non-emetic. One notable exception to this being *Suncus* murinus (musk shrews), which are capable of emesis.

Methods in this thesis are proxies of nausea and do not address the emetic properties of GDF15 or chemotherapy treatments. In order to so this, other species, such as the emetic musk shrew or lower order primates, would need to be used. Unfortunately, this was outside of the scope of the research performed in this thesis and these species were not included on any of the licences used.

Fortunately, emesis caused by GDF15 has been addressed elsewhere by other groups (Borner *et al.*, 2020; Breen *et al.*, 2020).

Although the data presented in chapter 3, regarding the valency of exogenous GDF15 treatment, does not directly address the nauseating properties of GDF15 or its emetic properties, it was published in 2020 (Worth *et al.*, 2020) and forms part of the current understanding of the effects of GDF15 treatment. This work fits alongside work by Borner et al. and Breen et al. who directly report on the effects of GDF15 and chemotherapies on vomiting in emetic species. Furthermore, a long-lasting GDF15 analogue has recently been tested in human subjects, causing nausea and emesis in a subset of individuals (Benichou *et al.*, 2023).

Therefore, despite flaws of using mouse models to assess nausea following GDF15 or chemotherapy treatment, useful information was still acquired.

My data, in conjunction with findings of other groups, allows us to draw reasonably reliable conclusions about the effects of GDF15 on nausea and emesis.

As prevention of CINV is clearly desirable, further exploration of the efficacy of blocking GFRAL activation against CINV will require the use of emetic species and ultimately human trial, so that feelings of nausea can be directly surveyed.

9.3.4 Assessment of anorexia and cachexia

Anorexia and cachexia most often appear together in cancer patients and those undergoing chemotherapy treatment. Whilst both cause a large negative impact on patient quality of life and prognosis, anorexia was more thoroughly explored in this thesis. The reason for this was predominantly dictated by licencing, time, and the coronavirus 19 pandemic.

In this thesis, body weight was used as a proxy for cachexia. This does not describe where weight was being lost from (fat, lean, or water). In order to address this, all mice undergoing chemotherapy treatment used in this thesis were scanned using an EchoMRI (see General Methods 2.6) to measure changes in lean and fat mass (data not shown) and tibialis anterior muscle, gastrocnemius muscle, inguinal white adipose, epididymal white adipose (where available), and interscapular brown adipose tissue were dissected and weighed (data not shown). These tissues, along with several others including heart and liver, were divided and one part rapidly frozen

on dry ice and kept for later assessment of inflammatory markers or markers or proteolysis/lipolysis using qPCR. The other part was formalin-fixed and paraffin-embedded for histological analysis. Unfortunately, due to the pandemic, there was not time to perform either molecular or histological analysis of these tissues.

As cachexia is an important and debilitating element of ACS, further investigation of the effects of blocking GFRAL on cachexia should be explored going forwards. This can immediately be done by assessing existing tissue from the studies performed here, and can in future encompass more thorough in vivo investigation, pending additions to animal licencing.

9.3.5 Preventing GFRAL signalling during chemotherapy in different mouse models

In chapter 7, a range of chemotherapy treatments were tested in WT mice. The two treatments which showed an impact on both food intake and body weight (CIS and CA), were selected for use in chapter 8. The reasoning behind this being that other therapies tested did not show effects on food intake or body weight anyway, so it would be hard to discern the effects of blocking GFRAL signalling.

Whilst the efficacy of the GFRAL mAb against anorexia and weight loss was tested in both CIS- and CA-treated WT mice, only CA was tested in GFRAL KO mice. The rationale behind this was twofold. Firstly, a similar experiment, in which GFRAL KO mice were treated with CIS and food intake and body weight measured, had already been published (Hsu *et al.*, 2017). Secondly, there were limitations in the number of GFRAL KO mice I was able to breed in the given timeframe.

Whilst it was relatively easy to generate *Gfral*$^{+/-}$ animals, producing *Gfral*$^{-/-}$ and *Gfral*$^{+/+}$ animals was much more challenging. To obtain a whole cohort suitable for one of these studies, more of the existing *Gfral*$^{-/-}$ and *Gfral*$^{+/+}$ animals would have been needed for breeding, increasing the time before the study could be run. Due to the pandemic and other university closures, this time was just not available. As it was, this study with CA in GFRAL KO mice was run in two parts due to lack of numbers, and this work was completed at the very end of the available time.

The *Gfral*-Cre line could also have been used in chapter 8 to trial different chemotherapies. For example, a similar study as in Chapter 4 could have been performed, in which *Gfral*-Cre mice would be injected into the DVC with a caspase virus, then treated with chemotherapy and food intake and body weight measured. However, as explained earlier, due to the coronavirus pandemic and Brexit, these mice only became available during the last few months of my time. Therefore, I only had time to validate this model. With this validation in place, these experiments provide a very interesting avenue of research for the future. Unfortunately, this was just not possible withing the scope of my own project.

9.4 The possibility of GDF15/GFRAL signalling as a therapeutic target

9.4.1 ACS or obesity?

At the commencement of the research presented here, it was not clear how GDF15/GFRAL signalling were causing anorexia and weight loss. The potential success of manipulating this signalling system during disease and therapy depends heavily on how anorexia and weight loss are achieved, and what role GDF15/GFRAL signalling is playing during disease.

Evidence now indicates that whilst intact GDF15/GFRAL signalling may be protective from obesity (Macia *et al.*, 2012; Mullican *et al.*, 2017; Tran *et al.*, 2018; Tsai *et al.*, 2019), this signalling network is activated by cellular stress, such as is caused by disease and certain drug therapies and is not a part of homeostatic control of energy balance. In terms of GDF15 as a therapeutic target, current evidence shows GDF15 to be highly aversive (Fig.3.2) (Borner, Shaulson, *et al.*, 2020; Borner, Wald, *et al.*, 2020; Sabatini *et al.*, 2021), and whilst increases in GDF15 do reduce food intake and cause weight loss, there is evidence that GDF15/GFRAL can cause cachexia (Tsai *et al.*, 2012; Lerner, Tao, *et al.*, 2016; Suriben *et al.*, 2020; Albuquerque *et al.*, 2022). These qualities would make GFRAL signalling a poor target to agonise to treat obesity but does suggest that GFRAL antagonism might be a useful target against ACS during diseases and therapies, which cause anorexia, cachexia, nausea, and/or emesis. The

GDF15/GFRAL signalling network therefore seems a promising target against cancer and chemotherapy-induced ACS.

In addition to cancer, GDF15 has been linked to ACS during other diseases such as human immunodeficiency virus infection, chronic heart failure, aging/sarcopenia, and COPD (Kempf *et al.*, 2007; Patel *et al.*, 2016; Johann, Kleinert and Klaus, 2021; Agarwal *et al.*, 2022). As evidence of the role of GDF15 in disease progression is conflicting or absent in many cases, further research would need to be done to find whether GDF15 is increased in cases where disease causes ACS and what role it may be playing in that particular disease scenario. For example, combatting chemotherapy-induced ACS in a cancer in which GDF15 is repressing tumour cell proliferation could be detrimental to overall prognosis. On the other hand, if preventing GDF15/GFRAL signalling prevents ACS from decreasing the efficacy of cytotoxic therapy, then the overall effect on prognosis could be a positive one. Further research is also required to establish whether GDF15/GFRAL signalling is causative of ACS in other diseases outside of cancer and chemotherapy.

It is possible that different parts of the GFRAL signalling network are responsible for the different effects of GDF15. For example, activation of one neuronal pathway may cause nausea, but not aversion. Another may decrease food intake, but not affect gastric emptying. If this is true and the different parts of this signalling network could be dissected, then it may be possible to induce or prevent certain effects of GDF15 which are beneficial, without causing effects which would be detrimental to the health and well-being of a patient.

There is already some evidence for this in available literature. For example, both Luan *et al.* (2019) and Suriben *et al.* (2020) found that by preventing peripheral adrenergic signalling, they were able to prevent weight loss in disease models, without affecting food intake (Luan *et al.*, 2019; Suriben *et al.*, 2020). There is also a lot of *in vitro* data showing the effects of GDF15 on cancer cells (Griner, Joshi and Nahta, 2013; Wang, Baek and Eling, 2013; Aw Yong *et al.*, 2014; Ünal *et al.*, 2015; Li *et al.*, 2016). With regards to this data, caution should be followed as commercially available GDF15 used in early studies, was shown to be contaminated with small quantities of TGFβs

which may affect results (Olsen *et al.*, 2017). It is possible, therefore, that GDF15 may have peripheral targets in disease situations, which produce separate effects. Future work could be directed to discover if GDF15 does have additional targets and/or GFRAL is more widely expressed during disease.

It may also be true that different parts of the central GFRAL signalling network perform different functions. To investigate this we must further understand pathways activated by GDF15 that are downstream of GFRAL neurons. This could provide avenues by which to target different parts of the GFRAL signalling network to understand what each part does. This is something for which the *Gfral*-Cre mouse will be extremely useful.

In terms of an obesity therapy, the aversive effects of GDF15 mean that the GDF15/GFRAL signalling system would only provide a good target if the weight loss effects can be uncoupled from the nauseating and cachectic effects. This could be made possible by targeting specific GDF15 signalling pathways, having established which signalling pathways carry out different functions.

9.4.2 Cancer and chemotherapy

Historically, there have been many studies investigating the role of GDF15 in cancer. In these studies, circulating GDF15 has had a variable correlation with prognosis. In addition to reported negative effects on cancer growth and proliferation, GDF15 has been connected to anorexia, weight loss, and cachexia during cancer in mice, rats, and humans (Tsai *et al.*, 2012; Lerner, Tao, *et al.*, 2016; Borner *et al.*, 2017; Suriben *et al.*, 2020; Ahmed *et al.*, 2021). In addition, many chemotherapy drugs are known to cause anorexia, cachexia, and nausea.

Although I was not able to identify a suitable model of cancer-induced ACS, there is still compelling evidence that prevention of GDF15/GFRAL signalling during cancer can alleviate cachexia in several preclinical mouse models (Lerner, Tao, *et al.*, 2016; Suriben *et al.*, 2020). Although they did not measure food intake, Lerner *et al.* (2016) found that prevention of GDF15/GFRAL signalling using an anti-GDF15 mAb could reverse cancer-induced cachexia. Suriben *et al.* (2020) similarly showed that blockade

of GFRAL signalling did prevent or reverse cachexia. Interestingly, in their study, whilst their anti-GFRAL mAb did not prevent anorexia, though it also did not have a negative impact on cancer progression.

In murine chemotherapy models, prevention of GDF15/GFRAL signalling has also proven useful against weight loss and anorexia. Breen *et al.* (2020) also found that prevention of GDF15 signalling using a mAb or GDF15 KO could prevent or reverse weight loss during chemotherapy, lessen the impact of chemotherapy on food intake, and did not negatively impact cancer progression in a preclinical mouse model, and this held true even during chemotherapy treatment (Breen *et al.*, 2020). Hsu *et al.* (2017) similarly showed that food intake and body weight were protected during treatment with CIS in GFRAL KO mice. These results correspond with my own findings in Chapter 8, that GFRAL KO or an anti-GFRAL mAb can protect mice from anorexia and weight loss during treatment with either CIS (Fig. 8.3A/B) or CA (Fig. 8.1A/B and 8.3C/D). Some of the data regarding treatment of mice with CIS and the anti-GFRAL mAb were published by us in Worth *et al*. (2020) and contributes to current knowledge of the involvement of GFRAL signalling in chemotherapy-induced anorexia and weight loss.

Though anorexia has a negative impact on quality of life, cachexia has a greater impact on cancer disease progression, efficacy of cancer therapies, and currently has no effective treatment. Therefore, even if prevention of GDF15/GFRAL signalling during cancer can reliably combat cachexia but not anorexia, it may be possible to have a positive impact on patient survival and quality of life by treating with an anti-GDF15 or -GFRAL mAb alongside an appetite stimulant, such as megace or a ghrelin analogue.

That blocking GDF15/GFRAL signalling can prevent the development of, or even reverse, cachexia (Lerner, Tao, *et al.*, 2016; Suriben *et al.*, 2020) is an extremely significant. As this has only been shown in mice with cancer, it will be important to ensure that the same holds true in other species, and that prevention of GDF15/GFRAL signalling continues not to have a negative impact on the progression of cancers. Indeed, there is a body of evidence showing that GDFD15/GFRAL

signalling has a negative impact on cancer progression depending on type and severity of the disease. In cases where GDF15 is associated with tumour growth, metastasis and neoangiogenesis, treatment with an anti-GDF15 or anti-GFRAL mAb could prove beneficial by targeting cancer growth and progression in addition to ACS.

10 Conclusions

- GDF15 is aversive and is released endogenously in response to treatment with certain cytotoxic drugs.

- GDF15 release and GFRAL activation do not occur after normal feeding stimuli and, therefore, are unlikely to perform a role in the day-to-day regulation of food intake and body weight.

- The GFRAL signalling network includes several known aversive, pathways.

- GFRAL neurons use CCK as a neurotransmitter to induce anorexia.

- GDF15 is increased and GFRAL^DVC neurons are activated by chemotherapy drugs which induce anorexia and weight loss.

- Chemotherapy-induced anorexia and weight loss can be reduced or prevented in mice by preventing GDFD15/GFRAL signalling, making the GDF15/GFRAL signalling network an attractive target to reduce chemotherapy-induced ACS.

Appendix

Publications from this work:

Worth, A.A., Shoop, R., Tye, K., Feetham, C.H., D'agostino, G., Dodd, G.T., Reimann, F., Gribble, F.M., Beebe, E.C., Dunbar, J.D., Alexander-Chacko, J.T., Sindelar, D.K., Coskun, T., Emmerson, P.J., and Luckman, S.M. (2020) '**The cytokine GDF15 signals through a population of brainstem cholecystokinin neurons to mediate anorectic signalling**', *eLife*, 9, pp. 1–19. Available at: https://doi.org/10.7554/eLife.55164.

References

Abizaid, A., Liu, Z.W., Andrews, Z.B., Shanabrough, M., Borok, E., Elsworth, J.D., Roth, R.H., Sleeman, M.W., Picciotto, M.R., Tschöp, M.H., Gao, X.B., and Horvath, T.L. (2006) 'Ghrelin modulates the activity and synaptic input organization of midbrain dopamine neurons while promoting appetite', *J Clin Invest*, 116(12), pp. 3229–3239. Available at: https://doi.org/10.1172/jci29867.

Adela, R. and Banerjee, S.K. (2015) 'GDF-15 as a target and biomarker for diabetes and cardiovascular diseases: A translational prospective', *Journal of Diabetes Research*, 2015(490842). Available at: https://doi.org/10.1155/2015/490842.

Agarwal, N., Ramirez Bustamante, C.E., Wu, H., Armamento-Villareal, R., Lake, J.E., Balasubramanyam, A., and Hartig, S.M. (2022) 'Heightened levels of plasma growth differentiation factor 15 in men living with HIV', *Physiological Reports*, 10(9), p. e15293. Available at: https://doi.org/10.14814/PHY2.15293.

Ahmad, A.S., Ormiston-Smith, N., and Sasieni, P.D. (2015) 'Trends in the lifetime risk of developing cancer in Great Britain: comparison of risk for those born from 1930 to 1960', *British Journal of Cancer*, 112(5), pp. 943–947. Available at: https://doi.org/10.1038/BJC.2014.606.

Ahmed, D.S., Isnard, S., Lin, J., Routy, B., and Routy, J.P. (2021) 'GDF15/GFRAL pathway as a metabolic signature for cachexia in patients with cancer', *Journal of Cancer*, 12(4), pp. 1125–1132. Available at: https://doi.org/10.7150/JCA.50376.

Albertoni, M., Shaw, P.H., Nozaki, M., Sophie, G., Tenan, M., Hamou, M.F., Fairlie, D.W., Breit, S.N., Paralkar, V.M., De Tribolet, N., Van Meir, E.G., and Hegi, M.E. (2002) 'Anoxia induces macrophage inhibitory cytokine-1 (MIC-1) in glioblastoma cells independently of p53 and HIF-1', *Oncogene*, 21(27), pp. 4212–4219. Available at: https://doi.org/10.1038/sj.onc.1205610.

Albuquerque, B., Chen, X., Hirenallur-Shanthappa, D., Zhao, Y., Stansfield, J.C., Zhang, B.B., Sheikh, A., and Wu, Z. (2022) 'Neutralization of GDF15 prevents anorexia and weight loss in the monocrotaline-induced cardiac cachexia rat model', *Cells*, 11(7), p. 1073. Available at: https://doi.org/10.3390/CELLS11071073.

Alhadeff, A.L., Holland, R.A., Nelson, A., Grill, H.J., and De Jonghe, B.C. (2015) 'Glutamate receptors in the central nucleus of the amygdala mediate cisplatin-induced malaise and energy balance dysregulation through direct hindbrain projections', *Journal of Neuroscience*, 35(31), pp. 11094–11104. Available at: https://doi.org/10.1523/JNEUROSCI.0440-15.2015.

Alhadeff, A.L., Holland, R.A., Zheng, H., Rinaman, L., Grill, H.J., and De Jonghe, B.C.

(2017) 'Excitatory hindbrain-forebrain communication is required for cisplatin-induced anorexia and weight loss', *The Journal of Neuroscience*, 37(2), pp. 362–370. Available at: https://doi.org/10.1523/JNEUROSCI.2714-16.2017.

Altena, R., Fehrmann, R.S.N., Boer, H., De Vries, E.G.E., Meijer, C., and Gietema, J.A. (2015) 'Growth differentiation factor 15 (GDF-15) plasma levels increase during bleomycin- and cisplatin-based treatment of testicular cancer patients and relate to endothelial damage', *PLoS ONE*, 10(1), pp. 1–15. Available at: https://doi.org/10.1371/journal.pone.0115372.

Altorki, N.K., Markowitz, G.J., Gao, D., Port, J.L., Saxena, A., Stiles, B., McGraw, T., and Mittal, V. (2019) 'The lung microenvironment: an important regulator of tumour growth and metastasis', *Nature Reviews Cancer*, 19(1), pp. 9–31. Available at: https://doi.org/10.1038/s41568-018-0081-9.

Anderberg, R.H., Anefors, C., Bergquist, F., Nissbrandt, H., and Skibicka, K.P. (2014) 'Dopamine signaling in the amygdala, increased by food ingestion and GLP-1, regulates feeding behavior', *Physiology & Behavior*, 136, pp. 135–144. Available at: https://doi.org/10.1016/J.PHYSBEH.2014.02.026.

Ando, K., Takahashi, F., Kato, M., Kaneko, N., Doi, T., Ohe, Y., Koizumi, F., Nishio, K., and Takahashi, K. (2014) 'Tocilizumab, a proposed therapy for the cachexia of interleukin6-expressing lung cancer', *PLoS ONE*, 9(7), p. e102436. Available at: https://doi.org/10.1371/JOURNAL.PONE.0102436.

Andrade-Franzé, G.M.F., Andrade, C.A.F., Gasparini, S., De Luca, L.A., De Paula, P.M., Colombari, D.S.A., Colombari, E., and Menani, J. V. (2015) 'Importance of the central nucleus of the amygdala on sodium intake caused by deactivation of lateral parabrachial nucleus', *Brain Research*, 1625, pp. 238–245. Available at: https://doi.org/10.1016/J.BRAINRES.2015.08.044.

Andrews, P.L.R. and Horn, C.C. (2006) 'Signals for nausea and emesis: Implications for models of upper gastrointestinal diseases', *Autonomic neuroscience : basic & clinical*, 125(1–2), pp. 100–115. Available at: https://doi.org/10.1016/J.AUTNEU.2006.01.008.

Andrews, P.L.R. and Sanger, G.J. (2014) 'Nausea and the quest for the perfect anti-emetic', *European Journal of Pharmacology*, 722(1), pp. 108–121. Available at: https://doi.org/10.1016/j.ejphar.2013.09.072.

Anesten, F., Dalmau Gasull, A., Richard, J.E., Farkas, I., Mishra, D., Taing, L., Zhang, F., Poutanen, M., Palsdottir, V., Liposits, Z., Skibicka, K.P., and Jansson, J.O. (2019) 'Interleukin-6 in the central amygdala is bioactive and co-localised with glucagon-like peptide-1 receptor', *Journal of Neuroendocrinology*, 31(6), p. 12722. Available at:

https://doi.org/10.1111/JNE.12722.

Anker, M.S., Holcomb, R., Muscaritoli, M., von Haehling, S., Haverkamp, W., Jatoi, A., Morley, J.E., Strasser, F., Landmesser, U., Coats, A.J.S., and Anker, S.D. (2019) 'Orphan disease status of cancer cachexia in the USA and in the European Union: a systematic review', *Journal of Cachexia, Sarcopenia and Muscle*, 10(1), pp. 22–34. Available at: https://doi.org/10.1002/JCSM.12402.

Aapro, M. (2016) 'CINV: still troubling patients after all these years'. Available at: https://doi.org/10.1007/s00520-018-4131-3.

Argilés, J.M., Busquets, S., Moore-Carrasco, R., Figueras, M., Almendro, V., and López-Soriano, F.J. (2007) 'Targets in clinical oncology: the metabolic environment of the patient', *Frontiers in Bioscience*, 12, pp. 3024–3051.

Argilés, J.M., Busquets, S., Stemmler, B., and López-Soriano, F.J. (2014) 'Cancer cachexia: Understanding the molecular basis', *Nature Reviews Cancer*, 14(11), pp. 754–762. Available at: https://doi.org/10.1038/nrc3829.

Arruda, A.P., Milanski, M., Romanatto, T., Solon, C., Coope, A., Alberici, L.C., Festuccia, W.T., Hirabara, S.M., Ropelle, E., Curi, R., Carvalheira, J.B., Vercesi, A.E., and Velloso, L.A. (2010) 'Hypothalamic actions of tumor necrosis factor α provide the thermogenic core for the wastage syndrome in cachexia', *Endocrinology*, 151(2), pp. 683–694. Available at: https://doi.org/10.1210/EN.2009-0865.

Arthur, S.T., Van Doren, B.A., Roy, D., Noone, J.M., Zacherle, E., and Blanchette, C.M. (2016) 'Cachexia among US cancer patients', *Journal of Medical Economics*, 19(9), pp. 874–880. Available at: https://doi.org/10.1080/13696998.2016.1181640.

Aviello, G., Cristiano, C., Luckman, S.M., and D'Agostino, G. (2021) 'Brain control of appetite during sickness', *British journal of pharmacology*, 178(10), pp. 2096–2110. Available at: https://doi.org/10.1111/BPH.15189.

Aw Yong, K.M., Zeng, Y., Vindivich, D., Phillip, J.M., Wu, P.H., Wirtz, D., and Getzenberg, R.H. (2014) 'Morphological effects on expression of growth differentiation factor 15 (GDF15), a marker of metastasis', *Journal of Cellular Physiology*, 229(3), pp. 362–373. Available at: https://doi.org/10.1002/jcp.24458.

Bachmann, J., Heiligensetzer, M., Krakowski-Roosen, H., Büchler, M.W., Friess, H., and Martignoni, M.E. (2008) 'Cachexia worsens prognosis in patients with resectable pancreatic cancer', *Journal of Gastrointestinal Surgery*, 12(7), pp. 1193–1201. Available at: https://doi.org/10.1007/s11605-008-0505-z.

Bae, T., Jang, J., Lee, H., Song, J., Chae, S., Park, M., Son, C.-G., Yoon, S., and Yoon, Y. (2019) 'Paeonia lactiflora root extract suppresses cancer cachexia by down-

regulating muscular NF-κB signalling and muscle-specific E3 ubiquitin ligases in cancer-bearing mice', *Journal of Ethnopharmacology*, 246(112222). Available at: https://doi.org/10.1016/j.jep.2019.112222.

Baek, S.J., Kim, K.-S., Nixon, J.B., Wilson, L.C., and Eling, T.E. (2000) 'Cyclooxygenase inhibitors regulate the expression of a TGF-β superfamily member that has proapoptotic and antitumorigenic activities', *Molecular Pharmacology*, 59(4), pp. 901–908. Available at: https://doi.org/10.1088/1742-6596/1013/1/012062.

Baile, C., Zinn, W., and Mayer, J. (2017) 'Effects of lactate and other metabolites on food intake of monkeys', *American Journal of Physiology-Legacy Content*, 219(6), pp. 1606–1613. Available at: https://doi.org/10.1152/ajplegacy.1970.219.6.1606.

Bajic, J.E., Johnston, I.N., Howarth, G.S., and Hutchinson, M.R. (2018) 'From the bottom-up: chemotherapy and gut-brain axis dysregulation', *Frontiers in Behavioral Neuroscience*, 12(104), pp. 1–16. Available at: https://doi.org/10.3389/FNBEH.2018.00104.

Baldini, G. and Phelan, K.D. (2019) 'The melanocortin pathway and control of appetite-progress and therapeutic implications', *Journal of Endocrinology*, 241(1), pp. R1–R33. Available at: https://doi.org/10.1530/JOE-18-0596.

Ballarò, R., Costelli, P., and Penna, F. (2016) 'Animal models for cancer cachexia', *Current Opinion in Supportive and Palliative Care*, 10(4), pp. 281–287. Available at: https://doi.org/10.1097/SPC.0000000000000233.

Baracos, V.E., Martin, L., Korc, M., Guttridge, D.C., and Fearon, K.C.H. (2018) 'Cancer-associated cachexia', *Nature Reviews Disease Primers*, 4(17105). Available at: https://doi.org/10.1038/nrdp.2017.105.

Bauskin, A.R. *et al.* (2005) 'The propeptide mediates formation of stromal stores of PROMIC-1: role in determining prostate cancer outcome', *Cancer Res*, 65(6), pp. 2330–2336. Available at: www.aacrjournals.org.

Bauskin, A.R., Jiang, L., Luo, X.W., Wu, L., Brown, D.A., and Breit, S.N. (2010) 'The TGF-β superfamily cytokine MIC-1/GDF15: Secretory mechanisms facilitate creation of latent stromal stores', *Journal of Interferon and Cytokine Research*, 30(6), pp. 389–397. Available at: https://doi.org/10.1089/JIR.2009.0052/ASSET/IMAGES/LARGE/FIGURE4.JPEG.

Bellio, C., Emperador, M., Castellano, P., Gris-Oliver, A., Canals, F., Sánchez-Pla, A., Zamora, E., Arribas, J., Saura, C., Serra, V., Tabernero, J., Littlefield, B.A., and Villanueva, J. (2022) 'GDF15 is an eribulin response biomarker also required for survival of DTP breast cancer cells', *Cancers*, 14(10), p. 2562. Available at: https://doi.org/10.3390/CANCERS14102562.

Benichou, O. *et al.* (2023) 'Discovery, development, and clinical proof of mechanism of LY3463251, a long-acting GDF15 receptor agonist', *Cell Metabolism*, 35(2), pp. 274-286.e10. Available at: https://doi.org/10.1016/j.cmet.2022.12.011.

Berna, M.J., Tapia, J.A., Sancho, V., and Jensen, R.T. (2007) 'Progress in developing cholecystokinin (CCK)/gastrin receptor ligands which have therapeutic potential', *Current opinion in pharmacology*, 7(6), pp. 583–592. Available at: https://doi.org/10.1016/J.COPH.2007.09.011.

Berthoud, H. -R, Jedrzejewska, A., and Powley, T.L. (1990) 'Simultaneous labeling of vagal innervation of the gut and afferent projections from the visceral forebrain with Dil injected into the dorsal vagal complex in the rat', *Journal of Comparative Neurology*, 301(1), pp. 65–79. Available at: https://doi.org/10.1002/cne.903010107.

Betley, N.J., Xu, S., Fang, Z., Cao, H., Gong, R., Magnus, C.J., Yu, Y., and Sternson, S.M. (2015) 'Neurons for hunger and thirst transmit a negative-valence teaching signal', *Nature*, 521(7551), pp. 180–185. Available at: https://doi.org/10.1038/nature14416.

Billig, I., Yates, B.J., and Rinaman, L. (2001) 'Plasma hormone levels and central c-Fos expression in ferrets after systemic administration of cholecystokinin', *American Journal of Physiology-Regulatory, Integrative and Comparative Physiology*, 281(4), pp. R1243–R1255. Available at: https://doi.org/10.1152/ajpregu.2001.281.4.r1243.

Blasio, A., Steardo, L., Sabino, V., and Cottone, P. (2014) 'Opioid system in the medial prefrontal cortex mediates binge-like eating', *Addiction biology*, 19(4), pp. 652–662. Available at: https://doi.org/10.1111/ADB.12033.

Di Bonaventura, M.V.M., Ciccocioppo, R., Romano, A., Bossert, J.M., Rice, K.C., Ubaldi, M., St. Laurent, R., Gaetani, S., Massi, M., Shaham, Y., and Cifani, C. (2014) 'Role of bed nucleus of the stria terminalis corticotrophin-releasing factor receptors in frustration stress-induced binge-like palatable food consumption in female rats with a history of food restriction', *Journal of Neuroscience*, 34(34), pp. 11316–11324. Available at: https://doi.org/10.1523/JNEUROSCI.1854-14.2014.

Bootcov, M.R., Bauskin, A.R., Valenzuela, S.M., Moore, A.G., Bansal, M., He, X.Y., Zhang, H.P., Donnellan, M., Mahler, S., Pryor, K., Walsh, B.J., Nicholson, R.C., Fairlie, W.D., Por, S.B., Robbins, J.M., and Breit, S.N. (1997) 'MIC-1, a novel macrophage inhibitory cytokine, is a divergent member of the TGF- superfamily', *Proceedings of the National Academy of Sciences*, 94(21), pp. 11514–11519. Available at: https://doi.org/10.1073/pnas.94.21.11514.

Borner, T., Arnold, M., Ruud, J., Breit, S.N., Langhans, W., Lutz, T.A., Blomqvist, A., and Riediger, T. (2017) 'Anorexia-cachexia syndrome in hepatoma tumour-bearing rats requires the area postrema but not vagal afferents and is paralleled by increased

MIC-1/GDF15', *Journal of Cachexia, Sarcopenia and Muscle*, 8(3), pp. 417–427. Available at: https://doi.org/10.1002/jcsm.12169.

Borner, T., Wald, H.S., Ghidewon, M.Y., Zhang, B., Wu, Z., De Jonghe, B.C., Breen, D., and Grill, H.J. (2020) 'GDF15 induces an aversive visceral malaise state that drives anorexia and weight loss', *Cell Reports*, 31(3), p. 107543. Available at: https://doi.org/10.1016/J.CELREP.2020.107543.

Borner, T., Shaulson, E.D., Ghidewon, M.Y., Grill, H.J., Hayes, M.R., Jonghe, B.C. De, Borner, T., Shaulson, E.D., Ghidewon, M.Y., Barnett, A.B., Horn, C.C., and Doyle, R.P. (2020) 'GDF15 induces anorexia through nausea and emesis', *Cell Metabolism*, 31(2), pp. 351–362. Available at: https://doi.org/10.1016/j.cmet.2019.12.004.

Borison, H.L. (1974) 'Area postrema: Chemoreceptor trigger zone for vomiting - is that all?', *Life Scineces*, 14(10), pp. 1807–1817.

Braun, T.P., Zhu, X., Szumowski, M., Scott, G.D., Grossberg, A.J., Levasseur, P.R., Graham, K., Khan, S., Damaraju, S., Colmers, W.F., Baracos, V.E., and Marks, D.L. (2011) 'Central nervous system inflammation induces muscle atrophy via activation of the hypothalamic-pituitary-adrenal axis', *The Journal of experimental medicine*, 208(12), pp. 2449–2463. Available at: https://doi.org/10.1084/JEM.20111020.

Bredholt, G., Mannelqvist, M., Stefansson, I.M., Birkeland, E., Bø, T.H., Øyan, A.M., Trovik, J., Kalland, K.H., Jonassen, I., Salvesen, H.B., Wik, E., and Akslen, L.A. (2015) 'Tumor necrosis is an important hallmark of aggressive endometrial cancer and associates with hypoxia, angiogenesis and inflammation responses', *Oncotarget*, 6(37), pp. 39676–39691. Available at: https://doi.org/10.18632/ONCOTARGET.5344.

Breen, D.M., Kim, H., Bennett, D., Wu, Z., Zhang, B.B., Birnbaum, M.J., Breen, D.M., Kim, H., Bennett, D., Calle, R.A., Collins, S., Esquejo, R.M., He, T., Weber, G., Wu, Z., Zhang, B.B., and Birnbaum, M.J. (2020) 'Clinical and translational report GDF-15 neutralization alleviates platinum-based chemotherapy-induced emesis, anorexia, and weight loss in mice and nonhuman primates', *Cell Metabolism*, 32(6), pp. 938–950. Available at: https://doi.org/10.1016/j.cmet.2020.10.023.

Breit, S.N., Johnen, H., Cook, A.D., Tsai, V.W.W., Mohammad, M.G., Kuffner, T., Zhang, H.P., Marquis, C.P., Jiang, L., Lockwood, G., Lee-Ng, M., Husaini, Y., Wu, L., Hamilton, J.A., and Brown, D.A. (2011) 'The TGF-β superfamily cytokine, MIC-1/GDF15: A pleotrophic cytokine with roles in inflammation, cancer and metabolism', *Growth Factors*, 29(5), pp. 187–195. Available at: https://doi.org/10.3109/08977194.2011.607137.

Brierley, D.I., Holt, M.K., Singh, A., de Araujo, A., McDougle, M., Vergara, M., Afaghani, M.H., Lee, S.J., Scott, K., Maske, C., Langhans, W., Krause, E., de Kloet, A.,

Gribble, F.M., Reimann, F., Rinaman, L., de Lartigue, G., and Trapp, S. (2021) 'Central and peripheral GLP-1 systems independently suppress eating', *Nature metabolism*, 3(2), pp. 258–273. Available at: https://doi.org/10.1038/S42255-021-00344-4.

Brown, D., Bauskin, A., Fairlie, W.D., Smith, M.D., Liu, T., Xu, N., and Breit, S.N. (2002) 'Antibody-based approach to high-volume genotyping for MIC-1 polymorphism', *BioTechniques*, 33(1), pp. 118–126.

Brown, D.A., Ward, R.L., Buckhaults, P., Liu, T., Romans, K.E., Hawkins, N.J., Bauskin, A.R., Kinzler, K.W., Vogelstein, B., and Breit, S.N. (2003) 'MIC-1 serum level and genotype: Associations with progress and prognosis of colorectal carcinoma', *Clinical Cancer Research*, 9(7), pp. 2642–2650. Available at: https://doi.org/10.1016/S1570-7946(03)80397-8.

Brown, D.A., Moore, J., Johnen, H., Smeets, T.J., Bauskin, A.R., Kuffner, T., Weedon, H., Milliken, S.T., Tak, P.P., Smith, M.D., and Breit, S.N. (2007) 'Serum macrophage inhibitory cytokine 1 in rheumatoid arthritis: A potential marker of erosive joint destruction', *Arthritis and Rheumatism*, 56(3), pp. 753–764. Available at: https://doi.org/10.1002/art.22410.

Brown, J.M. and Wilson, W.R. (2004) 'Exploiting tumour hypoxia in cancer treatment', *Nature Reviews Cancer*, 4(6), pp. 437–447. Available at: https://doi.org/10.1038/nrc1367.

Browning, K.N. and Travagli, R.A. (2016) 'Central nervous system control of gastrointestinal motility and secretion and modulation of gastrointestinal functions', *Comprehensive Physiology*, 4(4), pp. 1339–1368. Available at: https://doi.org/10.1002/cphy.c130055.Central.

Bruzzese, F., Hagglof, C., Leone, A., Sjoberg, E., Roca, M.S., Kiflemariam, S., Sjoblom, T., Hammarsten, P., Egevad, L., Bergh, A., Ostman, A., Budillon, A., and Augsten, M. (2014) 'Local and systemic protumorigenic effects of cancer-associated fibroblast-derived GDF15', *Cancer Research*, 74(13), pp. 3408–3417. Available at: https://doi.org/10.1158/0008-5472.CAN-13-2259.

Busquets, S., Toledo, M., Orpí, M., Massa, D., Porta, M., Capdevila, E., Padilla, N., Frailis, V., López-Soriano, F.J., Han, H.Q., and Argilés, J.M. (2012) 'Myostatin blockage using actRIIB antagonism in mice bearing the Lewis lung carcinoma results in the improvement of muscle wasting and physical performance', *Journal of Cachexia, Sarcopenia and Muscle*, 3(1), pp. 37–43. Available at: https://doi.org/10.1007/S13539-011-0049-Z.

Cai, H., Haubensak, W., Anthony, T.E., and Anderson, D.J. (2014) 'Central amygdala PKC-δ+ neurons mediate the influence of multiple anorexigenic signals', *Nature*

neuroscience, 17(9), pp. 1240–1248. Available at: https://doi.org/10.1038/NN.3767.

Campos, C.A., Bowen, A.J., Schwartz, M.W., and Palmiter, R.D. (2016) 'Parabrachial CGRP Neurons Control Meal Termination', *Cell Metabolism*, 23(5), pp. 811–820. Available at: https://doi.org/10.1586/14737175.2015.1028369.Focused.

Campos, C.A., Bowen, A.J., Han, S., Wisse, B.E., Palmiter, R.D., and Schwartz, M.W. (2017) 'Cancer-induced anorexia and malaise are mediated by CGRP neurons in the parabrachial nucleus', *Nature Neuroscience*, 20(7), pp. 934–942. Available at: https://doi.org/10.1038/nn.4574.

Cao, Z., Zhao, K., Jose, I., Hoogenraad, N.J., and Osellame, L.D. (2021) 'Biomarkers for cancer cachexia: A mini review', *International Journal of Molecular Sciences*, 22(9), pp. 1–15. Available at: https://doi.org/10.3390/ijms22094501.

Carson, D.A., Bhat, S., Hayes, T.C.L., Gharibans, A.A., Andrews, C.N., O'Grady, G., and Varghese, C. (2022) 'Abnormalities on electrogastrography in nausea and vomiting syndromes: A systematic review, meta-analysis, and comparison to other gastric disorders', *Digestive Diseases and Sciences*, 67(3), pp. 773–785. Available at: https://doi.org/10.1007/S10620-021-07026-X/FIGURES/3.

Carter, M.E., Soden, M.E., Zweifel, L.S., and Palmiter, R.D. (2013) 'Genetic identification of a neural circuit that suppresses appetite', *Nature*, 503(7474), pp. 111–114. Available at: https://doi.org/10.1038/nature12596.

Carter, M.E., Han, S., and Palmiter, R.D. (2015) 'Parabrachial calcitonin gene-related peptide neurons mediate conditioned taste aversion', *Journal of Neuroscience*, 35(11), pp. 4582–4586. Available at: https://doi.org/10.1523/JNEUROSCI.3729-14.2015.

Chen, C.Y., Asakawa, A., Fujimiya, M., Lee, S.D., and Inui, A. (2009) 'Ghrelin gene products and the regulation of food intake and gut motility', *Pharmacological Reviews*, 61(4), pp. 430–481. Available at: https://doi.org/10.1124/PR.109.001958.

Chen, J.Y., Campos, C.A., Jarvie, B.C., and Palmiter, R.D. (2018) 'Parabrachial CGRP neurons establish and sustain aversive taste memories', *Neuron*, 100(4), pp. 891–899. Available at: https://doi.org/10.1016/j.neuron.2018.09.032.

Chen, S.-J., Karan, D., Johansson, S.L., Lin, F.-F., Zeckser, J., Singh, A.P., Batra, S.K., and Lin, M.-F. (2007) 'Prostate-derived factor as a paracrine and autocrine factor for the proliferation of androgen receptor-positive human prostate cancer cells', *The Prostate*, 67(5), pp. 557–571. Available at: https://doi.org/10.1002/pros.

Chiavenna, S.M., Jaworski, J.P., and Vendrell, A. (2017) 'State of the art in anti-cancer mAbs', *Journal of Biomedical Science*, 24(15), pp. 1–12. Available at:

https://doi.org/10.1186/s12929-016-0311-y.

Chow, C.F.W. *et al.* (2022) 'Body weight regulation via MT1-MMP-mediated cleavage of GFRAL', *Nature Metabolism*, 4(2), pp. 203–212. Available at: https://doi.org/10.1038/s42255-022-00529-5.

Christiansen, A.M., Herman, J.P., and Ulrich-Lai, Y.M. (2011) 'Regulatory interactions of stress and reward on rat forebrain opioidergic and GABAergic circuitry', *Stress*, 14(2), pp. 205–215. Available at: https://doi.org/10.3109/10253890.2010.531331.

Chrysovergis, K., Wang, X., Kosak, J., Lee, S.H., Kim, J.S., Foley, J.F., Travlos, G., Singh, S., Baek, S.J., and Eling, T.E. (2014) 'NAG-1/GDF-15 prevents obesity by increasing thermogenesis, lipolysis and oxidative metabolism', *International Journal of Obesity*, 38(12), pp. 1555–1564. Available at: https://doi.org/10.1038/ijo.2014.27.

Chung, H.K. *et al.* (2017) 'Growth differentiation factor 15 is a myomitokine governing systemic energy homeostasis', *Journal of Cell Biology*, 216(1), pp. 149–165. Available at: https://doi.org/10.1083/jcb.201607110.

Ciccocioppo, R., Cippitelli, A., Economidou, D., Fedeli, A., and Massi, M. (2004) 'Nociceptin/orphanin FQ acts as a functional antagonist of corticotropin-releasing factor to inhibit its anorectic effect', *Physiology & Behavior*, 82(1), pp. 63–68. Available at: https://doi.org/10.1016/J.PHYSBEH.2004.04.035.

Cifuentes, L. and Acosta, A. (2022) 'Homeostatic regulation of food intake', *Clinics and Research in Hepatology and Gastroenterology*, 46, p. 101794. Available at: https://doi.org/10.1016/j.clinre.2021.101794

Cimino, I. *et al.* (2021) 'Activation of the hypothalamic–pituitary–adrenal axis by exogenous and endogenous GDF15', *Proceedings of the National Academy of Sciences*, 118(27), p. e2106868118. Available at: https://doi.org/10.1073/pnas.2106868118.

Clement-Jones, V. and Rees, L.H. (1982) *Neuroendocrine correlates of the endorphins and enkephalins, Clinical Neuroendocrinology*. Edited by G. Besser and L. Martini. ACADEMIC PRESS, INC. Available at: https://doi.org/10.1016/b978-0-12-093602-1.50010-4.

Coats, Andrew J Stewart *et al.* (2011) 'The ACT-ONE trial, a multicentre, randomised, double-blind, placebo-controlled, dose-finding study of the anabolic/catabolic transforming agent, MT-102 in subjects with cachexia related to stage III and IV non-small cell lung cancer and colorectal cancer: study design', *Journal of Cachexia, Sarcopenia and Muscle*, 2(4), pp. 201–207. Available at: https://doi.org/10.1007/S13539-011-0046-2.

Coll, A.P. *et al.* (2019) 'GDF15 mediates the effects of metformin on body weight and energy balance.', *Nature*, 578(7795), pp. 444–448. Available at: https://doi.org/10.1038/s41586-019-1911-y.

Cone, R.D. *et al.* (2001) 'The arcuate nucleus as a conduit for diverse signals relevant to energy homeostasis', *International Journal of Obesity*, 25(5), pp. 63–67. Available at: www.nature.com/ijo

Crawford, J. (2019) 'What are the criteria for response to cachexia treatment?', *Annals of Palliative Medicine*, 8(1), pp. 439–449. Available at: https://doi.org/10.21037/APM.2018.12.08.

D'Agostino, G., Lyons, D.J., Cristiano, C., Burke, L.K., Madara, J.C., Campbell, J.N., Garcia, A.P., Land, B.B., Lowell, B.B., Dileone, R.J., and Heisler, L.K. (2016) 'Appetite controlled by a cholecystokinin nucleus of the solitary tract to hypothalamus neurocircuit', *eLife*, 5(e12225), pp. 1–15. Available at: https://doi.org/10.7554/eLife.12225.

D'Agostino, G., Lyons, D., Cristiano, C., Lettieri, M., Olarte-Sanchez, C., Burke, L.K., Greenwald-Yarnell, M., Cansell, C., Doslikova, B., Georgescu, T., Martinez de Morentin, P.B., Myers, M.G., Rochford, J.J., and Heisler, L.K. (2018) 'Nucleus of the solitary tract serotonin 5-HT 2C receptors modulate food intake', *Cell metabolism*, 28(4), pp. 619-630.e5. Available at: https://doi.org/10.1016/J.CMET.2018.07.017.

Daly, L.E., Ní Bhuachalla, É.B., Power, D.G., Cushen, S.J., James, K., and Ryan, A.M. (2018) 'Loss of skeletal muscle during systemic chemotherapy is prognostic of poor survival in patients with foregut cancer', *Journal of Cachexia, Sarcopenia and Muscle*, 9(2), pp. 315–325. Available at: https://doi.org/10.1002/JCSM.12267.

Day, E.A., Ford, R.J., Smith, B.K., Mohammadi-Shemirani, P., Morrow, M.R., Gutgesell, R.M., Lu, R., Raphenya, A.R., Kabiri, M., McArthur, A.G., McInnes, N., Hess, S., Paré, G., Gerstein, H.C., and Steinberg, G.R. (2019) 'Metformin-induced increases in GDF15 are important for suppressing appetite and promoting weight loss', *Nature metabolism*, 1(12), pp. 1202–1208. Available at: https://doi.org/10.1038/S42255-019-0146-4.

Dewys, W.D., Begg, C., Ph, D., Lavin, P.T., Ph, D., Band, P.R., Bertino, J.R., Cohen, M.H., Douglass, H.O., Engstrom, P.F., Ezdinli, E., Horton, J., Johnson, G.J., Moertel, C.G., Oken, M.M., Perlia, C., Rosenbaum, C., and Silverstein, M.N. (1980) 'Prognostic effect of weight loss prior to chemotherapy in cancer patients', 69(4), pp. 491–497.

Ding, Y., Hao, K., Li, Z., Ma, R., Zhou, Y., Zhou, Z., Wei, M., Liao, Y., Dai, Y., Yang, Y., Zhang, X., and Zhao, L. (2020) 'c-Fos separation from Lamin A/C by GDF15 promotes colon cancer invasion and metastasis in inflammatory microenvironment', *Journal of*

cellular physiology, 235(5), pp. 4407–4421. Available at: https://doi.org/10.1002/JCP.29317.

Dobs, A.S., Boccia, R. V., Croot, C.C., Gabrail, N.Y., Dalton, J.T., Hancock, M.L., Johnston, M.A., and Steiner, M.S. (2013) 'Effects of enobosarm on muscle wasting and physical function in patients with cancer: a double-blind, randomised controlled phase 2 trial', *The Lancet. Oncology*, 14(4), pp. 335–345. Available at: https://doi.org/10.1016/S1470-2045(13)70055-X.

Dodd, G.T., Worth, A.A., Nunn, N., Korpal, A.K., Bechtold, D.A., Allison, M.B., Myers, M.G., Statnick, M.A., and Luckman, S.M. (2014) 'The thermogenic effect of leptin is dependent on a distinct population of prolactin-releasing peptide neurons in the dorsomedial hypothalamus', *Cell metabolism*, 20(4), pp. 639–649. Available at: https://doi.org/10.1016/J.CMET.2014.07.022.

Donohoe, C.L., Ryan, A.M., and Reynolds, J. V. (2011) 'Cancer cachexia: Mechanisms and clinical implications', *Gastroenterology Research and Practice*, 2011(601434), pp. 1–13. Available at: https://doi.org/10.1155/2011/601434.

Douglass, A.M., Kucukdereli, H., Ponserre, M., Markovic, M., Gründemann, J., Strobel, C., Alcala Morales, P.L., Conzelmann, K.K., Lüthi, A., and Klein, R. (2017) 'Central amygdala circuits modulate food consumption through a positive-valence mechanism', *Nature neuroscience*, 20(10), pp. 1384–1394. Available at: https://doi.org/10.1038/NN.4623.

Duan, K., Gao, X., and Zhu, D. (2021) 'The clinical relevance and mechanism of skeletal muscle wasting', *Clinical Nutrition*, 40(1), pp. 27–37. Available at: https://doi.org/10.1016/J.CLNU.2020.07.029.

Elmquist, J.K., Scammell, T.E., Jacobson, C.D., and Saper, C.B. (1996) 'Distribution of Fos-like immunoreactivity in the rat brain following intravenous lipopolysaccharide administration', *Journal of Comparative Neurology*, 371(1), pp. 85–103. Available at: https://doi.org/10.1002/(SICI)1096-9861(19960715)371:1<85::AID-CNE5>3.0.CO;2-H.

Elsea, Collin R, Kneiss, J.A., and Wood, L.J. (2015) 'Induction of IL-6 by cytotoxic chemotherapy is assiociated with loss of lean body and fat mass in tumour-free female mice', *Biological Research for Nursing*, 17(5), pp. 549–557. Available at: https://doi.org/10.1177/1099800414558087.Induction.

Elsea, Collin R., Kneiss, J.A., and Wood, L.J. (2015) 'Induction of IL-6 by Cytotoxic Chemotherapy Is Associated With Loss of Lean Body and Fat Mass in Tumor-free Female Mice', *Biological Research for Nursing*, 17(5), pp. 549–557. Available at: https://doi.org/10.1177/1099800414558087.

Emmerson, P.J. *et al.* (2017) 'The metabolic effects of GDF15 are mediated by the orphan receptor GFRAL', *Nature Medicine*, 23(10), pp. 1215–1219. Available at: https://doi.org/10.1038/nm.4393.

Emmerson, P.J., Duffin, K.L., Chintharlapalli, S., and Wu, X. (2018) 'GDF15 and growth control', *Frontiers in Physiology*, 9(1712), pp. 1–7. Available at: https://doi.org/10.3389/fphys.2018.01712.

Ezeoke, C.C. and Morley, J.E. (2015) 'Pathophysiology of anorexia in the cancer cachexia syndrome', *Journal of Cachexia, Sarcopenia and Muscle*, 6(4), pp. 287–302. Available at: https://doi.org/10.1002/jcsm.12059.

Fairlie, W.D., Moore, A.G., Bauskin, A.R., Russell, P.K., Zhang, H.R., and Breit, S.N. (1999) 'MIC-1 is a novel TGF-β superfamily cytokine associated with macrophage activation', *Journal of Leukocyte Biology*, 65(1), pp. 2–5. Available at: https://doi.org/10.1002/jlb.65.1.2.

Fearon, K. *et al.* (2011) 'Definition and classification of cancer cachexia: An international consensus', *The Lancet Oncology*, 12(5), pp. 489–495. Available at: https://doi.org/10.1016/S1470-2045(10)70218-7.

Fearon, K., Arends, J., and Baracos, V. (2013) 'Understanding the mechanisms and treatment options in cancer cachexia', *Nature Reviews Clinical Oncology*, 10(2), pp. 90–99. Available at: https://doi.org/10.1038/nrclinonc.2012.209.

Fearon, K.C.H., Glass, D.J., and Guttridge, D.C. (2012) 'Cancer cachexia: Mediators, signaling, and metabolic pathways', *Cell Metabolism*, 16(2), pp. 153–166. Available at: https://doi.org/10.1016/j.cmet.2012.06.011.

Fejzo, M.S. *et al.* (2018) 'Placenta and appetite genes GDF15 and IGFBP7 are associated with hyperemesis gravidarum', *Nature Communications*, 9(1178), pp. 1–9. Available at: https://doi.org/10.1038/s41467-018-03258-0.

Fejzo, M.S., Trovik, J., Grooten, I.J., Sridharan, K., Roseboom, T.J., Vikanes, Å., Painter, R.C., and Mullin, P.M. (2019) 'Nausea and vomiting of pregnancy and hyperemesis gravidarum', *Nature Reviews Disease Primers*, 5(1), pp. 1–17. Available at: https://doi.org/10.1038/s41572-019-0110-3.

Fejzo, M.S., MacGibbon, K.W., First, O., Quan, C., and Mullin, P.M. (2022) 'Whole-exome sequencing uncovers new variants in GDF15 associated with hyperemesis gravidarum', *Bjog*, 129(11), pp. 1845–1852. Available at: https://doi.org/10.1111/1471-0528.17129.

Fortin, S.M., Chen, J., and Hayes, M.R. (2020) 'Hindbrain melanocortin 3/4 receptors modulate the food intake and body weight suppressive effects of the GLP-1 receptor

agonist, liraglutide', *Physiology & behavior*, 220(112870). Available at: https://doi.org/10.1016/j.physbeh.2020.112870.Hindbrain.

Frikke-Schmidt, H., Hultman, K., Galaske, J.W., Jørgensen, S.B., Myers, M.G., and Seeley, R.J. (2019) 'GDF15 acts synergistically with liraglutide but is not necessary for the weight loss induced by bariatric surgery in mice', *Molecular Metabolism*, 21, pp. 13–21. Available at: https://doi.org/10.1016/j.molmet.2019.01.003.

Fujita, Y., Taniguchi, Y., Shinkai, S., Tanaka, M., and Ito, M. (2016) 'Secreted growth differentiation factor 15 as a potential biomarker for mitochondrial dysfunctions in aging and age-related disorders', *Geriatrics & Gerontology International*, 16, pp. 17–29. Available at: https://doi.org/10.1111/GGI.12724.

Fung, E. *et al.* (2021) 'Fc-GDF15 glyco-engineering and receptor binding affinity optimization for body weight regulation', *Scientific reports*, 11(8921), pp. 1–12. Available at: https://doi.org/10.1038/S41598-021-87959-5.

Garcia-Jimenez, C. and Goding, C.R. (2019) 'Perspective starvation and pseudo-starvation as drivers of cancer metastasis through translation reprogramming', *Cell Metabolism*, 29(2), pp. 254–267. Available at: https://doi.org/10.1016/j.cmet.2018.11.018.

Garfield, A.S., Li, C., Madara, J.C., Shah, B.P., Webber, E., Steger, J.S., Campbell, J.N., Gavrilova, O., Lee, C.E., Olson, D.P., Elmquist, J.K., Tannous, B.A., Krashes, M.J., and Lowell, B.B. (2015) 'A neural basis for melanocortin-4 receptor-regulated appetite', *Nature neuroscience*, 18(6), pp. 863–871. Available at: https://doi.org/10.1038/NN.4011.

Gatenby, R.A. and Gillies, R.J. (2004) 'Why do cancers have high aerobic glycolysis?', *Nature Reviews Cancer 2004 4:11*, 4(11), pp. 891–899. Available at: https://doi.org/10.1038/nrc1478.

Geary, N. (2020) 'Control-theory models of body-weight regulation and body-weight-regulatory appetite', *Appetite*, 144(104440). Available at: https://doi.org/10.1016/J.APPET.2019.104440.

Ghosh, S. (2019) 'Cisplatin: The first metal based anticancer drug', *Bioorganic Chemistry*, 88(102925). Available at: https://doi.org/10.1016/J.BIOORG.2019.102925.

Glass, C.K. and Olefsky, J.M. (2012) 'Inflammation and lipid signaling in the etiology of insulin resistance', *Cell metabolism*, 15(5), pp. 635–645. Available at: https://doi.org/10.1016/J.CMET.2012.04.001.

Graham, Z.A., Lavin, K.M., O'Bryan, S.M., Thalacker-Mercer, A.E., Buford, T.W., Ford,

K.M., Broderick, T.J., and Bamman, M.M. (2021) 'Mechanisms of exercise as a preventative measure to muscle wasting', *American journal of physiology*, 321(1), pp. C40–C57. Available at: https://doi.org/10.1152/AJPCELL.00056.2021.

Grant, C. V, Loman, B.R., Bailey, M.T., and Pyter, L.M. (2021) 'Manipulations of the gut microbiome alter chemotherapy- induced inflammation and behavioral side effects in female mice', *Brain Behav Immun*, 95, pp. 401–412. Available at: https://doi.org/10.1016/j.bbi.2021.04.014.

Greenway, F.L. (2015) 'Physiological adaptations to weight loss and factors favouring weight regain', *International Journal of Obesity (2005)*, 39(8), pp. 1188–1196. Available at: https://doi.org/10.1038/IJO.2015.59.

Grill, H.J. and Hayes, M.R. (2012) 'Hindbrain neurons as an essential hub in the neuroanatomically distributed control of energy balance', *Cell Metabolism*, 16(3), pp. 296–309. Available at: https://doi.org/10.1016/j.cmet.2012.06.015.

Griner, S.E., Joshi, J.P., and Nahta, R. (2013) 'Growth differentiation factor 15 stimulates rapamycin-sensitive ovarian cancer cell growth and invasion', *Biochemical Pharmacology*, 85(1), pp. 46–58. Available at: https://doi.org/10.1016/j.bcp.2012.10.007.

Gropp, E., Shanabrough, M., Borok, E., Xu, A.W., Janoschek, R., Buch, T., Plum, L., Balthasar, N., Hampel, B., Waisman, A., Barsh, G.S., Horvath, T.L., and Brüning, J.C. (2005) 'Agouti-related peptide-expressing neurons are mandatory for feeding', *Nature Neuroscience*, 8(10), pp. 1289–1291. Available at: https://doi.org/10.1038/nn1548.

Guan, L., Qiao, H., Wang, N., Luo, X., and Yan, J. (2018) 'The purinergic mechanism of the central nucleus of amygdala is involved in the modulation of salt intake in sodium-depleted rats', *Brain research bulletin*, 143, pp. 132–137. Available at: https://doi.org/10.1016/J.BRAINRESBULL.2018.08.018.

von Haehling, S. and Anker, S.D. (2010) 'Cachexia as a major underestimated and unmet medical need: Facts and numbers', *Journal of Cachexia, Sarcopenia and Muscle*, 1(1), pp. 1–5. Available at: https://doi.org/10.1007/s13539-010-0002-6.

Hao, S., Yang, H., Wang, X., He, Y., Xu, Haifeng, Wu, X., Pan, L., Liu, Y., Lou, H., Xu, Han, Ma, H., Xi, W., Zhou, Y., Duan, S., and Wang, H. (2019) 'The lateral hypothalamic and BNST GABAergic projections to the anterior ventrolateral periaqueductal gray regulate feeding', *Cell Reports*, 28(3), pp. 616-624.e5. Available at: https://doi.org/10.1016/J.CELREP.2019.06.051.

Hardaway, J.A. *et al.* (2019) 'Central amygdala prepronociceptin-expressing neurons mediate palatable food consumption and reward', *Neuron*, 102(5), pp. 1037-1052.e7.

Available at: https://doi.org/10.1016/j.neuron.2019.03.037.

Hardee, J.P., Counts, B.R., and Carson, J.A. (2019) 'Understanding the role of exercise in cancer cachexia therapy', *American Journal of Lifestyle Medicine*, 13(1), pp. 46–60. Available at: https://doi.org/10.1177/1559827617725283.

Haubensak, W., Kunwar, P.S., Cai, H., Ciocchi, S., Wall, N.R., Ponnusamy, R., Biag, J., Dong, H.W., Deisseroth, K., Callaway, E.M., Fanselow, M.S., Lüthi, A., and Anderson, D.J. (2010) 'Genetic dissection of an amygdala microcircuit that gates conditioned fear', *Nature*, 468(7321), pp. 270–276. Available at: https://doi.org/10.1038/NATURE09553.

Heeley, N. and Blouet, C. (2016) 'Central amino acid sensing in the control of feeding behavior', *Frontiers in Endocrinology*, 7(148), pp. 1–11. Available at: https://doi.org/10.3389/fendo.2016.00148.

Hendifar, A.E., Petzel, M.Q.B., Zimmers, T.A., Denlinger, C.S., Matrisian, L.M., Picozzi, V.J., and Rahib, L. (2019) 'Pancreas cancer-associated weight loss', *The Oncologist*, 24(5), pp. 691–701. Available at: https://doi.org/10.1634/theoncologist.2018-0266.

Heymsfield, S.B., Gonzalez, M.C.C., Shen, W., Redman, L., and Thomas, D. (2014) 'Weight loss composition is one-fourth fat-free mass: A critical review and critique of this widely cited rule', *Obesity Reviews*, 15(4), pp. 310–321. Available at: https://doi.org/10.1111/OBR.12143.

Hinke, S.A., Cavanaugh, C.R., Kirchner, T., Lang, W., Meng, R., Wallace, N.H., Liu, J.J., D'Aquino, K.E., Ho, G., Rankin, M.M., Wang, S.-P., Chavez, J.A., Nelson, S.M., Furman, J., Mullican, S., Rangwala, S.M., and Nawrocki, A.R. (2018) 'Growth differentiation factor-15 (GDF-15) inhibits gastric emptying in rodents as part of its anorectic mechanism of action', *Diabetes*, 67. Available at: https://doi.org/10.2337/DB18-283-LB.

Hinoi, E., Ochi, H., Takarada, T., Nakatani, E., Iezaki, T., Nakajima, H., Fujita, H., Takahata, Y., Hidano, S., Kobayashi, T., Takeda, S., and Yoneda, Y. (2012) 'Positive regulation of osteoclastic differentiation by growth differentiation factor 15 upregulated in osteocytic cells under hypoxia', *Journal of bone and mineral research*, 27(4), pp. 938–949. Available at: https://doi.org/10.1002/JBMR.1538.

Ho, J.E., Hwang, S.-J., Wollert, K.C., Larson, M.G., Cheng, S., Kempf, T., Vasan, R.S., Januzzi, J.L., Wang, T.J., and Fox, C.S. (2013) 'Biomarkers of cardiovascular stress and incident chronic kidney disease', *Clin Chem.*, 59(11), pp. 1613–1620. Available at: https://doi.org/10.1188/08.ONF.909-915.Effects.

Holt, M.K., Richards, J.E., Cook, D.R., Brierley, D.I., Williams, D.L., Reimann, F., Gribble, F.M., and Trapp, S. (2019) 'Preproglucagon neurons in the nucleus of the

solitary tract are the main source of brain GLP-1, mediate stress-induced hypophagia, and limit unusually large intakes of food', *Diabetes*, 68(1), pp. 21–33. Available at: https://doi.org/10.2337/DB18-0729/-/DC1.

Horvath, T.L., Warden, C.H., Hajos, M., Lombardi, A., Goglia, F., and Diano, S. (1999) 'Brain uncoupling protein 2: uncoupled neuronal mitochondria predict thermal synapses in homeostatic centers.', *The Journal of neuroscience : the official journal of the Society for Neuroscience*, 19(23), pp. 10417–27. Available at: https://doi.org/10.1523/JNEUROSCI.19-23-10417.1999.

Hromas, R., Hufford, M., Sutton, J., Xu, D., Li, Y., and Lu, L. (1997) 'PLAB, a novel placental bone morphogenetic protein', *Biochimica et Biophysica Acta*, 1354(1), pp. 40–44. Available at: https://doi.org/10.1016/S0167-4781(97)00122-X.

Hsu, J.Y. *et al.* (2017) 'Non-homeostatic body weight regulation through a brainstem-restricted receptor for GDF15', *Nature*, 551(7680), pp. 255–259. Available at: https://doi.org/10.1038/nature24042.

Huang, D., Grady, F.S., Peltekian, L., Laing, J.J., and Geerling, J.C. (2021) 'Efferent projections of CGRP/Calca-expressing parabrachial neurons in mice', *Journal of Comparative Neurology*, 529(11), pp. 2911–2957. Available at: https://doi.org/10.1002/CNE.25136.

Huh, S.J., Chung, C.Y., Sharma, A., and Robertson, G.P. (2010) 'Macrophage inhibitory cytokine-1 regulates melanoma vascular development', *American Journal of Pathology*, 176(6), pp. 2948–2957. Available at: https://doi.org/10.2353/ajpath.2010.090963.

Husaini, Y., Lockwood, G.P., Nguyen, T. V., Tsai, V.W.W., Mohammad, M.G., Russell, P.J., Brown, D.A., and Breit, S.N. (2015) 'Macrophage inhibitory cytokine-1 (MIC-1/GDF15) gene deletion promotes cancer growth in TRAMP prostate cancer prone mice', *PLoS ONE*, 19(10), pp. 1–12. Available at: https://doi.org/10.1371/journal.pone.0115189.

Iemolo, A., Blasio, A., St Cyr, S.A., Jiang, F., Rice, K.C., Sabino, V., and Cottone, P. (2013) 'CRF-CRF1 receptor system in the central and basolateral nuclei of the amygdala differentially mediates excessive eating of palatable food', *Neuropsychopharmacology*, 38(12), pp. 2456–2466. Available at: https://doi.org/10.1038/NPP.2013.147.

Ito, T., Igarashi, H., and Jensen, R.T. (2012) 'Pancreatic neuroendocrine tumors: Clinical features, diagnosis and medical treatment: Advances', *Best Practice and Research: Clinical Gastroenterology*, 26(6), pp. 737–753. Available at: https://doi.org/10.1016/J.BPG.2012.12.003.

Johann, K., Kleinert, M., and Klaus, S. (2021) 'The role of GDF15 as a myomitokine', *Cells*, 10(11), pp. 1–16. Available at: https://doi.org/10.3390/cells10112990.

Johnen, H. *et al.* (2007) 'Tumor-induced anorexia and weight loss are mediated by the TGF-β superfamily cytokine MIC-1', *Nature Medicine*, 13(11), pp. 1333–1340. Available at: https://doi.org/10.1038/nm1677.

Joint Formulary Committee (2022) 'Cytotoxic drugs | Treatment summaries | BNF | NICE Available at: https://bnf.nice.org.uk/treatment-summaries/cytotoxic-drugs/ (Accessed: 25 February 2023).

Joint Formulary Committee (2023) 'Clozapine | Drugs | BNF | NICE (2023). Available at: https://bnf.nice.org.uk/drugs/clozapine/ (Accessed: 2 September 2023).

Jones, J.E., Cadena, S.M., Gong, C., Wang, X., Chen, Z., Wang, S.X., Vickers, C., Chen, H., Lach-Trifilieff, E., Hadcock, J.R., and Glass, D.J. (2018) 'Supraphysiologic administration of GDF11 induces cachexia in part by upregulating GDF15', *Cell Reports*, 22(6), pp. 1522–1530. Available at: https://doi.org/10.1016/j.celrep.2018.01.044.

Jones, J.M., Qin, R., Bardia, A., Linquist, B., Wolf, S., and Loprinzi, C.L. (2011) 'Antiemetics for chemotherapy-induced nausea and vomiting occurring despite prophylactic antiemetic therapy', *Journal of Palliative Medicine*, 14(7), pp. 810–814. Available at: https://doi.org/10.1089/JPM.2011.0058.

Joshi, J.P., Brown, N.E., Griner, S.E., and Nahta, R. (2011) 'Growth differentiation factor 15 (GDF15)-mediated HER2 phosphorylation reduces trastuzumab sensitivity of HER2-overexpressing breast cancer cells', *Biochemical pharmacology*, 82(9), pp. 1090–1099. Available at: https://doi.org/10.1016/J.BCP.2011.07.082.

Kang, S.G., Choi, M.J., Jung, S.B., Chung, H.K., Chang, J.Y., Kim, J.T., Kang, Y.E., Lee, J.H., Hong, H.J., Jun, S.M., Ro, H.J., Suh, J.M., Kim, H., Auwerx, J., Yi, H.S., and Shong, M. (2021) 'Differential roles of GDF15 and FGF21 in systemic metabolic adaptation to the mitochondrial integrated stress response', *iScience*, 24(3), p. 102181. Available at: https://doi.org/10.1016/J.ISCI.2021.102181.

Kempf, T., von Haehling, S., Peter, T., Allhoff, T., Cicoira, M., Doehner, W., Ponikowski, P., Filippatos, G.S., Rozentryt, P., Drexler, H., Anker, S.D., and Wollert, K.C. (2007) 'Prognostic utility of growth differentiation factor-15 in patients with chronic heart failure', *Journal of the American College of Cardiology*, 50(11), pp. 1054–1060. Available at: https://doi.org/10.1016/j.jacc.2007.04.091.

Khachaturian, H., Lewis, M. and Watson, S. (1983) 'Enkephalin systems in diencephalon and brainstem of the rat.', *J Comp Neurol*, 220(3), pp. 310–320.

Kim, D.Y., Heo, G., Kim, M., Kim, H., Jin, J.A., Kim, H.K., Jung, S., An, M., Ahn, B.H., Park, J.H., Park, H.E., Lee, M., Lee, J.W., Schwartz, G.J., and Kim, S.Y. (2020) 'A neural circuit mechanism for mechanosensory feedback control of ingestion', *Nature*, 580(7803), pp. 376–380. Available at: https://doi.org/10.1038/S41586-020-2167-2.

Klaus, S., Igual Gil, C., and Ost, M. (2021) 'Regulation of diurnal energy balance by mitokines', *Cellular and Molecular Life Sciences*, 78(7), pp. 3369–3384. Available at: https://doi.org/10.1007/s00018-020-03748-9.

Kleinert, M., Clemmensen, C., Sjøberg, K.A., Carl, C.S., Jeppesen, J.F., Wojtaszewski, J.F.P., Kiens, B., and Richter, E.A. (2018) 'Exercise increases circulating GDF15 in humans', *Molecular Metabolism*, 9, pp. 187–191. Available at: https://doi.org/10.1016/j.molmet.2017.12.016.

Kojima, M., Hosoda, H., Date, Y., Nakazato, M., Matsuo, H., and Kangawa, K. (1999) 'Ghrelin is a growth-hormone-releasing acylated peptide from stomach', *Letters to Nature*, 402(6762), pp. 656–660. Available at: https://www.nature.com/articles/45230.pdf (Accessed: 20 February 2023).

Könner, A.C., Janoschek, R., Plum, L., Jordan, S.D., Rother, E., Ma, X., Xu, C., Enriori, P., Hampel, B., Barsh, G.S., Kahn, C.R., Cowley, M.A., Ashcroft, F.M., and Brüning, J.C. (2007) 'Insulin action in AgRP-expressing neurons is required for suppression of hepatic glucose production', *Cell Metabolism*, 5(6), pp. 438–449. Available at: https://doi.org/10.1016/j.cmet.2007.05.004.

Konturek, S., Konturek, J., Pawlik, T., and Brzozowki, T. (2004) 'Brain-gut axis and its role in the control of food intake', *Journal of physiology and pharmacology*, 55(1), pp. 137–154.

Korneev, K. V., Atretkhany, K.S.N., Drutskaya, M.S., Grivennikov, S.I., Kuprash, D. V., and Nedospasov, S.A. (2017) 'TLR-signaling and proinflammatory cytokines as drivers of tumorigenesis', *Cytokine*, 89, pp. 127–135. Available at: https://doi.org/10.1016/J.CYTO.2016.01.021.

Kovács, A., László, K., Gálosi, R., Tóth, K., Ollmann, T., Péczely, L., and Lénárd, L. (2012) 'Microinjection of RFRP-1 in the central nucleus of amygdala decreases food intake in the rat', *Brain research bulletin*, 88(6), pp. 589–595. Available at: https://doi.org/10.1016/J.BRAINRESBULL.2012.06.001.

Lacy, B.E., Parkman, H.P., and Camilleri, M. (2018) 'Chronic nausea and vomiting: Evaluation and treatment', *American Journal of Gastroenterology*, 113(5), pp. 647–659. Available at: https://doi.org/10.1038/S41395-018-0039-2.

Lau, S.K.M. and Iyengar, P. (2017) 'Implications of weight loss for cancer patients receiving radiotherapy', *Current Opinion in Supportive and Palliative Care*, 11(4), pp. 261–265. Available at: https://doi.org/10.1097/SPC.0000000000000298.

Laurens, C. *et al.* (2020) 'Growth and differentiation factor 15 is secreted by skeletal muscle during exercise and promotes lipolysis in humans', *JCI insight*, 5(6), pp. 1–14. Available at: https://doi.org/10.1172/jci.insight.131870.

Lawrence, C.B., Ellacott, K.L.J., and Luckman, S.M. (2002) 'PRL-releasing peptide reduces food intake and may mediate satiety signaling', *Endocrinology*, 143(2), pp. 360–367. Available at: https://doi.org/10.1210/ENDO.143.2.8609.

Leon, R.M., Borner, T., Stein, L.M., Urrutia, N.A., De Jonghe, B.C., Schmidt, H.D., and Hayes, M.R. (2021) 'Activation of PPG neurons following acute stressors differentially involves hindbrain serotonin in male rats', *Neuropharmacology*, 187, p. 108477. Available at: https://doi.org/10.1016/J.NEUROPHARM.2021.108477.

Lerner, L., Hayes, T.G., Tao, N., Krieger, B., Feng, B., Wu, Z., Nicoletti, R., Isabel Chiu, M., Gyuris, J., and Garcia, J.M. (2015) 'Plasma growth differentiation factor 15 is associated with weight loss and mortality in cancer patients', *Journal of Cachexia, Sarcopenia and Muscle*, 6(4), pp. 317–324. Available at: https://doi.org/10.1002/jcsm.12033.

Lerner, L., Gyuris, J., Nicoletti, R., Gifford, J., Krieger, B., and Jatoi, A. (2016) 'Growth differentiating factor-15 (GDF-15): A potential biomarker and therapeutic target for cancer-associated weight loss', *Oncology Letters*, 12(5), pp. 4219–4223. Available at: https://doi.org/10.3892/ol.2016.5183.

Lerner, L., Tao, J., Liu, Q., Nicoletti, R., Feng, B., Krieger, B., Mazsa, E., Siddiquee, Z., Wang, R., Huang, L., Shen, L., Lin, J., Vigano, A., Chiu, M.I., Weng, Z., Winston, W., Weiler, S., and Gyuris, J. (2016) 'MAP3K11/GDF15 axis is a critical driver of cancer cachexia', *Journal of Cachexia, Sarcopenia and Muscle*, 7(4), pp. 467–482. Available at: https://doi.org/10.1002/jcsm.12077.

Li, C., Wang, J., Kong, J., Tang, J., Wu, Y., Xu, E., Zhang, H., and Lai, M. (2016) 'GDF15 promotes EMT and metastasis in colorectal cancer', *Oncotarget* [Preprint]. Available at: https://doi.org/10.18632/oncotarget.6205.

Lin, L., Saha, P.K., Ma, X., Henshaw, I.O., Shao, L., Chang, B.H.J., Buras, E.D., Tong, Q., Chan, L., Mcguinness, O.P., and Sun, Y. (2011) 'Ablation of ghrelin receptor reduces adiposity and improves insulin sensitivity during aging by regulating fat metabolism in white and brown adipose tissues', *Aging cell*, 10(6), pp. 996–1010. Available at: https://doi.org/10.1111/J.1474-9726.2011.00740.X.

Lin, T.C. and Hsiao, M. (2017) 'Ghrelin and cancer progression', *Biochimica et*

Biophysica Acta (BBA) - Reviews on Cancer, 1868(1), pp. 51–57. Available at: https://doi.org/10.1016/J.BBCAN.2017.02.002.

Lincová, E., Hampl, A., Pernicová, Z., Staršíchová, A., Krčmář, P., Machala, M., Kozubík, A., and Souček, K. (2009) 'Multiple defects in negative regulation of the PKB/Akt pathway sensitise human cancer cells to the antiproliferative effect of non-steroidal anti-inflammatory drugs', *Biochemical Pharmacology*, 78(6), pp. 561–572. Available at: https://doi.org/10.1016/j.bcp.2009.05.001.

Liu, H., Huang, Y., Lyu, Y., Dai, W., Tong, Y., and Li, Y. (2021) 'GDF15 as a biomarker of ageing', *Exp Gerontol.*, 146(1112228). Available at: https://doi.org/10.1016/j.exger.2021.111228.

Liu, Y., Wang, D., Li, T., Yang, F., Li, Z., Bai, X., and Wang, Y. (2022) 'The role of NLRP3 inflammasome in inflammation-related skeletal muscle atrophy', *Frontiers in Immunology*, 13(1035709.), pp. 1–10. Available at: https://doi.org/10.3389/FIMMU.2022.1035709.

Lockhart, S.M., Saudek, V., and O'Rahilly, S. (2020) 'GDF15: A hormone conveying somatic distress to the brain', *Endocrine reviews*, 41(4). Available at: https://doi.org/10.1210/endrev/bnaa007.

Loman, B.R., Jordan, K.R., Haynes, B., Bailey, M.T., and Pyter, L.M. (2019) 'Chemotherapy-induced neuroinflammation is associated with disrupted colonic and bacterial homeostasis in female mice', *Scientific Reports*, 9(1). Available at: https://doi.org/10.1038/S41598-019-52893-0.

Low, J.K., Ambikairajah, A., Shang, K., Brown, D.A., Tsai, V.W.W., Breit, S.N., and Karl, T. (2017) 'First behavioural characterisation of a knockout mouse model for the transforming growth factor (TGF)-β superfamily cytokine, MIC-1/GDF15', *PLoS ONE*, 12(1), p. e0168416. Available at: https://doi.org/10.1371/journal.pone.0168416.

Lu, J.F., Zhu, M.Q., Xie, B.C., Shi, X.C., Liu, H., Zhang, R.X., Xia, B., and Wu, J.W. (2022) 'Camptothecin effectively treats obesity in mice through GDF15 induction', *PLOS Biol*, 20(2), p. e3001517. Available at: https://doi.org/10.1371/journal.pbio.3001517.

Lu, X., He, X., Su, J., Wang, J., Liu, X., Xu, K., De, W., Zhang, E., Guo, R., and Shi, Y.E. (2018) 'EZH2-mediated epigenetic suppression of GDF15 predicts a poor prognosis and regulates cell proliferation in non-small-cell lung cancer', *Molecular Therapy - Nucleic Acids*, 12, pp. 309–318. Available at: https://doi.org/10.1016/j.omtn.2018.05.016.

Luan, H.H., Wang, A., Hilliard, B.K., Carvalho, F., Rosen, C.E., Ahasic, A.M., Herzog, E.L., Kang, I., Pisani, M.A., Yu, S., Zhang, C., Ring, A.M., and Young, L.H. (2019) 'GDF15 is an Inflammation-Induced Central Mediator of Tissue Tolerance', *Cell*, 178(5), pp.

1231–1244. Available at: https://doi.org/10.1016/j.cell.2019.07.033.GDF15.

Luquet, S., Perez, F.A., Hnasko, T.S., and Palmiter, R.D. (2005) 'NPY/AgRP neurons are essentials for feeding in adult mice but can be ablated in neonates', *Science*, 310(5748), pp. 683–685. Available at: https://doi.org/10.1126/SCIENCE.1115524/SUPPL_FILE/LUQUET.SOM.PDF.

Lutz, T.A. (2016) 'Gut hormones such as amylin and GLP-1 in the control of eating and energy expenditure', *International Journal of Obesity Supplements*, 6(Suppl 1), p. S15. Available at: https://doi.org/10.1038/IJOSUP.2016.4.

Ma, L., Wang, D.D., Zhang, T.Y., Yu, H., Wang, Y., Huang, S.H., Lee, F.S., and Chen, Z.Y. (2011) 'Region-specific involvement of BDNF secretion and synthesis in conditioned taste aversion memory formation', *The Journal of Neuroscience*, 31(6), pp. 2079–2090. Available at: https://doi.org/10.1523/JNEUROSCI.5348-10.2011.

MacDougall, M.R. and Sharma, S. (2023) 'Physiology, Chemoreceptor Trigger Zone', *StatPearls* [Preprint]. Available at: https://www.ncbi.nlm.nih.gov/books/NBK537133/ (Accessed: 3 September 2023).

Macia, L., Tsai, V.W.W., Nguyen, A.D., Johnen, H., Kuffner, T., Shi, Y.C., Lin, S., Herzog, H., Brown, D.A., Breit, S.N., and Sainsbury, A. (2012) 'Macrophage inhibitory cytokine 1 (MIC-1/GDF15) decreases food intake, body weight and improves glucose tolerance in mice on normal & obesogenic diets', *PLoS ONE*, 7(4), p. e34868. Available at: https://doi.org/10.1371/journal.pone.0034868.

Mahler, S. V and Aston-Jones, G. (2018) 'CNO Evil? Considerations for the Use of DREADDs in Behavioral Neuroscience', 43, pp. 934–936. Available at: https://doi.org/10.1038/npp.2017.299

Majchrzak, K., Pawłowski, K.M., Orzechowska, E.J., Dolka, I., Mucha, J., Motyl, T., and Król, M. (2012) 'A role of ghrelin in canine mammary carcinoma cells proliferation, apoptosis and migration', *BMC Veterinary Research*, 8(170), pp. 1–18. Available at: https://doi.org/10.1186/1746-6148-8-170.

Majem, M., de las Peñas, R., Virizuela, J. A., Cabezón-Gutiérrez, L., Cruz, P., Lopez-Castro, R., Méndez, M., Mondéjar, R., Muñoz, M. del M., & Escobar, Y. (2022). SEOM Clinical Guideline update for the prevention of chemotherapy-induced nausea and vomiting (2021). *Clinical & Translational Oncology*, *24*(4), 712. https://doi.org/10.1007/S12094-022-02802-1

Malla, J., Zahra, A., Venugopal, S., Selvamani, T.Y., Shoukrie, S.I., Selvaraj, R., Dhanoa, R.K., Hamouda, R.K., and Mostafa, J. (2022) 'What role do inflammatory cytokines play in cancer cachexia?', *Cureus*, 14(7), p. e26798. Available at: https://doi.org/10.7759/CUREUS.26798.

Maniam, J. and Morris, M.J. (2012) 'The link between stress and feeding behaviour', *Neuropharmacology*, 63(1), pp. 97–110. Available at: https://doi.org/10.1016/j.neuropharm.2012.04.017.

Maracle, A.C., Normandeau, C.P., Dumont, É.C., and Olmstead, M.C. (2019) 'Dopamine in the oval bed nucleus of the stria terminalis contributes to compulsive responding for sucrose in rats', *Neuropsychopharmacology*, 44(2), pp. 381–389. Available at: https://doi.org/10.1038/S41386-018-0149-Y.

Martín-García, E., Burokas, A., Kostrzewa, E., Gieryk, A., Korostynski, M., Ziolkowska, B., Przewlocka, B., Przewlocki, R., and Maldonado, R. (2011) 'New operant model of reinstatement of food-seeking behavior in mice', *Psychopharmacology*, 215(1), pp. 49–70. Available at: https://doi.org/10.1007/S00213-010-2110-6.

Martinez, J.M., Sali, T., Okazaki, R., Anna, C., Hollingshead, M., Hose, C., Monks, A., Walker, N.J., Baek, S.J., and Eling, T.E. (2006) 'Drug-induced expression of nonsteroidal anti-inflammatory drug-activated gene/macrophage inhibitory cytokine-1/prostate-derived factor, a putative tumor suppressor, inhibits tumor growth.', *The Journal of pharmacology and experimental therapeutics*, 318(2), pp. 899–906. Available at: https://doi.org/10.1124/jpet.105.100081.rectal.

Matson, D.R. and Stukenberg, P.T. (2011) 'Spindle poisons and cell fate: A tale of two pathways', *Molecular Interventions*, 11(2), pp. 141–150. Available at: https://doi.org/10.1124/mi.11.2.12.

May, A.A., Liu, M., Woods, S.C., and Begg, D.P. (2016) 'CCK increases the transport of insulin into the brain', *Physiology & behavior*, 165, pp. 392–397. Available at: https://doi.org/10.1016/J.PHYSBEH.2016.08.025.

McQuade, R.M., Stojanovska, V., Donald, E., Abalo, R., Bornstein, J.C., and Nurgali, K. (2016) 'Gastrointestinal dysfunction and enteric neurotoxicity following treatment with anticancer chemotherapeutic agent 5-fluorouracil', *Neurogastroenterology & Motility*, 28(12), pp. 1861–1875. Available at: https://doi.org/10.1111/NMO.12890.

Melvin, A., Chantzichristos, D., Kyle, C.J., Mackenzie, S.D., Walker, B.R., Johannsson, G., Stimson, R.H., and O'Rahilly, S. (2020) 'GDF15 is elevated in conditions of glucocorticoid deficiency and is modulated by glucocorticoid replacement', *The Journal of clinical endocrinology and metabolism*, 105(5), pp. 1427–1434. Available at: https://doi.org/10.1210/CLINEM/DGZ277.

Mendes, M.C.S., Pimentel, G.D., Costa, F.O., and Carvalheira, J.B.C. (2015) 'Molecular and neuroendocrine mechanisms of cancer cachexia', *Journal of Endocrinology*, 226(3), pp. R29–R43. Available at: https://doi.org/10.1530/JOE-15-0170.

Le Merrer, J., Becker, J.A.J., Befort, K., and Kieffer, B.L. (2009) 'Reward processing by

the opioid system in the brain', *Physiological reviews*, 89(4), pp. 1379–1412. Available at: https://doi.org/10.1152/PHYSREV.00005.2009.

Molfino, A., Laviano, A., and Fanelli, F.R. (2010) 'Contribution of anorexia to tissue wasting in cachexia', *Current Opinion in Supportive and Palliative Care*, 4(4), pp. 249–253. Available at: https://doi.org/10.1097/SPC.0b013e32833e4aa5.

Mullican, S.E., Lin-Schmidt, X., Chin, C.N., Chavez, J.A., Furman, J.L., Armstrong, A.A., Beck, S.C., South, V.J., Dinh, T.Q., Cash-Mason, T.D., Cavanaugh, C.R., Nelson, S., Huang, C., Hunter, M.J., and Rangwala, S.M. (2017) 'GFRAL is the receptor for GDF15 and the ligand promotes weight loss in mice and nonhuman primates', *Nature Medicine*, 23(10), pp. 1150–1157. Available at: https://doi.org/10.1038/nm.4392.

Mullur, R., Liu, Y.Y., and Brent, G.A. (2014) 'Thyroid hormone regulation of metabolism', *Physiological Reviews*, 94(2), pp. 355–382. Available at: https://doi.org/10.1152/PHYSREV.00030.2013.

Nagy, J.A., Chang, S.H., Dvorak, A.M., and Dvorak, H.F. (2009) 'Why are tumour blood vessels abnormal and why is it important to know?', *British Journal of Cancer*, 100(6), pp. 865–869. Available at: https://doi.org/10.1038/sj.bjc.6604929.

Nair, V. *et al.* (2017) 'Growth differentiation factor–15 and risk of CKD progression', *Journal of the American Society of Nephrology*, 28(7), pp. 2233–2240. Available at: https://doi.org/10.1681/ASN.2016080919.

Narsale, A.A. and Carson, J.A. (2014) 'Role of IL-6 in cachexia – therapeutic implications', *Current opinion in supportive and palliative care*, 8(4), pp. 321–327. Available at: https://doi.org/10.1097/SPC.0000000000000091.

Neary, N.M., Small, C.J., Wren, A.M., Lee, J.L., Druce, M.R., Palmieri, C., Frost, G.S., Ghatei, M.A., Coombes, R.C., and Bloom, S.R. (2004) 'Ghrelin increases energy intake in cancer patients with impaired appetite: Acute, randomized, placebo-controlled trial', *The Journal of Clinical Endocrinology & Metabolism*, 89(6), pp. 2832–2836. Available at: https://doi.org/10.1210/JC.2003-031768.

NICE (2016) 'Prevention of chemotherapy induced nausea and vomiting in adults: netupitant/palonosetron Evidence summary Key points from the evidence'. Available at: www.nice.org.uk/guidance/esnm69 (Accessed: 25 February 2023).

NICE (2019) *British National Formulary*.

Norris, A.J. *et al.* (2021) 'Parabrachial opioidergic projections to preoptic hypothalamus mediate behavioral and physiological thermal defenses', *eLife*, 10, p. e60779.

O'Rahilly, S. (2017) 'GDF15—From biomarker to allostatic hormone', *Cell*

Metabolism, 26(6), pp. 807–808. Available at: https://doi.org/10.1016/j.cmet.2017.10.017.

Okere, C.O., Kaba, H., and Higuchi, T. (2000) 'Importance of endogenous nitric oxide synthase in the rat hypothalamus and amygdala in mediating the response to capsaicin', *Journal of Comparative Neurology*, 423(4), pp. 670–686. Available at: https://onlinelibrary.wiley.com/doi/epdf/10.1002/1096-9861%2820000807%29423%3A4%3C670%3A%3AAID-CNE11%3E3.0.CO%3B2-S?saml_referrer (Accessed: 27 December 2022).

Olsen, O.E., Skjærvik, A., Størdal, B.F., Sundan, A., and Holien, T. (2017) 'TGF-β contamination of purified recombinant GDF15', *PLoS ONE*, 12(11). Available at: https://doi.org/10.1371/journal.pone.0187349.

Onesti, J.K. and Guttridge, D.C. (2014) 'Inflammation based regulation of cancer cachexia', *BioMed Research International*, 2014, pp. 1–7. Available at: https://doi.org/10.1155/2014/168407.

Ost, M., Igual Gil, C., Coleman, V., Keipert, S., Efstathiou, S., Vidic, V., Weyers, M., and Klaus, S. (2020) 'Muscle-derived GDF15 drives diurnal anorexia and systemic metabolic remodeling during mitochondrial stress', *EMBO reports*, 21(3). Available at: https://doi.org/10.15252/EMBR.201948804.

Palmiter, R.D. (2018) 'The parabrachial nucleus: CGRP neurons function as a general alarm', *Trends in Neurosciences*, 41(5), pp. 280–293. Available at: https://doi.org/10.1016/j.tins.2018.03.007.

Paredes, F., Williams, H.C., and San Martin, A. (2021) 'Metabolic adaptation in hypoxia and cancer', *Cancer letters*, 502, pp. 133–142. Available at: https://doi.org/10.1016/J.CANLET.2020.12.020.

Park-York, M., Boghossian, S., Oh, H., and York, D.A. (2013) 'PKCθ expression in the amygdala regulates insulin signaling, food intake and body weight', *Obesity (Silver Spring, Md.)*, 21(4), pp. 755–764. Available at: https://doi.org/10.1002/OBY.20278.

Park, H., Nam, K.-S., Lee, H.-J., and Kim, K.S. (2022) 'Ionizing radiation-induced GDF15 promotes angiogenesis in human glioblastoma models by promoting VEGFA expression through p-MAPK1/SP1 signaling.', *Frontiers in oncology*, 12(801230), pp. 1–12. Available at: https://doi.org/10.3389/fonc.2022.801230.

Park, S.B., Goldstein, D., Krishnan, A. V, Cindy, ;, Lin, S.-Y., Friedlander, M.L., Cassidy, J., Koltzenburg, M., Matthew, ;, and Kiernan, C. (2013) 'Chemotherapy-induced peripheral neurotoxicity: A critical analysis', *CA: A Cancer Journal for Clinicians*, 63(6), pp. 419–437. Available at: https://doi.org/10.3322/CAAC.21204.

Park, S.H., Choi, H.J., Yang, H., Do, K.H., Kim, J., Kim, H.H., Lee, H., Oh, C.G., Lee, D.W., and Moon, Y. (2012) 'Two in-and-out modulation strategies for endoplasmic reticulum stress-linked gene expression of pro-apoptotic macrophage-inhibitory cytokine 1', *The Journal of biological chemistry*, 287(24), pp. 19841–19855. Available at: https://doi.org/10.1074/JBC.M111.330639.

Parker, H.E., Adriaenssens, A., Rogers, G., Richards, P., Koepsell, H., Reimann, F., and Gribble, F.M. (2012) 'Predominant role of active versus facilitative glucose transport for glucagon-like peptide-1 secretion', *Diabetologia*, 55(9), pp. 2445–2455. Available at: https://doi.org/10.1007/s00125-012-2585-2.

Parker, J.A., McCullough, K.A., Field, B.C.T., Minnion, J.S., Martin, N.M., Ghatei, M.A., and Bloom, S.R. (2013) 'Glucagon and GLP-1 inhibit food intake and increase c-fos expression in similar appetite regulating centres in the brainstem and amygdala', *International Journal of Obesity*, 37(10), pp. 1391–1398. Available at: https://doi.org/10.1038/ijo.2012.227.

Patel, M.S., Lee, J., Baz, M., Wells, C.E., Bloch, S., Lewis, A., Donaldson, A. V., Garfield, B.E., Hopkinson, N.S., Natanek, A., Man, W.D.C., Wells, D.J., Baker, E.H., Polkey, M.I., and Kemp, P.R. (2016) 'Growth differentiation factor-15 is associated with muscle mass in chronic obstructive pulmonary disease and promotes muscle wasting in vivo', *Journal of Cachexia, Sarcopenia and Muscle*, 7(4), pp. 436–448. Available at: https://doi.org/10.1002/jcsm.12096.

Patel, S. *et al.* (2019) 'GDF15 provides an endocrine signal of nutritional stress in mice and humans', *Cell Metabolism*, 29, pp. 1–12. Available at: https://doi.org/10.1016/j.cmet.2018.12.016.

Paxinos, G. and Franklin, K.B. (2001) *Mouse Brain in Stereotaxic Coordinates*. 2nd edn. London: Academic Press.

Peckett, A.J., Wright, D.C., and Riddell, M.C. (2011) 'The effects of glucocorticoids on adipose tissue lipid metabolism', *Metabolism: Clinical and Experimental*, 60(11), pp. 1500–1510. Available at: https://doi.org/10.1016/j.metabol.2011.06.012.

Pérez De La Mora, M., Hernández-Gómez, A.M., Arizmendi-García, Y., Jacobsen, K.X., Lara-García, D., Flores-Gracia, C., Crespo-Ramírez, M., Gallegos-Cari, A., Nuche-Bricaire, A., and Fuxe, K. (2007) 'Role of the amygdaloid cholecystokinin (CCK)/gastrin-2 receptors and terminal networks in the modulation of anxiety in the rat. Effects of CCK-4 and CCK-8S on anxiety-like behaviour and [3H]GABA release', *European Journal of Neuroscience*, 26(12), pp. 3614–3630. Available at: https://doi.org/10.1111/J.1460-9568.2007.05963.X.

Petry, C.J., Ong, K.K., Burling, K.A., Barker, P., Perry, J.R., Acerini, C.L., Hughes, I.A.,

Dunger, D.B., and O'Rahilly, S. (2018) 'GDF15 concentrations in maternal serum associated with vomiting in pregnancy: the Cambridge baby growth study', *bioRxiv*, 3(123), pp. 1–14. Available at: https://doi.org/10.1101/221267.

Plunkett, W., Huang, P., Xu, Y., Heinemann, V., Grunewald, R., and Gandhi, V. (1995) 'Gemcitabine: metabolism, mechanisms of action, and self-potentiation', *Seminars in Oncology*, 22(4), pp. 3–10.

Porporato, P.E. *et al.* (2013) 'Acylated and unacylated ghrelin impair skeletal muscle atrophy in mice', *The Journal of Clinical Investigation*, 123(2), p. 611. Available at: https://doi.org/10.1172/JCI39920.

Powley, T.L. (2021) 'Brain-gut communication: vagovagal reflexes interconnect the two "brains"', *American journal of physiology*, 321(5), pp. G576–G587. Available at: https://doi.org/10.1152/AJPGI.00214.2021/ASSET/IMAGES/LARGE/AJPGI.00214.2021_F003.JPEG.

Pradhan, G., Samson, S.L., and Sun, Y. (2013) 'Ghrelin: much more than a hunger hormone', *Current Opinion in Clinical Nutrition and Metabolic Care*, 16(6), pp. 619–624. Available at: https://doi.org/10.1097/MCO.

Prado, C.M.M., Baracos, V.E., McCargar, L.J., Mourtzakis, M., Mulder, K.E., Reiman, T., Butts, C.A., Scarfe, A.G., and Sawyer, M.B. (2007) 'Body composition as an independent determinant of 5-fluorouracil-based chemotherapy toxicity', *Clinical Cancer Research*, 13(11), pp. 3264–3268. Available at: https://doi.org/10.1158/1078-0432.CCR-06-3067.

Prado, C.M.M., Birdsell, L.A., and Baracos, V.E. (2009) 'The emerging role of computerized tomography in assessing cancer cachexia', *Current Opinion in Supportive and Palliative Care*, 3(4), pp. 269–275. Available at: https://doi.org/10.1097/SPC.0B013E328331124A.

Prunier, C., Baker, D., ten Dijke, P., and Ritsma, L. (2018) 'TGF-β Family Signaling Pathways in Cellular Dormancy', *Trends in Cancer*, 5(1), pp. 66–78. Available at: https://doi.org/10.1016/j.trecan.2018.10.010.

Pursey, K.M., Contreras-Rodriguez, O., Collins, C.E., Stanwell, P., and Burrows, T.L. (2019) 'Food addiction symptoms and amygdala response in fasted and fed states', *Nutrients*, 11(1285), pp. 1–10. Available at: https://doi.org/10.3390/NU11061285.

Ramos, E.J.B., Suzuki, S., Marks, D., Inui, A., Asakawa, A., and Meguid, M.M. (2004) 'Cancer anorexia-cachexia syndrome: Cytokines and neuropeptides', *Current Opinion in Clinical Nutrition and Metabolic Care*, 7(4), pp. 427–434. Available at: https://doi.org/10.1097/01.mco.0000134363.53782.cb.

Rapoport, B.L. (2017) 'Delayed chemotherapy-induced nausea and vomiting: Pathogenesis, incidence, and current management', *Frontiers in Pharmacology*, 8(19), pp. 1–10. Available at: https://doi.org/10.3389/fphar.2017.00019.

Ratnam, N.M., Peterson, J.M., Talbert, E.E., Ladner, K.J., Rajasekera, P. V., Schmidt, C.R., Dillhoff, M.E., Swanson, B.J., Haverick, E., Kladney, R.D., Williams, T.M., Leone, G.W., Wang, D.J., and Guttridge, D.C. (2017) 'NF-κB regulates GDF-15 to suppress macrophage surveillance during early tumor development', *Journal of Clinical Investigation*, 127(10), pp. 3796–3809. Available at: https://doi.org/10.1172/JCI91561.

Rausch, V., Sala, V., Penna, F., Porporato, P.E., and Ghigo, A. (2021) 'Understanding the common mechanisms of heart and skeletal muscle wasting in cancer cachexia', *Oncogenesis*, 10(1), pp. 1–13. Available at: https://doi.org/10.1038/s41389-020-00288-6.

Reddy, N.L., Tan, B.K., Barber, T.M., and Randeva, H.S. (2014) 'Brown adipose tissue: Endocrine determinants of function and therapeutic manipulation as a novel treatment strategy for obesity', *BMC Obesity*, 1(1), pp. 1–12. Available at: https://doi.org/10.1186/s40608-014-0013-5.

Reidelberger, R.D., Heimann, D., Kelsey, L., and Hulce, M. (2003) 'Effects of peripheral CCK receptor blockade on feeding responses to duodenal nutrient infusions in rats', *American Journal of Physiology - Regulatory Integrative and Comparative Physiology*, 284(2), pp. 389–398. Available at: https://doi.org/10.1152/AJPREGU.00529.2002/ASSET/IMAGES/LARGE/H6023154900 05.JPEG.

Riddell, I.A. and Lippard, S.J. (2018) 'Cisplatin and oxaliplatin: Our current understanding of their actions', in *Metallo-Drugs: Development and Action of Anticancer Agents*. Walter de Gruyter GmbH, pp. 1–42. Available at: https://doi.org/10.1515/9783110470734-001/MACHINEREADABLECITATION/RIS.

Rinaman, L. (1999) 'A functional role for central glucagon-like peptide-1 receptors in lithium chloride-induced anorexia', *American Journal of Physiology*, 277(5), pp. 1537–1540. Available at: https://doi.org/10.1152/AJPREGU.1999.277.5.R1537/ASSET/IMAGES/LARGE/AREG7 1140002X.JPEG.

Roila, F. *et al.* (2016) '2016 MASCC and ESMO guideline update for the prevention of chemotherapy- and radiotherapy-induced nausea and vomiting and of nausea and vomiting in advanced cancer patients', *Annals of Oncology*, 27, pp. v119–v133. Available at: https://doi.org/10.1093/annonc/mdw270.

Roman, C.W., Derkach, V.A., and Palmiter, R.D. (2016) 'Genetically and functionally defined NTS to PBN brain circuits mediating anorexia', *Nature Communications*, 7, pp. 1–11. Available at: https://doi.org/10.1038/ncomms11905.

Roman, C.W., Sloat, S.R., and Palmiter, R.D. (2017) 'A tale of two circuits: CCK NTS neuron stimulation controls appetite and induces opposing motivational states by projections to distinct brain regions', *Neuroscience*, 358, pp. 316–324. Available at: https://doi.org/10.1016/j.neuroscience.2017.06.049.

Russell JA. Core affect and the psychological construction of emotion. Psychol Rev. 2003 Jan;110(1):145-72. doi: 10.1037/0033-295x.110.1.145. PMID: 12529060.

Ryu, J.S., Robinson, L. and Raucher, D. (2019) 'Elastin-Like Polypeptide Delivers a Notch Inhibitory Peptide to Inhibit Tumor Growth in Combination with Paclitaxel', *Journal of Chemotherapy (Florence, Italy)*, 31(1), pp. 23–29. Available at: https://doi.org/10.1080/1120009X.2018.1537554.

Sabatini, P. V., Frikke-Schmidt, H., Arthurs, J., Gordian, D., Patel, A., Rupp, A.C., Adams, J.M., Wang, J., Jørgensen, S.B., Olson, D.P., Palmiter, R.D., Myers, M.G., and Seeley, R.J. (2021) 'GFRAL-expressing neurons suppress food intake via aversive pathways', *Proceedings of the National Academy of Sciences*, 118(8). Available at: https://doi.org/10.1073/PNAS.2021357118.

Saito, K., Cao, X., He, Y., and Xu, Y. (2015) 'Progress in the molecular understanding of central regulation of body weight by estrogens', *Obesity (Silver Spring)*, 23(5), pp. 919–926. Available at: https://doi.org/10.1002/OBY.21099.

Sanchez, M.R., Wang, Y., Cho, T.S., Schnapp, W.I., Schmit, M.B., Fang, C., and Cai, H. (2022) 'Dissecting a disynaptic central amygdala-parasubthalamic nucleus neural circuit that mediates cholecystokinin-induced eating suppression', *Molecular metabolism*, 58(101433), pp. 1–9. Available at: https://doi.org/10.1016/J.MOLMET.2022.101443.

Sándor, N., Schilling-Tóth, B., Kis, E., Benedek, A., Lumniczky, K., Sáfrány, G., and Hegyesi, H. (2015) 'Growth Differentiation Factor-15 (GDF-15) is a potential marker of radiation response and radiation sensitivity', *Mutation Research - Genetic Toxicology and Environmental Mutagenesis*, 793, pp. 142–149. Available at: https://doi.org/10.1016/j.mrgentox.2015.06.009.

Sanger, G.J. and Andrews, P.L.R. (2018) 'A history of drug discovery for treatment of nausea and vomiting and the implications for future research', *Frontiers in Pharmacology*, 9(913), pp. 1–35. Available at: https://doi.org/10.3389/fphar.2018.00913.

Scheffer, D., Kulcsár, G., Nagyéri, G., Kiss-Merki, M., Rékási, Z., Maloy, M., and

Czömpöly, T. (2020) 'Active mixture of serum-circulating small molecules selectively inhibits proliferation and triggers apoptosis in cancer cells via induction of ER stress', *Cellular signalling*, 65(109426). Available at: https://doi.org/10.1016/J.CELLSIG.2019.109426.

Schindelin, J., Arganda-Carreras, I., Frise, E., and Al., E. (2012) 'Fiji: an open-source platform for biological-image analysis', *Nature methods*, 9(7), pp. 676–682. Available at: https://doi.org/10.1038/nmeth.2019.

Seebacher, N.A., Stacy, A.E., Porter, G.M., and Merlot, A.M. (2019) 'Clinical development of targeted and immune based anti-cancer therapies', *Journal of Experimental & Clinical Cancer Research*, 38(156), pp. 1–39. Available at: https://doi.org/10.1186/S13046-019-1094-2.

Seeley, R.J., Blake, K., Rushing, P.A., Benoit, S., Eng, J., Woods, S.C., and D'Alessio, D. (2000) 'The Role of CNS Glucagon-Like Peptide-1 (7-36) Amide Receptors in Mediating the Visceral Illness Effects of Lithium Chloride', *The Journal of Neuroscience*, 20(4), pp. 1616–1621. Available at: https://doi.org/10.1523/JNEUROSCI.20-04-01616.2000.

Senapati, S., Rachagani, S., Chaudhary, K., Johansson, S.L., Singh, R.K., and Batra, S.K. (2010) 'Overexpression of macrophage inhibitory cytokine-1 induces metastasis of human prostate cancer cells through the FAK-RhoA signaling pathway', *Oncogene*, 29(9), pp. 1293–1302. Available at: https://doi.org/10.1038/onc.2009.420.

Siddiqui, J.A., Seshacharyulu, P., Muniyan, S., Pothuraju, R., Khan, P., Vengoji, R., Chaudhary, S., Maurya, S.K., Lele, S.M., Jain, M., Datta, K., Nasser, M.W., and Batra, S.K. (2022) 'GDF15 promotes prostate cancer bone metastasis and colonization through osteoblastic CCL2 and RANKL activation', *Bone Research*, 10(1), pp. 1–15. Available at: https://doi.org/10.1038/s41413-021-00178-6.

Side effects of radiotherapy - NHS (2023). Available at: https://www.nhs.uk/conditions/radiotherapy/side-effects/ (Accessed: 29 January 2023).

Siff, T., Parajuli, P., Razzaque, M.S., and Atfi, A. (2021) 'Cancer-Mediated Muscle Cachexia: Etiology and Clinical Management', *Trends in Endocrinology & Metabolism*, 32(6), pp. 382–402. Available at: https://doi.org/10.1016/j.tem.2021.03.007.

Singh, P. and Kuo, B. (2016) 'Central Aspects of Nausea and Vomiting in GI Disorders', *Current Treatment Options in Gastroenterology*, 14(4), pp. 444–451. Available at: https://doi.org/10.1007/s11938-016-0107-x.

Siren, P.M.A. and Siren, M.J. (2010) 'Systemic zinc redistribution and dyshomeostasis in cancer cachexia', *Journal of Cachexia, Sarcopenia and Muscle*, 1(1), pp. 23–33.

Available at: https://doi.org/10.1007/S13539-010-0009-Z.

Sominsky, L. and Spencer, S.J. (2014) 'Eating behavior and stress: A pathway to obesity', *Frontiers in Psychology*, 5, pp. 1–8. Available at: https://doi.org/10.3389/fpsyg.2014.00434.

Song, H., Yin, D., and Liu, Z. (2012) 'GDF-15 promotes angiogenesis through modulating p53/HIF-1α signaling pathway in hypoxic human umbilical vein endothelial cells', *Molecular Biology Reports*, 39(4), pp. 4017–4022. Available at: https://doi.org/10.1007/s11033-011-1182-7.

Sonis, S.T. (2004) 'The pathobiology of mucositis', *Nature Reviews Cancer 2004 4:4*, 4(4), pp. 277–284. Available at: https://doi.org/10.1038/nrc1318.

Strelau, J., Böttner, M., Lingor, P., Suter-Crazzolara, C., Galter, D., Jaszai, J., Sullivan, A., Schober, A., Krieglstein, K., and Unsicker, K. (2000) 'GDF-15/MIC-1 a novel member of the TGF-beta superfamily', *Journal of neural transmission. Supplementum*, 60, pp. 273–276. Available at: https://doi.org/10.1007/978-3-7091-6301-6_18.

Sullivan, K.A., Grant, C. V., Jordan, K.R., Vickery, S.S., and Pyter, L.M. (2021) 'Voluntary wheel running ameliorates select paclitaxel chemotherapy-induced sickness behaviors and associated melanocortin signaling', *Behavioural brain research*, 399, p. e113041. Available at: https://doi.org/10.1016/J.BBR.2020.113041.

Sun, Y., Wang, P., Zheng, H., and Smith, R.G. (2004) 'Ghrelin stimulation of growth hormone release and appetite is mediated through the growth hormone secretagogue receptor', *Proceedings of the National Academy of Sciences of the United States of America*, 101(13), pp. 4679–4684. Available at: https://doi.org/10.1073/PNAS.0305930101.

Suriben, R. *et al.* (2020) 'Antibody-mediated inhibition of GDF15–GFRAL activity reverses cancer cachexia in mice', *Nature Medicine*, 26(8), pp. 1264–1270. Available at: https://doi.org/10.1038/s41591-020-0945-x.

Suzuki, H., Asakawa, A., Amitani, H., Nakamura, N., and Inui, A. (2013) 'Cancer cachexia - Pathophysiology and management', *Journal of Gastroenterology*, 48(5), pp. 574–594. Available at: https://doi.org/10.1007/s00535-013-0787-0.

Tazi, E. and Errihani, H. (2010) 'Treatment of cachexia in oncology.', *Indian Journal of Palliative Care*, 16(3), pp. 129–137. Available at: https://doi.org/10.4103/0973-1075.73644.

Tijerina, A.J. (2004) 'The Biochemical Basis of Metabolism in Cancer Cachexia', *Dimens Crit Care Nurs.*, 23(6), pp. 237–243.

Tisdale, M.J. (2004) 'Cancer cachexia', *Langenbeck's Archives of Surgery*, 389(4), pp. 299–305. Available at: https://doi.org/10.1007/S00423-004-0486-7/METRICS.

Townsend, L.K., Weber, A.J., Day, E.A., Shamshoum, H., Shaw, S.J., Perry, C.G.R., Kemp, B.E., Steinberg, G.R., and Wright, D.C. (2021) 'AMPK mediates energetic stress-induced liver GDF15', *FASEB journal : official publication of the Federation of American Societies for Experimental Biology*, 35(1). Available at: https://doi.org/10.1096/FJ.202000954R.

Tran, T., Yang, J., Gardner, J., and Xiong, Y. (2018) 'GDF15 deficiency promotes high fat diet-induced obesity in mice', *PLoS ONE*, 13(8), pp. 1–13. Available at: https://doi.org/10.1371/journal.pone.0201584.

Travagli, R.A. and Anselmi, L. (2016) 'Vagal neurocircuitry and its influence on gastric motility', *Nature Reviews Gastroenterology and Hepatology*, 13(7), pp. 389–401. Available at: https://doi.org/10.1038/nrgastro.2016.76.

Tsai, V.W., Zhang, H.P., Manandhar, R., Lee-Ng, K.K.M., Lebhar, H., Marquis, C.P., Husaini, Y., Sainsbury, A., Brown, D.A., and Breit, S.N. (2018) 'Treatment with the TGF-b superfamily cytokine MIC-1/GDF15 reduces the adiposity and corrects the metabolic dysfunction of mice with diet-induced obesity', *International Journal of Obesity*, 42(3), pp. 561–571. Available at: https://doi.org/10.1038/ijo.2017.258.

Tsai, V.W.W., Husaini, Y., Manandhar, R., Lee-Ng, K.K.M., Zhang, H.P., Harriott, K., Jiang, L., Lin, S., Sainsbury, A., Brown, D.A., and Breit, S.N. (2012) 'Anorexia/cachexia of chronic diseases: a role for the TGF-β family cytokine MIC-1/GDF15', *Journal of cachexia, sarcopenia and muscle*, 3(4), pp. 239–243. Available at: https://doi.org/10.1007/S13539-012-0082-6.

Tsai, V.W.W., Macia, L., Johnen, H., Kuffner, T., Manadhar, R., Jørgensen, S.B., Lee-Ng, K.K.M., Zhang, H.P., Wu, L., Marquis, C.P., Jiang, L., Husaini, Y., Lin, S., Herzog, H., Brown, D.A., Sainsbury, A., and Breit, S.N. (2013) 'TGF-b superfamily cytokine MIC-1/GDF15 is a physiological appetite and body weight regulator', *PLoS ONE*, 8(2), pp. 1–9. Available at: https://doi.org/10.1371/journal.pone.0055174.

Tsai, V.W.W. *et al.* (2015) 'Serum levels of human MIC-1/GDF-15 vary in a diurnal pattern, do not display a profile suggestive of a satiety factor and are related to BMI', *PLoS ONE*, 10(7), pp. 1–15. Available at: https://doi.org/10.1371/journal.

Tsai, V.W.W., Lin, S., Brown, D.A., Salis, A., and Breit, S.N. (2016) 'Anorexia-cachexia and obesity treatment may be two sides of the same coin: Role of the TGF-b superfamily cytokine MIC-1/GDF15', *International Journal of Obesity*, 40, pp. 193–197. Available at: https://doi.org/10.1038/ijo.2015.242.

Tsai, V.W.W., Zhang, H.P., Manandhar, R., Schofield, P., Christ, D., Lee-Ng, K.K.M.,

Lebhar, H., Marquis, C.P., Husaini, Y., Brown, D.A., and Breit, S.N. (2019) 'GDF15 mediates adiposity resistance through actions on GFRAL neurons in the hindbrain AP/NTS', *International journal of obesity (2005)*, 43(12), pp. 2370–2380. Available at: https://doi.org/10.1038/S41366-019-0365-5.

Turnbull, A. V. and Rivier, C.L. (1999) 'Regulation of the hypothalamic-pituitary-adrenal axis by cytokines: Actions and mechanisms of action', *Physiological Reviews*, 79(1), pp. 1–71. Available at: https://doi.org/10.1152/PHYSREV.1999.79.1.1/ASSET/IMAGES/LARGE/JNP.OC11F4.JPEG.

Ünal, B., Alan, S., Başsorgun, C.İ., Karakaş, A.A., Elpek, G.Ö., and Çiftçioğlu, M.A. (2015) 'The divergent roles of growth differentiation factor-15 (GDF-15) in benign and malignant skin pathologies', *Archives of Dermatological Research*, 307, pp. 551–557. Available at: https://doi.org/10.1007/s00403-015-1546-2.

Unsicker, K., Spittau, B., and Krieglstein, K. (2013) 'The multiple facets of the TGF-β family cytokine growth/differentiation factor-15/macrophage inhibitory cytokine-1', *Cytokine and Growth Factor Reviews*, 24, pp. 373–384. Available at: https://doi.org/10.1016/j.cytogfr.2013.05.003.

Vaughan, V.C., Martin, P., and Lewandowski, P.A. (2013) 'Cancer cachexia: Impact, mechanisms and emerging treatments', *Journal of Cachexia, Sarcopenia and Muscle*, 4(2), pp. 95–109. Available at: https://doi.org/10.1007/S13539-012-0087-1.

Vassileva, V. *et al.* (2008) 'Efficacy assessment of sustained intraperitoneal paclitaxel therapy in a murine model of ovarian cancer using bioluminescent imaging', *British Journal of Cancer*, 99(12), p. 2037. Available at: https://doi.org/10.1038/SJ.BJC.6604803.

Venkatesh, P. and Kasi, A. (2022) 'StatPearls (Internet)', in *StatPearls (Internet)*. Florida: Treasure Island, StatPearls Publishing. Available at: https://www.ncbi.nlm.nih.gov/books/NBK538187.

Wafai, L., Taher, M., Jovanovska, V., Bornstein, J.C., Dass, C.R., and Nurgali, K. (2013) 'Effects of oxaliplatin on mouse myenteric neurons and colonic motility', *Frontiers in neuroscience*, 7, pp. 1–8. Available at: https://doi.org/10.3389/FNINS.2013.00030.

Wang, D., Wei, X., Geng, X., Li, P., and Li, L. (2022) 'GDF15 enhances proliferation of aged chondrocytes by phosphorylating SMAD2', *Journal of Orthopaedic Science*, 27(1), pp. 249–256. Available at: https://doi.org/10.1016/J.JOS.2020.12.004.

Wang, X., Baek, S.J., and Eling, T.E. (2013) 'The Diverse Roles of Nonsteroidal Anti-inflammatory Drug Activated Gene (NAG-1/GDF15) in Cancer', *Biochemical pharmacology*, 85(5), p. 597. Available at:

https://doi.org/10.1016/J.BCP.2012.11.025.

Wang, X.B., Jiang, X.R., Yu, X.Y., Wang, L., He, S., Feng, F.Y., Guo, L.P., Jiang, W., and Lu, S.H. (2014) 'Macrophage inhibitory factor 1 acts as a potential biomarker in patients with esophageal squamous cell carcinoma and is a target for antibody-based therapy', *Cancer science*, 105(2), pp. 176–185. Available at: https://doi.org/10.1111/CAS.12331.

Wang, Y., Kim, J.M., Schmit, M.B., Cho, T.S., Fang, C., and Cai, H. (2019) 'A bed nucleus of stria terminalis microcircuit regulating inflammation-associated modulation of feeding', *Nature Communications*, 10(2769), pp. 1–13. Available at: https://doi.org/10.1038/S41467-019-10715-X.

Wang, Z. *et al.* (2021) 'GDF15 induces immunosuppression via CD48 on regulatory T cells in hepatocellular carcinoma', *Journal for immunotherapy of cancer*, 9(e002787), pp. 1–16. Available at: https://doi.org/10.1136/JITC-2021-002787.

Wasserman, D.H. (2009) 'Four grams of glucose', *American Journal of Physiology - Endocrinology and Metabolism*, 296(1), pp. 11–21. Available at: https://doi.org/10.1152/AJPENDO.90563.2008/ASSET/IMAGES/LARGE/ZH10120855 100011.JPEG.

Waterson, M.J. and Horvath, T.L. (2015) 'Neuronal regulation of energy homeostasis: Beyond the hypothalamus and feeding', *Cell Metabolism*, 22(6), pp. 962–970. Available at: https://doi.org/10.1016/j.cmet.2015.09.026.

Webb WW, Fogel RP. (1995) 'Gastroparesis: current management', *Compr Ther*. 21(12), pp. 741-45. PMID: 8789140.

Weber, B.Z.C., Arabaci, D.H., and Kir, S. (2022) 'Metabolic reprogramming in adipose tissue during cancer cachexia', *Frontiers in Oncology*, 12, pp. 1–9. Available at: https://doi.org/10.3389/FONC.2022.848394.

Welch, C.C., Kim, E.M., Grace, M.K., Billington, C.J., and Levine, A.S. (1996) 'Palatability-induced hyperphagia increases hypothalamic dynorphin peptide and mRNA levels', *Brain Research*, 721(1–2), pp. 126–131. Available at: https://doi.org/10.1016/0006-8993(96)00151-5.

Welsh, J.B., Sapinoso, L.M., Kern, S.G., Brown, D.A., Liu, T., Bauskin, A.R., Ward, R.L., Hawkins, N.J., Quinn, D.I., Russell, P.J., Sutherland, R.L., Breit, S.N., Moskaluk, C.A., Frierson, H.F., and Hampton, G.M. (2003) 'Large-scale delineation of secreted protein biomarkers overexpressed in cancer tissue and serum', *Proceedings of the National Academy of Sciences*, 100(6), pp. 3410–3415. Available at: https://doi.org/10.1073/pnas.0530278100.

Welsh, P., Kimenai, D.M., Marioni, R.E., Hayward, C., Campbell, A., Porteous, D., Mills, N.L., O'Rahilly, S., and Sattar, N. (2022) 'Reference ranges for GDF-15, and risk factors associated with GDF-15, in a large general population cohort', *Clinical Chemistry and Laboratory Medicine*, 60(11), pp. 1820–1829. Available at: https://doi.org/10.1515/CCLM-2022-0135.

Wen, X., Zhang, B., Wu, B., Xiao, H., Li, Z., Li, R., Xu, X., and Li, T. (2022) 'Signaling pathways in obesity: mechanisms and therapeutic interventions', *Signal Transduction and Targeted Therapy*, 7(298). Available at: https://doi.org/10.1038/S41392-022-01149-X.

Williams, D.L., Lilly, N.A., Edwards, I.J., Yao, P., Richards, J.E., and Trapp, S. (2018) 'GLP-1 action in the mouse bed nucleus of the stria terminalis', *Neuropharmacology*, 131, pp. 83–95. Available at: https://doi.org/10.1016/J.NEUROPHARM.2017.12.007.

Wischhusen, J., Melero, I., and Fridman, W.H. (2020) 'Growth/differentiation factor-15 (GDF-15): From biomarker to novel targetable immune checkpoint', *Frontiers in Immunology*, 11(951), pp. 1–21. Available at: https://doi.org/10.3389/FIMMU.2020.00951.

Wollert, K.C., Kempf, T., and Wallentin, L. (2017) 'Growth differentiation factor 15 as a biomarker in cardiovascular disease', *Clinical Chemistry*, 63(1), pp. 140–151. Available at: https://doi.org/10.1373/clinchem.2016.255174.

Woltman, T.A., Hulce, M., and Reidelberger, R.D. (1999) 'Relative blood-brain barrier permeabilities of the cholecystokinin receptor antagonists devazepide and A-65186 in rats', *J. Pharm. Pharmacol*, 51, pp. 917–920. Available at: https://doi.org/10.1211/0022357991773348.

Wong, J., Tran, L.T., Lynch, K.A., and Wood, L.J. (2018) 'Dexamethasone exacerbates cytotoxic chemotherapy induced lethargy and weight loss in female tumor free mice', *Cancer Biology and Therapy*, 19(1), pp. 87–96. Available at: https://doi.org/10.1080/15384047.2017.1394549.

Worth, A.A., Shoop, R., Tye, K., Feetham, C.H., D'agostino, G., Dodd, G.T., Reimann, F., Gribble, F.M., Beebe, E.C., Dunbar, J.D., Alexander-Chacko, J.T., Sindelar, D.K., Coskun, T., Emmerson, P.J., and Luckman, S.M. (2020) 'The cytokine GDF15 signals through a population of brainstem cholecystokinin neurons to mediate anorectic signalling', *eLife*, 9, pp. 1–19. Available at: https://doi.org/10.7554/eLife.55164.

Wu, C.S., Wei, Q., Wang, H., Kim, D.M., Balderas, M., Wu, G., Lawler, J., Safe, S., Guo, S., Devaraj, S., Chen, Z., and Sun, Y. (2020) 'Protective effects of ghrelin on fasting-induced muscle atrophy in aging mice', *The journals of gerontology. Series A, Biological sciences and medical sciences*, 75(4), pp. 621–630. Available at:

https://doi.org/10.1093/GERONA/GLY256.

Wu, Q., Clark, M.S., and Palmiter, R.D. (2012) 'Deciphering a neuronal circuit that mediates appetite', *Nature*, 483, pp. 594–297. Available at: https://doi.org/10.1038/nature10899.

Xiong, Y., Walker, K., Min, X., Hale, C., Tran, T., Komorowski, R., Yang, J., Davda, J., Nuanmanee, N., Kemp, D., Wang, X., Liu, H., Miller, S., Lee, K.J., Wang, Z., and Véniant, M.M. (2017) 'Long-acting MIC-1/GDF15 molecules to treat obesity: Evidence from mice to monkeys', *Science Translational Medicine*, 9(8732), pp. 1–11. Available at: https://doi.org/10.1126/scitranslmed.aan8732.

Xu, J., Kimball, T.R., Lorenz, J.N., Brown, D.A., Bauskin, A.R., Klevitsky, R., Hewett, T.E., Breit, S.N., and Molkentin, J.D. (2006) 'GDF15/MIC-1 functions as a protective and antihypertrophic factor released from the myocardium in association with SMAD protein activation', *Circulation Research*, 98(3), pp. 342–350. Available at: https://doi.org/10.1161/01.RES.0000202804.84885.d0.

Yagi, T., Asakawa, A., Ueda, H., Ikeda, S., Miyawaki, S., and Inui, A. (2013) 'The role of zinc in the treatment of taste disorders', *Recent Patents on Food, Nutrition & Agriculture*, 5(1), pp. 44–51. Available at: https://doi.org/10.2174/2212798411305010007.

Yang, Linda *et al.* (2017) 'GFRAL is the receptor for GDF15 and is required for the anti-obesity effects of the ligand', *Nature Medicine*, 23, pp. 1158–1166. Available at: https://doi.org/10.1038/nm.4394.

Yang, Liu, Yu, H., Dong, S., Zhong, Y., and Hu, S. (2017) 'Recognizing and managing on toxicities in cancer immunotherapy', *http://dx.doi.org/10.1177/1010428317694542*, 39(3), pp. 1–13. Available at: https://doi.org/10.1177/1010428317694542.

Yeh, S.-S. and Schuster, M.W. (2006) 'Megestrol acetate in cachexia and anorexia', *International Journal of Nanomedicine*, 1(4), pp. 411–416.

Yeh, S.S. and Schuster, M.W. (1999) 'Geriatric cachexia: the role of cytokines', *The American Journal of Clinical Nutrition*, 70(2), pp. 183–197. Available at: https://doi.org/10.1093/AJCN.70.2.183.

Yu, S., Li, Q., Yu, Y., Cui, Y., Li, W., Liu, T., and Liu, F. (2020) 'Activated HIF1α of tumor cells promotes chemoresistance development via recruiting GDF15-producing tumor-associated macrophages in gastric cancer', *Cancer immunology, immunotherapy* 69(10), pp. 1973–1987. Available at: https://doi.org/10.1007/S00262-020-02598-5.

Zeng, Q., Ou, L., Wang, W., and Guo, D.Y. (2020) 'Gastrin, cholecystokinin, signaling,

and biological activities in cellular processes', *Frontiers in Endocrinology*, 11(112), pp. 1–16. Available at: https://doi.org/10.3389/FENDO.2020.00112.

Zhang, C., Kaye, J.A., Cai, Z., Wang, Y., Prescott, S.L., Liberles, S.D., Zhang, C., Kaye, J.A., Cai, Z., Wang, Y., Prescott, S.L., and Liberles, S.D. (2021) 'Area postrema cell types that mediate nausea- associated behaviors', *Neuron*, 109, pp. 461–472. Available at: https://doi.org/10.1016/j.neuron.2020.11.010.

Zhang, H., Fealy, C.E., and Kirwan, J.P. (2019) 'Exercise training promotes a GDF15-associated reduction in fat mass in older adults with obesity', *American Journal of Physiology - Endocrinology and Metabolism*, 316(5), pp. E829–E836. Available at: https://doi.org/10.1152/ajpendo.00439.2018.

Zhang, L., Koller, J., Gopalasingam, G., Qi, Y., and Herzog, H. (2022) 'Central NPFF signalling is critical in the regulation of glucose homeostasis', *Molecular Metabolism*, 62(101525), pp. 1–9. Available at: https://doi.org/10.1016/J.MOLMET.2022.101525.

Zhang, X., Huang, H.J., Feng, D., Yang, D.J., Wang, C.M., and Cai, Q.P. (2014) 'Is concomitant radiotherapy necessary with gemcitabine-based chemotherapy in pancreatic cancer?', *World Journal of Gastroenterology : WJG*, 20(46), pp. 17648–17655. Available at: https://doi.org/10.3748/WJG.V20.I46.17648.

Zhong, W., Shahbaz, O., Teskey, G., Beever, A., Kachour, N., Venketaraman, V., and Darmani, N.A. (2021) 'Mechanisms of nausea and vomiting: Current knowledge and recent advances in intracellular emetic signaling systems', *International Journal of Molecular Sciences*, 22(5797), pp. 1–33. Available at: https://doi.org/10.3390/IJMS22115797.

Zimmers, T.A., Gutierrez, J.C., and Koniaris, L.G. (2010) 'Loss of GDF-15 abolishes sulindac chemoprevention in the ApcMin/+ mouse model of intestinal cancer', *Journal of Cancer Research and Clinical Oncology*, 136, pp. 571–576. Available at: https://doi.org/https://doi.org/10.1007/s00432-009-0691-4.

Zséli, G., Vida, B., Martinez, A., Lechan, R.M., Khan, A.M., and Fekete, C. (2016) 'Elucidation of the anatomy of a satiety network: Focus on connectivity of the parabrachial nucleus in the adult rat', *Journal of Comparative Neurology*, 524(14), pp. 2803–2827. Available at: https://doi.org/10.1002/cne.23992.

Zséli, G., Vida, B., Szilvásy-Szabó, A., Tóth, M., Lechan, R.M., and Fekete, C. (2018) 'Neuronal connections of the central amygdalar nucleus with refeeding-activated brain areas in rats', *Brain structure & function*, 223(1), pp. 391–414. Available at: https://doi.org/10.1007/S00429-017-1501-4.